Interaction and toxicological studies of compounds on membrane models, cell cultures and 3D tissue models

by

Melinda Bartok, M.Sc.

A Thesis submitted in partial fulfillment
of the requirements for the degree of

Doctor of Philosophy
in Biochemical Engineering

Approved Dissertation Committee

_____
Prof. Dr. Detlef Gabel (Chair)

_____
PD Dr. Stephan Reichl

_____
Prof. Dr. Mathias Winterhalter

_____
Dr. Maria Engelke

Date of Defense: 7th October 2014

Engineering and Science

Acknowledgements

My profound appreciation goes to Prof. Dr. Detlef Gabel, who gave me the opportunity to work on several interesting projects during my PhD, who identified my interest and guided me through my experiments with so much patience. I would like to thank him for the helpful advices, interesting discussions and always new ideas, which made my work successful and easy every day.

My gratitude goes also to Dr. Maria Engelke, who introduced me into the science of tissue engineering and gave me the possibility to work on the hemi-cornea project in collaboration with University Hospital Hamburg-Eppendorf and Henkel from Düsseldorf. I am very grateful for her kind supervision and tutelage at the early stages of my work and for the interesting scientific and not so scientific discussions.

I am highly indebted to Prof. Dr. Mathias Winterhalter for his kind help in the bilayer experiments, for his interest in teaching me a new method and also for the interesting discussions during the experiments.

Sincere thanks goes to PD Dr. Stephan Reichl from the University of Braunschweig for kindly providing us the HCE cells and for accepting to be my external PhD committee member.

Special thanks for all my recent and former colleges in the working group of Prof. Dr. Detlef Gabel, Prof. Dr. Mathias Winterhalter and Prof. Dr. Roland Benz for making my days so enjoyable and the work less difficult than it always seemed to be.

Finally I would like to express my sincere gratitude to my wonderful parents and husband for supporting, guiding me in my life and giving me so much love day by day, without them I would not be able to reach where I am.

Table of Contents

Thesis Abstract

The first part of the study introduces two biotechnologically produced *in vitro* human cell based 3D hemi-cornea test systems, which aim at the complete replacement of the Draize Eye Irritation test. These test systems allow the assessment of chemicals of any physical-chemical properties and their proper categorization in different GHS categories. The first test system comprises an epithelium and a stroma with a collagen membrane embedded between them. The membrane allows the separation and the independent assessment of the damages in both compartments separately. The cell viability, measured with the MTT assay, was used as a toxicological endpoint. The second test system includes cornea models, which comprise epithelium and stroma without a collagen membrane. A test method based on these models was developed, which quantitatively determines the initial depth of injury (DoI) after chemical treatment of the tissues, combining the MTT assay with cryosectioning procedures. The areas of the metabolically inactive tissue are used as a visible correlate of the DoI. Both newly developed test systems could correctly classify and discriminate the GHS 1 and GHS 2 chemicals, but are over-predictive for GHS no category chemicals. Additionally, a 3D conjunctiva based test system was introduced to help in the classification of conjunctiva specific chemicals. However, the test materials tested on these models showed similar results to the 3D cornea models; in conclusion, no additional information was obtained.

The second part of the thesis describes the protective effect of brilliant blue G (BBG) on the cytotoxicity of trypan blue (TB), octenidine (Oct) and benzalkonium chloride (BAK). TB is a vital dye used for the staining of the internal limiting membrane during eye surgery. In the presence of TB, BBG significantly increased the cell survival of ARPE (human retinal pigment epithelium) cells, even at high TB concentrations, whereas at the same concentrations TB alone led to considerable cell damage. In the mixture with BAK, a widely used preservative in ophthalmologic solutions, or Oct, an antiseptic used for skin and wound disinfection, BBG decreased the cytotoxic effects of the two compounds on HCE (human corneal epithelial) cells. Although BBG is a well known $P2X_7$ receptor antagonist, other $P2X_7$ receptor antagonists did not show any protective effect on BAK or Oct. Therefore, it is assumed that the protective effect of BBG is not due to its action on the $P2X_7$ receptor. Brilliant blue R (BBR), a dye similar to BBG, showed protective effects only for Oct. The protective effects of BBR were comparable

with that of BBG. The bacterial inhibitory tests on different Gram-positive and Gram-negative bacteria revealed that high concentrations of BBG or BBR (above 0.025%) in mixture with either BAK or Oct no longer inhibited the bacterial growth of Gram-negative bacteria. However, the Gram-positive bacteria were hindered at all tested concentrations.

A third part of the present work includes two closely related studies. The first study describes the interaction of halogenated dodecaborate clusters with liposomal membranes, characterized by using different biophysical techniques. The Zeta potential measurements showed strong interaction of the cluster molecules to the liposomal membrane surface. These interactions led to significant changes in enthalpies of the transition temperatures of the lipids. The changes in enthalpies could be due to the morphological changes of the lipids in presents of high cluster concentrations, as revealed from cryo-TEM (cryo-transmission electron microscopy) and AFM (atomic force microscopy) images. The release of the liposomal contents was also achieved in presence of the clusters. It is assumed that the leakage occurred either through the pores formed by the cluster molecules within the liposomal bilayer, or through complete destruction of the liposomes. As the toxicity of the clusters on mammalian cells was not significantly high, the use of these molecules is proposed for the targeted release of drugs from liposomes used in cancer therapy.

In a second study the association and uptake of liposomes containing the dodecaborate cluster lipid in endothelial and cancer cell lines is described. The association was cell type dependent and HUVEC (endothelial) cells showed the strongest uptake of lipids. The fluorescent microscopy images showed uptake for both boron-lipid, followed by immuno-staining, and fluorescent marker lipid, even when the liposomes were sterically stabilized by pegylation. However, these interactions with Kelly and V79 (immortalized cancer cell lines) were concentration dependent and different for different boron-lipids liposomes. Interestingly, HUVEC showed for all boron-lipids an association of 90%-100%, even when the incubation took place at 4°C. Therefore, the use of these liposomes as drug delivery agents might be limited, as they would probably be taken up mostly in the vasculature.

Part 1: Two *in vitro* eye irritation test methods suitable for the complete replacement of the *in vivo* Draize Eye Irritation Test

1.1. Introduction

In the present study we report two newly developed *in vitro* eye irritation test methods, based on the 3D human hemi-cornea models described by Engelke et al. (2013), and show that both methods are able to classify the chemicals in the three GHS (Globally Harmonized System of Classification and Labeling of Chemicals) categories, defined by the United Nations in 1992 (United Nations 2011). The first publication (Appendix I) describes a new 3D hemi-cornea test system, which allows the separation and the independent quantification of the cellular damage in the epithelium and the stroma by the insertion of a collagen membrane between these two tissue compartments. The second manuscript (Appendix II) introduces a new method for the quantification of the initial depth of injury in 3D hemi-cornea models and 3D conjunctiva models, by using the MTT viability assay combined with cryosectioning procedures. The third manuscript (Appendix III) contains data from a comparison study between the eye irritation test system, named IRE-DOI (depth of injury measurement in *ex vivo* isolated rabbit eye) introduced by Jester et al. (2010), and the two new test methods we have recently developed. The outcome of the comparison study revealed that both recently introduced methods have a higher predictive capacity for all tested chemicals with regard to the GHS categories, compared to the IRE-DOI method, which misclassified several test substances used in the study.

1.1.1. GHS classification of chemicals based on their eye irritation potential

To ensure the protection of the consumers and the environment, each raw material and chemical must be tested with an extensive toxicological assessment procedure prior to usage. It is regulated by law (Regulation (EC) No 1272/2008) that these investigations have to be performed regarding to the GHS. The GHS was first introduced in 1992 in a mandate published after the UNCED (United Nations Conference on Environment and Development), where they mentioned the need of harmonization of the already existent systems of classification and labeling of the chemicals in different countries (United Nations 2011). A vital component of the toxicological examinations, according to the GHS, represents the assessment of the eye irritation potential of different substances. To date, there are three GHS categories defined to predict the eye irritation

of chemicals. The substances which fall in GHS 1 category, cause severe eye damage with irreversible effects within a 21 day observation period, i.e. destruction of the cornea, persistent corneal opacity, interference with the functions of the iris. GHS 2 substances are divided in two subcategories, GHS 2A (moderate eye irritants) and GHS 2B (mild eye irritants). GHS 2A substances produce eye irritations, such as conjunctival redness, edema or corneal opacity that are fully reversible in a period of 21 days. A substance is categorized as GHS 2B if these eye irritations recover in a maximum of 7 days. Those chemicals which cause no or slight eye irritation fall in the group of GHS not classified (GHS nc) substances (United Nations 2011).

At the present moment, the only OECD approved test for the determination of the whole range of eye irritating potential of chemicals is the rabbit Draize eye irritation test (Draize et al. 1944; OECD 2012a). In the interest of animal protection, it is regulated by law (Directive 86/609/EEC, Regulation (EC) No. 1907/2006 and Council Regulation (EC) No. 440/2008) that the research done on animals has to be waived as long as there are other possible methods to get relevant information about the substance to be tested. The European Union (EU) implemented an absolute prohibition of the tests on animals in the EU cosmetic research (Regulation (EC) No. 1223/2009). The use of the Draize eye irritation test, where the eyes of living rabbits are exposed to several test chemicals, as a last step in an integrated test strategy is impossible since 2009 after this policy was introduced in the EU. This fact forces the cosmetic industry and the raw material manufacturer to develop and validate alternative test methods to be able to bring always new products with innovative additives on the market.

1.1.2. Existent alternative test methods to replace the Draize eye irritation test

The Draize eye irritation test was developed by Draize et al. (1944) to test the products that are intended to come in contact with the human eye, such as ophthalmological preparation and cosmetics, and to provide handling guidelines and labeling precautions for these products. This test method involves the application of a defined volume (0.1 ml or 0.1 g) of the undiluted test materials *in vivo* on the rabbit eyes and the assessment of the irritation potential of these substances on the cornea, conjunctiva and iris, up to 21 days after application (York & Steiling 1998). The assessment system is totally subjective and includes as eye response: the corneal opacity, the area of the cornea involved, the damage to the iris and to the conjunctiva (ECETOC 1998). The Draize test method has been increasingly criticized in the past, not only due to cruelty

to animals, but also because of inconsistency of the generated data and overestimation of human responses (Christian & Diener 1996; Barile 2010). Several *in vitro* methods have been developed in the past to replace the Draize eye irritation test. The most promising alternative methods can be divided in two groups. The first group includes test systems which can accurately identify non-irritant (GHS nc) substances and distinguish them from other classes, such as GHS 2 or GHS 1 chemicals. The second group contains test methods that can predict the severe irritants (GHS 1) from other GHS classes. No test method has been developed yet, which could clearly identify the GHS 2 chemicals from other categories. In the first group several cell culture based assays are included, such as the Cytosensor Microphysiometer (CM), the Red Blood Cell Hemolysis (RBCH), the Neutral Red Release (NRR) and the Fluorescein Leakage assay (FL), as well as 3D epithelial models of the cornea such as the Human Corneal Epithelium, HCE™ (from SkinEthic, Lyon, France) and the EpiOcular™ (from MatTek, Ashland, USA) model. Also the Hen's Egg Test on the Chorio-Allantoic Membrane (HET-CAM) is designed to predict if a substance is a non-irritant or not. The CM assay is a cytotoxicity and cell function based in vitro test method that is performed on a monolayer of adherent mouse fibroblast cells, exposed to increasing concentrations of a test chemical and determines the metabolic rate of the cells by measuring the changes in pH per a time unit (Harbell et al. 1999). The RBCH assay is based on the photometrical measurement of the hemoglobin leakage and the denaturation of oxyhemoglobin from freshly isolated red blood cells in presence of potentially irritant chemicals (Pape et al. 1999). In the NRR assay monolayer cell cultures are pre-incubated with the neutral red dye, which binds to the lysosomes of the cells. After chemical exposure, the assay measures the direct toxicity of the test substance related to the damages on the cell membrane and the integrity of the lysosomes, by measuring the amount of the dye released after the exposure (Zuang 2000). The FL assay measures the sodium fluorescein leakage through an adherent dog kidney epithelial cell line (MDCK) due to the damage in the cell structure and disruption of the cell layer after exposure to chemical substances (Shaw et al. 1991). The MDCK are confluently grown cells, reported to easily form tight junction proteins. Therefore, they are a good model for the corneal epithelial barrier functions (Clothier et al. 1999). All these cell culture based assays predict the eye irritation of a chemical mostly based on the damages induced in the cell integrity after exposure and only discriminate irritants from non-irritants. Another problem with these assays is that they are limited to water soluble test substances (McNamee et al. 2009). The bio-

artificial 3D tissue models (HCE™ and EpiOcular™) have a multilayered epithelium reconstructed from human corneal epithelial cells (HCE™) or human epidermal keratinocytes (EpiOcular™). Both can only predict non-irritant and mild or moderate eye irritant chemicals, determined by the vitality of the tissues, measured usually by using the MTT assay or LDH (lactate dehydrogenase) release as a toxicological endpoint (Eskes et al. 2005). The HET-CAM assay was developed to mimic the effects of the test substances on the conjunctival tissue of the eye. The test system is based on the exposure of the chorio-allatoic membrane of 9 days old fertilized chicken eggs to chemicals, to identify the irritative reactions within a 5 minute observation period. Usually three reactions are to be observed: hemorrhage, lysis or coagulation (Steiling et al. 1999).

According to Scott et al. (2010) only test methods that include also a stroma could distinguish severe eye irritants from other classes, because the eye irritation of non classified substances are limited to the epithelium of the cornea, while the mild, moderate or severe irritants cause damage to the stroma, with different depth of stromal injuries depending on the severity of the eye irritant. Therefore, in the second group only test systems using ex-vivo isolated animal eyes from bovine (Bovine Corneal Opacity and Permeability test - BCOP), chicken (Isolated Chicken Eye test - ICE) or rabbit (Isolated Rabbit Eye test - IRE) are included. The BCOP test method is based on the topical exposure with test chemicals of the isolated corneas from freshly slaughtered cattle. The toxic effects of the chemicals are assessed by the induced opacity and the increased permeability of the corneal tissue (Gautheron et al. 1992). The ICE and IRE tests use whole eyes of the animals, but the attention during the test is focused on the cornea, which is exposed to a test chemical for 10 seconds. After exposure, the damage to the cornea is assessed by the permeability, opacity, swelling or other macroscopic changes of the cornea tissue (Prinsen & Koeter 1993; Eskes et al. 2005). A histological analysis on the exposed corneas is possible and could help in the determination of the depth of injury produced by the chemicals (Maurer et al. 2002; Jester 2006).

To date, only one cell-based test system (FL) and two ex vivo animal test systems (BCOP and ICE) have reached official regulatory acceptance (OECD 2012b; 2013b; 2013a).

None of these presented methods can clearly classify the chemicals in all three GHS categories; therefore, none of them is able to replace the Draize eye test as a stand-alone test system. Scott et al. (2010) described that, if more test systems are included in an integrated testing strategy, they

could possibly give a better classification of the chemicals according to their GHS class. Therefore, he introduced two possible test strategies, the top-down and the bottom-up approach. A top-down approach is used, when a test substance is assumed, according to his physico-chemical properties, to be a severe or moderate irritant and it begins with a test method that can accurately determine the severe irritants (GHS 1) and continues with a method that would identify the non- or slight irritants (GHS nc), if the first method gives a negative response. If both test methods give a negative response, the test substance is assumed to be a GHS 2 chemical. The bottom-up approach functions in the opposite way, by starting with a chemical which is assumed to be a non-irritant substance (Scott et al. 2010). Several combinations have been proposed for both of these test strategies, but none of them could correctly classify all the chemicals in the three GHS categories (Kolle et al. 2011; Hayashi et al. 2012).

1.1.3. Cornea models

The cornea is a clear, avascular barrier of the eye, which on one hand protects the intraocular tissues from the outer environment and the exogenous substances that may interact with the eye and on the other hand is part of the visual system due to its transparency and high refractive index. A human cornea contains five tissue layers: coneal epithelium, basement membrane, Bowman's layer, stroma, Descemet's membrane and endothelium (Hornof et al. 2005). In order to develop a test system which could completely replace the tests on the animal eyes *in vivo*, several layers of such a complex cornea must be included in an *in vitro* bioengineered 3D cornea model. Therefore, many scientists have focused on the development of a biotechnologically produced 3D cornea model, which comprises the three major cellular layers: a monolayered endothelium, a collagenous stromal compartment and a multilayered epithelium. The first *in vitro* reconstruction of such a cornea model was described by Minami et al. (1993) using isolated bovine corneal cells. They also introduced the usefulness of the air-liquid interface for the differentiation and proliferation of the epithelial cells in these constructs to a multilayered structure. Schneider et al. (1999) also developed an *in vitro* cornea model from isolated primary cornea cells of fetal pigs. This model contained a monolayered endothelium under a collagenous stromal part and on top two to three layered epithelium was obtained. Whether these tissues were suitable for exposure to different chemicals was not tested in the studies. Later, Griffith et al. (1999) succeeded to reconstruct a human 3D cornea model from immortalized human corneal

cell lines. They showed that these models have similarities to human corneas in their morphology, histology, transparency, biological marker expression and ion/fluid transport. Several types of surfactants were tested on these models and the tissue damage was comparable to that of human or rabbit corneas (Griffith et al. 1999). Reichl et al. (2004) has also introduced an organotypic cornea equivalent, by using immortalized epithelial and endothelial cell lines and a primary human stromal cell line. They reported that the constructs presented typical corneal structures and drug permeation studies showed that the constructs are 1.6 – 1.8 times more permeable than ex-vivo porcine corneas. At the same time, Engelke et al. (2004) and Zorn-Kruppa et al. (2005) described a new 3D hemi-cornea model based on SV-40 immortalized human corneal epithelial cells (HCE), human corneal keratocytes (HCK) and human corneal endothelial cells (HCEC). The epithelium presented a 5-7 multilayered tight tissue, grown on the stroma of homogenously distributed HCK cells embedded in a collagen matrix. The monolayered endothelium was grown underneath the stroma. Later, they have optimized the cell growth of both the HCE and the HCK cells to serum free condition (Seeber et al. 2008; Manzer et al. 2009). And finally, Engelke et al. (2013) have published an interlaboratory prevalidation study of a slightly modified cornea equivalent, consisting only a stromal and an epithelial layer. In their study they have shown that the models could predict a broad range of potential eye irritants from different GHS categories and of different physico-chemical properties. The results show a reliable predictivity of the GHS 1 category chemicals, but in some cases does not sufficiently discriminate the GHS nc and GHS 2 chemicals (Engelke et al. 2013). An improvement of this method, based on the separation of the epithelium and the stroma by the insertion of a collagen membrane between these compartments, and independent quantification of the damages in both compartments after chemical exposure, is one of the main subject of this present thesis. This new approach significantly improved the classification of the GHS 1 and GHS 2 chemicals; however, the test system has an over-predictivity for the GHS nc test substances (Appendix I).

1.1.4. Conjunctiva models

The conjunctiva is a mucous membrane having a thin epithelial layer with a vascularized tissue under it. Similar to the cornea, it plays an important role as protective barrier to the eye. It also contributes to the production of mucous glycoproteins for the tear film maintenance of the eye

(Hornof et al. 2005). The conjunctiva has a 15 to 25 times higher permeability than the cornea; hence, the conjunctiva plays an important role in the drug absorptions during ocular treatments (Hämäläinen et al. 1997). The Draize eye irritation test predicts not only the corneal damage, but also the damages induced in the conjunctiva and iris by the test chemicals. There are some reported chemicals which are more conjunctiva specific, such as anisole, isopropyl acetoacetate, isopropanol and allylalcohol (ECETOC 1998). Therefore, for the complete replacement of the Draize test one might need to take in consideration two test systems instead of one; one based on reconstructed 3D human hemi-cornea models and an additional one based on 3D human conjunctiva models, to obtain a precise classification of the chemicals. In the past, several conjunctival epithelium models were constructed, based on primary conjunctiva epithelial cells from either rabbit or bovine origin (Saha et al. 1996; Civiale et al. 2003). Both types of models expressed a multilayered conjuntival epithelium, however, only the rabbit conjunctiva epithelial models have shown transepithelial electrical resistence (TER) similar to that of *ex vivo* conjunctiva (Kompella et al. 1993). Yang et al. (2000) observed that if the tissue is transferred at air-liquid interface on the day 4 after seeding, the bioelectric parameters and the transport properties are in a closer correlation with that of the ex-vivo rabbit conjunctiva. More recently, two immortalized human conjunctival cell line became available. One is a spontaneously immortalized conjuntival epithelial cell line, named IOBA-NHC, from a human donor (Diebold et al. 2003). The cell line was mainly used as a monolayer culture to test the ophthalmological drugs for sensitivity of or damage to the conjunctiva (Huhtala et al. 2009). Another available human conjunctival cell line was obtained from a bulbar conjunctiva of a donor and was hTERT immortalized as described by Gipson et al. (2003). The cell line, named HCjE, was shown to express membrane-associated mucin production similar to their native conjunctival epithelium, when cultured in a multilayered model. The models reconstructed from this cell line were used mostly to study the regulation of the expression, glycosylation and function of the membrane mucins in the conjunctival epithelium, to understand how to overcome ocular surface diseases (Govindarajan & Gipson 2010). The idea to construct a full thickness conjunctiva model for the prediction of eye irritation potential of chemicals has not yet been described in the literature. Therefore we aimed at the successful reconstruction of a 3D human conjunctiva model with a thin stromal compartment and a multilayered epithelium on top of it.

1.1.5. The initial depth of injury after chemical exposure

The concept of the initial depth of injury (DoI) of chemicals on a cornea tissue, after topical exposure to different test chemicals, has been introduced by Jester et al. (1998). They showed that the surface area and the DoI in the epithelium and in stroma of a rabbit eye, after the exposure to different test substances, are directly correlated with the macroscopical severity of the test substance observed *in vivo*. Later, Jester et al. (2001) described the extent of the DoI after the treatment of the cornea of *ex vivo* rabbit eyes with chemicals from different GHS categories. They concluded that the slightly irritant substances damaged just the upper cell layer of the epithelium, while chemicals with mild or moderated irritation effect showed an impact on the whole epithelium and on the anterior stroma as well, and the severe irritant agents damaged the whole cornea down to the endothelium, and even the endothelium in some cases. Some substances were found to deviate from this concept, for example H_2O_2 and $NaBO_3$, which damage the stroma much more than the overlying epithelium (Maurer et al. 2001). Other chemicals, such as 8% NaOH were found more harmful for the conjunctiva than for the cornea (Maurer & Parker 2000). This observation suggests the need of an *in vitro* conjunctiva tissue, as an additional test system, to accurately assess the eye irritation potential of all test substances. More recently, Jester (2006) characterized the DoI of 22 chemicals, differing in type and severity of corneal injury, by using the low volume eye test, which is a refinement method of the Draize rabbit eye test. He observed that the extent of the corneal injury following exposure to ocular irritants significantly correlates with the initial injury previously measured in living animals. However, the presented methods used by Jester et al. to assess the DoI in the *in vivo* rabbit cornea were based on the live-dead fluorescent staining method and a microscopical analysis of the stained full corneal tissues. Recently, Jester et al. (2010) described a novel method to determine the depth of injury in corneal tissues of *ex vivo* rabbit eyes, after chemical exposure, by using cryosectioning procedures combined with fluorescent detection of biomarkers in the tissue section. They observed that the damaged cells, which entered in apoptosis, were easily marked by Tunel labeling, while living cells, which are apoptosis negative, showed an intact F-Actin-cytoskeleton with palloidin-rhodamin staining. The test substance dependent DoI of the epithelium and the stroma was separately assessed by calculating the Tunel positive tissue part and subtracting it from the palloidin stained negative control (water). A prediction model for the classification of the tested chemicals in three GHS categories was also described in this study;

however, the GHS classification was significantly different from the existing data obtained in the Draize eye irritation tests. Based on these findings from Jester et al. (2010), we established a method for the DoI quantification after topical treatment of the reconstructed human 3D hemi-cornea and conjunctiva models. The method combines the MTT viability assay of the reconstructed tissues, after chemical treatment, with cryosectioning procedures. The DoI is assessed by subtracting the formazan stained tissue length from the whole tissue length. Based on the prediction model developed on the basis of 25 test chemicals, all GHS 1 chemicals, 89 % of GHS 2 chemicals and 57 % of GHS nc substances were classified correctly with this method (Appendix II).

1.2. Results and Outcomes

1.2.1. Development of an in vitro ocular test system for the prediction of all three GHS categories (Appendix I)

Authors: **M. Bartok**, D. Gabel, M. Zorn-Kruppa, M. Engelke

Status of the publication: Available online in *Toxicology in Vitro* since 27th September 2014 **DOI:** 10.1016/j.tiv.2014.09.005; will be printed in: *Toxicology in Vitro* (2015), 29(1): 72-80.

Contribution of M. Bartok to the work: Developed the insertion method of the CCC membranes between the epithelium and the stroma of the hemi-cornea models. Co-developed the chemical test protocol of the new ocular test system. Contributed for the acquisition, analysis and interpretation of the experimental data, wrote the manuscript together with M. Engelke.

Contribution of the coauthors: M. Engelke co-developed the chemical test protocol for the new ocular test system, contributed for the acquisition, analysis and interpretation of the experimental data and helped with the coordination of the study. D. Gabel and M. Zorn-Kruppa helped with guiding the development of the insertion method for the CCC membranes and revised the manuscript.

1.2.2. Determining the depth of injury in bioengineered tissue models of cornea and conjunctiva for the prediction of all three ocular GHS categories (Appendix II)

Authors: M. Zorn-Kruppa, P. Houdek, E. Wladikowsky, M. Engelke, **M. Bartok**, K.R. Mewes, I. Moll, J. M. Brandner

Status of the publication: Published in *PLoS One* 9(12) on the 10th of December 2014.

DOI: 10.1371/journal.pone.0114181

Contribution of M. Bartok to the work: Transferred and modified the test protocol for the measurement of the depth of injury of chemicals for use at JUB. Tested a selected number of test chemicals to prove the interlaboratory transferability of the test system, contributed for the writing of the manuscript and in the review process.

Contribution of the coauthors: M. Zorn-Kruppa conducted the study, developed the test method for the measurement of the depth of injury and wrote the manuscript together with M.

Bartok and M. Engelke. P. Houdek and E. Wladikowsky helped with the data acquisition and analysis. M. Engelke, K.R. Mewes, I. Moll and J. M. Brandner reviewed the manuscript.

1.2.3. Predicting the eye irritation potential of chemicals: A comparison study between two test systems based on human 3D hemi-cornea models (Appendix III)

Authors: R. Tandon, **M. Bartok**, M. Zorn-Kruppa, J. M. Brandner, D. Gabel and M. Engelke

Status of the publication: Prepared for submission in *Toxicology in Vitro*.

Contribution of M. Bartok to the work: Described the plan of the work and supervised the first author (Rashmi Tandon) in the data acquisition and analysis, contributed for the writing of the manuscript and in the review process.

Contribution of the coauthors: R. Tandon did the data acquisition and analysis, and wrote the manuscript together with M. Bartok. M. Engelke helped in conducting the study, in data analysis and reviewed the manuscript. M. Zorn-Kruppa, J. M. Brandner and D. Gabel reviewed the manuscript.

1.3. Conclusions and Outlook

Several alternative methods have been proposed in the past, but none of these has given results on the chemical classification, which could meet the validation criteria of OECD (Organization for Economic Co-operation and Development) for the complete replacement of the in vivo Draize eye irritation test as a stand-alone test system. Therefore, we propose the two new test methods, developed in this study, to be suitable as a complete replacement for the Draize eye irritation test. These test methods are based on the human 3D hemi-cornea models previously introduced by Engelke et al. (2013) for the prediction of the eye irritation potential of chemicals. In the first test system, a collagen membrane was inserted between the epithelium and the stroma, to allow the separation and the individual quantification of the damages in both compartments. This slight modification of the previously reported test system (Engelke et al. 2013) helped in improving the ability of the system to correctly categorize the ocular irritant substances. The developed prediction model, based on the combinations of the cut-off values for both the epithelium and stroma, helped in the optimal classification of the test materials according to their GHS categories. In consequence, from 30 test chemicals with balanced GHS classes, all GHS 1 chemicals, 80 % of the GHS 2 chemicals and only 50 % of the GHS nc chemicals were predicted correctly. For the test substances which were not predicted correctly the test system showed an over-predictivity for a higher GHS class.

The second test method used both the previously described 3D hemi-cornea tissues (Engelke et al. 2013) as well as the newly developed 3D conjunctiva models for the topical exposure of the test chemicals. In both cases, the tissues, after exposure, were stained with the MTT reagent, to identify the viable cells, and frozen for cryosectioning. The formazan-free areas of the tissues were correlated to the DoI. The defined prediction model, based on 25 test chemicals from balanced GHS classes, helped to clearly discriminate the GHS 1 and GHS 2 chemicals. However, as with the previous method, an over-predictivity of 43 % was seen for the GHS nc substances. The 3D conjunctiva models, in comparison to the 3D hemi-cornea models, had no significant difference in their sensitivity towards the test chemicals; in conclusion, they showed a classification of the tested substances similar to that of the cornea models.

We also performed a comparison study between the predictivity of the two newly developed test methods based on the 3D hemi-cornea models, and the test method based on *ex vivo* rabbit corneas presented by Jester et al. (2010). In summary, the study demonstrates that both test

methods introduced by us can predict the GHS class of an eye irritant chemical more accurately, while the IRE-DoI method (Jester et al. 2010) resulted in under-prediction of numerous severe irritant substances (GHS 1) as GHS 2 or GHS nc category. We also observed a very good concordance between the prediction capacities of the GHS classes of the two new methods introduced by us.

For the first time, two cell-based in vitro test systems were introduced, which could clearly distinguish between GHS 1 and GHS 2 chemicals. Both test systems proved to be suitable to define the eye irritation potential of chemicals under standard conditions and independent from animal materials. We suggest that these *in vitro* test systems are suitable for the complete replacement of the Draize eye irritation test, despite the over-predictivity of the GHS nc chemicals in comparison to results obtained in the Draize eye irritation test.

As a future perspective, we must also take in consideration that the definition of the irritating effect is not the only characteristic which differentiates the substances in categories; rather, is also very important to include a study regarding the regeneration possibility with time of the in vitro cornea models after induction of damage. Usually the depth of injury influences the regeneration of the cornea significantly. In presence of the moderate and severe eye irritants, which damage the stroma significantly, the corneal tissues have less chance to recover either partially or completely.

References

Barile, F. A. (2010). Validating and troubleshooting ocular in vitro toxicology tests. *J Pharmacol Toxicol Methods,* 61, 136-145. doi: 10.1016/j.vascn.2010.01.001

Christian, M. S., Diener, R. M. (1996). Soaps and detergents: Alternatives to animal eye irritation tests. *Int J Toxicol,* 15, 1-44. doi: 10.3109/10915819609008705

Civiale, C., Paladino, G., Marino, C., Trombetta, F., Pulvirenti, T., Enea, V. (2003). Multilayer primary epithelial cell culture from bovine conjunctiva as a model for in vitro toxicity tests. *Ophthalmic Res,* 35, 126-136. doi: 10.1159/000070047

Clothier, R., Starzec, G., Stipho, S., Kwong, Y. C. (1999). Assessment of Initial Damage and Recovery Following Exposure of MDCK Cells to an Irritant. *Toxicol In Vitro,* 13, 713-717. doi: 10.1016/S0887-2333(99)00054-5

COUNCIL DIRECTIVE of 24 November 1986 on the approximation of laws, regulations and administrative provisions of the Member states regarding the protection of animals used for experimental and other scientific purposes (86/609/EEC)

COUNCIL REGULATION (EC) No 440/2008 of 30 May 2008 laying down test methods pursuant to Regulation (EC) No 1907/2006 of the European Parliament and of the Council on the Registration, Evaluation, Authorisation and Restriction of Chemicals (REACH)

Diebold, Y., Calonge, M., de Salamanca, A. E., Callejo, S., Corrales, R. M., Sáez, V., Siemasko, K. F., Stern, M. E. (2003). Characterization of a spontaneously immortalized cell line (IOBA-NHC) from normal human conjunctiva. *Invest Ophthalmol Vis Sci,* 44, 4263-4274. doi: 10.1167/iovs.03-0560

Draize, J., Woodward, G., Calvery, H. (1944). Methods for the study of irritation and toxicity of substances applied topically to the skin and mucous membranes. *J Pharmacol Exp Ther,* 82, 377-390.

ECETOC (1998). Eye Irritation: Reference Chemicals Data Bank. Technical Report No. 48 (2), European Center for Ecotoxicology and Toxicology of Chemicals, Brussels, Belgium.

Engelke, M., Patzke, J., Tykhonova, S., Zorn-Kruppa, M. (2004). Assessment of ocular irritation by image processed quantification of cell injury in human corneal cell cultures and in corneal constructs. *Altern Lab Anim,* 32, 345-353.

Engelke, M., Zorn-Kruppa, M., Gabel, D., Reisinger, K., Rusche, B., Mewes, K. R. (2013). A human hemi-cornea model for eye irritation testing: quality control of production, reliability and predictive capacity. *Toxicol In Vitro,* 27, 458-468. doi: 10.1016/j.tiv.2012.07.011

Eskes, C., Bessou, S., Bruner, L., Curren, R., Harbell, J., Jones, P., Kreiling, R., Liebsch, M., McNamee, P., Pape, W., Prinsen, M. K., Seidle, T., Vanparys, P., Worth, A., Zuang, V. (2005). Eye irritation. *Altern Lab Anim,* 33 Suppl 1, 47-81.

Gautheron, P., Dukic, M., Alix, D., Sina, J. F. (1992). Bovine corneal opacity and permeability test: an in vitro assay of ocular irritancy. *Fundam Appl Toxicol,* 18, 442-449.

Gipson, I. K., Spurr-Michaud, S., Argüeso, P., Tisdale, A., Ng, T. F., Russo, C. L. (2003). Mucin gene expression in immortalized human corneal–limbal and conjunctival epithelial cell lines. *Invest Ophthalmol Vis Sci,* 44, 2496-2506. doi: 10.1167/iovs.02-0851

Govindarajan, B., Gipson, I. K. (2010). Membrane-tethered mucins have multiple functions on the ocular surface. *Exp Eye Res,* 90, 655-663. doi: 10.1016/j.exer.2010.02.014

Griffith, M., Osborne, R., Munger, R., Xiong, X., Doillon, C. J., Laycock, N. L., Hakim, M., Song, Y., Watsky, M. A. (1999). Functional human corneal equivalents constructed from cell lines. *Science,* 286, 2169-2172. doi: 10.1126/science.286.5447.2169

Hämäläinen, K., Kananen, K., Auriola, S., Kontturi, K., Urtti, A. (1997). Characterization of paracellular and aqueous penetration routes in cornea, conjunctiva, and sclera. *Invest Ophthalmol Vis Sci,* 38, 627-634.

Harbell, J. W., Osborne, R., Carr, G. J., Peterson, A. (1999). Assessment of the Cytosensor Microphysiometer Assay in the COLIPA In Vitro Eye Irritation Validation Study. *Toxicol In Vitro,* 13, 313-323.

Hayashi, K., Mori, T., Abo, T., Ooshima, K., Hayashi, T., Komano, T., Takahashi, Y., Sakaguchi, H., Takatsu, A., Nishiyama, N. (2012). Two-stage bottom-up tiered approach combining several alternatives for identification of eye irritation potential of chemicals including insoluble or volatile substances. *Toxicol In Vitro,* 26, 1199-1208. doi: 10.1016/j.tiv.2012.06.008

Hornof, M., Toropainen, E., Urtti, A. (2005). Cell culture models of the ocular barriers. *Eur J Pharm Biopharm,* 60, 207-225. doi: 10.1016/j.ejpb.2005.01.009

Huhtala, A., Rönkkö, S., Teräsvirta, M., Puustjärvi, T., Sihvola, R., Vehanen, K., Laukkanen, A., Anttila, J., Urtti, A., Pohjonen, T. (2009). The effects of 5-fluorouracil on ocular tissues in vitro and in vivo after controlled release from a multifunctional implant. *Invest Ophthalmol Vis Sci,* 50, 2216-2223. doi: 10.1167/iovs.08-3016

Jester, J. V. (2006). Extent of corneal injury as a biomarker for hazard assessment and the development of alternative models to the Draize rabbit eye test. *Cutan Ocul Toxicol,* 25, 41-54. doi: 10.1080/15569520500536626

Jester, J. V., Li, H. F., Petroll, W. M., Parker, R. D., Cavanagh, H. D., Carr, G. J., Smith, B., Maurer, J. K. (1998). Area and depth of surfactant-induced corneal injury correlates with cell death. *Invest Ophthalmol Vis Sci,* 39, 922-936.

Jester, J. V., Li, L., Molai, A., Maurer, J. K. (2001). Extent of initial corneal injury as a basis for alternative eye irritation tests. *Toxicol In Vitro,* 15, 115-130.

Jester, J. V., Ling, J., Harbell, J. (2010). Measuring depth of injury (DOI) in an isolated rabbit eye irritation test (IRE) using biomarkers of cell death and viability. *Toxicol In Vitro,* 24, 597-604. doi: 10.1016/j.tiv.2009.10.010

Kolle, S. N., Kandarova, H., Wareing, B., van Ravenzwaay, B., Landsiedel, R. (2011). In-house validation of the EpiOcular(TM) eye irritation test and its combination with the bovine corneal opacity and permeability test for the assessment of ocular irritation. *Altern Lab Anim,* 39, 365-387.

Kompella, U. B., Kim, K.-J., Lee, V. H. (1993). Active chloride transport in the pigmented rabbit conjunctiva. *Curr Eye Res,* 12, 1041-1048.

Manzer, A. K., Lombardi-Borgia, S., Schafer-Korting, M., Seeber, J., Zorn-Kruppa, M., Engelke, M. (2009). SV40-transformed human corneal keratocytes: optimisation of serum-free culture conditions. *Altex,* 26, 33-39.

Maurer, J. K., Molai, A., Parker, R. D., Li, L., Carr, G. J., Petroll, W. M., Cavanagh, H. D., Jester, J. V. (2001). Pathology of ocular irritation with bleaching agents in the rabbit low-volume eye test. *Toxicol Pathol,* 29, 308-319. doi: 10.1080/019262301316905264

Maurer, J. K., Parker, R. D. (2000). Microscopic changes with acetic acid and sodium hydroxide in the rabbit low-volume eye test. *Toxicol Pathol,* 28, 679-687. doi: 10.1177/019262330002800507

Maurer, J. K., Parker, R. D., Jester, J. V. (2002). Extent of initial corneal injury as the mechanistic basis for ocular irritation: key findings and recommendations for the development of alternative assays. *Regul Toxicol Pharmacol,* 36, 106-117.

McNamee, P., Hibatallah, J., Costabel-Farkas, M., Goebel, C., Araki, D., Dufour, E., Hewitt, N. J., Jones, P., Kirst, A., Le Varlet, B., Macfarlane, M., Marrec-Fairley, M., Rowland, J., Schellauf, F., Scheel, J. (2009). A tiered approach to the use of alternatives to animal testing for the safety assessment of cosmetics: eye irritation. *Regul Toxicol Pharmacol,* 54, 197-209. doi: 10.1016/j.yrtph.2009.04.004

Minami, Y., Sugihara, H., Oono, S. (1993). Reconstruction of cornea in three-dimensional collagen gel matrix culture. *Invest Ophthalmol Vis Sci,* 34, 2316-2324.

OECD (2012a). Acute Eye Irritation/Corrosion. OECD Guidline for Testing of Chemicals No. 405, Organisation for Economic Cooperation and Development, Paris, France. Retrieved from http://www.oecd-ilibrary.org/environment/oecd-1039-guidelines-for-the-testing-of-chemicals-section-4-health-effects_20745788.

OECD (2012b). Fluorescein Leakage Test Method for Identifying Ocular Corrosives and Severe Irritants. OECD Guidline for the Testing of Chemicals No. 460, Organisation for Economic Cooperation and Development, Paris, France. Retrieved from http://www.oecd-ilibrary.org/environment/oecd-guidelines-for-the-testing-of-chemicals-section-4-health-effects_20745788.

OECD (2013a). Bovine Corneal Opacity and Permeability Test method for identifying i) chemicals inducing serious eye damage and ii) chemicals not requiring classification for eye irritation or serious eye damage. OECD Guidline for the Testing of Chemicals No. 437, Organisation for Economic Cooperation and Development. Retrieved from http://www.oecd-ilibrary.org/environment/oecd-guidelines-for-the-testing-of-chemicals-section-4-health-effects_20745788.

OECD (2013b). Test Guideline 438: Isolated Chicken Eye Test method for identifying i) chemicals inducing serious eye damage and ii) chemicals not requiring classifications for eye irritation or serious eye damage. OECD Guidline for the Testing of Chemicals No. 438, Organisation for Economic Cooperation and Development, Paris, France. Retrieved from http://www.oecd-ilibrary.org/environment/oecd-guidelines-for-the-testing-of-chemicals-section-4-health-effects_20745788.

Pape, W., Pfannenbecker, U., Argembeaux, H., Bracher, M., Esdaile, D., Hagino, S., Kasai, Y., Lewis, R. (1999). COLIPA validation project on in vitro eye irritation tests for cosmetic ingredients and finished products (phase I): the red blood cell test for the estimation of acute eye irritation potentials. Present status. *Toxicol In Vitro,* 13, 343-354.

Prinsen, M. K., Koeter, H. B. (1993). Justification of the enucleated eye test with eyes of slaughterhouse animals as an alternative to the Draize eye irritation test with rabbits. *Food Chem Toxicol,* 31, 69-76.

REGULATION (EC) No 1272/2008 OF THE EUROPEAN PARLIAMENT AND OF THE COUNCIL of 16 December 2008 on classification, labelling and packaging of substances and mixtures, amending and repealing Directives 67/548/EEC and 1999/45/EC, and amending Regulation (EC) No 1907/2006

REGULATION (EC) No 1907/2006 OF THE EUROPEAN PARLIAMENT AND OF THE COUNCIL of 18 December 2006 concerning the Registration, Evaluation, Authorisation and Restriction of Chemicals (REACH), establishing a European Chemicals Agency, amending Directive 1999/45/EC and repealing Council Regulation (EEC) No 793/93 and

Commission Regulation (EC) No 1488/94 as well as Council Directive 76/769/EEC and Commission Directives 91/155/EEC, 93/67/EEC, 93/105/EC and 2000/21/EC

REGULATION (EC) No 1223/2009 OF THE EUROPEAN PARLIAMENT AND OF THE COUNCIL of 30 November 2009 on cosmetic products

Reichl, S., Bednarz, J., Muller-Goymann, C. C. (2004). Human corneal equivalent as cell culture model for in vitro drug permeation studies. *Br J Ophthalmol,* 88, 560-565.

Saha, P., Kim, K.-J., Lee, V. H. (1996). A primary culture model of rabbit conjunctival epithelial cells exhibiting tight barrier properties. *Curr Eye Res,* 15, 1163-1169.

Schneider, A. I., Maier-Reif, K., Graeve, T. (1999). Constructing an in vitro cornea from cultures of the three specific corneal cell types. *In Vitro Cell Dev Biol Anim,* 35, 515-526. doi: 10.1007/s11626-999-0062-0

Scott, L., Eskes, C., Hoffmann, S., Adriaens, E., Alepee, N., Bufo, M., Clothier, R., Facchini, D., Faller, C., Guest, R., Harbell, J., Hartung, T., Kamp, H., Varlet, B. L., Meloni, M., McNamee, P., Osborne, R., Pape, W., Pfannenbecker, U., Prinsen, M., Seaman, C., Spielmann, H., Stokes, W., Trouba, K., Berghe, C. V., Goethem, F. V., Vassallo, M., Vinardell, P., Zuang, V. (2010). A proposed eye irritation testing strategy to reduce and replace in vivo studies using Bottom-Up and Top-Down approaches. *Toxicol In Vitro,* 24, 1-9. doi: 10.1016/j.tiv.2009.05.019

Seeber, J. W., Zorn-Kruppa, M., Lombardi-Borgia, S., Scholz, H., Manzer, A. K., Rusche, B., Schafer-Korting, M., Engelke, M. (2008). Characterisation of human corneal epithelial cell cultures maintained under serum-free conditions. *Altern Lab Anim,* 36, 569-583.

Shaw, A., Balls, M., Clothier, R., Bateman, N. (1991). Predicting ocular irritancy and recovery from injury using Madin-Darby canine kidney cells. *Toxicol In Vitro,* 5, 569-571. doi: 10.1016/0887-2333(91)90095-U

Steiling, W., Bracher, M., Courtellemont, P., de Silva, O. (1999). The HET-CAM, a Useful In Vitro Assay for Assessing the Eye Irritation Properties of Cosmetic Formulations and Ingredients. *Toxicol In Vitro,* 13, 375-384.

United Nations (UN) (2011). Globally Harmonized System of Classification and Labelling of Chemicals (GHS), Fourth revised edition, UN New York and Geneva, 2011. Retrieved from http://www.unece.org/trans/danger/publi/ghs/ghs_rev04/04files_e.html.

Yang, J. J., Ueda, H., Kim, K.-J., Lee, V. H. (2000). Meeting future challenges in topical ocular drug delivery:: Development of an air-interfaced primary culture of rabbit conjunctival epithelial cells on a permeable support for drug transport studies. *J Control Release,* 65, 1-11. doi: 10.1016/S0168-3659(99)00226-6

York, M., Steiling, W. (1998). A critical review of the assessment of eye irritation potential using the Draize rabbit eye test. *J Appl Toxicol,* 18, 233-240. doi: 10.1002/(SICI)1099-1263(199807/08)18:4<233::AID-JAT496>3.0.CO;2-Y

Zorn-Kruppa, M., Tykhonova, S., Belge, G., Bednarz, J., Diehl, H. A., Engelke, M. (2005). A human corneal equivalent constructed from SV40-immortalised corneal cell lines. *Altern Lab Anim,* 33, 37-45.

Zuang, V. (2000). The neutral red release assay: a review. *Altern Lab Anim,* 29, 575-599.

Part 2: The protective effect of brilliant blue G on human eye epithelial cells towards the cell toxicity of trypan blue, octenidine and benzalkonium chloride

2.1. Introduction

The irritation of vital dyes and preservatives found in ophthalmological solutions is a consistent problem for the patients. Hence, the reduction of the toxicity of these compounds with a non-toxic substance, is a desirable effect. Brilliant blue G (BBG) was shown to meet the expected effect on trypan blue (TB), octenidine (Oct) and benzalkonium chloride (BAK) toxicity when tested with ARPE (human retinal pigment epithelium) and HCE (human corneal epithelium) cells. The first manuscript (Appendix IV) describes the protective effect of BBG on TB toxicity and proposes several combinations of the two dyes for the future preparations of staining solutions for epiretinal membrane (ERM) and internal limiting membrane (ILM). The second manuscript (Appendix V) contains data of the remarkable protective effect of BBG on the cytotoxicity of Oct and BAK and proposes to include BBG in ready-to-use antiseptic preparations to reduce the possible irritations and inflammations caused by the antiseptics.

2.1.1. Staining of the internal limiting membrane

The internal limiting membrane (ILM) represents the innermost layer of the retina being the boundary between the retina and the vitreous humor. The ILM is described as a periodic acid Schiff positive basement membrane, which has a smooth inner surface and an irregular retinal surface (Abdelkader & Lois 2008). The astrocytes and the Müller glial cells are the two main type of macroglial cells in the mammalian retina, which contribute together to the formation of the ILM (Ramirez et al. 1996). The membrane itself consists of collagen fibrils, proteoglycans, plasma membrane of the Müller cells and basement membrane (Bron et al. 1997). Distortions of this membrane can lead to pathological effects, resulting in vitreomacular interface disorders, such as epiretinal membranes (ERM), macular holes and vitreomacular traction syndrome (Yuen et al. 2009). These disorders can considerably deteriorate the vision of the affected eye. The restoration of the vision can be achieved with the removal of the ERM. Since there is a possibility of ERM recurrence because of incomplete removal of the membrane during the surgery, the concomitant removal of the ILM is suggested (Kwok et al. 2005). Also, for the surgery of idiopathic macular holes, the removal of the ILM is necessary (Christensen et al.

2009). The ILM is a thin, transparent membrane and its removal is difficult even for an experienced eye surgeon because of poor visibility of the membrane. The inappropriate removal of the ILM poses a risk to damage the retina resulting retinal edema or retinal pigment epithelium alterations (Kadonosono et al. 2000). The staining of the membrane is necessary to avoid complications during and after surgery. There are several vital dyes already in clinical use for this purpose. A combination of some of these dyes, trypan blue (TB) and brilliant blue G (BBG), has been only recently proposed by us (Awad et al. 2013). These combinations would be advantageous for staining of both the ILM and ERM in one step and for safer and easier removal of the membranes during eye surgery.

2.1.2. Toxicity of vital dyes

The clinically widely used vital dyes for the staining of ILM or ERM during eye surgery are TB, BBG and indocyanine green (ICG). TB is an anionic hydrophilic azo dye advocated since many years as a vital stain in macular hole surgery in order to enhance visualization of optically clear tissues, like ILM. Although this chromophore is a useful surgical tool, clinical studies on retinal pigment epithelium (ARPE) cells reported functional visual loss after its use, and many investigators suggested more safety testing (Jackson et al. 2004). The clinically used concentrations for TB are between 0.15% and 0.25% (wt %) (Rodrigues et al. 2009).

ICG is a tricarbocyanine anionic dye, which has been used in ophthalmologic practice for many years as a successful ILM vital stain in macular hole surgery, to perform angiograms of the choroid and also for cataract surgery (Kadonosono et al. 2000). ICG was reported as a safe vital stain for the macular hole surgery, the clinical data showing that the macular closure rate may be achieved in 74-100% of the patients, but recently it was found that the dye may persist in the vitreous cavity after macular hole surgery for up to 36 months (Gale et al. 2004). Other clinical studies have attributed decreased visual acuity, visual field defects and ARPE atrophy and optic nerve atrophy after the use of ICG (Yuen et al. 2009). Being the most popular ILM stain, ICG continues to be the most widely used intraocular dye in membrane peeling surgery despite the recent reports that it may not be safe.

Studies that have compared ICG with TB directly have found that TB appears to be safer, but inferior in its ILM staining ability (Lee et al. 2005). Actually TB appears to have a higher affinity for the ERM because of the many dead glial cells within those membranes (Rodrigues et

al. 2009), and is defined by many investigators as the blue dye, which enables complete identification of the entire ERM surface (Feron et al. 2002). However, a controlled clinical study, which evaluated patients that underwent ERM surgery, showed that ICG does not stain the ERM (Hillenkamp et al. 2005; Hillenkamp et al. 2007). BBG produces appropriate ILM staining at a concentration of 0.025%, when used for idiopathic ERM and macular hole treatment, emerging as a good alternative for ICG, although the data on its toxicity are limited (Rodrigues et al. 2009).

In 2006, a dye known as BBG, which is a blue anionic aminotriarylmethane compound, was shown to stain the ILM with no significant in vivo toxicity in rats, primates and humans (Enaida et al. 2006). This dye is commonly used for protein determination and gel electrophoresis, because it has affinity to bind nonspecifically to virtually all proteins (Congdon et al, 1993; Westermeier, 2006). In 2009 Yuen et al. found that BBG has a dose- and time-dependent toxicity on ARPE cells and retinal ganglion/Müller glial primary cells in every cell viability assays they performed. The minimal concentration needed to produce high quality staining is 0.025% (Rodrigues et al. 2009). Brilliant blue R (BBR) is a dye very similar to BBG, which has two methyl groups less in its molecular formula. The slight difference in the name of the two compounds describes the colors of them. The suffix G was added by Max Weiler in 1913 to describe the slightly greenish color of the blue dye, and the suffix R is an abbreviation for red as the blue color of the dye has a reddish tint. The toxicity of BBR on ARPE or other eye cells had not been established and studied in the past, nor had this dye been used in any clinical staining procedures. This led us to characterize the effect of the dye on the eye cells and describe the difference between the individual toxicity of BBR and BBG, and their protective activity in presence of other compounds.

2.1.3. Toxicity of preservatives and antiseptics used in medical care

2.1.3.1. Benzalkonium chloride

Ophthalmic solutions as well as nasal sprays and nebulizer compounds contain preservatives to prevent the bacterial growth in the solutions in case of a regular use. Benzalkonium chloride (BAK), a cationic detergent with a broad range of antimicrobial activity, is the most commonly used preservative in ophthalmic solutions even though it is known to have prominent side effects at clinically used concentrations (Okahara et al. 2013), which are between 0.004% and 0.02%

(Liang et al. 2012). BAK is also known to interact with high affinity with membrane proteins, like guanine nucleotide triphosphate-binding proteins, affecting signal transduction and other processes in cells (Patarca & Fletcher 1995). Beside this, BAK was reported to exert its toxic effect by damaging the cytoplasmic membranes of the cells and as a consequence affecting the metabolic cellular function (Lapalus et al. 1990). However, the BAK induced cell death is dose dependent. At a concentration of 0.01%, which is used in most of the ophthalmic preparations, BAK causes immediate cell retractions and degeneration of human corneal epithelial (HCE) cells within only two hours (Tripathi et al. 1992). The frequent adverse effects attributed to ophthalmic solutions containing BAK, in a long term treatment, are corneal cytotoxicity, tear film instability, conjunctival inflammation, trabecular meshwork cell apoptosis, cataract development and macular edema (Rosin & Bell 2013). Ways to reduce the toxic effects of the preservative on the eyes, for example by the presence of another compound, either as a pretreatment prior to BAK application or in combination with BAK, has only been introduced very recently by Feng et al. (2014) and by us. Feng et al. (2014) described that lacritin, a human tear glycoprotein, secreted from the lacrimal glands can hinder the toxic stress of BAK at a concentration of 1 nM on HCE cells if is pretreated 24 hour prior to the application of BAK containing compounds. We have reported that BBG, a vital dye used for the staining of the ILM shows significant protective effect for BAK toxicity on the HCE cells, increasing the cell survival up to 51% in presence of 0.01% BAK at 30 minutes incubation. Without BBG, after 5 minutes incubation, only 10% of the HCE cells were found metabolically active at the same BAK concentration (Appendix V).

2.1.3.2. Octenidine dihydrochloride

Another important group of medical products, which often causes irritation when used at a daily basis, are the skin and wound disinfectants. One of them is octenidine dihydrochloride (Oct), an antiseptic compound, introduced about 30 years ago for the treatment of skin, mucous membranes and wounds (Sedlock & Bailey 1985; Heeg 1990). Usually, it is found in the final product at concentrations between 0.05% - 0.2% in mixture with alcohols (disinfectant solutions) or glycerol and detergents (antiseptic soap) (Dabek et al. 2007). In some cases is also recommended to use as a single substance, i.e. neonatal skin antisepsis, because some alcohols, like 2-phenoxyethanol, which is the mostly used alcohol in combination with Oct, absorbs

through the skin and may cause central nervous system toxicity (Bührer et al. 2002). In comparison to other antiseptic compounds, like Chlorhexidine, Cetylpyridinium chloride, BAK, Polyhexanide or Triclosan, Oct showed better antibacterial and antifungal efficiency, even for the most resistant test organisms, like *Pseudomonas aeruginosa*, *Staphylococcus aureus* and *Candida albicans* (Koburger et al. 2010). In *C. albicans*, Oct at a concentration of 1.5 mg/l is reported to induce extensive cell damage, lysis and collapse of the cell structure with leakage of the cellular content, when incubated together for 24 hours (Ghannoum et al. 1990). Oct is a cationic surface-active agent with two cationic centers in its molecule, separated by a long aliphatic hydrocarbon chain, which gives special features to the compound, resulting in unspecific modes of action (Hübner et al. 2010). It has four tertiary amino groups in his structure, two of which are protonated, and is known to be stable under exposition to light, temperature and in the pH range of 1.6 to 12.2 (Stahl et al. 2011). Oct binds strongly to negatively charged surfaces, like lipid bacterial cell membrane components and epithelial cell membranes and it cannot be removed easily. Both of these effects are described as beneficial (Hübner et al. 2010). It was not found to be absorbed in the intact skin of humans and animals and only a low amount was found to be absorbed in case of a compromised bovine skin, 2.64% of the total Oct applied. The reason was thought to be the high molecular weight of the compound, 550.9 g/mol (Stahl et al. 2011). Due to these finding, no further pharmacokinetic or drug metabolic studies have been conducted. Oct was found to build stable complexes with the *stratum corneum* of the skin, thereby exerting a sustained antimicrobial effect, acting as an antimicrobial shield on the disinfected surface for a longer time interval after the topical application (Hübner et al. 2010). However, although in clinical trials Oct has been described as a very successful antiseptic agent in skin, mucous membranes and wounds disinfection, in vitro studies shows that Oct has high toxicity towards mammalian cells (Kramer et al. 2004; Hirsch et al. 2009). In our studies Oct led to considerable decrease in cell survival. After only 5 minutes incubation, at 0.003% Oct, there were only a few percent of HCE cells alive. In order to hinder the pronounced toxic effect of the substance we have combined Oct with BBG and observed that BBG increased the cell survival in presence of Oct even more than in combination with BAK. For all concentrations between 0.002% and 0.009% Oct, together with 0.025% BBG, a cell survival of over 80% was seen for either 5 or 30 minutes incubations (Appendix V).

2.1.4. The $P2X_7$ receptor and its antagonists

P2X receptors are a family of non-selective membrane cation channels, gated in the presence of extracellular ATP (adenosine triphosphate) (McLarnon et al. 2006). The activation of the receptors by extracellular ATP leads to transmembrane pore opening and the influx of ions such as sodium, potassium, magnesium, calcium and some organic ions (Xin et al. 2011). These receptors mediate many physiological processes throughout the whole body, including synaptic transmission, thrombocyte aggregation, regulation of renal blood flow, and immunological responses (Surprenant & North 2009). They are also involved in pathological states by signaling neuropathic pain, chronic inflammation and are related to epilepsy, Parkinson's and Alzheimer's disease (McLarnon et al. 2006; Hracskó et al. 2011; Engel et al. 2012). Among the seven different P2X receptor isoforms, the $P2X_7$ receptor has a unique role in the body. The $P2X_7$ receptor was found to be mostly responsible in immunoreactivity and in controlling microglia proliferation and cell death (Bianco et al. 2006; Surprenant & North 2009). In the immune system it is expressed in mast cells, monocytes, macrophages, dendritic cells, erythrocytes and T and B lymphocytes (Skaper et al. 2010). In the nervous system it was found to be expressed in astrocytes, microglia, neurons and Schwann cells (Pannicke et al. 2000). In the literature this receptor is also called the cell death receptor, because it mainly acts as a pro-apoptotic receptor, inducing cell death in response to pathological insults. The $P2X_7$ receptor was also found to be part of many epithelial cells in the rat, such as cornea, esophagus, soft palate, tongue, vagina and foot pad, playing a role in the physiologic turnover of continuously regenerating epithelial tissues (Gröschel-Stewart et al. 1999). Recently, Dutot et al. (2008) reported the expression of the $P2X_7$ receptor in four different human eye epithelial cell lines as well, such as human conjunctival epithelial, corneal epithelial, retinal pigment epithelial and lens epithelial cells. The $P2X_7$ receptor is known to possess unusual properties, changing its selectivity for molecules during prolonged activation in presence of ATP. At short exposure to ATP it is permeable to sodium and calcium ions, but a prolonged exposure leads to the opening of a large pore and an accumulation of molecules such as ethidium bromide, propidium iodide, YO-PRO-1 (quinolinium, 4-[(3-methyl-2(3H)-benzoxazolylidene)methyl]-1-[3-(trimethylammonio) propyl]di-iodide) and other compounds up to 900 Da (Dutot et al. 2008). The opening of a large pore leads not only to large ion influxes, but also to the leakage of small metabolites (Chung et al. 2000). At long exposure to high amounts of ATP, as it would be in case of a trauma related to

an injury or an infection, the activated receptor leads to cell death. The reason for inducing cell death can be also beneficial; for example in the immune response of the body, this receptor induces the death of the macrophages by simultaneously killing the intracellular bacterial organism (Placido et al. 2006). However, there are several pathological responses of the body to traumatic injuries. These injuries are associated with decrease in extracellular calcium, enhancing the ATP release from the mechanically traumatized cells and by this activating the $P2X_7$ receptors, which then mediates the cell death in the surrounding tissue (Wang et al. 2004). Based on these findings, the $P2X_7$ receptor was proposed to be a potential target for drug development, to synthesize potent antagonists of the receptor in order to hinder the activation of it in pathological states and induce a faster healing after injury. As the interest of the researchers towards these receptors raised in the past few years, several antagonists have been developed to hinder the activation of the $P2X_7$ receptors. Among these antagonists, special emphasis was put on BBG, OxATP (adenosine 5'-triphosphate-2',3'-dialdehyde) and DPPH (N'-(3,5-dichloropyridin-4-yl)-3-phenylpropane- hydrazide).

BBG is known to be a noncompetitive, highly selective $P2X_7$ receptor antagonist, inhibiting the receptor with nanomolar affinity. Since BBG is a polysulfonated molecule, it is thought to bind to the positively charged amino acids on the ectodomain of the $P2X_7$ receptor (Jiang et al. 2000). In the literature it was reported to block the activation of $P2X_7$ receptor at 10 μM concentration, when incubated 30 minutes prior to the addition of BAK (Dutot et al. 2008). Peng et al. (2009) described that BBG has a unique therapeutic profile, due to multiple cellular targets in the body, including neurons, astrocytes and microglia. He also reported that an intravenous administration of BBG 15 minutes after an induced spinal cord injury in rats significantly improved functional recovery and reduced posttraumatic inflammatory responses and tissue damage, by hindering the activation of $P2X_7$ receptors in the traumatized tissue (Peng et al. 2009). Jiang et al. (2000) mentioned that the inhibition of the $P2X_7$ receptors by BBG is only slowly reversible.

OxATP, in contrast to BBG, is an irreversible, noncompetitive $P2X_7$ receptor antagonist, known to block the human $P2X_7$ receptor at 10 μM concentration in vitro (Hibell et al. 2001). Murgia et al. (1993) described that OxATP covalently binds to the unprotonated lysine residues at the nucleotide binding site of the receptor molecule, and as a result the maximal inhibitory effect of the compound is obtained after a preincubation with the cultured cells for 30 – 120 minutes, prior to exposure to high amounts of ATP. According to Chung et al. (2000) 300 μM of OxATP,

incubated 2 hours with GH3 cells (rat pituitary epithelial-like tumor cells) prior to addition of ATP, completely inhibited the ATP-induced $P2X_7$ receptor activation and as an outcome inhibited the increase of intracellular Ca^{2+}. The differences between the maximal inhibitory concentrations of OxATP in human versus rat $P2X_7$ receptors (10 μM and 300 μM, respectively) is related to the high selectivity of the antagonist for human $P2X_7$ receptors (Hibell et al. 2001).Wang et al. (2004) showed that OxATP, when injected directly in the spinal cord, 1 hour after the spinal cord injury in rat, reduced neuronal death and improved motor recovery. However, Peng et al. (2009) mentioned that the injection in an already injured spinal cord is rarely feasible clinically and that this application will have no immediate clinical use in the future.

DPPH is a newly synthesized, selective $P2X_7$ receptor antagonist, introduced recently by Lee et al. (2012). He reported that in $hP2X_7$ expressing HEK 293 cells (human embryonic kidney cells), DPPH showed an inhibitory constant of 650 nM (IC_{50}) for the $P2X_7$ receptor, in presence of BzATP (benzoylbenzoyl ATP), with the ethidium bromide assay (Lee et al. 2012). To date, no *in vivo* applications appear to be published related to this substance.

2.2. Results and Outcomes

2.2.1. Brilliant Blue G as protective agent against trypan blue toxicity in human retinal pigment epithelial cells in vitro (Appendix IV)

Authors: D. Awad, I. Schrader, **M. Bartok**, N. Sudumbrekar, A. Mohr, D. Gabel

Status of the publication: Published in *Graefes Arch Clin Exp Ophthalmol*. 2013, 251:1735-40

DOI: 10.1007/s00417-013-2342-3

Contribution of M. Bartok to the work: Contributed for the acquisition, analysis and interpretation of the experimental data, partially wrote the Material and Methods section and reviewed the manuscript.

Contribution of the coauthors: D. Awad conducted the study, helped in the acquisition, analysis and interpretation of the experimental data, wrote the manuscript. I. Schrader and N. Sudumbrekar helped in the acquisition, analysis and interpretation of the experimental data. A. Mohr and D. Gabel helped in the preparation, review and approval of the manuscript.

2.2.2. Reduction of cytotoxicity of benzalkonium chloride and octenidine by Brilliant Blue G (Appendix V)

Authors: M. Bartok, R. Tandon, G. Alfaro-Espinoza, M. S. Ullrich and D. Gabel

Status of the publication: Accepted for publication in *EXCLI* journal (in press).

Contribution of M. Bartok to the work: Conducted the study, contributed for the acquisition, analysis and interpretation of the experimental data, wrote the manuscript.

Contribution of the coauthors: R. Tandon helped in the acquisition of the cell toxicity data. G. Alfaro-Espinoza performed and analysed the bacterial toxicity experiments. M. S. Ullrich and D. Gabel helped with the coordination of the study and reviewed the manuscript.

2.3. Conclusions and Outlook

These studies describe a remarkable protective effect of BBG on antiseptics and vital dyes. In the first publication (Appendix IV), we reported that BBG in combination with TB, even above 0.075% concentration of TB, significantly increased the cell survival of ARPE cells after 5 or 30 minutes incubation, whereas TB alone at the mentioned concentrations and incubation times showed considerable cell damage. During the study, efforts have been made to conclude whether the protective effect of the BBG is related to its ability to act as a $P2X_7$ receptor antagonist on ARPE cells. The propidium iodide (PI) uptake showed staining of the entire cell body, and not only the nucleus, which we concluded as a secondary effect of the TB staining, as the vital dye was present on the cell surface even after a tedious washing procedure. Therefore, we could not conclude that the protective effect of BBG is due to its activity as a $P2X_7$ receptor antagonist. The tested combinations of TB and BBG in this study may help to find an appropriate combination of these two vital dyes, in order to increase the dye effectiveness in staining of both ERM and ILM in one step, as well as to choose a combination which will be safer to the eye.

In the second manuscript (Appendix V), we described that the cytotoxicity of BAK and Oct on HCE cells is significantly reduced in the presence of BBG. BBR, a dye similar to BBG, showed protective effect only in the presence of Oct; however, this effect was lower than the one obtained in presence of BBG. Although BBG is a well known $P2X_7$ receptor antagonist, other selective $P2X_7$ antagonists, OxATP and DPPH did not show any protective effect on the cells in the presence of BAK nor of Oct. Therefore we concluded that the protective effect of BBG is not due to its action on the $P2x_7$ receptor. However, we do not know if the protective effect of BBG is due to its action on another cell receptor or if this effect is only due to its chemical interaction with the positively charged antiseptics, resulting in a complex, which is no longer toxic to the cells. BBR, in contrast to BBG, has been used in the past only as a sensitive protein stain in polyacrylamide gel electrophoresis. Whether it has any activity on the $P2X_7$ receptor is not yet known. According to our bacterial inhibitory tests on several Gram-negative and Gram-positive bacteria, there are only limited numbers of combinations between BBG and BAK or Oct, or BBR and Oct, at which the bacterial growth is inhibited. High concentrations of BBG or BBR (0.03% or higher) in presence of either BAK or Oct, at the tested concentrations (between 0.001% and 0.01%) does not inhibit the growth of Gram-negative bacteria. However, the growth of Gram-positive bacteria was hindered at all tested combinations. Based on these findings, we proposed

several combinations of BBG with Oct or BAK, which could be useful in antiseptic preparations, because it might reduce possible irritations and inflammations, caused by the antiseptics, as well as helps in marking the disinfected area prior to surgery.

References

Abdelkader, E., Lois, N. (2008). Internal limiting membrane peeling in vitreo-retinal surgery. *Surv Ophthalmol,* 53, 368-396. doi: 10.1016/j.survophthal.2008.04.006

Awad, D., Schrader, I., Bartok, M., Sudumbrekar, N., Mohr, A., Gabel, D. (2013). Brilliant Blue G as protective agent against trypan blue toxicity in human retinal pigment epithelial cells in vitro. *Graefes Arch Clin Exp Ophthalmol,* 251, 1735-1740. doi: 10.1007/s00417-013-2342-3

Bianco, F., Ceruti, S., Colombo, A., Fumagalli, M., Ferrari, D., Pizzirani, C., Matteoli, M., Di Virgilio, F., Abbracchio, M. P., Verderio, C. (2006). A role for P2X7 in microglial proliferation. *J Neurochem,* 99, 745-758. doi: 10.1111/j.1471-4159.2006.04101.x

Bron, A., Tripathi, R., Tripathi, B. (1997). *Wolff's anatomy of the eye.(The inner limiting membrane).* England: Chapman & Hall, London.

Bührer, C., Bahr, S., Siebert, J., Wettstein, R., Geffers, C., Obladen, M. (2002). Use of 2% 2-phenoxyethanol and 0.1% octenidine as antiseptic in premature newborn infants of 23–26 weeks gestation. *J Hosp Infect,* 51, 305-307. doi: 10.1053/jhin.2002.1249

Christensen, U. C., Kroyer, K., Sander, B., Larsen, M., Henning, V., Villumsen, J., la Cour, M. (2009). Value of internal limiting membrane peeling in surgery for idiopathic macular hole stage 2 and 3: a randomised clinical trial. *Br J Ophthalmol,* 93, 1005-1015. doi: 10.1136/bjo.2008.151266

Chung, H. S., Park, K. S., Cha, S. K., Kong, I. D., Lee, J. W. (2000). ATP-induced [Ca(2+)](i) changes and depolarization in GH3 cells. *Br J Pharmacol,* 130, 1843-1852. doi: 10.1038/sj.bjp.0703253

Dabek, S. D., Krug, B. D., Müller, K. M., Ostermeyer, C., Pietsch, H. D., Rudolf, M. D. (2007). Germany Patent No. DE 102005058978 A1.

Dutot, M., Liang, H., Pauloin, T., Brignole-Baudouin, F., Baudouin, C., Warnet, J. M., Rat, P. (2008). Effects of toxic cellular stresses and divalent cations on the human P2X7 cell death receptor. *Mol Vis,* 14, 889-897.

Enaida, H., Hisatomi, T., Hata, Y., Ueno, A., Goto, Y., Yamada, T., Kubota, T., Ishibashi, T. (2006). Brilliant blue G selectively stains the internal limiting membrane/brilliant blue G-assisted membrane peeling. *Retina,* 26, 631-636. doi: 10.1097/01.iae.0000236469.71443.aa

Engel, T., Jimenez-Pacheco, A., Miras-Portugal, M. T., Diaz-Hernandez, M., Henshall, D. C. (2012). P2X7 receptor in epilepsy; role in pathophysiology and potential targeting for seizure control. *Int J Physiol Pathophysiol Pharmacol,* 4, 174.

Feng, M. M., Baryla, J., Liu, H., Laurie, G. W., McKown, R. L., Ashki, N., Bhayana, D., Hutnik, C. M. (2014). Cytoprotective effect of lacritin on human corneal epithelial cells exposed to benzalkonium chloride in vitro. *Curr Eye Res,* 39, 604-610. doi: 10.3109/02713683.2013.859275

Feron, E. J., Veckeneer, M., Parys-Van Ginderdeuren, R., Van Lommel, A., Melles, G. R., Stalmans, P. (2002). Trypan blue staining of epiretinal membranes in proliferative vitreoretinopathy. *Arch Ophthalmol,* 120, 141-144.

Gale, J. S., Proulx, A. A., Gonder, J. R., Mao, A. J., Hutnik, C. M. (2004). Comparison of the in vitro toxicity of indocyanine green to that of trypan blue in human retinal pigment epithelium cell cultures. *Am J Ophthalmol,* 138, 64-69. doi: 10.1016/j.ajo.2004.02.061

Ghannoum, M. A., Elteen, K. A., Ellabib, M., Whittaker, P. A. (1990). Antimycotic effects of octenidine and pirtenidine. *J Antimicrob Chemother,* 25, 237-245.

Gröschel-Stewart, U., Bardini, M., Robson, T., Burnstock, G. (1999). Localisation of P2X5 and P2X7 receptors by immunohistochemistry in rat stratified squamous epithelia. *Cell Tissue Res,* 296, 599-605. doi: 10.1007/s004410051321

Heeg, P. (1990). [Antisepsis of mucous membranes--current status and aspects of future development]. *Z Gesamte Hyg,* 36, 83-86.

Hibell, A., Thompson, K., Xing, M., Humphrey, P., Michel, A. (2001). Complexities of Measuring Antagonist Potency at P2X7Receptor Orthologs. *Journal of Pharmacology and Experimental Therapeutics,* 296, 947-957.

Hillenkamp, J., Saikia, P., Gora, F., Sachs, H. G., Lohmann, C. P., Roider, J., Baumler, W., Gabel, V. P. (2005). Macular function and morphology after peeling of idiopathic epiretinal membrane with and without the assistance of indocyanine green. *Br J Ophthalmol,* 89, 437-443. doi: 10.1136/bjo.2004.051250

Hillenkamp, J., Saikia, P., Herrmann, W. A., Framme, C., Gabel, V. P., Sachs, H. G. (2007). Surgical removal of idiopathic epiretinal membrane with or without the assistance of indocyanine green: a randomised controlled clinical trial. *Graefes Arch Clin Exp Ophthalmol,* 245, 973-979. doi: 10.1007/s00417-006-0485-1

Hirsch, T., Jacobsen, F., Rittig, A., Goertz, O., Niederbichler, A., Steinau, H., Seipp, H., Steinstraesser, L. (2009). Vergleichende in-vitro-Studie zur Zytotoxizität klinisch eingesetzter Antiseptika. *Der Hautarzt,* 60, 984-991. doi: 10.1007/s00105-009-1842-x

Hracskó, Z., Baranyi, M., Csölle, C., Gölöncsér, F., Madarász, E., Kittel, Á., Sperlágh, B. (2011). Lack of neuroprotection in the absence of P 2 X 7 receptors in toxin-induced animal models of Parkinson's disease. *Mol Neurodeg,* 6. doi: 10.1186/1750-1326-6-28

Hübner, N.-O., Siebert, J., Kramer, A. (2010). Octenidine dihydrochloride, a modern antiseptic for skin, mucous membranes and wounds. *Skin Pharmacol Phys,* 23, 244-258. doi: 10.1159/000314699

Jackson, T. L., Hillenkamp, J., Knight, B. C., Zhang, J. J., Thomas, D., Stanford, M. R., Marshall, J. (2004). Safety testing of indocyanine green and trypan blue using retinal pigment epithelium and glial cell cultures. *Invest Ophthalmol Vis Sci,* 45, 2778-2785. doi: 10.1167/iovs.04-0320

Jiang, L.-H., Mackenzie, A. B., North, R. A., Surprenant, A. (2000). Brilliant blue G selectively blocks ATP-gated rat P2X7 receptors. *Mol Pharmacol,* 58, 82-88. doi: 10.1124/mol.58.1.82

Kadonosono, K., Itoh, N., Uchio, E., Nakamura, S., Ohno, S. (2000). Staining of internal limiting membrane in macular hole surgery. *Arch Ophthalmol,* 118, 1116-1118.

Koburger, T., Hübner, N.-O., Braun, M., Siebert, J., Kramer, A. (2010). Standardized comparison of antiseptic efficacy of triclosan, PVP–iodine, octenidine dihydrochloride, polyhexanide and chlorhexidine digluconate. *J Antimicrob Chemother,* 65, 1712-1719. doi: 10.1093/jac/dkq212

Kramer, A., Roth, B., Müller, G., Rudolph, P., Klöcker, N. (2004). Influence of the antiseptic agents polyhexanide and octenidine on FL cells and on healing of experimental superficial aseptic wounds in piglets. A double-blind, randomised, stratified, controlled, parallel-group study. *Skin Pharmacol Physiol,* 17, 141-146. doi: 10.1159/000077241

Kwok, A., Lai, T. Y., Yuen, K. S. (2005). Epiretinal membrane surgery with or without internal limiting membrane peeling. *Clin Experiment Ophthalmol,* 33, 379-385. doi: 10.1111/j.1442-9071.2005.01015.x

Lapalus, P., Ettaiche, M., Fredj-Reygrobellet, D., Jambou, D., Elena, P. P. (1990). Cytotoxicity studies in ophthalmology. *Lens Eye Toxic Res,* 7, 231-242.

Lee, K. L., Dean, S., Guest, S. (2005). A comparison of outcomes after indocyanine green and trypan blue assisted internal limiting membrane peeling during macular hole surgery. *Br J Ophthalmol,* 89, 420-424. doi: 10.1136/bjo.2004.049684

Lee, W. G., Lee, S. D., Cho, J. H., Jung, Y., Kim, J. H., Hien, T. T., Kang, K. W., Ko, H., Kim, Y. C. (2012). Structure-activity relationships and optimization of 3,5-dichloropyridine derivatives as novel P2X(7) receptor antagonists. *J Med Chem,* 55, 3687-3698. doi: 10.1021/jm2012326

Liang, H., Brignole-Baudouin, F., Riancho, L., Baudouin, C. (2012). Reduced in vivo ocular surface toxicity with polyquad-preserved travoprost versus benzalkonium-preserved travoprost or latanoprost ophthalmic solutions. *Ophthalmic Res,* 48, 89-101. doi: 10.1159/000335984

McLarnon, J. G., Ryu, J. K., Walker, D. G., Choi, H. B. (2006). Upregulated expression of purinergic P2X(7) receptor in Alzheimer disease and amyloid-beta peptide-treated microglia and in peptide-injected rat hippocampus. *J Neuropathol Exp Neurol,* 65, 1090-1097. doi: 10.1097/01.jnen.0000240470.97295.d3

Murgia, M., Hanau, S., Pizzo, P., Rippa, M., Di Virgilio, F. (1993). Oxidized ATP. An irreversible inhibitor of the macrophage purinergic P2Z receptor. *J Biol Chem,* 268, 8199-8203.

Okahara, A., Tanioka, H., Takada, K., Kawazu, K. (2013). Ocular toxicity of benzalkonium chloride homologs compared with their mixtures. *J Toxicol Pathol,* 26, 343-349. doi: 10.1293/tox.2013-0022

Pannicke, T., Fischer, W., Biedermann, B., Schädlich, H., Grosche, J., Faude, F., Wiedemann, P., Allgaier, C., Illes, P., Burnstock, G. (2000). P2X7 receptors in Müller glial cells from the human retina. *J Neurosci,* 20, 5965-5972.

Patarca, R., Fletcher, M. A. (1995). Effects of benzalkonium salts on eukaryotic and microbial G-protein-mediated processes and surface membranes. *Crit Rev Oncog,* 6, 327-356.

Peng, W., Cotrina, M. L., Han, X., Yu, H., Bekar, L., Blum, L., Takano, T., Tian, G.-F., Goldman, S. A., Nedergaard, M. (2009). Systemic administration of an antagonist of the ATP-sensitive receptor P2X7 improves recovery after spinal cord injury. *Proc Natl Acad Sci,* 106, 12489-12493. doi: 10.1073/pnas.0902531106

Placido, R., Auricchio, G., Falzoni, S., Battistini, L., Colizzi, V., Brunetti, E., Di Virgilio, F., Mancino, G. (2006). P2X7 purinergic receptors and extracellular ATP mediate apoptosis of human monocytes/macrophages infected with Mycobacterium tuberculosis reducing the intracellular bacterial viability. *Cell Immunol,* 244, 10-18. doi: 10.1016/j.cellimm.2007.02.001

Ramirez, J. M., Trivino, A., Ramirez, A. I., Salazar, J. J., Garcia-Sanchez, J. (1996). Structural specializations of human retinal glial cells. *Vision Res,* 36, 2029-2036. doi: 10.1016/0042-6989(95)00322-3

Rodrigues, E. B., Costa, E. F., Penha, F. M., Melo, G. B., Bottós, J., Dib, E., Furlani, B., Lima, V. C., Maia, M., Meyer, C. H. (2009). The use of vital dyes in ocular surgery. *Surv Ophthalmol,* 54, 576-617. doi: 10.1016/j.survophthal.2009.04.011

Rosin, L. M., Bell, N. P. (2013). Preservative toxicity in glaucoma medication: clinical evaluation of benzalkonium chloride-free 0.5% timolol eye drops. *Clinical ophthalmology,* 7, 2131-2135. doi: 10.2147/OPTH.S41358

Sedlock, D. M., Bailey, D. M. (1985). Microbicidal activity of octenidine hydrochloride, a new alkanediylbis [pyridine] germicidal agent. *Antimicrob Agents and Chemother,* 28, 786-790. doi: 10.1128/AAC.28.6.786

Skaper, S. D., Debetto, P., Giusti, P. (2010). The P2X7 purinergic receptor: from physiology to neurological disorders. *The FASEB Journal,* 24, 337-345. doi: 10.1096/fj.09-138883

Stahl, J., Braun, M., Siebert, J., Kietzmann, M. (2011). The percutaneous permeation of a combination of 0.1% octenidine dihydrochloride and 2% 2-phenoxyethanol (octenisept(R)) through skin of different species in vitro. *BMC veterinary research,* 7, 44. doi: 10.1186/1746-6148-7-44

Surprenant, A., North, R. A. (2009). Signaling at purinergic P2X receptors. *Annu Rev Physiol,* 71, 333-359. doi: 10.1146/annurev.physiol.70.113006.100630

Tripathi, B. J., Tripathi, R. C., Kolli, S. P. (1992). Cytotoxicity of ophthalmic preservatives on human corneal epithelium. *Lens Eye Toxic Res,* 9, 361-375.

Wang, X., Arcuino, G., Takano, T., Lin, J., Peng, W. G., Wan, P., Li, P., Xu, Q., Liu, Q. S., Goldman, S. A., Nedergaard, M. (2004). P2X7 receptor inhibition improves recovery after spinal cord injury. *Nat Med,* 10, 821-827. doi: 10.1038/nm1082

Xin, L., Yanjuan, X., Zhiyuan, L. (2011). P2X Receptors as New Therapeutic Targets. In C. Rundfeldt (Ed.), Drug Development - A Case Study Based Insight into Modern Strategies (pp. 313-336): InTech. Retrieved from http://www.intechopen.com/books/drug-development-a-case-study-based-insight-into-modern-strategies/p2x-receptors-as-new-therapeutic-targets. doi: 10.5772/27012

Yuen, D., Gonder, J., Proulx, A., Liu, H., Hutnik, C. (2009). Comparison of the in vitro safety of intraocular dyes using two retinal cell lines: a focus on brilliant blue G and indocyanine green. *Am J Ophthalmol,* 147, 251-259 e252. doi: 10.1016/j.ajo.2008.08.031

Part 3: Interaction of dodecaborate cluster lipids and dodecahalo-dodecaborates with liposomes and mammalian cells

3. 1. Introduction

This present study introduces new biological relevancies of the halogenated dodecaborate clusters and boron-lipid liposomes, where the boron-lipid has as a charged headgroup the dodecaborate cluster molecule. The first manuscript (Appendix VI) describes the strong interaction of dodecahalo-dodecaborate clusters with different liposomal membranes by using numerous biophysical techniques such as zeta potential, differential scanning calorimetry, cryo-transmission electron microscopy, atomic force microscopy and fluorophore leakage measurements. We observed that the strength of the interaction increases with increasing the halogen size. As an outcome, we propose the use of these cluster molecules for targeted release of the drugs from liposomes used as delivery agents. The second manuscript (Appendix VII) presents the strong association and high uptake of the boron-lipid liposomes in primary endothelial cells and cancer cells, measured by flow cytometry and fluorescence microscopy. The high uptake of boron-lipid liposomes in endothelial cells, even when the liposomes were sterically stabilized by pegylation, may limit their use as delivery vehicles in certain therapies.

3.1.1. Liposomes

Liposomes were first described in 1965 by Bangham et al. (1965), who observed that the closely packed phospholipid molecules can form vesicles when swollen in a buffer system. These vesicles present a multilayered structure with an interior aqueous core. Later, Sessa and Weissmann (1968) and de Gier et al. (1968) presented in more detail the properties of the liposomes. Since then they have become very versatile tools in biology, biochemistry and medicine. Liposomes are the smallest artificial vesicles with spherical shape, formed by lipid bilayers. The lipids used to form the liposomes are mostly nontoxic phospholipids.

Phospholipids are amphipathic molecules, which contain a hydrophilic polar head group (e.g. choline) and a non-polar hydrophobic lipid backbone. The chemical structure of phospholipids contains a glycerol molecule, which is esterified in position one and two with fatty acids and in the third position with a phosphate group. The fatty acids can vary in their length between 10 and 18 carbon atoms, and they could also contain cis-configured double bonds. If the phospholipids

are dispersed in water, the formation of bilayers occurs spontaneously because of the hydrophobic effect (Voet et al. 2002). This means that the fatty acids will join together to avoid the water, whereas the polar head groups will associate with the water, forming small, closed vesicles, containing an aqueous core.

In experimental procedures usually either small unilamellar vesicles (SUV) or large unilamellar vesicles (LUV) are used. Both of these vesicles are formed from multilamellar vesicles (MLV). The MLVs are obtained by dissolving the lipids in an organic solvent (e.g. chloroform), drying to obtain a lipid film, and finally hydrating above the phase transition temperature of the lipid. SUVs are formed from MLVs by sonication, which creates 30-60 nm diameter vesicles (Ulrich 2002). LUVs are prepared from MLVs by repeated extrusion trough a polycarbonate membrane with defined pore diameter (Hope et al. 1985). The formed liposomes can be used as carriers, loaded with a great variety of molecules, such as small drugs, proteins, nucleotides, and even plasmids (Ulrich 2002). The encapsulation efficiency can be enhanced if the liposomal suspension is frozen and thawed prior the extrusion (Mayer et al. 1985).

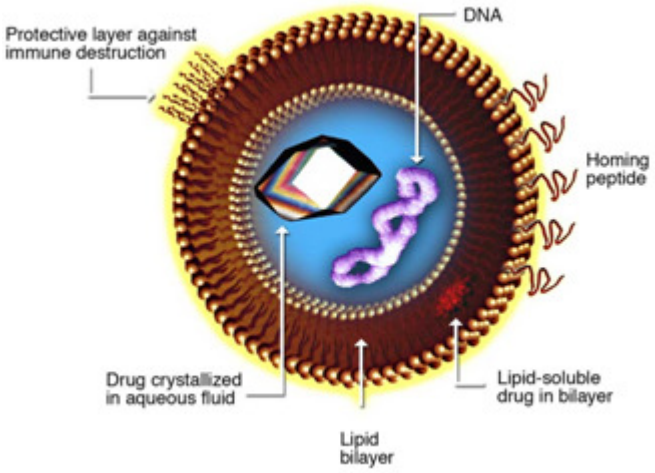

Figure 1. Schematic representation of liposomes as drug carriers (http://www.equidblog.com/2009/11/articles/test-category/antibiotics-1/putting-a-new-spin-on-old-drugs/)

3.1.2. Liposomes as delivery agents

Liposomes are ideal drug carriers, because they are non-toxic and biodegradable. When liposomes are injected into the bloodstream, they go all over the body, but they tend to

accumulate in inflamed tissues (Awasthi et al. 2002). The high accumulation of the liposomes in these tissues is due to the "leaky" blood vessels of the tissues, allowing the liposomes to escape from the bloodstream (Parikh 2013). Liposomes also show tendency to accumulate in tumors; therefore, they are attractive delivery agents of anti-neoplastic chemotherapy drugs (Mittal et al. 2014). By having a targeted delivery system with liposomes, the toxic side effects of drugs can be reduced, while achieving the same or even higher concentrations of drug at the site of interest. However, one of the most important disadvantage in using liposomes as drug delivery agents is the short circulation time of liposomes in blood (Momekova et al. 2010). To overcome this problem, the liposomal surface needs to be modified. The sterical stabilization of liposomes with long flexible polymer residues will increase the circulation time in the body and delay the clearance from the blood stream through the reticulo-endothelial system (Drummond et al. 1999; Hashizaki et al. 2003). Polyethylene glycol (PEG) labeled phosphatidyl ethanolamine is the mostly used molecule for the steric stabilization of liposomes. These PEG containing lipids are easily included within the liposomal membrane during the liposome preparation. Including PEG lipids in the liposomal membrane leads to changes in the physical-chemical properties of liposomes such as reduces the size of liposomes with the increasing percentage of PEG lipids (Sriwongsitanont & Ueno 2002). At high concentrations of PEG lipids in a liposomal formulation the formation of liposomes is disfavored; instead, the formation of liposomal disks is favored (Edwards et al. 1997).

3.1.3. Targeted delivery of liposomes

To ensure that liposomes will accumulate selectively in tumor cells, they can be labeled with tumor seeking units. There are various possible ligands described in the literature, which can serve as a tumor seeking unit. For example, it is known that epidermal growth factor receptors are over-expressed in tumors; therefore, the epidermal growth factor (EGF) can be used as a tumor seeking entity (Chaidarun et al. 1994). Bohl Kullberg et al. (2002) introduced a method to bind EGF to DSPC/Cholesterol/DSPE-PEG liposomes. The *in vitro* experiments performed with EGF-liposomes demonstrated that they had EGF-receptor specific cellular binding (Bohl Kullberg et al. 2002).

Another possible tumor seeking entity could be the folic acid. It plays a major role in rapid cell division and growth. The folate receptor, known as a glycosyl-phosphatidylinositol-anchored

glycoprotein, is amplified in many human tumors (Carlsson et al. 2003). The coupling of folate group to the liposomes via the outer end of the PEG-lipid (DSPE-PEG) proved suitability of the liposomes as delivery systems *in vitro* (Pan et al. 2002), but *in vivo* they showed a rapid clearance by the liver and therefore, no specific accumulation in the tumor (Gabizon et al. 2003).

The growth receptor $p185^{HER2}$, encoded by HER2 proto-oncogene, is also known to be over-expressed in cancer cells, in comparison with normal tissues. Park et al. (1995) showed that the immuno-liposomes having anti-$p185^{HER2}$ units were suitable tumor targeting vesicles, which internalized in the tumor cells via receptor mediated endocytosis. However, the internalization of these immuno-liposomes in cells was reduced by the incorporation of PEG-lipids into the liposomal structure (Park et al. 1995).

To target the liposomes towards the CD44 receptor, which is present in carcinoma, melanoma, lymphoma and lung tumor cells, the liposomes were modified by incorporating hyaluronic acid (HA) in their membrane (Eliaz & Szoka 2001). The HA is an oligosaccharide present in the extracellular matrix, which helps in tissue hydration and water transport within the cells (Necas et al. 2008). The *in vitro* studies demonstrated that the uptake of these functionalized liposomes is higher than that of non-modified liposomes in B16F10 murine melanoma cells. However, in non-cancerous cells, where CD44 is only expressed at low levels, the uptake of HA-modified liposomes was very low. Therefore, the authors concluded that liposomes modified with HA are potent transporters for drug delivery in cancer cells (Eliaz & Szoka 2001).

The transferrin is a glycoprotein responsible for the iron transport in the body via receptor mediated endocytosis. The transferrin receptor is found at high concentration in the tumor cells in comparison with normal cells. Therefore, the pegylated liposomes, modified with transferring molecules attached to the distal terminal of the PEG-chains, are promising as intracellular targeting carriers in the treatment of cancer (Ishida et al. 2001). The *in vivo* studies, which used transferrin modified liposomes to transport encapsulated BSH (mercapto-undecahydro-dodecaborate) into the tumor cells, showed that high amounts of BSH reached the site of interest, with a very low plasma boron concentration (Maruyama et al. 2004).

3.1.4. Interaction of liposomes with cells

The interaction of liposomes with biological systems is very complex. There are four possible mechanisms of liposome-cell interaction by which the liposomes can deliver their contents to the

cell. The occurrence of any of these interactions depends on the liposome characteristics such as size, charge, composition and the presence of targeting devices. Also a major determinant of liposome-cell interaction is the type of the cell and the environmental factors such as the presence of serum in the cell culture media (Torchilin & Weissig 2003).

The liposome binding or adsorption to cells without uptake of the liposomes is found in literature for both targeted and non-targeted liposomes. The mechanism of adsorption with content release is believed to take place at liposome-cell membrane contact. This contact could lead to a higher permeability of the liposomal membrane and the release of the liposomal content into the cytoplasm (Torchilin & Weissig 2003). The contact mediated transfer of liposomal content take place with an exchange of lipids between the liposomes and the cell membrane. This could help to transfer mostly lipophilic materials and drugs to the cells (Sandra & Pagano 1979).The fusion of the liposomes with the cells involves the complete mixing of the liposomal membrane with the cell membrane and the release of the liposomal content into the cytoplasm of the cell (van der Meel et al. 2014). It is believed that fusion does not occur at the cell membrane when using plain liposomes, because such a process would need specific fusion inducing agents, like fusion proteins and peptides (Versluis et al. 2013). The endocytotic internalization of the liposomes by invagination of the cell membrane into endosomal compartments is another possible way for liposome-cell interaction. The liposomes containing endosomes will fuse with the lysosomes, which result in the lysosomal digestion of the endosomal contents and the release of the liposomal content into the cell by exocytosis (van der Meel et al. 2014).

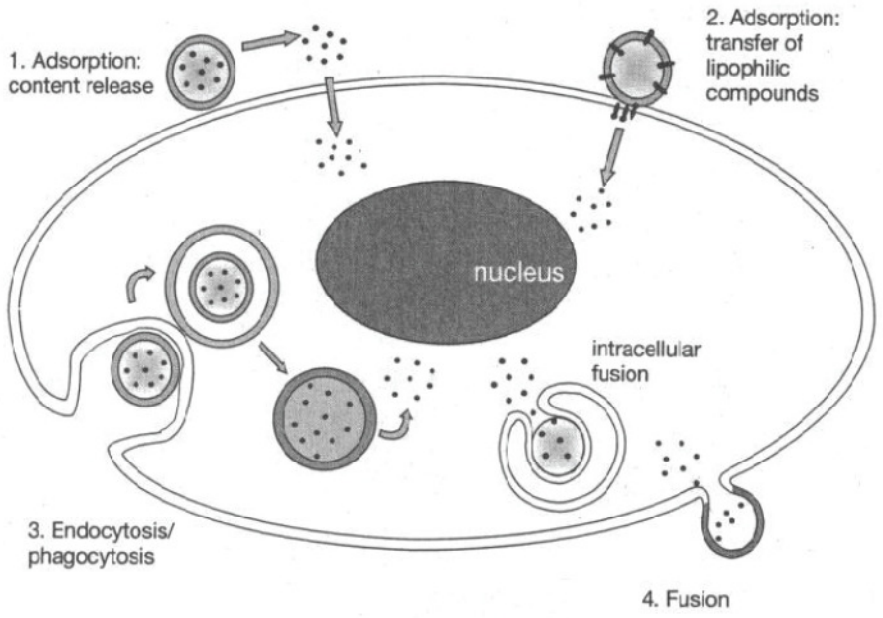

Figure 2. Schematic mechanism of the four types of interactions of liposomes with cells (Torchilin & Weissig 2003)

3.1.5. Specific accumulation of liposomes in tumors

Tumor tissues require a functioning vasculature for the delivery of nutrients and the removal of toxic waste products associated with cellular metabolism. This vasculature has to expand continuously to serve an essential requirement for tumor initiation, progression and metastasis (Siemann 2006). The vasculature expansion, which leads to the tumor mass expansion, requires the formation of new blood vessels with chaotic architecture and aberrant branching. This process is called neovascularization, and is relatively uncommon in most normal tissues, but is an important feature of solid tumors (Konerding et al. 2002). The tumor vasculature is typically characterized by dilated vessels, large inter-capillary distances and decreased vessel density. Because the vessel network that is formed in tumors is typically unable to keep proliferating as rapidly as the growing tumor cell mass, it will inevitably fail to ensure the nutritional needs of the tumor cells (Siemann 2006). This is the reason why these tumor blood vessels have gaps as large as 600 to 800 nm between adjacent endothelial cells, which makes possible to the liposomes with certain sizes to enter through these gaps into the tumor interstitial space.

The accumulation level of liposomes in tumor tissues usually depend on the liposome size, has to be smaller than the vessel gaps of the tumor; molecular weight and charge; the circulation time

of the liposomes, which can be enhanced with PEG; the level of tumor vascularization, that means the better the vascularization is, the more liposomes can accumulate in the tumor tissue; and the size of the gaps, if they are smaller than the liposomes, no extravasation into the tumor tissue will be possible.

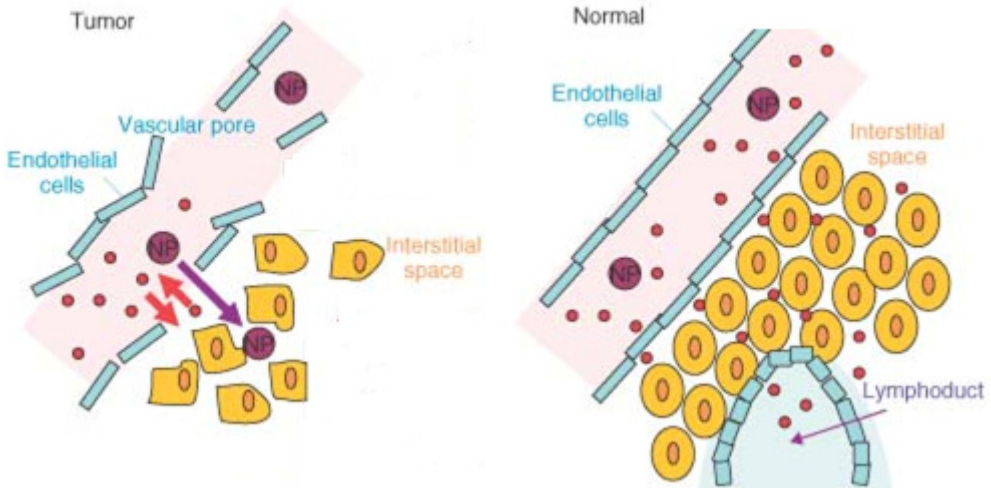

Figure 3. Comparative representation of tumor and normal tissue blood vessels (http://wires.wiley.com/WileyCDA/WiresArticle/wisId-WNAN66.html)

3.1.6. Boron Neutron Capture Therapy

The clinical interest in boron neutron capture therapy (BNCT) is focused mostly on the treatment of cerebral metastases of melanoma and high grade gliomas (Barth et al. 2005). These types of cancers are very resistant to all forms of currently available therapies, including surgery, chemotherapy, radiotherapy, immunotherapy, or gene therapy. Combinations of these therapies were also tried in United States, but lead to death in majority of the patients, due to the aggressive treatment (Lacroix et al. 2001). It would be useful to find methods and molecular strategies, which can target selectively malignant cells, and has no or slight effect on normal tissue, adjacent to the tumor tissue.

BNCT was designed in a way to selectively destroy malignant cells and skip the normal tissue. The therapy is based on the nuclear reaction, which occurs when the boron atom (^{10}B) is irradiated with low-energy thermal neutrons. The irradiation is followed by a nuclear fission resulting high energy α-particles (^{4}He) and lithium nuclei (^{7}Li) with around 2.31 MeV of energy. The resulted high energy is deadly to the cells where the reaction occurs (Barth et al. 2005). The

produced particles have to act in a short range to ensure that the adjacent normal tissue will not be affected by this therapy. A major challenge to make this therapy successful is to selectively deliver and accumulate sufficient amounts of boron atoms in the tumor tissues. The concentration of boron in the target tumor tissue should be at least 10^9 atoms/cell or 20-30 µg/g of tumor. It is also very important to ensure that enough thermal neutrons are absorbed by the boron atoms to induce a lethal $^{10}B(n,\alpha)^7Li$ capture reaction (Barth et al. 2005). The high energy α-particles have a limited path length in the cancer tissue, which is about 5-9 µm, due to this the destructive effects of the high energy particles is limited to boron containing cells (Sivaev & Bregadze 2009); therefore, much more boron has to be accumulated in the tumor tissues than in the surrounding normal tissue.

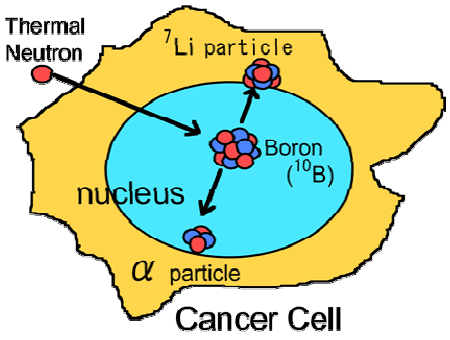

Figure 4. Schematic representation of the boron neutron capture reaction (http://www.osaka-med.ac.jp/deps/neu/omcBNCT/BNCT_E/BNCT_E1.html)

3.1.7. Boron containing compounds

The promising development of BNCT in clinical treatment, which started around 60 years ago, led to the synthesis of several boron containing compounds, which could successfully deliver the therapeutic concentration of boron to the tumor tissue. For such boron delivery agents to be effective, they must fulfill some criteria: first, they should have low systemic toxicity and high tumor/brain and tumor/blood concentrations; second, they should achieve concentrations of at least 20 µg of boron per gram of tumor; they should present rapid clearance from blood and normal tissue, but persistence in tumor for BNCT. However, to date, no single boron delivery agent was found to fulfill all the above mentioned criteria (Barth et al. 2005).

3.1.8. Dodecaborate cluster compounds

Polyhedral boron hydride structures are formed from boranes by the elimination of protons. All of these structures are characterized by electron deficient bonding (Lipscomb 1963), and they exhibit aromatic properties (King 2001).

The dodecahydro-closo-dodecaborate ($Na_2B_{12}H_{12}$) was first synthesized by Pitochelli and Hawthorne (1960). These molecules and their derivatives showed interesting characteristics such as thermal and chemical stability and low in vitro toxicity. Based on the $Na_2B_{12}H_{12}$, other halogenated derivatives of dodecaborate clusters were synthesized by an electrophile substitution reaction (Knoth et al. 1964). The early studies on these dodecahalogen-closo-dodecaborate structures showed that they have high thermal and chemical stability. Recently, we have studied the *in vitro* toxicity of these halogenated cluster compounds. Our results revealed that the toxicities of dodecahalogen-dodecaborates are higher in comparison with $Na_2B_{12}H_{12}$. The EC_{50} values are 0.44, 0.25 and 0.14 mM for $Na_2B_{12}Cl_{12}$, $Na_2B_{12}Br_{12}$ and $Na_2B_{12}I_{12}$, respectively (Appendix VI).

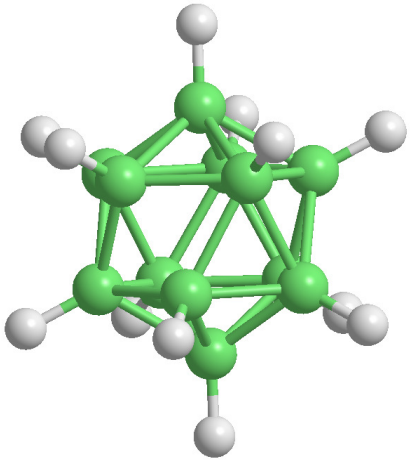

Figure 5. 3D structure of dodecahalo-closo-dodecaborate clusters: ● **= B**; ● **= Cl, Br, I**

Recent studies on leakage experiment with the halogenated derivatives of $Na_2B_{12}H_{12}$ showed that they are capable to induce leakage of the liposomal contents much better than BSH; therefore, they became great potential inducers for drug release (Appendix VI).

3.1.9. Liposomes in BNCT

Liposomes as promising drug carriers show a great tendency for boron delivery to the tumor tissue. Small, water soluble boron compounds can be encapsulated in the aqueous core of liposome vesicles. After intravenous administration these liposomes can penetrate the tumor tissue and localize intra-cellularly. It is known that boron compounds in their free form have no affinity to the tumor cells and they are rapidly cleared from the body. Instead, encapsulated in liposomes they can reach therapeutic ranges of boron concentrations in the tumor (Carlsson et al. 2003). To enhance the selective boron transport to the tumor tissue, the liposomes can be tagged with tumor seeking entities (Maruyama et al. 2004).

Numerous disadvantages in the encapsulation of the boron compounds into liposomes have been described in the literature, including low encapsulation efficiency, leakage upon storage, or modification of the liposome structures by the boron clusters (Gabel et al. 2007). These problems led to the synthesis of new lipid structures which have as charged head group a boron cluster compound, linked to a lipid backbone. These boron containing lipids can be incorporated directly into the liposomal membrane (Schaffran et al. 2009) and will avoid problems involving leakage of the agent due to improper encapsulation.

3.1.10. Saint lipids

The first dodecaborate cluster lipids were described by Lee et al. (2007). These boron-lipids have the BSH molecule as head-group, they are doubly negatively charged and showed similarly low *in vitro* toxicity as BSH. Later, Schaffran et al. (2009) described the first dodecaborate cluster lipids with only one negative charge. These boron-lipids will help to decrease the clearance of the liposomes from the bloodstream and will lead to longer retention times in the body in comparison with doubly negatively charged dodecaborate cluster lipids. These lipids, named also Saint-lipids, contain a pyridinium core with two chains of 12, 14 or 16 carbon atoms as lipid backbone, connected through the nitrogen atom with the help of butylene, pentylene or ethylenoxyethylene linker to the oxygen atom on the dodecaborate cluster as headgroup. They can form closed liposomes in the presence or even absence of helper lipids such as DSPC and cholesterol. For the preparation of boron lipid liposomes, the helper lipids should not differ very much in their chain length from the boron lipid; therefore, DSPC was chosen as a desirable helper lipid for the formation of stable Saint-lipids liposomes (Schaffran et al., 2009).

These boron-lipids showed a low impact on cell viability, their EC_{50} range was between 1.5 and 4.8 mM, except for the Dioxan-Saint-12 and Dioxan-Saint-14, which showed higher toxicities (Schaffran et al. 2009).

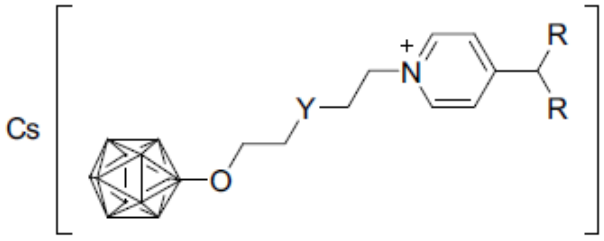

Y = no atom: THF-Saint-12 (R=$C_{12}H_{25}$); THF-Saint-14 (R=$C_{14}H_{29}$); THF-Saint-16 (R=$C_{16}H_{33}$)

O: Dioxan-Saint-12 (R=$C_{12}H_{25}$); Dioxan-Saint-14 (R=$C_{14}H_{29}$); Dioxan-Saint-16 (R=$C_{16}H_{33}$)

CH_2: Pyran-Saint-12 (R=$C_{12}H_{25}$); Pyran-Saint-14 (R=$C_{14}H_{29}$); Pyran-Saint-16 (R=$C_{16}H_{33}$)

Figure 6. The structures of the Saint-lipids (Schaffran et al. 2009)

3.2. Results and Outcomes

3.2.1. Halogenated dodecaborate clusters as agents to trigger release of liposomal contents (Appendix VI)

Authors: D. Awad, **M. Bartok**, F. Mostaghimi, I. Schrader, N. Sudumbrekar, T. Schaffran, C. Jenne, J. Eriksson, M. Winterhalter, J. Fritz, K. Edwards, D. Gabel

Status of the publication: Accepted for publication in *ChemPlusChem* journal (in press).

Contribution of M. Bartok to the work: Contributed for the acquisition, analysis and interpretation of the experimental data, partially wrote the Material and Methods section and reviewed the manuscript.

Contribution of the coauthors: D. Awad, F. Mostaghimi, I. Schrader and N. Sudumbrekar contributed for the data acquisition, analysis and interpretation. D. Gabel wrote the manuscript. T. Schaffran, C. Jenne, J. Eriksson, M. Winterhalter, J. Fritz and K. Edwards reviewed the manuscript.

3.2.2. Cellular interaction and uptake of liposomes containing dodecaborate cluster lipids: Implications for boron neutron capture therapy (Appendix VII)

Authors: M. Bartok, D. Awad, J. Wilinska, M. Kirihata, R. Schubert, R. Süss and D. Gabel

Status of the publication: In preparation.

Contribution of M. Bartok to the work: Co-developed the immuno-staining method, contributed for the acquisition, analysis and interpretation of the experimental data, wrote the manuscript together with D. Gabel.

Contribution of the coauthors: D. Awad conducted the preliminary experiments and co-developed the immuno-staining method. J. Wilinska helped with the acquisition of the FACS data. M. Kirihata developed the primary antibodies for the immuno-staining. R. Schubert, R. Süss and D. Gabel helped with the coordination of the study and reviewed the manuscript.

3.3. Conclusions and Outlook

The first study (Appendix VI) reveals a strong interaction of the dodecahalogen dodecaborate clusters with DPPC (dipalmitoyl-phosphatidylcholine) and DSPC (distearoyl-phosphatidylcholine) liposomes. The interaction was characterized using different biophysical techniques. The zeta potential measurements showed that the cluster molecules easily form stable and strong interactions with the liposomal membrane surface. The Cryo-TEM (cryo-transmission electron microscopy) and AFM (atomic force microscopy) images revealed that these interactions are not only limited to the liposomal surfaces, but they induce drastic changes in the morphology of the liposomes. For example, in the presence of high BI (dodecaiodo-dodecaborate) concentration the liposome structures disappear and instead only long needle-shaped structures were found. These long electron dense structures are thought to be rich in iodine. The leakage of the CF (carboxyfluorescein) is induced by the halogenated clusters not only in DPPC or DSPC liposomes, but also in cholesterol containing and sterically stabilized liposomes. In all preparations BI was the most effective cluster to induce leakage. The toxicity of the halogenated clusters was also measured on a lung fibroblast cell line. We found that none of the clusters had a considerably high toxicity; therefore, we suggest the use of these cluster molecules, mostly of BI, to trigger the release of liposome-encapsulated drugs after the accumulation at the site of interest in cancer therapy.

In the second manuscript (Appendix VII) we report the uptake and localization of boron-lipid liposomes in three different cell lines, a primary endothelial cell line (HUVEC) and two tumor cell lines (Kelly and V79). We found that the uptake of the boron lipid, measured by immuno-staining, and the fluorescent lipid from sterically stabilized liposomes is concentration dependent and different when using different boron-lipids. The highest uptake of boron-lipid was obtained by using THF-S-14, THP-S-14 and THP-S-16 containing liposomes at 2.5 mM concentration. However, in several preparations the uptake of boron-lipid and fluorescent lipid did not coincide completely. In the flow cytometry measurements the strongest association was obtained by using HUVEC endothelial cells. At the lowest liposome concentration tested (0.01 mM), these cells showed between 90% and 100% cell association, even at low incubation temperatures (4°C). In contrast, Kelly and V79 cells at this concentration had slight (Kelly) or no (V79) association with the liposomes. Reducing the incubation temperature of the cells with the liposomes affected the cellular uptake drastically in case of V79 and only slightly in case of Kelly. These results

indicate that the boron-lipids may preferentially be taken up in the endothelial cells from the vasculature, which might limit their use in the boron neutron capture therapy. The reason for such interactions between the boron-lipids liposomes and the cells was not yet elucidated. However, we think that the uptake could be caused by the strong interactions of the boron cluster headgroups with the cell surface, as described in the previous study (see Appendix VI).

References

Awasthi, V. D., Goins, B., Klipper, R., Phillips, W. T. (2002). Accumulation of PEG-liposomes in the inflamed colon of rats: potential for therapeutic and diagnostic targeting of inflammatory bowel diseases. *J Drug Target,* 10, 419-427. doi: 10.1080/1061186021000001878

Bangham, A. D., Standish, M. M., Watkins, J. C. (1965). Diffusion of univalent ions across the lamellae of swollen phospholipids. *J Mol Biol,* 13, 238-252.

Barth, R. F., Coderre, J. A., Vicente, M. G. H., Blue, T. E. (2005). Boron neutron capture therapy of cancer: current status and future prospects. *Clin Cancer Res,* 11, 3987-4002.

Bohl Kullberg, E., Bergstrand, N., Carlsson, J., Edwards, K., Johnsson, M., Sjoberg, S., Gedda, L. (2002). Development of EGF-conjugated liposomes for targeted delivery of boronated DNA-binding agents. *Bioconjug Chem,* 13, 737-743.

Carlsson, J., Kullberg, E. B., Capala, J., Sjoberg, S., Edwards, K., Gedda, L. (2003). Ligand liposomes and boron neutron capture therapy. *J Neurooncol,* 62, 47-59.

Chaidarun, S. S., Eggo, M. C., Sheppard, M. C., Stewart, P. M. (1994). Expression of epidermal growth factor (EGF), its receptor, and related oncoprotein (erbB-2) in human pituitary tumors and response to EGF in vitro. *Endocrinology,* 135, 2012-2021. doi: 10.1210/endo.135.5.7956924

de Gier, J., Mandersloot, J. G., van Deenen, L. L. (1968). Lipid composition and permeability of liposomes. *Biochim Biophys Acta,* 150, 666-675. doi: 10.1016/0005-2736(68)90056-4

Drummond, D. C., Meyer, O., Hong, K., Kirpotin, D. B., Papahadjopoulos, D. (1999). Optimizing liposomes for delivery of chemotherapeutic agents to solid tumors. *Pharmacol Rev,* 51, 691-743.

Edwards, K., Johnsson, M., Karlsson, G., Silvander, M. (1997). Effect of polyethyleneglycol-phospholipids on aggregate structure in preparations of small unilamellar liposomes. *Biophys J,* 73, 258-266. doi: 10.1016/S0006-3495(97)78066-4

Eliaz, R. E., Szoka, F. C., Jr. (2001). Liposome-encapsulated doxorubicin targeted to CD44: a strategy to kill CD44-overexpressing tumor cells. *Cancer Res,* 61, 2592-2601.

Gabel, D., Awad, D., Schaffran, T., Radovan, D., Dărăban, D., Damian, L., Winterhalter, M., Karlsson, G., Edwards, K. (2007). The anionic boron cluster (B12H11SH) 2– as a means to trigger release of liposome contents. *ChemMedChem,* 2, 51-53. doi: 10.1002/cmdc.200600227

Gabizon, A., Horowitz, A. T., Goren, D., Tzemach, D., Shmeeda, H., Zalipsky, S. (2003). In vivo fate of folate-targeted polyethylene-glycol liposomes in tumor-bearing mice. *Clin Cancer Res,* 9, 6551-6559.

Hashizaki, K., Taguchi, H., Itoh, C., Sakai, H., Abe, M., Saito, Y., Ogawa, N. (2003). Effects of poly(ethylene glycol) (PEG) chain length of PEG-lipid on the permeability of liposomal bilayer membranes. *Chem Pharm Bull (Tokyo),* 51, 815-820.

Hope, M. J., Bally, M. B., Webb, G., Cullis, P. R. (1985). Production of large unilamellar vesicles by a rapid extrusion procedure: characterization of size distribution, trapped volume and ability to maintain a membrane potential. *Biochim Biophys Acta,* 812, 55-65.

Ishida, O., Maruyama, K., Tanahashi, H., Iwatsuru, M., Sasaki, K., Eriguchi, M., Yanagie, H. (2001). Liposomes bearing polyethyleneglycol-coupled transferrin with intracellular targeting property to the solid tumors in vivo. *Pharm Res,* 18, 1042-1048.

King, R. B. (2001). Three-dimensional aromaticity in polyhedral boranes and related molecules. *Chem Rev,* 101, 1119-1152.

Knoth, W. H., Miller, H., Sauer, J. C., Balthis, J., Chia, Y., Muetterties, E. (1964). Chemistry of boranes. IX. Halogenation of B10H10-2 and B12H12-2. *Inorg Chem,* 3, 159-167. doi: 10.1021/ic50012a002

Konerding, M., Van Ackern, C., Fait, E., Steinberg, F., Streffer, C. (2002). *Morphological aspects of tumor angiogenesis and microcirculation* (M. Molls & P. Vaupel Eds.). Berlin: Springer.

Lacroix, M., Abi-Said, D., Fourney, D. R., Gokaslan, Z. L., Shi, W., DeMonte, F., Lang, F. F., McCutcheon, I. E., Hassenbusch, S. J., Holland, E., Hess, K., Michael, C., Miller, D., Sawaya, R. (2001). A multivariate analysis of 416 patients with glioblastoma multiforme: prognosis, extent of resection, and survival. *J Neurosurg,* 95, 190-198. doi: 10.3171/jns.2001.95.2.0190

Lee, J. D., Ueno, M., Miyajima, Y., Nakamura, H. (2007). Synthesis of boron cluster lipids: closo-dodecaborate as an alternative hydrophilic function of boronated liposomes for neutron capture therapy. *Org Lett,* 9, 323-326. doi: 10.1021/ol062840+

Lipscomb, W. N. (1963). *Boron hydrides*. New York: W. A. Benjamin Inc.

Maruyama, K., Ishida, O., Kasaoka, S., Takizawa, T., Utoguchi, N., Shinohara, A., Chiba, M., Kobayashi, H., Eriguchi, M., Yanagie, H. (2004). Intracellular targeting of sodium mercaptoundecahydrododecaborate (BSH) to solid tumors by transferrin-PEG liposomes, for boron neutron-capture therapy (BNCT). *J Control Release,* 98, 195-207. doi: 10.1016/j.jconrel.2004.04.018

Mayer, L. D., Hope, M. J., Cullis, P. R., Janoff, A. S. (1985). Solute distributions and trapping efficiencies observed in freeze-thawed multilamellar vesicles. *Biochim Biophys Acta,* 817, 193-196.

Mittal, N. K., Bhattacharjee, H., Mandal, B., Balabathula, P., Thoma, L. A., Wood, G. C. (2014). Targeted liposomal drug delivery systems for the treatment of B cell malignancies. *J Drug Target,* 22, 372-386. doi: 10.3109/1061186X.2013.878942

Momekova, D., Rangelov, S., Lambov, N. (2010). Long-circulating, pH-sensitive liposomes. *Methods Mol Biol,* 605, 527-544. doi: 10.1007/978-1-60327-360-2_35

Necas, J., Bartosikova, L., Brauner, P., Kolar, J. (2008). Hyaluronic acid (hyaluronan): a review. *Vet Med,* 53, 397-411.

Pan, X. Q., Wang, H., Shukla, S., Sekido, M., Adams, D. M., Tjarks, W., Barth, R. F., Lee, R. J. (2002). Boron-containing folate receptor-targeted liposomes as potential delivery agents for neutron capture therapy. *Bioconjug Chem,* 13, 435-442.

Parikh, S. M. (2013). Dysregulation of the angiopoietin-Tie-2 axis in sepsis and ARDS. *Virulence,* 4, 517-524. doi: 10.4161/viru.24906

Park, J. W., Hong, K., Carter, P., Asgari, H., Guo, L. Y., Keller, G. A., Wirth, C., Shalaby, R., Kotts, C., Wood, W. I., et al. (1995). Development of anti-p185HER2 immunoliposomes for cancer therapy. *Proc Natl Acad Sci U S A,* 92, 1327-1331.

Pitochelli, A. R., Hawthorne, F. M. (1960). The isolation of the icosahedral B12H12-2 Ion. *J Am Chem Soc,* 82, 3228-3229. doi: 10.1021/ja01497a069

Sandra, A., Pagano, R. E. (1979). Liposome-cell interactions. Studies of lipid transfer using isotopically asymmetric vesicles. *J Biol Chem,* 254, 2244-2249.

Schaffran, T., Burghardt, A., Barnert, S., Peschka-Suss, R., Schubert, R., Winterhalter, M., Gabel, D. (2009). Pyridinium lipids with the dodecaborate cluster as polar headgroup: synthesis, characterization of the physical-chemical behavior, and toxicity in cell culture. *Bioconjug Chem,* 20, 2190-2198. doi: 10.1021/bc900147w

Sessa, G., Weissmann, G. (1968). Phospholipid spherules (liposomes) as a model for biological membranes. *J Lipid Res,* 9, 310-318.
Siemann, D. W. (2006). *Vascular-targeted therapies in oncology*: Wiley Online Library.
Sivaev, I. B., Bregadze, V. V. (2009). Polyhedral boranes for medical applications: current status and perspectives. *Eur J Inorg Chem,* 2009, 1433-1450. doi: 10.1002/ejic.200900003
Sriwongsitanont, S., Ueno, M. (2002). Physicochemical properties of PEG-grafted liposomes. *Chem Pharm Bull (Tokyo),* 50, 1238-1244.
Torchilin, V. P., Weissig, V. (2003). *Liposomes: a practical approach* (second ed.). Boston: Oxford University Press.
Ulrich, A. S. (2002). Biophysical aspects of using liposomes as delivery vehicles. *Biosci Rep,* 22, 129-150. doi: 10.1023/A:1020178304031
van der Meel, R., Fens, M. H., Vader, P., van Solinge, W. W., Eniola-Adefeso, O., Schiffelers, R. M. (2014). Extracellular vesicles as drug delivery systems: Lessons from the liposome field. *J Control Release*. doi: 10.1016/j.jconrel.2014.07.049
Versluis, F., Voskuhl, J., van Kolck, B., Zope, H., Bremmer, M., Albregtse, T., Kros, A. (2013). In situ modification of plain liposomes with lipidated coiled coil forming peptides induces membrane fusion. *J Am Chem Soc,* 135, 8057-8062. doi: 10.1021/ja4031227
Voet, D., Voet, J., Pratt, C. (2002). *Lehrbuch der Biochemie* (S. Weinheim Ed.): Wiley-VCH.

Appendices

Appendix I

Toxicology in Vitro 29 (2015) 72–80

Contents lists available at ScienceDirect

Toxicology in Vitro

journal homepage: www.elsevier.com/locate/toxinvit

Development of an *in vitro* ocular test system for the prediction of all three GHS categories

M. Bartok [a,*], D. Gabel [a], M. Zorn-Kruppa [b], M. Engelke [a]

[a] School of Engineering and Science, Jacobs University Bremen, Campus Ring 1, 28759 Bremen, Germany
[b] Department of Dermatology and Venerology, University Medical Center Hamburg-Eppendorf, Martinistraße 52, 20246 Hamburg, Germany

ARTICLE INFO

Article history:
Received 3 July 2014
Accepted 5 September 2014
Available online 27 September 2014

Keywords:
Eye irritation
Human hemi-cornea model
Prediction model
Predictive capacity
GHS classification

ABSTRACT

In the present study we considered a new approach that allows the individual quantification of damages induced in the epithelium and stroma of an *in vitro* hemi-cornea model after chemical treatment. We aimed at a stand-alone test system for classification according to the classification of the globally harmonized system of classification and labelling of chemicals (GHS).

We have modified a previously developed 3D hemi-cornea model by the insertion of a collagen membrane between epithelium and stroma. This membrane allows the separation and independent assessment of these compartments after topical exposure to potential eye irritants. The cell viability quantified by MTT assay was used as the toxicological endpoint. The prediction model based on the results obtained from 30 test chemicals uses a single exposure period and the combination of cut-off values in tissue viability from both epithelium and stroma.

The *in vitro*–*in vivo* concordance of the test system is 77%. All of the GHS category 1, 80% of the GHS category 2 and 50% of the GHS not categorized chemicals are predicted correctly. In conclusion, the test system predicts and discriminates GHS category 1 and GHS category 2 chemicals, but is over-predictive for GHS not categorized materials.

1. Introduction

In order to ensure consumer and environmental protection, chemicals and raw materials are subjected to extensive toxicological assessment according to the specific legislation regarding different industries and countries. The assessment of the eye-irritating potential of substances is an essential part of the toxicological examinations. To date, the rabbit Draize eye irritation test (Draize et al., 1944) is still the only OECD-approved test for the determination of the whole range of eye irritating effects from mild to severe (OECD, 2002). However, the Draize eye test has been increasingly criticized due to its lack of reproducibility, overestimation of human responses, and cruelty to animals (Weil and Scala, 1971).

In the past, a number of new *in vitro* methods have been developed in order to replace the Draize test. One group of test systems is based on isolated animal eyes, e.g. the Bovine Corneal Opacity and Permeation (BCOP) test and the Isolated Chicken Eye (ICE) test (Gautheron et al., 1992; Prinsen and Koeter, 1993; Barile, 2010; Verstraelen et al., 2013). A second group takes advantage of the reactions evoked by chemicals in incubated hen eggs (Eskes et al., 2005) or invertebrates (Adriaens et al., 2005, 2008). One test system is based on the perturbation and denaturation of corneal proteins; these processes are supposed to mimic the disruptive effect to ocular irritants (Eskes et al., 2014). Another group uses cultured cells of different origin to assess the eye-irritating potential of chemicals (Eskes et al., 2005; McNamee et al., 2009; Hartung et al., 2010; Takahashi et al., 2010, 2011; Sakaguchi et al., 2011).

As a further approach, 3D cornea epithelial models have been reconstructed (Doucet et al., 2006; Van Goethem et al., 2006; Huhtala et al., 2008; Seaman et al., 2010; Kaluzhny et al., 2011; Kolle et al., 2011; Katoh et al., 2013). Approaches using 3D epithelial models only discriminate between irritants (I) and non-irritants (NI) based on a classification (PM) with one viability cut-off value (Van Goethem et al., 2006; Kaluzhny et al., 2011). Due to the absence of stroma, further discrimination between chemicals classified as GHS2 (moderate irritants) and GHS1 (severe irritants) is not foreseen.

Currently, only one cell-based test system (Fluorescence leakage, FL) and two *ex vivo* animal test systems (BCOP and ICE) have reached official regulatory acceptance (OECD, 2012, 2013a,b). However, these test systems allow only the prediction of serious eye damage (GHS1, i.e., BCOP, ICE and FL), and of

* Corresponding author. Tel.: +49 421 2003253; fax: +49 421 2003249.
E-mail address: m.bartok@jacobs-university.de (M. Bartok).

http://dx.doi.org/10.1016/j.tiv.2014.09.005
0887-2333/

chemicals not requiring classification (GHSnc, i.e., BCOP and ICE), but not of GHS2. No single *in vitro* assay has been developed and validated as a full regulatory replacement for the Draize Eye Irritation test. Instead, the tests developed so far are intended to be used within the framework of an integrated testing strategy, either in a top–down or in a bottom–up approach (McNamee et al., 2009; Scott et al., 2010; Hayashi et al., 2012). These approaches, as *in vitro* alternatives to animal testing for the safety assessment, reveal their strengths preferably in the discrimination between severe and non-severe chemicals. Test systems predicting GHS2 substances directly are not yet available.

According to Scott et al. (2010), only those reconstructed corneal models that include both the epithelium and the stroma allow discrimination between all three GHS classes: severe/corrosive (GHS1), mild/moderate (GHS2) and not classified (GHSnc). This perception is based on studies by Jester and Maurer (Jester et al., 1998a,b, 2001, 2006, 2010; Maurer et al., 2002), who showed that the surface area and depth of initial corneal injury (DoI) in the epithelium and stroma, caused by chemicals of various classes in the rabbit eye, strongly correlate with the macroscopically observable severity and duration of ocular injury.

Consequently, we previously generated a 3D cornea model based on human SV40-immortalized corneal cell lines (Engelke et al., 2004; Zorn-Kruppa et al., 2004, 2005; Seeber et al., 2008; Manzer et al., 2009) which comprises both epithelium and stroma to provide an animal-free tool for eye irritation testing (Engelke et al., 2013) as well as for *in vitro* drug permeation studies (Hahne and Reichl, 2011; Hahne et al., 2012).

In a previous study (Engelke et al., 2013) we proved the reproducible construction and the transferability of the production of the complex 3D models into other laboratories. With this model, we developed a prediction model based on 20 test chemicals that reliably predicted GHS category 1 chemicals. The model did, however, not sufficiently discriminate between all 3 GHS categories

Since we assume that the individual assessment of the viability in the epithelium and stroma is essential for the GHS classification, we have expanded our previous model to include a membrane between these two compartments. This membrane allows us to separate the epithelium and stroma after exposure and to determine the cell viability individually. We have tested the model using thirty chemicals of balanced GHS classification. Based on suitable viability cut-off values for both the epithelium and stroma we developed a prediction model which allows the discrimination of all three GHS categories.

As a reproducible tissue reconstruction is crucial for the reliability of an *in vitro* test system we have assessed the intra-laboratory reproducibility. Acceptance criteria were defined based on the viabilities of the negative control (NC) and batch control (BC) in the epithelium (NC_{epi}, BC_{epi}) and stroma (NC_{stroma}, BC_{stroma}) from all batches produced over a 6-month period.

2. Materials and methods

2.1. Materials and reagents

Tissue culture flasks, flat bottomed multi-well plates (6-, 12-, 24- and 96-well plates), penicillin/streptomycin, PBS without Ca^{2+}, Mg^{2+} (PBS−−) and PBS with Ca^{2+}, Mg^{2+} (PBS++) were purchased from Biochrom (Berlin, Germany). $CaCl_2$, PBS−− tenfold concentrated powder, isopropanol, Nunc cell culture inserts (0.5 cm^2 surface area, 3 μm pore size, polycarbonate) were obtained from OmniLab (Bremen, Germany) and Bola Teflon O-rings (1 cm outer and 0.7 cm inner diameter) were from Bohlinger GmbH, Grünsfeld, Germany). The silicon O-rings were from Dichtungstechnik (Bensheim, Germany) and the electrospun membranes were from The Electrospinning Company (Harwell Oxford, UK). The rat tail collagen solution was obtained from CellSystems (Troisdorf, Germany). The media 199, Ham's F12 and TrypLE Express were from Invitrogen (Darmstadt, Germany). Triton X-100, thiazolyl blue tetrazolium bromide (MTT reagent), NaOH, $NaHCO_3$, Hepes, Bouin's solution was purchased from Sigma–Aldrich (Schnelldorf, Germany). The Collagen Cell Carrier (CCC) was from Viscofan Bioengineering (Weinheim, Germany). Keratinocyte Basal Medium (KBM) plus Bullet-kit as well as chemically defined Keratinocyte Growth Medium (KGM-CD) were obtained from Lonza (Basel, Switzerland).

2.2. Test chemicals and control materials

The test chemicals were chosen on the basis of eye irritation classifications derived from individual *in vivo* rabbits. We selected 30 test chemicals from the database of the Technical Report of the European Center for Ecotoxicology and Toxicology of Chemicals (ECETOC, 1998). Of these chemicals, 24 are liquids and 6 are solids. We have only selected 6 solid test substances, because similar to the *in vivo* test, testing of solids *in vitro* is more challenging, especially if particles remain on the tissue surface after the washing procedure. Solids may result in false classification as GHSnc only because they are not soluble under applied conditions. Details of the 30 selected chemicals, together with their *in vivo* eye irritation classification, are shown in Table 1. The test materials covered the whole range of eye irritation potencies and represented different chemical classes. PBS++ and 0.3% Triton X-100 served as the negative control (NC) and as the batch control (BC), respectively.

2.3. Solutions for the cell cultures and hemi-cornea reconstruction

The reconstruction buffer for neutralizing the acidic solution of the collagen was prepared by mixing together 2.2 g $NaHCO_3$ and 4.77 g Hepes in 100 ml of 0.5 N NaOH solution. The tenfold concentrated F99 medium was prepared according to Engelke et al. (2013). The O-ring attachment solution was made by mixing together 100 μl F99 medium, 250 μl reconstruction buffer, 100 μl KGM medium and 600 μl collagen solution. The MTT solution was prepared by first dissolving the MTT reagent in double-distilled water to a concentration of 5 mg/ml. This stock solution was stored at −20 °C for a maximum of 6 months in the dark. It was diluted with KGM medium to a final concentration of 1 mg/ml before use.

2.4. Cell culture and hemi-cornea reconstruction

The human corneal epithelial (HCE) cell line used in this study was immortalized by Araki-Sasaki et al. (1995). This cell line was kindly provided by Stephan Reichl, Technische Universität Braunschweig, Germany, who received it from the RIKEN cell bank (Tsukuba, Japan). The HCE cells were used between the 87th and 112th passage number. The HCE cells form a multilayered epithelium when cultivated at the air–liquid interface under serum-free conditions (Seeber et al., 2008). The human corneal keratocytes (HCK) were immortalized and established by Zorn-Kruppa et al. (2005) and Manzer et al. (2009). Also, the HCK cell line was only used for a limited number of passages (passage 13–26 in this study). Both HCE and HCK were cultured as described by Engelke et al. (2013).

The hemi-cornea models were prepared in three steps: preparation of the stroma equivalent, attachment and fixation of the CCC-membrane, and addition of the epithelial cells. For the stroma equivalent, per model 30 μl of F99 medium, 75 μl of reconstruction buffer, 30 μl of KGM medium containing 50,000 HCK cells and 180 μl of the collagen solution was mixed; 250 μl of this solution was placed into the cell culture insert and left for about 25 min

Table 1
List of the selected test chemicals used for the development and the assessment of a test system using the hemi-cornea model with inserted CCC-membrane.

Nos.	Test chemical	Cas No.	Purity (%)	Supplier	Physical state	Chemical class	*in vivo* GHS class[a]
1	3-Methoxy-1,2-propanediol[c]	623-39-2	98	Sigma	Liquid	Alcohol	nc
2	Glycerol[c]	56-81-5	⩾99	Sigma	Liquid	Alcohol	nc
3	3,3-Dimethylpentane[c]	562-49-2	99	Sigma	Liquid	Alkane	nc
4	Toluene[c]	108-88-3	99.8	Sigma	Liquid	Aromatic	nc
5	1-Bromohexane[c]	111-25-1	98	Sigma	Liquid	Brominated deriv.	nc
6	Ethylene glycol diethyl ether	629-14-1	99	Sigma	Liquid	Ether	nc
7	Potassium tetrafluoroborate	14075-53-7	⩾99.99	Sigma	Solid	Inorganic	nc
8	2-Heptanone[c]	110-43-0	99	Sigma	Liquid	Ketone	nc
9	Polyethylene glycol 400[c]	25322-68-3	[b]	Sigma	Liquid	Surfactant	nc
10	Tween 20	9005-64-5	[b]	Sigma	Liquid	Surfactant	nc
11	Methyl cyanoacetate	105-34-0	99	Sigma	Liquid	Acetate	2A
12	2,6-Dichlorobenzoyl chloride[c]	4659-45-4	99	Sigma	Liquid	Acyl halides	2A
13	2-Methyl-1-pentanol[c]	105-30-6	99	Sigma	Liquid	Alcohol	2B
14	Octan-1-ol[c]	111-87-5	>99.5	Sigma	Liquid	Alcohol	2A
15	Ethanol	64-17-5	99.5	AppliChem	Liquid	Alcohol	2A
16	2-Propanol[c]	67-63-0	99.7	AppliChem	Liquid	Alcohol	2A
17	Ammonium nitrate[c]	6484-52-2	>99	Sigma	Solid	Inorganic	2A
18	Acetone[c]	67-64-1	⩾99.7	Roth	Liquid	Ketone	2A
19	3-Chloropropionitrile[c]	542-76-7	98	Sigma	Liquid	Nitrile	2B
20	Dibenzyl phosphate	1623-08-1	99	Sigma	Solid	Organo phosphate	2A
21	2-Methoxyethyl acrylate[c]	3121-61-7	98	Sigma	Liquid	Acrylate	1
22	Cyclohexanol[c]	108-93-0	99	Sigma	Liquid	Alcohol	1
23	p-Fluoroaniline[c]	371-40-4	99	Sigma	Liquid	Aromatic	1[d]
24	Imidazole[c]	288-32-4	99	Sigma	Solid	Heterocyclic	1
25	Chlorhexidine	55-56-1	⩾99.5	Sigma	Solid	Miscellaneous	1
26	Quinacrine[c]	69-05-6	⩾90	Sigma	Solid	Miscellaneous	1
27	Benzalkonium chloride (1%)[c]	8001-54-5	Ultra	Sigma	Liquid	Surfactant	1
28	Cetylpyridinium bromide (6%)[c]	140-72-7	98	Sigma	Liquid	Surfactant	1
29	Trition X-100 (10%)	9002-93-1	[b]	Sigma	Liquid	Surfactant	1
30	Sodium lauryl sulfate (15%)	151-21-3	⩾99	Roth	Liquid	Surfactant	1

[a] *GHS classification:* (United Nations, 2011): nc: unclassified; category 2A/2B: mild/moderately irritating to the eye; 1: irreversible effects to the eye.
[b] Not specified.
[c] The test chemical was also in the test protocol using a 10 min exposure period.
[d] In the ECETOC database the study criteria were not met. Previously classified as severe irritant (R41) by Balls et al. (1999).

at 37 °C to polymerize. Then the CCC membrane was carefully placed on top of the stroma with sterile forceps, avoiding the formation of air bubbles under the membrane. In order to avoid propagation of the HCE cells underneath the CCC-membrane, i.e. on top of the stroma, the membrane was fixed with an O-ring which had been immersed in the attachment solution beforehand. These constructs were incubated for another 10 min at 37 °C until the attachment solution was polymerized and hence adhered to the CCC-membrane. Afterwards, 100,000 HCE cells suspended in 70 µl of KGM medium were plated in the center of the O-ring. An additional 230 µl of KGM medium was added to the insert the next day, after about 18 h. Usually, 20–30 hemi-cornea models were produced per batch. The models were cultured in 12-well plates for the first 6 days, submerged in 1.5 ml KGM medium which was changed once after 3 days. Then the inserts were transferred into 6-well plates and the amount of medium was lowered to 1.2 ml. The models were cultivated at the air liquid interface for the next 7 days with daily change of medium.

2.5. Histology

For histological evaluation of the tissue production, untreated tissues were fixed with Bouin's fixation fluid and embedded in paraffin. Cross-sections of 7 µm thickness were cut and stained either with Hematoxylin–Eosin or Azan using standard procedures.

2.6. Test protocol

The hemi-cornea tissues were exposed to the test chemicals at room temperature (RT). For liquid test chemicals, 50 µl was applied in the middle of the O-rings on the epithelium of the corneal tissues. Solid test substances were applied topically onto the epithelium of the hemi-cornea tissues using an oval, 6 mm Volkmann bone curette (Wittex, Simbach Germany), which was calibrated with a defined volume of about 50 mg NaCl. To ensure contact and spreading of the solids, 50 µl of PBS++ was additionally pipetted on top of the epithelium. The further treatments were the same as described for the liquid chemicals. All chemicals as well as NCs and BCs were tested at room temperature for 60 min exposure time. Selected chemicals were also incubated for 10 min in order to find the most suitable time point, resulting in the highest degree of separation between the GHS classes.

After exposure, the tissues were washed according to the protocol of Engelke et al. (2013), the O-rings were removed from the tissues and the inserts were transferred to a 24-well holding plate and incubated with 500 µl KGM medium. For the MTT viability assay the CCC membrane with the epithelial layer was separated from the stroma with forceps. The epithelia on the CCC-membrane were placed in a 24-well plate. The inserts with the stroma were placed in another 24-well plate. In this way the stroma and the epithelium could be assessed individually for cell survival. The preliminary results of the NC revealed that the separation of the epithelium and stroma does not effect the viability of the cells in the respective tissues. In contrast, the sum of optical densities of the separated tissues, compared to the unseparated tissues, had a tendency to give higher values. This may results from the fact that the diffusion is limiting for the MTT metabolism. Less MTT is metabolized to Formazan in the chosen incubation time due to the longer diffusion path in the unseparated tissue. The MTT solution, 1.5 ml per well, was added to each well of the 24-well plates and incubated for 3 h at 37 °C. For solubilization of the formazan, the MTT solution was removed from the wells and 1.5 ml isopropanol was added to each well and left overnight in a dark place at RT, sealed with parafilm to avoid the evaporation of the solvent.

The next day, 100 µl triplicate samples from each tissue were transferred to a 96-well plate and further diluted 1:1 with 100 µl of isopropanol. The optical densities (OD) were measured on a microplate reader (Dynatech MR5000, Dynex Technologies GmbH, Denkendorf, Germany) at 570 nm. 200 µl of isopropanol served as the blank. The relative tissue viability was determined for each tissue using the following formula:

$$\%\text{Viability} = [\text{OD(treated tissues}/\text{OD(NC)}] \times 100\%$$

The relative viability was calculated from the OD as a percentage of the NC (=100% viability) for each sample. The mean ± standard deviation (SD) was determined from triplicate tissues.

To avoid false negative results, possible direct interaction of the selected test chemicals with the MTT-assay was tested (see Engelke et al., 2013 for details).

2.7. Data analysis

All test chemicals were tested in three independent runs on triplicate tissues, each together with NCs and BCs. All further statistical calculations were performed using Microsoft Office Excel version 2013. The agreement between *in vivo* and *in vitro* data was assessed after classification of the tested chemicals into three GHS classes: GHS1, GHS2 and GHSnc. Cut-off values of obtained viability data were defined for both epithelium and stroma. Classification of the chemicals into the 3 GHS classes is based on the appropriate combination of these cut-offs.

Contingency tables were used to evaluate the agreement between *in vivo* and *in vitro* classifications. By means of this analysis, the calculation of the percentage of products correctly classified by the test system was possible, as well as the number of false positives (over-estimations) and false negatives (under-estimations).

The Kappa coefficient (κ) (Landis and Koch, 1977) was calculated to define the degree of concordance between both compared methods (*in vivo*/*in vitro*).

3. Results

3.1. Development of the hemi-cornea model with inserted CCC-membrane

In order to find the best method to successfully separate the epithelium from the stromal layer, we explored different attachment approaches by using different materials. We found that the best results, as well as the easiest procedure, were obtained with the use of a CCC-membrane attached directly on top of the stroma and fixed with a Teflon O-ring, which was previously immersed in a collagen solution. The hemi-cornea construct thus obtained exhibits a multilayer of epithelial cells on top of the CCC-membrane which separates the epithelium from the collagenous stromal matrix with embedded HCK cells (Fig. 1). The other attachment methods we initially explored included pretreating of the CCC-membrane with KGM medium or PBS−− for 30 min at room temperature prior to attachment, applying 50 µl of collagen solution on top of the stromal layer as an adhesive, or shortly immersing the membrane in the collagen solution. None of these methods helped to attach the CCC-membrane properly and the epithelial cells were found growing under the membrane. Other efforts, for instance the use of electrospun membranes of 10 µm or 20 µm thickness, silicon instead of Teflon O-rings and agarose or histo-acryl as glue were disappointing either due to cell toxicity or extensive preparation and migration of epithelial cells onto the stroma.

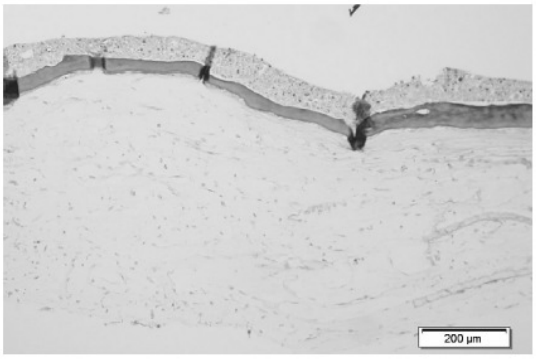

Fig. 1. Histological cross section of the hemi-cornea model with a CCC-membrane inserted between epithelium and stroma. The tissue section is 7 µm thick and was stained with Azan. The picture was taken at a 10× objective.

3.2. Development of a prediction model

For the development of an adequate prediction model, 30 chemicals with different physicochemical properties and irritation potentials were tested (Table 1). The means and standard deviations (SD) of three independent runs were calculated (Table 2). The average viability (%) of the epithelium was plotted versus the viability (%) of the stroma for each test substance (Fig. 2). The chemicals belonging to GHS1 (diamonds) show almost no epithelial viability and stromal viability <35%. These chemicals cluster in the lower left corner of the diagram. The separation between the GHS2 (squares) and GHSnc (circles) chemicals is less clear, but an epithelial viability >15% divides the two groups most clearly. Thus, an appropriate combination of epithelial and stromal viability may allow us to discriminate between severe/irreversible irritants (GHS1), chemicals which are mild or moderately irritating (GHS2) and chemicals which are slightly or not irritating to the eye (GHSnc). A horizontal and a vertical line mark the cut-offs for discrimination into these three groups. The combinations of the cut-off values from the epithelium and stroma define the prediction model (PM) for the classification of the test chemicals into the three GHS-classes as shown in Table 3. According to the PM, all test chemicals which induce a reduction of the stromal viability to less than 35% compared to the NC_{stroma} are predicted as GHS1. Test chemicals which reduce the epithelial viability to less than 15% of the NC_{epi}, but with a stromal viability higher than 35% compared to the NC_{stroma} are predicted as GHS2. Only test chemicals with an epithelial viability higher than 15% compared to NC_{epi} and a stromal viability higher than 35% of the NC_{stroma} are predicted as non-irritant according to the GHS system.

The classification of the tested chemicals according to the PM defined in Table 3 is included in the last column of Table 2. All falsely classified chemicals are shaded in grey. False classification results from the fact that either the stromal viability or/and the epithelial viability do not comply with the criteria defined in the PM (Table 3). The comparison of the *in vitro* classification with the *in vivo* classification of the 30 test chemicals in Table 1 demonstrates a perfect prediction of all severe irritants (GHS1). Eight out of ten GHS2 chemicals, but only five out of ten GHSnc test chemicals were predicted correctly. Thus, GHS1 and other GHS groups can be well discriminated. Discrimination between GHS2 and GHSnc does not perform as well, since four out of ten GHSnc chemicals were predicted to be GHS2, and one out of ten (tween 20) to be GHS1.

We tested whether the accuracy of the prediction could be improved by the reduction of the exposure period, assuming that

Table 2
Tissue viability (%) of epithelium and stroma from each run (means and standard deviations of three tissues per run) after exposure for 60 min with the test chemicals, as well as means and standard deviations of the three runs. The last column includes the *in vitro* predicted classification of each of the test chemicals. False predictions are highlighted.

Nr	Test chemical	Epithelial tissue viability (%)					Stromal tissue viability (%)					in vitro GHS class
	name	run 1	run 2	run 3	mean	SD	run 1	run 2	run 3	mean	SD	
1	3-Methoxy-1,2-propanediol	8,09	7,15	8,38	7,87	0,64	46,15	71,07	41,38	52,87	15,94	2
2	Glycerol	25,49	29,16	9,19	21,28	10,63	80,73	84,23	81,47	82,14	1,84	nc
3	3,3-Dimethylpentane	36,78	28,99	33,64	33,14	3,92	102,68	91,10	117,02	103,60	12,99	nc
4	Toluene	3,40	6,49	3,35	4,41	1,80	31,85	45,58	49,91	42,45	9,43	2
5	1-Bromohexane	26,39	22,16	22,35	23,63	2,39	87,68	88,14	68,13	81,32	11,43	nc
6	Ethylene glycol diethyl ether	3,20	0,71	1,84	1,92	1,24	61,97	38,57	32,52	44,35	15,55	2
7	Potassium tetrafluoroborate	77,69	113,03	82,03	90,92	19,27	78,93	92,84	89,95	87,24	7,34	nc
8	2-Heptanone	2,50	2,67	1,37	2,18	0,71	72,66	72,72	62,13	69,17	6,10	2
9	Polyethylene glycol 400	41,03	37,97	30,09	36,36	5,65	93,40	84,08	68,61	82,03	12,52	nc
10	Tween 20	21,32	33,06	19,67	24,68	7,30	15,61	26,74	9,40	17,25	8,79	1
11	Methyl cyanoacetate	5,40	2,53	2,32	3,42	1,72	31,53	51,69	45,54	42,92	10,33	2
12	2,6-Dichlorobenzoyl chloride	40,33	35,40	22,82	32,85	9,03	98,52	81,98	89,61	90,04	8,28	nc
13	2-Methyl-1-pentanol	3,02	3,24	2,81	3,02	0,21	55,56	42,63	38,91	45,70	8,74	2
14	Octan-1-ol	3,43	4,16	4,43	4,01	0,51	62,47	52,22	60,44	58,38	5,43	2
15	Ethanol	2,07	4,10	3,90	3,36	1,12	31,39	53,88	67,69	50,99	18,32	2
16	2-Propanol	4,50	2,55	4,21	3,75	1,05	59,15	49,31	41,86	50,11	8,67	2
17	Ammonium nitrate	2,52	1,15	1,88	1,85	0,69	49,41	28,70	39,20	39,11	10,35	2
18	Acetone	10,91	4,10	5,62	6,88	3,57	83,54	81,36	69,69	78,20	7,45	2
19	3-Chloropropionitrile	5,05	2,45	2,61	3,37	1,46	62,33	68,43	84,30	71,69	11,34	2
20	Dibenzyl phosphate	5,18	3,57	3,75	4,16	0,88	7,59	4,43	7,05	6,36	1,69	1
21	2-Methoxyethyl acrylate	2,21	1,65	0,94	1,60	0,64	38,05	23,63	32,44	31,38	7,27	1
22	Cyclohexanol	2,39	1,17	1,74	1,77	0,61	22,08	23,07	17,23	20,80	3,13	1
23	p-Fluoroaniline	2,44	3,11	2,66	2,74	0,34	6,12	4,47	6,01	5,53	0,93	1
24	Imidazole	3,41	1,94	3,97	3,11	1,05	9,64	7,32	16,58	11,18	4,82	1
25	Chlorhexidine	4,46	2,76	3,22	3,48	0,87	8,21	3,72	5,31	5,74	2,28	1
26	Quinacrine	83,96	89,05	72,25	81,75	8,61	24,18	24,18	20,18	22,85	2,31	1
27	Benzalkonium chloride (1%)	3,93	4,22	4,45	4,20	0,26	2,41	6,70	5,99	5,03	2,30	1
28	Cetylpyridinium bromide (6%)	4,03	2,91	3,81	3,58	0,59	9,66	5,02	11,44	8,71	3,31	1
29	Trition X-100 (10%)	2,83	2,08	1,12	2,01	0,86	3,59	5,18	2,72	3,83	1,25	1
30	Sodium lauryl sulfate (15%)	3,06	2,38	2,05	2,50	0,52	4,26	2,32	11,03	5,87	4,57	1

a short exposure period would increase the selectivity between GHSnc and GHS2. Hence, we repeated the test for a selected group of test chemicals with an exposure period of 10 min. The selected test chemicals are marked in Table 1. The plot of the mean viability (%) of the epithelium versus the viability (%) of the stroma for each test substance (Fig. 3) reveals that the shorter exposure time did not improve the discrimination between GHSnc and GHS2. Instead, the discriminatory power of the test systems was compromised and the selectivity between all three classes was dramatically reduced. Hence, we did not conduct a detailed analysis of the data obtained from the test protocol using the 10 min exposure protocol.

3.3. Reliability and predictive capacity of the test system

We performed a statistical analysis of the *in vitro* classification from the results using the 60 min exposure test protocol and the PM presented in Table 3 in order to assess the reliability and predictive capacity of the test system. The *in vitro* results and *in vivo* Draize test results are compared in a contingency table (Table 4). The bottom row lists the percentage of correct classifications (producer accuracy) for the three GHS categories, and the last column lists the user accuracy. The producer accuracy refers to the probability that a test chemical of a certain GHS class is correctly classified as such, while the user accuracy refers to the probability that a test chemical assigned as a certain GHS class using the *in vitro* test really belongs to this class.

Thus, all GHS1 test chemicals, 80% of the GHS2 test chemicals and 50% of the GHSnc test chemicals were predicted correctly. In conclusion, the selectivity between thesevere and the moderate/mild irritant is very good, but 50% of the non-irritants were overestimated. The user accuracies are 83%, 67% and 83% for the GHS1, GHS2 and GHSnc, respectively. According to these results, 83% of the substances classified as GHS1 and GHSnc *in vitro* test indeed belong to these classes. In contrast, 4 of 12 test chemicals

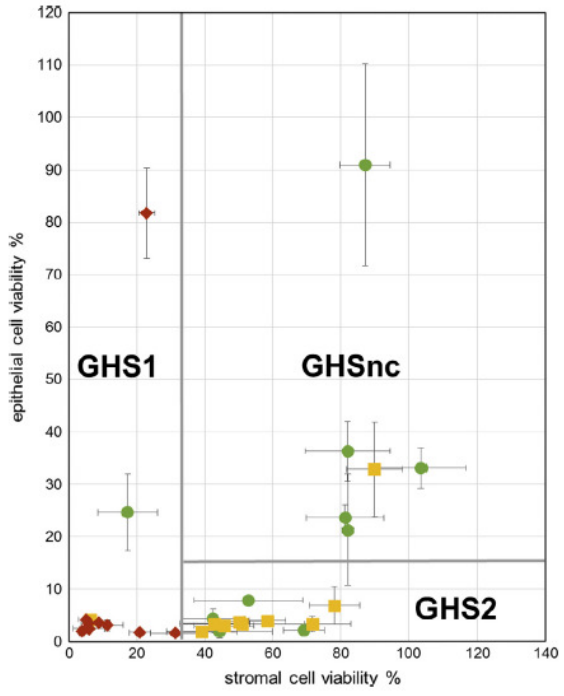

Fig. 2. Plot of epithelial versus stromal viabilities after 60 min exposure period for each test substance. A horizontal and a vertical line indicate the discrimination of the three groups. The data points represent the corresponding *in vivo* classification: GHS1 (◆), GHS2 (■) and GHSnc (●).

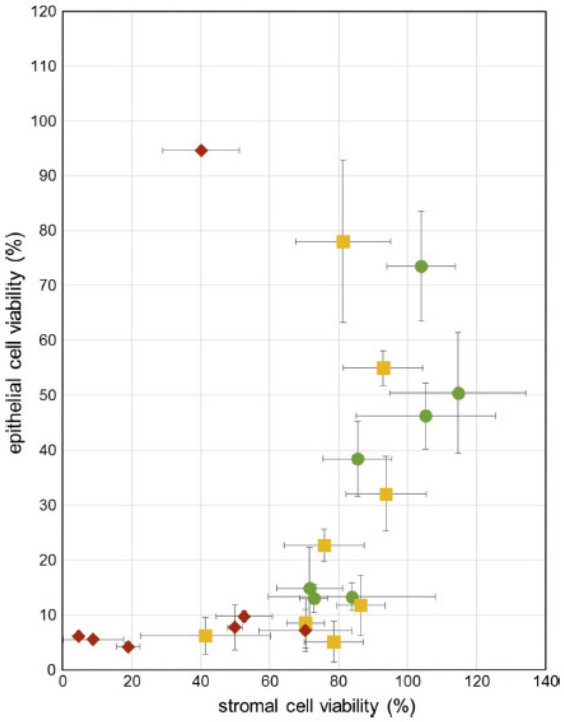

Fig. 3. Plot of epithelial versus stromal viabilities after 10 min exposure period for each test substance. The data points represent the corresponding *in vivo* classification: GHS1 (◆), GHS2 (■) and GHSnc (●).

Table 3
Prediction model based on the viabilities (%) from both the epithelium and the stroma (see Table 2) after chemical treatment. Cut-off values of obtained viability data were defined for both epithelium and stroma and their combination results in classification of the test chemicals into three classes.

Epithelial viability (%)	Operator	Stromal viability (%)	*In vitro* GHS class
>15	AND	>35	nc
<15	AND	>35	2
		<35	1

predicted as GHS2 were classified as GHSnc by the Draize test. In consequence, the test system is over-predictive with regard to the GHSnc chemicals.

Table 5 contains the statistical parameters obtained through concordance analysis of the *in vitro* test system. The kappa coefficient (κ) of 0.65 and a concordance rate of 77% imply a substantial agreement between the *in vitro* and *in vivo* estimates. The under-estimation rate of only 3% is very low, but the high percentage of over-predicted non-irritant test chemicals result in an overall over-estimation rate of 20%.

3.4. Reproducibility of the production over time

Fig. 4 represents the obtained MTT-derived OD-values of the NC for both the epithelium (NC_{epi}) and the stroma (NC_{stroma}) from all batches. The average ± standard deviation of the 26 batches are $NC_{epi} = 0.58 \pm 0.14$ for the epithelium, and $NC_{stroma} = 0.71 \pm 0.23$ for the stroma. Both NC_{epi} and NC_{stroma} exhibit a tendency to decrease over time beginning with batch number 14, but the BCs of both the epithelium (BC_{epi}) and the stroma (BC_{stroma}) remain relatively constant and outliers of the NC_{epi} did not inevitably affect the BC_{epi}. (Fig. 5). The averaged viability (%) and standard deviation of the 26 batches are: $BC_{epi} = 7.0\% \pm 3.3\%$ and for $BC_{stroma} = 31.9\% \pm 9.8\%$. Based on the obtained averages for both NCs and BCs, we defined threshold values $NC_{epi} > 0.4$ and $NC_{stroma} > 0.5$ and $BC_{epi} < 10\%$ and $BC_{stroma} < 50\%$, as acceptance criteria.

4. Discussion

A test system for eye irritation testing based on the hemi-cornea model has already been evaluated regarding quality control of production, reliability and predictive capacity (Engelke et al., 2013). The protocol of that study used the overall tissue viability (MTT assay) as the read-out parameter. The sensitivity of that test system was 77% and specificity varied between 57% and 86% (dependent on the laboratory) to discriminate classified from non-classified chemicals. We concluded that additional physiologically relevant endpoints in both epithelium and stroma have to be developed for the reliable prediction of all GHS classes of eye irritation in one stand-alone test system. In order to benefit from this sophisticated model we developed a method that allows the separation of the epithelium and stroma by the insertion of a membrane between these compartments during production. The insertion of the membrane has to fulfil several demands: on the one hand, the membrane has to attach directly to the surface of the stroma to avoid migration and expansion of the epithelial cells underneath, on the other hand, the membrane should not stick to the surface, because it has to be detached easily after chemical treatment. In addition, the inserted membrane should be made from a similar material (collagen) to the Bowman's membrane in the human cornea, otherwise it might reduce the irritation of the

Table 4
Contingency table of predicted GHS classes versus *in vivo* Draize test data including the resulting producer and user accuracy (%).

		In vivo/Draize-test			Total *in vitro*	User accuracy (%)
		GHS1	GHS2	GHSnc		
In vitro test	GHS1	10	1	1	12	83
	GHS2	0	8	4	12	67
	GHSnc	0	1	5	6	83
Total *in vivo*		10	10	10	30	
Producer accuracy (%)		100	80	50		

Table 5
Statistical analysis of obtained data using concordance analysis.

Nr of test chemicals (n)	30
Kappa coefficient (κ)	0.65
Concordance rate (%)	77
Under-estimated rate (%)	3
Over-estimated rate (%)	20

chemicals on the stromal compartment and in this way yield a false GHS classification. These requirements could only be achieved using the CCC-membrane and its immobilization with a Teflon O-ring. The unwanted growth of HCE cells on the stromal surface was only observed in case of an improper fixation of the CCC-membrane and could be detected from the folding of the membrane 2 or 3 days after production.

In order to assess the ability of this *in vitro* method to categorize ocular irritants, the effect of test chemicals on the epithelium and/or the stromal were compared. In general, the results show that the induced decrease in cell viability in the epithelium and/or stroma irritants correlates to the *in vivo* irritancy potential of the test chemicals. Irritants known to produce no or slight irritation in the Draize Test (ECETOC, 1998) produced a decrease in cellular viability that was mainly limited to the epithelium. Irritants classified as mild/moderate (GHS2) produced a complete viability loss to the corneal epithelium that extended into the stroma. Chemicals classified as severe/corrosive irritants (GHS1) produced an extensive stromal damage besides complete viability loss to the corneal epithelium. Consequently, these findings indicate that differences between different levels of irritants categorized by the Draize test can be simulated in the *in vitro* test system.

The complex test system requires cut-off value definition for both the epithelium and the stroma. With adequate combinations of these cut-offs, the tested chemicals can be classified into three groups. The cut-off values and their combinations were chosen so as to achieve an optimal assignment of the test chemicals according to the GHS classification. The comparison of the *in vitro* and *in vivo* classifications of the 30 test chemicals demonstrates the utility of the *in vitro* test in identifying and discriminating between severe irritants (GHS1) and substances which are mild

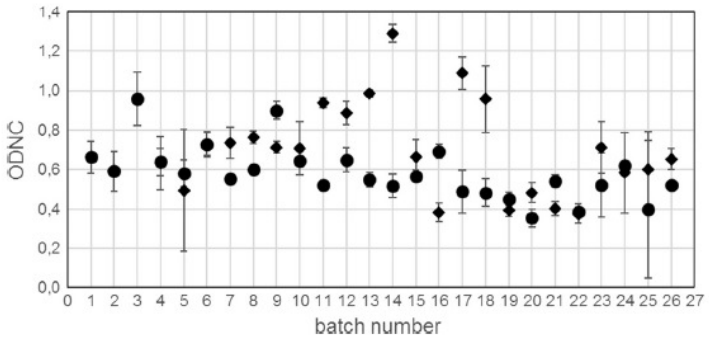

Fig. 4. Optical density of the NC from 26 independent batches for both epithelium (●) and stroma (♦). Data points represent the means of 3 tissues. NCs were treated for a 60 min exposure period with PBS^{++} at room temperature.

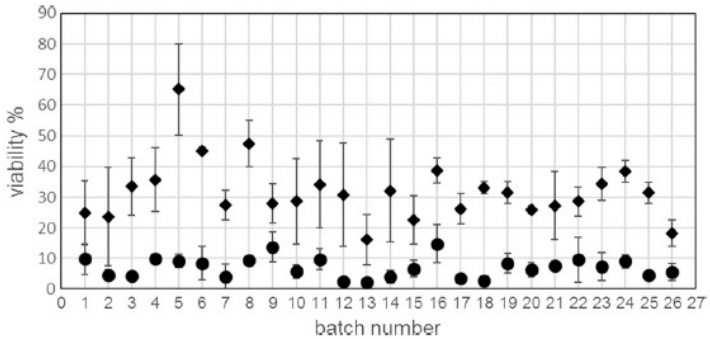

Fig. 5. Viability (%) of the BC from 26 independent batches for both epithelium (●) and stroma (♦). Data points represent the means of 3 tissues. BCs were treated for a 60 min exposure period with 0.3% Triton X-100 at room temperature.

or moderately irritant (GHS2). It also clearly reflects a high percentage of over-estimation of chemicals classified as non-irritant *in vivo* (GHSnc). All of the GHS1 test chemicals, 80% of the GHS2 test chemicals and 50% of the GHSnc test chemicals were predicted correctly. While the selectivity between the severe and the moderate/mild irritants is high, 50% of the non-irritants were over-estimated. In consequence, the test system is over-predictive with regard to the GHSnc chemicals.

For some substances, this may be explained by the fact that these substances are very viscous and hence carry away the upper epithelial cell layers during the washing procedure. Some GHSnc-classified test chemicals such as toluene, 3-methoxy-1,2-propanediol, ethylene glycol diethyl ether and 2-heptanone not only damaged the epithelium, but also led to a substantial loss in the stromal viability. In general, only if the residual viability of the epithelium was >20% compared to the NC_{epi}, did the stromal viability remain close to 100%. The sole exception was Tween 20, a surfactant that was also classified as GHSnc from the Draize test data, and which induced an extensive damage to the stromal viability despite an epithelial viability of >20%.

We obtained inconsistent results for 2,6-dichlorobenzoyl chloride. Despite the fact that 2,6-dichlorobenzoyl chloride is a GHS2 class chemical according to the Draize test, it had only little effect on the epithelium and almost no effect on the stroma. This may be ascribed to the fact that 2,6-dichlorobenzoyl chloride is insoluble in water and did not spread on the entire surface of the hemi-cornea.

Within the group of severe irritants, quinacrine forms an exception as it has little effect to the epithelium, but affects the stroma.

The dissatisfactory results obtained for GHSnc chemicals may be due to the fact that the epithelium of the hemi-cornea model displays no proper barrier function. This hypothesis is supported by the outcome of the previous inter-laboratory prevalidation study (Engelke et al., 2013). This study revealed that the time-dependent exponential decay of cell viability in the hemi-cornea model (without inserted CCC-membrane) is monophasic. Hence, the diffusion kinetics of the tested chemicals are comparable in both epithelium and stroma, because the epithelium does not exert a particular barrier function. The results of the present study also indicate that the decrease in tissue viability is a diffusion-controlled process which is basically dependent on the stromal part which constitutes at least 90% of the hemi-cornea thickness. The diffusion of the tested chemicals is limited by their diffusion coefficient in the hydrous collagen and the cells serve as toxic markers. From this point of view, the hemi-cornea model presents a 3D cell toxicity assay that, in contrast to standard cultured cell based assays, combines both the diffusion coefficient and inherent cell toxicity of a test chemical. However, the PM shows that both compartments are necessary for the prediction of all three GHS classes: the stroma compartment is sufficient to discriminate GHS1 from GHS2 and GHSnc chemicals, but the epithelium is essential for the discrimination of GHSnc from GHS1 and GHS2.

Obtained MTT-derived OD-values of NC and BC for both epithelium (NC_{epi}, BC_{epi}) and stroma (NC_{stroma}, BC_{stroma}) were collected to assess the reproducibility of production. For all the batches produced over the 6 months experimental period, we used 12 continuous passages for both cell lines, beginning from passage number 100 for HCE and passage 13 for HCK, respectively. The decrease in the number of epithelial cell layers and HCK growth rate may be attributed to an altered genomic content after extensive passages, as reported for other SV40-immortalized cell lines (Ray et al., 1990; Stewart and Bacchetti, 1991). In addition, the used HCE cell line is composed of numerous heterogeneous cell populations, since such genomic aberrations randomly occur and may vary among individual cells (Yamasaki et al., 2009).

5. Conclusions

The current report shows that the individual quantification of cell viability in the stroma and epithelium using the MTT-assay can be used to reflect all GHS categories. For the first time, a cell-based test system was developed which proved to be suitable for identifying and discriminating between severe irritants (GHS1) and substances which are mild or moderately irritant (GHS2). The kappa coefficient of 0.65 and a concordance rate of 77% imply a substantial agreement between *in vitro* and *in vivo* estimates, despite the over-predictivity of GHSnc classified chemicals. In addition, for the identification of GHSnc, the user accuracy was as good as for the identification of GHS1, suggesting that the method prediction of GHSnc materials is also good. However, for the prediction of all three GHS categories we suggest the combination of the presented test system with a method which more reliably identifies GHSnc materials.

Conflict of Interest

The authors declare that there are no conflicts of interest.

Transparency Document

The Transparency document associated with this article can be found in the online version.

Acknowledgments

This project was funded by the German Federal Ministry of Education and Research, FKZ 0316010C. The authors would like to acknowledge Dr. Miriam Grace for proofreading the manuscript.

References

Adriaens, E., Dhondt, M.M., Remon, J.P., 2005. Refinement of the Slug Mucosal Irritation test as an alternative screening test for eye irritation. Toxicol. In Vitro 19, 79–89. http://dx.doi.org/10.1016/j.tiv.2004.06.004.

Adriaens, E., Bytheway, H., De Wever, B., Eschrich, D., Guest, R., Hansen, E., Vanparys, P., Schoeters, G., Warren, N., Weltens, R., Whittingham, A., Remon, J.P., 2008. Successful prevalidation of the slug mucosal irritation test to assess the eye irritation potency of chemicals. Toxicol. In Vitro 22, 1285–1296. http://dx.doi.org/10.1016/j.tiv.2008.02.018.

Araki-Sasaki, K., Ohashi, Y., Sasabe, T., Hayashi, K., Watanabe, H., Tano, Y., Handa, H., 1995. An SV40-immortalized human corneal epithelial cell line and its characterization. Invest. Ophthalmol. Vis. Sci. 36, 614–621.

Balls, M., Berg, N., Bruner, L.H., Curren, R.D., de Silva, O., Earl, L.K., Esdaile, D.J., Fentem, J.H., Liebsch, M., Ohno, Y., Prinsen, M.K., Spielmann, H., Worth, A.P., 1999. Eye irritation testing: the way forward. Altern. Lab. Anim. 27, 53–77.

Barile, F.A., 2010. Validating and troubleshooting ocular in vitro toxicology tests. J. Pharmacol. Toxicol. Methods 61, 136–145. http://dx.doi.org/10.1016/j.vascn.2010.01.001.

Doucet, O., Lanvin, M., Thillou, C., Linossier, C., Pupat, C., Merlin, B., Zastrow, L., 2006. Reconstituted human corneal epithelium: a new alternative to the Draize eye test for the assessment of the eye irritation potential of chemicals and cosmetic products. Toxicol. In Vitro 20, 499–512. http://dx.doi.org/10.1016/j.tiv.2005.09.005.

Draize, J., Woodward, G., Calvery, H., 1944. Methods for the study of irritation and toxicity of substances applied topically to the skin and mucous membranes. J. Pharmacol. Exp. Ther. 82, 377–390.

ECETOC, 1998. Eye Irritation: Reference Chemicals Data Bank. Technical Report No. 48 (2), European Center for Ecotoxicology and Toxicology of Chemicals, Brussels, Belgium.

Engelke, M., Patzke, J., Tykhonova, S., Zorn-Kruppa, M., 2004. Assessment of ocular irritation by image processed quantification of cell injury in human corneal cell cultures and in corneal constructs. Altern. Lab. Anim. 32, 345–353.

Engelke, M., Zorn-Kruppa, M., Gabel, D., Reisinger, K., Rusche, B., Mewes, K.R., 2013. A human hemi-cornea model for eye irritation testing: quality control of production, reliability and predictive capacity. Toxicol. In Vitro 27, 458–468. http://dx.doi.org/10.1016/j.tiv.2012.07.011.

Eskes, C., Bessou, S., Bruner, L., Curren, R., Harbell, J., Jones, P., Kreiling, R., Liebsch, M., McNamee, P., Pape, W., Prinsen, M.K., Seidle, T., Vanparys, P., Worth, A., Zuang, V., 2005. Eye irritation. Altern. Lab. Anim. 33 (suppl. 1), 47–81.

Eskes, C., Hoffmann, S., Facchini, D., Ulmer, R., Wang, A., Flego, M., Vassallo, M., Bufo, M., van Vliet, E., d'Abrosca, F., Wilt, N., 2014. Validation study on the Ocular Irritection(R) assay for eye irritation testing. Toxicol. In Vitro. http://dx.doi.org/10.1016/j.tiv.2014.02.009.

Gautheron, P., Dukic, M., Alix, D., Sina, J.F., 1992. Bovine corneal opacity and permeability test: an in vitro assay of ocular irritancy. Fundam. Appl. Toxicol. 18, 442–449.

Hahne, M., Reichl, S., 2011. Development of a serum-free human cornea construct for in vitro drug absorption studies: the influence of varying cultivation parameters on barrier characteristics. Int. J. Pharm. 416, 268–279. http://dx.doi.org/10.1016/j.ijpharm.2011.07.004.

Hahne, M., Zorn-Kruppa, M., Guzman, G., Brandner, J.M., Haltner-Ukomado, E., Watzig, H., Reichl, S., 2012. Prevalidation of a human cornea construct as an alternative to animal corneas for in vitro drug absorption studies. J. Pharm. Sci. 101, 2976–2988. http://dx.doi.org/10.1002/jps.23190.

Hartung, T., Bruner, L., Curren, R., Eskes, C., Goldberg, A., McNamee, P., Scott, L., Zuang, V., 2010. First alternative method validated by a retrospective weight-of-evidence approach to replace the Draize eye test for the identification of non-irritant substances for a defined applicability domain. ALTEX 27, 43–51.

Hayashi, K., Mori, T., Abo, T., Ooshima, K., Hayashi, T., Komano, T., Takahashi, Y., Sakaguchi, H., Takatsu, A., Nishiyama, N., 2012. Two-stage bottom-up tiered approach combining several alternatives for identification of eye irritation potential of chemicals including insoluble or volatile substances. Toxicol. In Vitro 26, 1199–1208. http://dx.doi.org/10.1016/j.tiv.2012.06.008.

Huhtala, A., Salminen, L., Tähti, H., Uusitalo, H. (2008). Corneal Models for the Toxicity Testing of Drugs and Drug Releasing Materials. In: Ashammakhi, N. (Ed.), Topics in multifunctional biomaterials and devices.

Jester, J.V., 2006. Extent of corneal injury as a biomarker for hazard assessment and the development of alternative models to the Draize rabbit eye test. Cutan. Ocul. Toxicol. 25, 41–54. http://dx.doi.org/10.1080/15569520500536626.

Jester, J.V., Li, H.F., Petroll, W.M., Parker, R.D., Cavanagh, H.D., Carr, G.J., Smith, B., Maurer, J.K., 1998a. Area and depth of surfactant-induced corneal injury correlates with cell death. Invest. Ophthalmol. Vis. Sci. 39, 922–936.

Jester, J.V., Petroll, W.M., Bean, J., Parker, R.D., Carr, G.J., Cavanagh, H.D., Maurer, J.K., 1998b. Area and depth of surfactant-induced corneal injury predicts extent of subsequent ocular responses. Invest. Ophthalmol. Vis. Sci. 39, 2610–2625.

Jester, J.V., Li, L., Molai, A., Maurer, J.K., 2001. Extent of initial corneal injury as a basis for alternative eye irritation tests. Toxicol. In Vitro 15, 115–130.

Jester, J.V., Ling, J., Harbell, J., 2010. Measuring depth of injury (DOI) in an isolated rabbit eye irritation test (IRE) using biomarkers of cell death and viability. Toxicol. In Vitro 24, 597–604. http://dx.doi.org/10.1016/j.tiv.2009.10.010.

Kaluzhny, Y., Kandarova, H., Hayden, P., Kubilus, J., d'Argembeau-Thornton, L., Klausner, M., 2011. Development of the EpiOcular(TM) eye irritation test for hazard identification and labelling of eye irritating chemicals in response to the requirements of the EU cosmetics directive and REACH legislation. Altern. Lab. Anim. 39, 339–364.

Katoh, M., Hamajima, F., Ogasawara, T., Hata, K., 2013. Establishment of a new in vitro test method for evaluation of eye irritancy using a reconstructed human corneal epithelial model, LabCyte CORNEA-MODEL. Toxicol. In Vitro 27, 2184–2192. http://dx.doi.org/10.1016/j.tiv.2013.08.008.

Kolle, S.N., Kandarova, H., Wareing, B., van Ravenzwaay, B., Landsiedel, R., 2011. In-house validation of the EpiOcular(TM) eye irritation test and its combination with the bovine corneal opacity and permeability test for the assessment of ocular irritation. Altern. Lab. Anim. 39, 365–387.

Landis, J.R., Koch, G.G., 1977. The measurement of observer agreement for categorical data. Biometrics 33, 159–174.

Manzer, A.K., Lombardi-Borgia, S., Schafer-Korting, M., Seeber, J., Zorn-Kruppa, M., Engelke, M., 2009. SV40-transformed human corneal keratocytes: optimisation of serum-free culture conditions. ALTEX 26, 33–39.

Maurer, J.K., Parker, R.D., Jester, J.V., 2002. Extent of initial corneal injury as the mechanistic basis for ocular irritation: key findings and recommendations for the development of alternative assays. Regul. Toxicol. Pharmacol. 36, 106–117.

McNamee, P., Hibatallah, J., Costabel-Farkas, M., Goebel, C., Araki, D., Dufour, E., Hewitt, N.J., Jones, P., Kirst, A., Le Varlet, B., Macfarlane, M., Marrec-Fairley, M., Rowland, J., Schellauf, F., Scheel, J., 2009. A tiered approach to the use of alternatives to animal testing for the safety assessment of cosmetics: eye irritation. Regul. Toxicol. Pharmacol. 54, 197–209. http://dx.doi.org/10.1016/j.yrtph.2009.04.004.

OECD, 2002. Acute Eye Irritation/Corrosion. OECD Guidline for Testing of Chemicals No. 405, Organisation for Economic Cooperation and Development, Paris, France. Retrieved from <http://www.oecd-ilibrary.org/environment/oecd-1039-guidelines-for-the-testing-of-chemicals-section-4-health-effects_20745788>.

OECD, 2012. Fluorescein Leakage Test Method for Identifying Ocular Corrosives and Severe Irritants. OECD Guidline for the Testing of Chemicals No. 460, Organisation for Economic Cooperation and Development, Paris, France. Retrieved from <http://www.oecd-ilibrary.org/environment/oecd-guidelines-for-the-testing-of-chemicals-section-4-health-effects_20745788>.

OECD, 2013a. Test Guideline 438: Isolated Chicken Eye Test method for identifying i) chemicals inducing serious eye damage and ii) chemicals not requiring classifications for eye irritation or serious eye damage. OECD Guidline for the Testing of Chemicals No. 438, Organisation for Economic Cooperation and Development, Paris, France. Retrieved from <http://www.oecd-ilibrary.org/environment/oecd-guidelines-for-the-testing-of-chemicals-section-4-health-effects_20745788>.

OECD, 2013b. Bovine Corneal Opacity and Permeability Test method for identifying i) chemicals inducing serious eye damage and ii) chemicals not requiring classification for eye irritation or serious eye damage. OECD Guidline for the Testing of Chemicals No. 437, Organisation for Economic Cooperation and Development. Retrieved from <http://www.oecd-ilibrary.org/environment/oecd-guidelines-for-the-testing-of-chemicals-section-4-health-effects_20745788>.

Prinsen, M.K., Koeter, H.B., 1993. Justification of the enucleated eye test with eyes of slaughterhouse animals as an alternative to the Draize eye irritation test with rabbits. Food Chem. Toxicol. 31, 69–76.

Ray, F.A., Peabody, D.S., Cooper, J.L., Cram, L.S., Kraemer, P.M., 1990. SV40 T antigen alone drives karyotype instability that precedes neoplastic transformation of human diploid fibroblasts. J. Cell. Biochem. 42, 13–31. http://dx.doi.org/10.1002/jcb.240420103.

Sakaguchi, H., Ota, N., Omori, T., Kuwahara, H., Sozu, T., Takagi, Y., Takahashi, Y., Tanigawa, K., Nakanishi, M., Nakamura, T., Morimoto, T., Wakuri, S., Okamoto, Y., Sakaguchi, M., Hayashi, T., Hanji, T., Watanabe, S., 2011. Validation study of the Short Time Exposure (STE) test to assess the eye irritation potential of chemicals. Toxicol. In Vitro 25, 796–809. http://dx.doi.org/10.1016/j.tiv.2011.01.015.

Scott, L., Eskes, C., Hoffmann, S., Adriaens, E., Alepee, N., Bufo, M., Clothier, R., Facchini, D., Faller, C., Guest, R., Harbell, J., Hartung, T., Kamp, H., Varlet, B.L., Meloni, M., McNamee, P., Osborne, R., Pape, W., Pfannenbecker, U., Prinsen, M., Seaman, C., Spielmann, H., Stokes, W., Trouba, K., Berghe, C.V., Goethem, F.V., Vassallo, M., Vinardell, P., Zuang, V., 2010. A proposed eye irritation testing strategy to reduce and replace in vivo studies using Bottom–Up and Top–Down approaches. Toxicol. In Vitro 24, 1–9. http://dx.doi.org/10.1016/j.tiv.2009.05.019.

Seaman, C.W., Whittingham, A., Guest, R., Warren, N., Olson, M.J., Guerriero, F.J., Adriaens, E., De Wever, B., 2010. An evaluation of a cultured human corneal epithelial tissue model for the determination of the ocular irritation potential of pharmaceutical process materials. Toxicol. In Vitro 24, 1862–1870. http://dx.doi.org/10.1016/j.tiv.2010.03.004.

Seeber, J.W., Zorn-Kruppa, M., Lombardi-Borgia, S., Scholz, H., Manzer, A.K., Rusche, B., Schafer-Korting, M., Engelke, M., 2008. Characterisation of human corneal epithelial cell cultures maintained under serum-free conditions. Altern. Lab. Anim. 36, 569–583.

Stewart, N., Bacchetti, S., 1991. Expression of SV40 large T antigen, but not small t antigen, is required for the induction of chromosomal aberrations in transformed human cells. Virology 180, 49–57.

Takahashi, Y., Hayashi, T., Koike, M., Sakaguchi, H., Kuwahara, H., Nishiyama, N., 2010. An interlaboratory study of the short time exposure (STE) test using SIRC cells for predicting eye irritation potential. Cutan. Ocul. Toxicol. 29, 77–90. http://dx.doi.org/10.3109/15569521003587327.

Takahashi, Y., Hayashi, K., Abo, T., Koike, M., Sakaguchi, H., Nishiyama, N., 2011. The Short Time Exposure (STE) test for predicting eye irritation potential: intra-laboratory reproducibility and correspondence to globally harmonized system (GHS) and EU eye irritation classification for 109 chemicals. Toxicol. In Vitro 25, 1425–1434. http://dx.doi.org/10.1016/j.tiv.2011.04.012.

United Nations, 2011. Globally Harmonized System of Classification and Labelling of Chemicals (GHS), Fourth revised edition, UN New York and Geneva, 2011. Retrieved from <http://www.unece.org/trans/danger/publi/ghs/ghs_rev04/04files_e.html>.

Van Goethem, F., Adriaens, E., Alepee, N., Straube, F., De Wever, B., Cappadoro, M., Catoire, S., Hansen, E., Wolf, A., Vanparys, P., 2006. Prevalidation of a new in vitro reconstituted human cornea model to assess the eye irritating potential of chemicals. Toxicol. In Vitro 20, 1–17. http://dx.doi.org/10.1016/j.tiv.2005.05.002.

Verstraelen, S., Jacobs, A., De Wever, B., Vanparys, P., 2013. Improvement of the Bovine Corneal Opacity and Permeability (BCOP) assay as an *in vitro* alternative to the Draize rabbit eye irritation test. Toxicol. In Vitro 27, 1298–1311.

Weil, C.S., Scala, R.A., 1971. Study of intra- and interlaboratory variability in the results of rabbit eye and skin irritation tests. Toxicol. Appl. Pharmacol. 19, 276–360.

Yamasaki, K., Kawasaki, S., Young, R.D., Fukuoka, H., Tanioka, H., Nakatsukasa, M., Quantock, A.J., Kinoshita, S., 2009. Genomic aberrations and cellular heterogeneity in SV40-immortalized human corneal epithelial cells. Invest. Ophthalmol. Vis. Sci. 50, 604–613. http://dx.doi.org/10.1167/iovs.08-2239.

Zorn-Kruppa, M., Tykhonova, S., Belge, G., Diehl, H.A., Engelke, M., 2004. Comparison of human corneal cell cultures in cytotoxicity testing. ALTEX 21, 129–134.

Zorn-Kruppa, M., Tykhonova, S., Belge, G., Bednarz, J., Diehl, H.A., Engelke, M., 2005. A human corneal equivalent constructed from SV40-immortalised corneal cell lines. Altern. Lab. Anim. 33, 37–45.

Appendix II

PLOS ONE

RESEARCH ARTICLE

Determining the Depth of Injury in Bioengineered Tissue Models of Cornea and Conjunctiva for the Prediction of All Three Ocular GHS Categories

Michaela Zorn-Kruppa[1]*, Pia Houdek[1], Ewa Wladykowski[1], Maria Engelke[2], Melinda Bartok[2], Karsten R. Mewes[3], Ingrid Moll[1], Johanna M. Brandner[1]

1. University Medical Center Hamburg-Eppendorf, Department of Dermatology and Venerology, 20246 Hamburg, Germany, **2.** Jacobs University Bremen gGmbH, School of Engineering and Sciences, 28759 Bremen, Germany, **3.** Henkel AG & Co. KGaA, 40589 Düsseldorf, Germany

*m.zorn-kruppa@uke.de

OPEN ACCESS

Citation: Zorn-Kruppa M, Houdek P, Wladykowski E, Engelke M, Bartok M, et al. (2014) Determining the Depth of Injury in Bioengineered Tissue Models of Cornea and Conjunctiva for the Prediction of All Three Ocular GHS Categories. PLoS ONE 9(12): e114181. doi:10.1371/journal.pone.0114181

Editor: Alfred S. Lewin, University of Florida, United States of America

Received: September 22, 2014

Accepted: November 5, 2014

Published: December 10, 2014

Data Availability: The authors confirm that all data underlying the findings are fully available without restriction. All relevant data are within the paper.

Funding: The study was funded by German Federal Ministry of Education and Research Bundesministerium für Bildung und Forschung. BMBF-FKZ/grant number: 0316010. URL: http://www.bmbf.de (MZ-K ME MB KM JMB). The funders had no role in study design, data collection and analysis, decision to publish, or preparation of the manuscript.

Competing Interests: The authors confirm that co-author Johanna M. Brandner is a PLOS ONE Editorial Board member Furthermore, the authors confirm that co-author Karsten R. Mewes is currently an employee of the Henkel AG & Co. KGaA. This does not alter the authors' adherence to PLOS ONE policies on sharing data and materials.

Abstract

The depth of injury (DOI) is a mechanistic correlate to the ocular irritation response. Attempts to quantitatively determine the DOI in alternative tests have been limited to *ex vivo* animal eyes by fluorescent staining for biomarkers of cell death and viability in histological cross sections. It was the purpose of this study to assess whether DOI could also be measured by means of cell viability detected by the MTT assay using 3-dimensional (3D) reconstructed models of cornea and conjunctiva. The formazan-free area of metabolically inactive cells in the tissue after topical substance application is used as the visible correlate of the DOI. Areas of metabolically active or inactive cells are quantitatively analyzed on cryosection images with ImageJ software analysis tools. By incorporating the total tissue thickness, the relative MTT-DOI (rMTT-DOI) was calculated. Using the rMTT-DOI and human reconstructed cornea equivalents, we developed a prediction model based on suitable viability cut-off values. We tested 25 chemicals that cover the whole range of eye irritation potential based on the globally harmonized system of classification and labelling of chemicals (GHS). Principally, the MTT-DOI test method allows distinguishing between the cytotoxic effects of the different chemicals in accordance with all 3 GHS categories for eye irritation. Although the prediction model is slightly over-predictive with respect to non-irritants, it promises to be highly valuable to discriminate between severe irritants (Cat. 1), and mild to moderate irritants (Cat. 2). We also tested 3D conjunctiva models with the aim to specifically address conjunctiva-damaging substances. Using the MTT-DOI method in this model delivers comparable results as the cornea model, but does not add additional information. However, the MTT-DOI method using reconstructed cornea

models already provided good predictability that was superior to the already existing established *in vitro/ex vivo* methods.

Introduction

To date, the rabbit Draize eye irritation test [1] is still the only OECD-approved test for the prediction of all three GHS categories for eye irritation in one single test system [2]. In the past, a number of ex vivo and in vitro methods have been developed in order to replace the Draize test. For example, tests either based on isolated animal eyes, like the Bovine Corneal Opacity and Permeation (BCOP) test and the Isolated Chicken Eye (ICE) test [3], [4], [5], [6], or cell-based assays [7], [8], [9], [10], [11], [12] have been described. Furthermore, approaches have been published that take advantage of the reactions evoked by chemicals in incubated hen eggs [7] or invertebrates [13], [14]. Also a test system based on the perturbation and denaturation of corneal proteins which is supposed to mimic the disruptive effect of ocular irritants [15] and various 3D cornea epithelial models [16], [17], [18], [19], [20], [21], [22] have been developed. Currently some methods have gained regulatory acceptance for selected GHS categories. For example, both the BCOP and the ICE test method have been implemented at OECD level to screen for corrosives and severe eye irritants (Cat. 1) on the one hand and for non-classified chemicals on the other hand [23], [24]. In the European Union, the HET-CAM (Hen's Egg Test Chorioallantoic Membrane) and the Isolated Rabbit Eye (IRE) test have also been accepted for the identification of severe eye irritants [25]. In addition, the Cytosensor Microphysiometer test method has gained validation status for the identification of severe irritants (limited to water-soluble materials) and non-classified substances (limited to water-soluble surfactants and surfactant- containing mixtures) and is now the subject of a draft OECD guideline [26]. All available methods reveal their strengths preferably in the accurate identification of either severe eye-irritants or non-irritants. Test methods which reliably distinguish the mild/moderate irritatants (Cat. 2) from Cat. 1 and the non-irritants (No Cat.) directly, are not yet available. Therefore many of these test methods are intended to be used only within the framework of an integrated testing strategy, either in a top-down or in a bottom-up approach [8], [27], [28].

According to an expert group [27], only methods based on ocular tissues comprising both, the epithelium and the stroma, are thought to allow discrimination between all three GHS categories. This perception is based on studies by Jester and Maurer [29], [30], [31], [32], [33], [34] who showed that the surface area and depth of initial corneal injury (DOI) in epithelium and stroma of rabbit eyes strongly correlate with the eye-irritating potential of chemicals which had been topically applied to the eye. The conclusions of the authors are based on

in vivo rabbit studies using live/dead assay in combination with the low volume eye test (LVET) as well as on ex vivo studies on isolated rabbit eyes [33].

In the presented study we aimed to establish an in vitro test method which reliably predicts the eye-irritation potential of chemicals for all three GHS categories within one test. For this purpose the previously established and well characterized reconstructed cornea model, consisting of a collagenous stroma covered with a multilayered corneal epithelium [35], [36], [37], [38], [39], was used. Recently we had demonstrated reproducible production of the cornea equivalent model according to standard operation procedures as well as successful method transfer to other laboratories [40]. Furthermore, the corneal tissues had been treated with 20 chemicals of different eye-irritating potential and physical properties under blind conditions, and the relative viability of the whole tissue was used as endpoint to assess the performance and limitations of the models in two independent laboratories. The best-suited prediction model was based on a 60 minutes exposure period with the test substance and a cut-off value of 40% relative viability to discriminate between non-classified and GHS category 1/2 chemicals. The data revealed a high inter-laboratory concordance in predictivity. However, only those chemicals belonging to GHS Cat. 1 were classified correctly in both laboratories, while 3 out of 15 chemicals belonging to No Cat. or Cat. 2 had been concordantly misclassified in both laboratories.

Therefore it was our aim to increase the predictive capacity of the 3D cornea-based test system in order to eliminate false negative responses on the one hand and to discriminate between all 3 GHS categories in one stand-alone test system on the other hand. This method refinement was performed by integrating an additional physiologically relevant endpoint, namely the initial depth of injury in both epithelium and stroma, into the eye irritation assessment. We developed a new technique to quantify the initial DOI in the reconstructed cornea tissues by combining the MTT viability assay with cryosectioning procedures (MTT-DOI method). The formazan-free area of metabolically inactive cells in the tissue after topical substance application is used as the visible correlate of the DOI. A panel of 25 chemicals which covered all GHS categories in a balanced manner was tested on the cornea models in order to assess performance and predictivity of the MTT-DOI method. The test results were then compared with high-quality in vivo reference data.

Although corneal damage is the most influential driver of eye irritation for all GHS categories, also conjunctival damage was found to be of importance, particularly as driver of irritation for GHS Cat. 2 classification [41], [42]. Thus, some chemicals are categorized as Cat. 2 mainly due to severity and/or persistence of the damage they produce in the conjunctiva in vivo [43]. Furthermore, even if subclassification within Cat. 2 is not mandatory in the EU, US authorities prescribe to distinguish between mild (Category 2B) and moderate irritancy (Category 2A). A great significance of conjunctiva effects has been claimed in the discrimination of Category 2A versus 2B [44]. However, none of the already validated in vitro methods for eye irritation testing sufficiently addresses the conjunctiva involvement. Therefore we developed a 3D conjunctiva model from

immortalized human conjunctival cell lines. The conjunctiva model was characterized and subjected to the MTT-DOI measurements with a panel of 12 chemicals with a focus on the mild and moderate irritating Cat. 2 substances. Results from MTT-DOI measurements with 3D cornea and conjunctiva tissue equivalents were compared and critically discussed.

Materials and Methods

Materials

Thiazolyl blue tetrazolium bromide (MTT reagent), sodium hydroxide, sodium bicarbonate, HEPES and sucrose were obtained from Sigma-Aldrich (Schnelldorf, Germany). Calcium chloride, PBS without Ca^{2+} and Mg^{2+} (PBS−), isopropanol, Nunc cell culture inserts (0.5 cm^2 surface area, 0.4 and 3 µm pore size, polycarbonate) were from Thermo Scientific (Roskilde, Denmark). Rat tail collagen solution was purchased from CellSystems (Troisdorf, Germany). Media 199 and Ham's F12, as well as TrypLE Express were from Invitrogen (Darmstadt, Germany). For construction of cornea equivalents, Keratinocyte Basal Medium (KBM) with a Bullet-kit and the chemically defined Keratinocyte Growth Medium (KGM-CD) were obtained from Lonza (Basel, Switzerland). To build up the conjunctiva equivalents two different media were used: Keratinocyte serum-free medium was from Invitrogen (Darmstadt, Germany), and supplemented with 25 g/mL bovine pituitary extract, 0.2 ng/ml epidermal growth factor (Darmstadt, Germany), and 0.4 mM calcium chloride (Invitrogen, Darmstadt, Germany). DMEM/F12 (Sigma-Aldrich, Schnelldorf, Germany) supplemented with 10% newborn calf serum (Thermo Scientific, Schwerte, Germany) and 10 ng/mL EGF was used for stratification (stratification medium). Penicillin/streptomycin, PBS- and PBS with Ca^{2+}, Mg^{2+} (PBS+) were purchased from Biochrom (Berlin, Germany). Bola Teflon O-rings (with 3 inner and 6 outer diameter) were from Bohlender GmbH (Grünsfeld, Germany).

Test substances

Most of the test materials used in this study were chosen from the database published by the European Center for Ecotoxicology and Toxicology of Chemicals [43], according to the classification of the Globally Harmonized System [45] based on the in-vivo data obtained with the Draize eye irritation test. Dimethyl sulfoxide (DMSO) was chosen from the database from Laboratoire National de la Santé [3], isopropyl acetoacetate was collected from the ZEBET database [46], and glycolic acid from ICCVAM [47]. From the databases, a total of 25 test chemicals were chosen (see Table 1). PBS+ and iso-propanol were used as negative control (NC) and batch control (BC), respectively.

Table 1. List of the reference chemicals used in this study.

Chemical	CAS No	In vivo GHS category	Data source	Supplier	Physical state	Chemical class
Glycerol*	56-81-5	No Cat.	ECETOC	Roth	liquid	alcohol
PEG-400*	25322-68-3	No Cat.	ECETOC	Sigma	liquid	surfactant
DMSO*	67-68-5	No Cat.	LNS	Merck	liquid	surfactant
Toluene	108-88-3	No Cat.	ECETOC	Sigma	liquid	aromatic
3-methoxy-1,2-propanediol	623-39-2	No Cat.	ECETOC	Sigma	liquid	alcohol
2-heptanone	110-43-0	No Cat.	ECETOC	Sigma	liquid	ketone
n-bromohexane	111-25-1	No Cat.	ECETOC	Sigma	liquid	haloginated hydrocarbon
Isopropyl acetoacetate*	542-08-5	Cat. 2B	ZEBET	Sigma	liquid	ester
3-chloropropionitrile*	542-76-7	Cat. 2B	ECETOC	Sigma	liquid	nitrile
Glycolic acid (10%)	79-14-1	Cat. 2B	ICCVAM	Sigma	solid[b]	acids
2-methyl-1-pentanol*	105-30-6	Cat. 2B	ECETOC	Sigma	liquid	alcohol
Ammonium nitrate	6484-52-2	Cat. 2A	ECETOC	Sigma	solid	inorganic
Iso-propanol*	67-63-0	Cat. 2A	ECETOC	Roth	liquid	alcohol
Acetone*	67-64-1	Cat. 2A	ECETOC	Chemsolute	liquid	ketone
Ethanol*	64-17-5	Cat. 2A	ECETOC	Merck	liquid	alcohol
2,6-dichlorobenzoyl chloride	4659-45-4	Cat. 2A	ECETOC	Sigma	liquid	acyl halide
Sodium hydroxyde (1%)	1310-73-2	Cat. 2A	ECETOC	Merck	liquid	inorganic alkalies
Benzalkonium chloride (1%)*	8001-54-5	Cat. 1	ECETOC	Sigma	solid[b]	surfactant
Cyclohexanol*	108-93-0	Cat. 1	ECETOC	Sigma	liquid	alcohol
Triton X-100 (10%)*	9002-93-1	Cat. 1	ECETOC	Sigma	liquid	surfactant
Imidazole	288-32-4	Cat. 1	ECETOC	Sigma	solid	heterocydic
Quinacrine	69-05-6	Cat. 1	ECETOC	Sigma	solid	heterocydic
Cetylpyridinium bromide (6%)	140-72-7	Cat. 1	ECETOC	Sigma	solid[b]	surfactant
2-methoxyetyl acrylate	3121-61-7	Cat. 1	ECETOC	Sigma	liquid	acrylate
4-fluoroaniline	371-40-4	Cat. 1	ECETOC	Sigma	liquid	aromatic

The in vivo classification data, chemical and physical properties and suppliers of the reference substances are indicated.
*These chemicals were tested also with 10 min exposure on cornea and conjunctiva models.
[b]Solid chemicals were tested as liquids. DMSO: dimethyl sulfoxide, PEG-400: polyethylene glycol 400.

doi:10.1371/journal.pone.0114181.t001

Construction of 3D cornea models

The cornea model consists of a 3D stromal biomatrix with embedded human corneal keratocytes covered with a multilayer of human corneal epithelial cells. The corneal keratocytes (HCK), immortalized with SV-40 adenovirus, were established by Zorn-Kruppa [36] and further characterized by Manzer [38]. The corneal epithelial cells (HCE) were kindly provided by Stephan Reichl from Technical University of Braunschweig, Germany, who received them from the RIKEN cell bank (Tsukuba, Japan). The HCE cells were also immortalized with the SV-40 adenovirus and established by Araki-Sasaki [48]. Both cell lines were cultured as described [40].

The cornea models were prepared according to Engelke [40] with some minor modifications. Briefly, first the stromal layer was prepared in cell culture inserts (3 µm pore size) from collagen embedded HCK cells: six volumes of the collagen solution were gently mixed with one volume of ten-fold concentrated P99 medium (1:1 mixture of Media 199, Ham's F12), 2.5 volumes of reconstruction buffer (2.2 g sodium bicarbonate, 4.77 g HEPES and 100 ml 0.5 N sodium hydroxide), and one volume of KGM containing 50,000 HCK cells. Then, 150,000 HCE cells suspended in 300 µl of KGM medium were plated on top of each stroma. The constructs were cultured submerged for 6 days. Then the models were cultivated at air liquid interface for further 7 days to induce multilayer formation.

Construction, barrier function and immunohistochemical characterization of conjunctiva models

The human conjunctival epithelial cells (ConjEp-1/p53DD/cdk4R/TERT, shortly named HCjE), were kindly provided by Ilene Gipson from Schepens Eye Research Institute at Harvard Medical School in Boston, Massachusetts, USA. The cells were taken from a human bulbar conjunctiva, immortalized by expression of hTERT and characterized by Gipson and coworkers [49]. HCjE cells were cultured as described [49]. The collagenous stroma matrix of the conjunctiva equivalents was produced according to the method described above for the cornea models. Subsequently, 750,000 HCjE cells were placed on top. The equivalents were cultured submerged for two days, and then switched to air-liquid interphase conditions for a culture period of 6 days. Thereafter, stratification medium (see materials) was added topically for 24 h to induce stratification and formation of epithelial tight junctions.

When conjunctiva epithelial models lacking the collagen matrix were used, HCjE cells were directly plated into membrane inserts with 0.4 µm pore size and cultivated as described above for the full thickness models.

Barrier function testing by transepithelial electrical resistance (TER) measurements of conjunctiva epithelial models was carried out using the Endohm chamber and the EVOM resistance meter (World Precision Instruments, Sarasota, Florida).

Immunohistochemistry was conducted as described in [50]. For vertical images, paraffin sections (6 µm) of formaldehyde-fixed tissues were taken. For en-face (horizontal) images, cultures cells grown on membrane inserts were fixed in ice-cold methanol/acetone and processed as described. Primary antibodies against claudin-1 (Cldn-1, 1:3000), zona occludens protein 1 (ZO-1, 1:100) and occludin (Ocln, 1:20), were obtained from Zymed Laboratories (San Francisco, CA) and cytokeratin 13 (CK-13, 1:80) was purchased from Santa Cruz Biotechnology (Heidelberg, Germany). Alexa Fluor 488 Fab (Life technologies, Darmstadt, Germany) was used as secondary antibody (1:600). An Axiophot II microscope (Zeiss, Göttingen, Germany) and the software Openlab 2.0.9 (Improvision, Coventry, UK) were used for the evaluation of stainings. All images of stainings

from a series of experiments were acquired and processed at the same settings, and representative areas were photographed.

Test protocol for 3D cornea and conjunctiva models

The cornea models were treated topically with 50 µl of the liquid test substances described in Table 1, for an exposure time of 10 or 60 minutes at room temperature. Since conjunctiva tissues generally showed tendency to contract and shrink during construction, a limiting Teflon ring was fixed on the epithelium of these models with vaseline to avoid leakage of the applied chemicals. Proportionally, the applied volume of test substances were reduced to 10 µl. Solid test substances were applied topically onto the epithelium of the tissues using an oval, 6 mm Volkmann bone curette (Wittex, Simbach Germany), which was calibrated with a defined volume of about 50 mg sodium chloride. For each test substance, as well as for the NC and BC, 3 tissue models per batch were used. To prove good reproducibility of the data, all the test substances were tested in at least 3 separate batches. Following exposure, the tissues were extensively washed with PBS+, and transferred into 1.5 ml MTT solution (1 mg/ml) and incubated for 2 h at 37℃ and 5% CO_2. Then sucrose solution was added to a final concentration of 20% and incubated for another 60 min. Thereafter the tissues were removed from the inserts, transferred into cryomolds and embedded in cryomatrix. The tissues were placed at 4℃ for 30 minutes and then frozen in liquid nitrogen. The frozen tissues were stored at −20℃ prior to cryosectioning.

Cryosectioning of the MTT stained tissues and photo-documentation

The cornea and conjunctiva models were sectioned with a Leica CM3050 cryostat at a chamber temperature of −23 to −25℃ and object temperature of −19 to −21℃. The thickness of the cryosections was 30 µm. 3 sections per sample from the center of the models were taken for further analysis. For long time preservation, the cryosections were mounted in Fluoromount G. For evaluation, a Leica DMLS binocular transmitted light microscope (Wetzlar, Germany) equipped with a Leica EC3 digital imaging camera and LAS EZ software were used.

Quantitative analysis of the MTT-DOI

For the quantitative analysis of cell damage and for the determination of the DOI in both tissue models, the images of the sections were processed in ImageJ open source software [51], [52]. After a conversion of the number of pixels into mm, the total cross sectional lengths and the Formazan stained tissue lengths were measured 5 times per image using the straight line tool of the program. The rMTT-DOI was calculated as percentage of the non-viable tissue thickness, where no Formazan staining is present, of the total tissue thickness, as shown in Fig. 1.

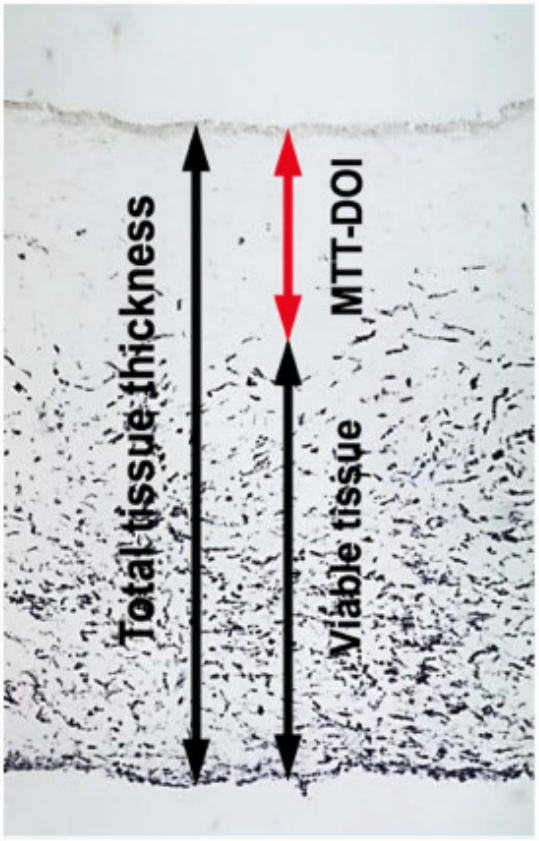

Fig. 1. Determination of the DOI from MTT stained cornea tissues after chemical exposure. The MTT-DOI is calculated in relation to total tissue thickness. The presented model was exposed to isopropanol for 60 minutes.

doi:10.1371/journal.pone.0114181.g001

Results

Development of the DOI-method based on cryosections of MTT-stained 3D-cornea equivalents

We developed a method to analyze the DOI by combining the MTT viability assay with cryosectioning techniques and computer-aided analysis with the aim to establish a prediction model to discriminate all three GHS classes for eye irritation within one model.

When applying common cryosectioning procedures to the bioengineered 3D-cornea models, insufficient tissue preservation was a general issue, in particular induced by shattering due to the high water content of the artificial collagenous stroma. To avoid these freezing artifacts, the unfixed MTT-stained tissues were saturated with 20% sucrose before embedding in cryomatrix [53]. Cutting at

approx. −20°C gave the best results for this watery tissue. Adjusting the thickness in the range of 25 to 35 microns was most suitable for sectioning. By using this method it was possible to detect the formazan crystals in the cryosections and to define a clear demarcation between dead and viable tissue areas (Fig. 1).

When testing the reference chemicals we observed that the overall tissue thickness of cornea models was influenced by the test substances itself during 60 min exposure (Fig. 2). This was especially obvious for 1% sodium hydroxide or 10% Triton X-100. Whereas sodium hydroxide led to contraction of the whole tissue, Triton X-100 caused tissue enlargement by swelling. In addition, the total tissue thickness of the NC models was found to vary between the different batches (mean value of the NC=1.65 mm ± 0.4). Thus, because of this observed inter-batch variability, it is not suitable to use the absolute DOI value. Instead, we used the relative DOI (rMTT-DOI) given as percent of the total tissue thickness which incorporates the variability in total thickness as a basis for out prediction model.

Fig. 3 summarizes the rMTT-DOI values of NCs and of BCs in the various batches over time. Both values remain relatively constant over time. The NC never exceed values of 0.5% of the total tissue thickness (mean ± SD=0.08 ± 0.11), whereas rMTT-DOI of the BC vary between 36 and 56% (mean ± SD= 41.99 ± 4.88).

Regarding the epithelial portion of the tissue model, multilayer growth was ensured in all cases.

Establishment of a preliminary prediction model based on MTT-DOI-measurements of cornea equivalents

To develop an adequate prediction model, 25 chemicals with different physicochemical properties were selected (Table 1). The chemicals cover all categories of eye irritation potential according to the GHS from non-irritant to severe irritant. Adopted from previous studies [40] we used a 60 min exposure times to establish a suitable protocol. In addition, for 12 selected substances also a 10 min exposure period was tested. NCs and BCs were included in each run. Means and standard deviations (SD) of the rMTT-DOIs of three independent batches were calculated (Table 2). In addition, boxplot analyses were prepared (Fig. 4 and 5) to display the characteristic distribution of the rMTT-DOI values for each single test substance in a series of experiments.

Using the 60 min exposition protocol, all rMTT-DOIs found for the Cat. 1 chemicals were higher than 90%, indicating that these chemicals severely damage the cells of the whole tissue models (Fig. 4). A second cluster of compounds is formed by the No Cat. chemicals with rMTT-DOIs below 5% (Fig. 4), indicating that the tissue damage induced by these substances occurs only at the superficial layers and is more or less restricted to the corneal epithelium.

However, when using the 10 min exposure protocol (Fig. 5), we observed that the DOIs of chemicals from different GHS classes cannot be separated satisfactorily. For example, the isopropyl acetoacetate belongs to GHS Cat. 2 but in our 10 min measurements it displays low rMTT-DOI values similar to that of

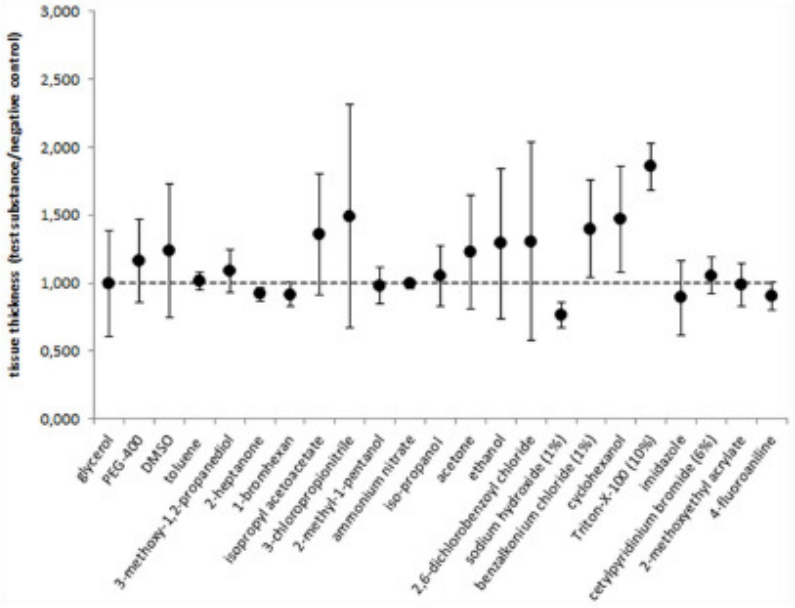

Fig. 2. Tissue thicknesses of cornea models after exposure with the chemicals in relation to the thickness of the corresponding negative controls. Means and SDs of 3 batches (3 models per batch).

doi:10.1371/journal.pone.0114181.g002

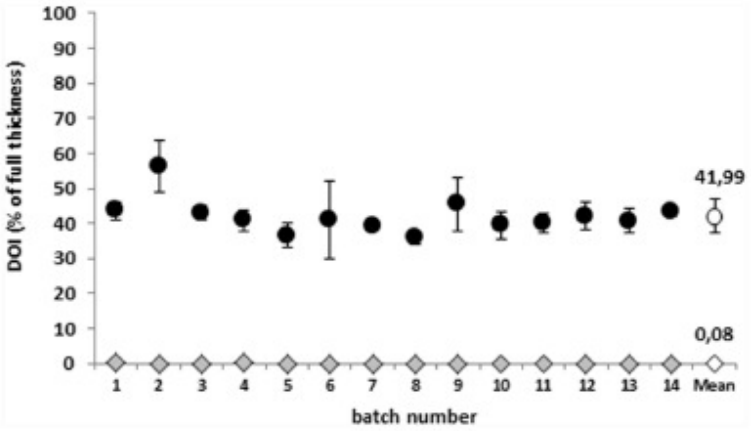

Fig. 3. Reproducibility of the rMTT-DOI values for negative controls (rhombs) and batch controls (circles) over 14 runs. Data points represent the means of 3 models. BCs were treated for a 60 min exposure period with iso-propanol, NCs were treated with PBS+ at room temperature.

doi:10.1371/journal.pone.0114181.g003

Table 2. MTT-DOI values in cornea and conjunctiva models after 10 and 60 min exposure with selected chemicals.

Chemical	In vitro MTT-DOI (% of total tissue thickness)						
	Cornea model 60 min			Cornea model 10 min		Conjunctiva model 10 min	
	Mean	SD	In vitro Cat.	Mean	SD	Mean	SD
Glycerol	2.94	0.95	No Cat.	1.64	1.00	0.61	0.3
PEG-400	1.48	0.99	No Cat.	0.46	0.37	0.18	0.22
DMSO	2.31	0.66	No Cat.	1.14	1.18	0.72	0.56
Toluene	48.60	1.78	Cat. 2	-	-	-	-
3-methoxy-1,2-propanediol	3.33	1.08	No Cat.	-	-	-	-
2-heptanone	26.00	0.99	Cat. 2	-	-	-	-
n-bromohexane	32.88	6.59	Cat. 2	-	-	-	-
Isopropyl acetoacetate	35.19	6.86	Cat. 2	0.61	0.21	0.5	0.68
3-chloropropionitrile	53.28	1.23	Cat. 2	16.19	1.17	8.79	4.87
Glycolic acid (10%)	nd	nd		-	-	-	-
2-methyl-1-pentanol	72.07	9.98	Cat. 2	28.10	1.20	18.05	3.76
Ammonium nitrate	16.45	2.33	Cat. 2	-	-	-	-
iso-propanol*	41.99	5.29	Cat. 2	29.41	7.09	24.02	8.86
Acetone	26.89	4.59	Cat. 2	21.56	6.70	19.61	5.14
Ethanol	37.48	1.83	Cat. 2	28.11	1.40	15.76	4.95
2,6-dichlorobenzoyl chloride	9.84	1.63	Cat. 2	-	-	-	-
Sodium hydroxyde (1%)	99.25	1.28	Cat. 1	-	-	-	-
Benzalkonium chloride (1%)	99.97	0.03	Cat. 1	96.03	6.46	88.17	18.43
Cyclohexanol	94.03	3.42	Cat. 1	33.81	13.55	28.25	7.21
Triton X-100 (10%)	99.93	0.07	Cat. 1	91.16	12.09	95.39	12.04
Imidazole	99.97	0.03	Cat. 1	-	-	-	-
Quinacrine	nd	nd		-	-	-	-
Cetylpyridinium bromide (6%)	99.98	0.04	Cat. 1	-	-	-	-
2-methoxyetyl acrylate	95.35	3.09	Cat. 1	-	-	-	-
4-fluoroaniline	99.69	0.54	Cat. 1	-	-	-	-

In vitro scores and classifications were calculated according to the prediction model using a 60 min exposure time, as depicted in Fig. 6. rMTT-DOI means and SDs of 3 individual runs are given.
*Iso-propanol was used as BC and therefore tested in each run. DMSO: dimethyl sulfoxide, PEG-400: polyethylene glycol 400.

doi:10.1371/journal.pone.0114181.t002

all tested No Cat. substances. In addition, the in vivo severely irritating cyclohexanol possessed a relatively low rMTT-DOI comparable with that of the tested mild and moderately irritating substances. Thus reduction of the exposure time from 60 to 10 min weakens the ability to discriminate between all three GHS categories and would lead to a higher incidence of false negative predictions when incorporated in a prediction model.

When comparing the rMTT-DOI values obtained after both exposure times, most of the substances led to higher values after 60 min than after 10 min. This was most noticeable for the Cat 2B substances.

According to the results of the 60 min exposures a preliminary prediction model was defined using two cut-off values for the in vitro classification of the

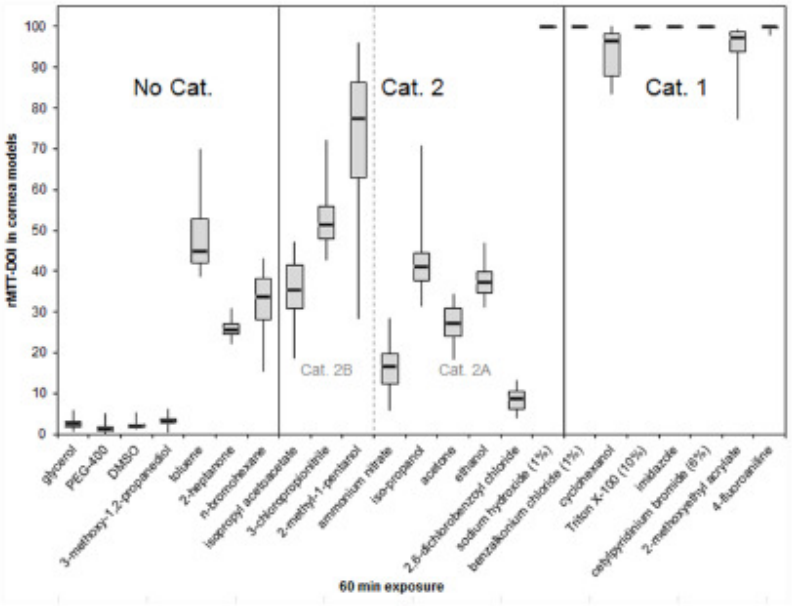

Fig. 4. Boxplot analyses showing the distribution of the rMTT-DOI values for 23 of the 25 selected chemicals in corneal models after 60 min exposure. The in vivo GHS categories of the selected chemicals are depicted within the figure. Medians and boxes for upper and lower quartiles are shown. Whiskers indicate minimum and maximum values. ($n=9$).

doi:10.1371/journal.pone.0114181.g004

test chemicals into the three GHS categories as shown in Fig. 6. In this prediction model test chemicals with rMTT-DOIs of ≤5% are assigned to the non-irritant class (No Cat.) and chemicals with rMTT-DOIs ≥90% are assigned to the severe irritant class (Cat. 1). All other chemicals with intermediate rMTT-DOIs are predicted as Cat 2 chemicals.

The outcome of the evaluation of all test substances and their predicted categorization according to the above defined prediction model is summarized in Table 2.

From the 25 substances tested, 19 were categorized correctly. Of the other six substances, toluene, 2-heptanone and n-bromohexane were classified false positive as Cat. 2, and 1% sodium hydroxide false positive as Cat. 1.

For two chemicals no reliable MTT-DOIs could be determined: Glycolic acid led to a complete decomposition of the collagen matrix. Quinacrine resulted in a patchy MTT-formazan stain even in the epithelium, indicating some remaining viability, although Quinacrine seemed to affect the whole tissue.

Reliability and predictive capacity of the test system

To assess the relevance of the test system, reliability and predictive capacity were determined from a contingency table (Table 3).

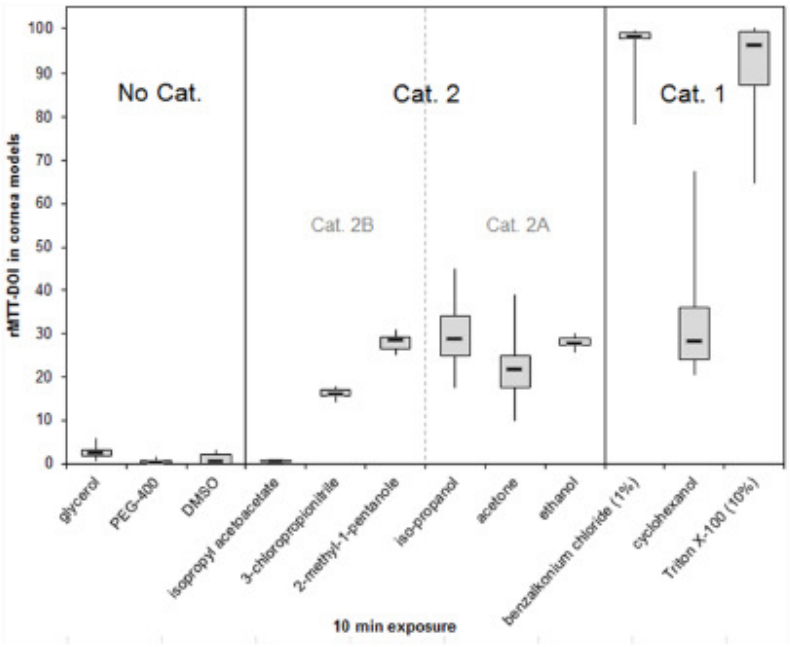

Fig. 5. Boxplots presenting rMTT-DOIs in cornea models after 10 min exposure with 12 chemicals with different eye irritating potential. The in vivo GHS categories of the selected chemicals are depicted within the figure. Medians and boxes of 3 batches (3 models per batch) for upper and lower quartiles are shown. Whiskers indicate minimum and maximum values.

doi:10.1371/journal.pone.0114181.g005

Accordingly, using the 60 min exposure times, all Cat. 1 chemicals and 89% of the Cat. 2 chemicals were predicted correctly. Thus the accuracy of prediction for the severe and the mild and moderate irritant substances is very good. Furthermore, no compound was false negative predicted in the MTT-DOI test, but 43% of the non-irritants were overestimated.

In consequence, the overall concordance rate of 83% implies a substantial agreement between the in vitro and in vivo estimates. However, the test system is over-predictive with regard to non-irritant chemicals.

Regarding the physicochemical properties, all alcohols and surfactants and 2 of the 3 solid compounds were correctly predicted. However the pH extreme compounds were over-predicted or led to no result, especially strongly acidic compounds destroy the collagen matrix, as it was found for 10% glycolic acid.

Successful establishment of 3D conjunctiva equivalent models

With the aim to test its ability to improve predictivity of the 3D cornea model, we established human 3D conjunctiva equivalent models (conjunctiva epithelial model and full conjunctiva model) constructed from human immortalized conjunctiva cells (see materials and methods for establishment).

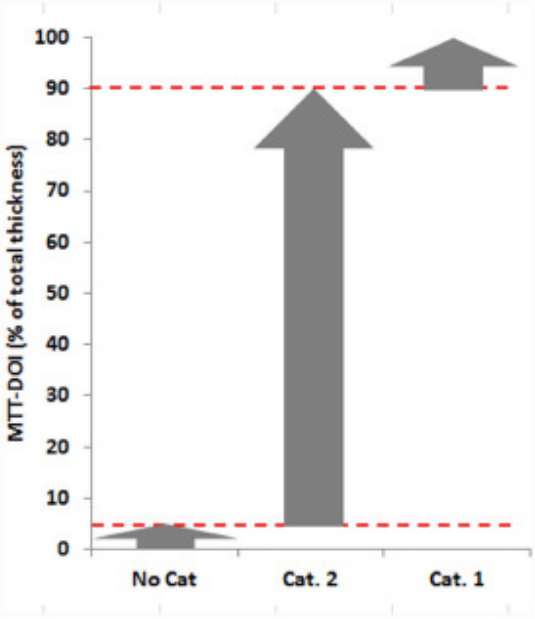

Fig. 6. Preliminary prediction model for the MTT-DOI in vitro classification of chemicals, based on the cornea equivalent system and a 60 min exposure protocol.

doi:10.1371/journal.pone.0114181.g006

Barrier function measurements confirmed an increase of transepithelial resistance in conjunctiva epithelial models after 9 days of cultivation (Fig. 7C). When mimicking chemical exposure conditions by 1 h incubation with PBS+, no significant influence on TER was observed. Thus, the conjunctiva cells are able to form a barrier under these culture conditions.

The stromal layers of the full conjunctiva models underwent contraction and shrinkage during construction which was even increased during final stratification phase. Therefore measurements of the TER with conjunctiva models did not reveal reliable results due to voltage leakage at the margins of the reconstructed tissues. However, as depicted in Fig. 7A, the 3D conjunctiva models consist of 4–8 layers of epithelial cells, and compared with the epithelial models (Fig. 7B),

Table 3. Contingency table showing the in vivo Draize test data versus the in vitro predicted categories, based on the prediction model utilizing the cornea equivalent system and a 60 min exposure protocol.

Category	In vivo Cat. 1	In vivo Cat. 2	In vivo No Cat.	Sum
In vitro Cat. 1	7	1	0	8
In vitro Cat. 2	0	8	3	11
In vitro No Cat.	0	0	4	4
Sum	7	9	7	23

doi:10.1371/journal.pone.0114181.t003

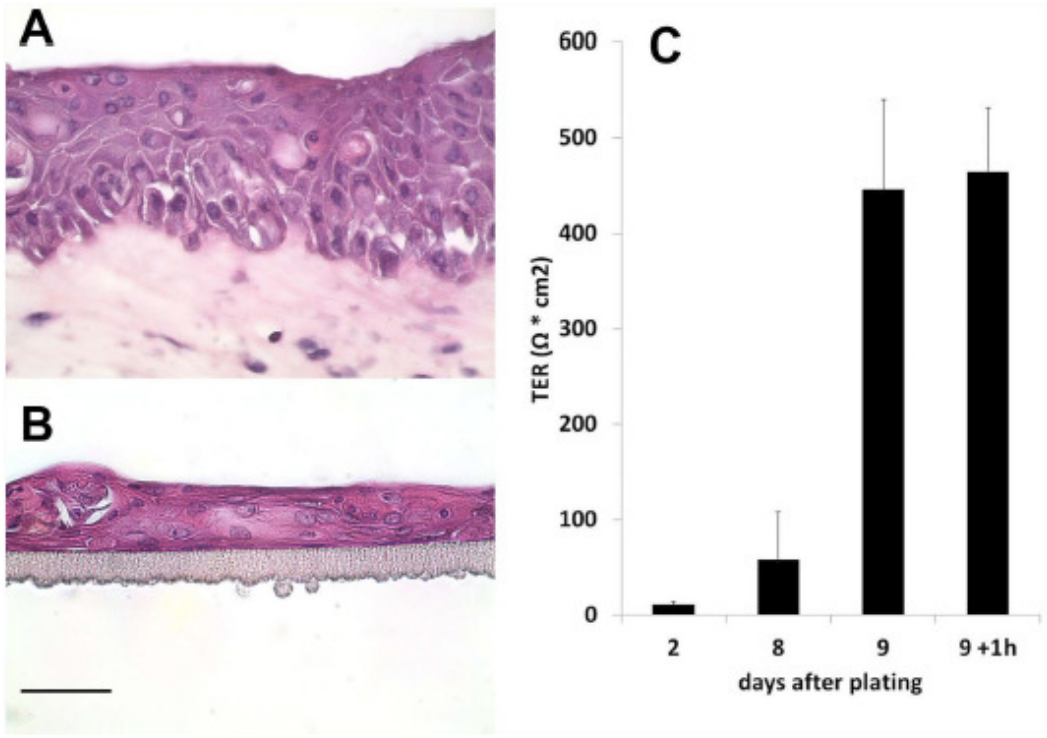

Fig. 7. H&E stain of paraffin sections of conjunctiva models at 40-fold magnification (A, B). A shows a conjunctiva full thickness model with stratified epithelial layers on top of the stromal matrix with embedded fibroblasts. B shows a conjunctiva epithelial model without stromal matrix. (Scale bar represents 50 μm.) C: Diagram summarizing the TER values of conjunctiva epithelial models after 2 to 9 days after construction. Note: Measurements on day 8 were just before addition of serum/EGF-containing stratification medium. On day 9 epithelial constructs were measured before and directly after 1 h incubation with PBS+.

doi:10.1371/journal.pone.0114181.g007

multilayer formation and stratification was even enhanced on top of collagen matrices. For further biochemical characterization of barrier function in both conjunctiva models expression and localization of the tight junction components Cldn-1, ZO-1, Ocln, and of conjunctiva-specific CK-13 were analyzed. Immunofluorescence images show conjunctiva–characteristic expression of the different proteins in the cross sections of both models (Fig. 8). The microscopic evaluation reveals an overall expression of Cldn-1 and a more apical expression of CK-13 whereas ZO-1 and Ocln are localized at the apical superficial membranes of the epithelial cells.

MTT-DOI-measurements of conjunctiva equivalents

For reasons of comparison with the corneal model, the MTT-DOI-measurements were only performed with the full conjunctiva equivalents also consisting of epithelium and collagen embedded cells.

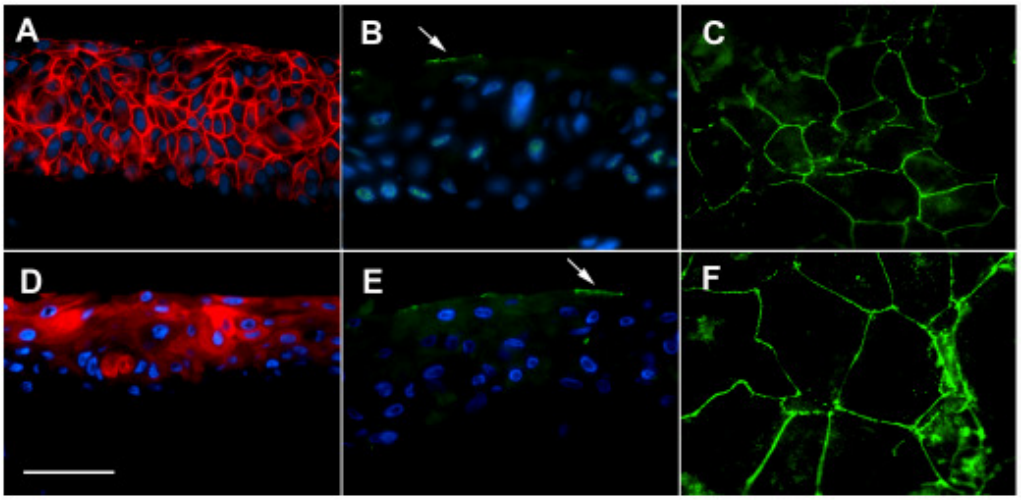

Fig. 8. Immunofluorescence localization of tight junction components Cldn-1 (A red), ZO-1, (B, C, green), and Ocln) (E, F, green), and of conjunctiva-specific CK-13 (D, green) in conjunctiva full thickness tissue models. Note: localization of ZO-1 and Odn is restricted to the apical membrane of superficial epithelial cells (red arrows). A, B, D, E: vertical sections; C, F: horizontal sections. Scale bar represents 50 μm.

doi:10.1371/journal.pone.0114181.g008

For substance application to conjunctiva models we used a limiting Teflon ring affixed with Vaseline in order to avoid leakage of the chemicals since conjunctiva tissues showed tendency to contract and shrink during construction (see also 3.4). When testing these models we generally took a 10 min exposure to minimize the time of usage of the Teflon ring which might affect the measurements.

Twelve reference substances with different physicochemical properties were tested on conjunctiva models. Boxplot analysis of the resulting rMTT-DOI values are depicted in Fig. 9. Means ± SDs of rMTT-DOI values are summarized in Table 2. Quite similar to the studies using cornea models, rMTT-DOIs from Cat 2A and 2B obtained with conjunctiva models lay close together and could not be separated satisfactory. When comparing the rMTT-DOI values obtained with conjunctiva and cornea models after 10 min, it is obvious that both tissues generate very similar results with respect to their susceptibilities towards the selected chemicals of all categories. In particular chemicals which have been shown to react in vivo primarily on the conjunctiva like isopropyl acetoacetate and iso-propanol did not result in higher rMTT-DOI values in conjunctiva models compared to cornea models.

Discussion

In order to provide a straightforward and reliable method to predict the eye irritation potential of chemicals, we developed a cryosectioning procedure for MTT-stained unfixed 3D cornea equivalents to measure the initial depth of injury

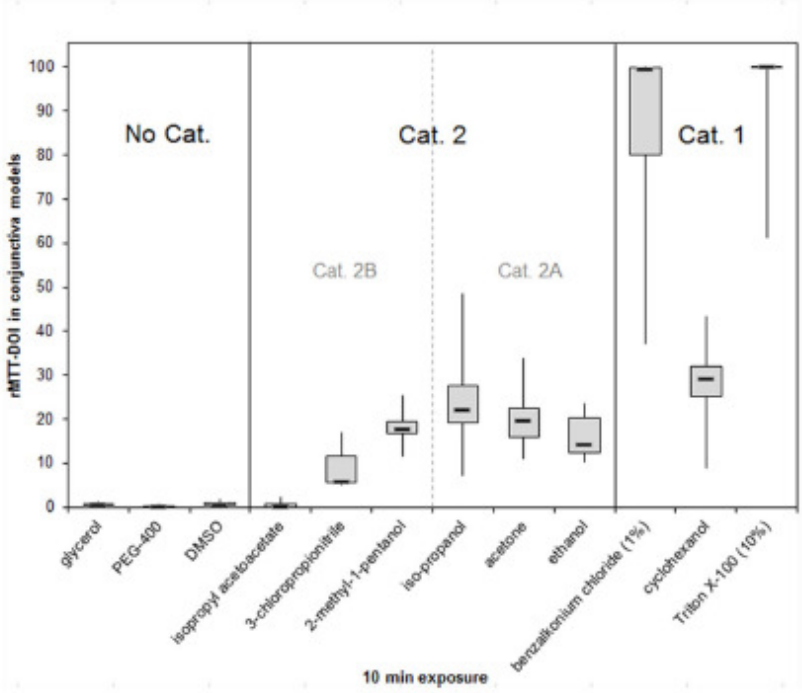

Fig. 9. Boxplot analyses presenting the MTT-DOIs generated with conjunctiva models after 10 min exposure with 12 chemicals. The in vivo GHS categories of the selected chemicals are depicted within the figure. Medians and boxes for upper and lower quartiles are shown. Whiskers indicate minimum and maximum values. ($n = 9$).

doi:10.1371/journal.pone.0114181.g009

in relation to the total tissue thickness. By using this method supplemented by ImageJ-based quantitative analysis tools, we can clearly distinguish reference substances of different GHS categories by means of their rMTT-DOIs.

In contrast to the ex vivo DOI measurements on isolated rabbit eyes (IRE-DOI) described by Jester [33], where classification is based on differential DOI values from both epithelium and stroma, our classification system is exclusively based on DOI in the entire tissue. This modification is due to the fact that in the cornea equivalent stromal cell death almost always occurs only after total loss of epithelial viability. With respect to the choice of a suitable endpoint, MTT reduction to formazan by living cells was preferred over of f-actin/TUNEL staining used by Jester, because the latter, apoptosis-specific staining method failed to give any reliable and reproducible results when adapting it to our cornea equivalent system. This might be due to the different embedding procedures necessary for the native animal corneas on one hand and the artificial stromal tissue on the other hand. However, measurement of MTT-derived formazan offers a valid, simple and widely used method of assessing cell viability. Moreover, contrary to f-actin/TUNEL, which is based on the detection of apoptosis-associated DNA strand

breaks, MTT reduction is a marker reflecting viable cell metabolism. Therefore it is independent from the mechanism or timing of the detected cell death which plays a role in TUNEL staining.

In the presented study, 23 of the selected 25 test chemicals caused MTT-DOIs which were detectable with our MTT-DOI/cornea model test system. 10% glycolic acid did not result in any measurable MTT-DOI, because it dissolved the collagenous stromal matrix leading to total destruction of the reconstructed tissue. Since also 1% sodium hydroxide was over-predicted as a severe irritant compound, we conclude that pH extreme compounds (pH<2.0 or >11.5) in general might be overestimated or rather incompatible with the MTT-DOI test in reconstructed cornea models as it has already been described for other in vitro methods [54]. An overestimation of acids and alkalines in our system might be caused by the fact that any pH buffering mucous- and/or tearfilm-producing component, which is present in vivo, is missing. However, it has often been described that alkalines induce chemical burns to the ocular surface resulting in disastrous and challenging injuries in vivo [55], [56], [57].

The second substance which could not be evaluated with our method was quinacrine. In contrast to all the other test chemicals, quinacrine induces cell death in the stroma while parts of the epithelium are still viable. This observation indicates that the impact on the epithelium is not preceding the impact on the stromal keratocytes. Our observation corresponds to the European Commission/ British Home Office (EC/HO) validation study which showed that also the BCOP test cannot predict the actual degree or depth of injury for quinacrine [58], [59]. Presumably, this chemical leads to a delayed onset of full degree of irritation.

The investigation of our test substances showed, that all severe irritant substances were categorized correctly. Further this was true for 89% of the mild and moderate irritant substances and 57% of non-irritants. Hence, the MTT-DOI test method promises to be suitable to discriminate between severe irritants (Cat. 1), and mild to moderately irritant Cat. 2 substances, which cannot be covered by any other test system published so far.

According to the ECETOC database, toluene, 2-heptanone and n-bromohexane, belong to the non-irritant GHS category and are therefore over-predicted as mild and moderate irritants using the MTT-DOI method. However, toluene has also been misclassified in other studies: For example, the European Union Risk Assessment Report [60] reported from different eye irritation studies in rabbits where toluene was found to be irritant in 2 of 3 studies [61], [62],. In addition, two studies reported eye irritation in toluene-exposed humans [63], [64],. Also von Burg and coworkers confirmed the eye irritating potential of toluene in rabbits and humans [65]. Eye irritation induced by toluene was also detected with alternative test methods such as the BCOP test [66], [67], the HCE assay [17], and the SMI test [13]. Therefore, the rabbit Draize test data reported in the ECETOC data base [43], are thought to underestimate the irritation potential of this chemical.

Also for 2-heptanone and n-bromohexane contradicting results to the Draize test exist in literature. According to NIOSH Pocket Guide to Chemical Hazards,

2-heptanone is indeed irritating to the eye and for n-bromohexane it was found by Kojima that this substance could only be correctly predicted with modification of the rinsing protocol within their in vitro test system [68]. In addition, n-bromohexane is classified as a skin-irritating substance [69].

Taken into account these fundamental limitations in reliability of predictions due to inconsistent in vivo data, the MTT-DOI test method promises to be suitable to discriminate not only between severe irritants (Cat. 1), and mild to moderately irritant Cat. 2 substances but also identify the non-irritating substances with high accuracy.

It is worth mentioning that no compound was false negative predicted in the MTT-DOI test and no surfactant and no alcohol resulted in a false prediction. Thus, compared to BCOP and ICE tests, the MTT-DOI test promises to cause less false results of alcohols, surfactants as well as ketones [70]. Since two of the three solid chemicals were correctly predicted, the MTT-DOI method is also not necessarily restricted to liquids as it is for example the case for the Fluorescein Leakage test or the Cytosensor Microphysiometer test method [2], [26].

Further, the predictive capacity of the MTT-DOI method for volatile chemicals seems to be higher than in other in vitro systems [67] since all tested volatile chemicals (vapor pressure>6 kilopascal at 25 ℃), as there are ethanol, acetone and iso-propanol, were correctly predicted.

Compared to the prediction models from our previous studies where spectrophotometric determination of MTT reduction of the whole tissue was used as endpoint, the prediction model based on rMTT-DOI values thus represents a significant and promising improvement.

In our hands, 60 min of incubation showed a more reliable result to categorize the test substances compared to 10 min of incubation. However, in view of quickness of the method, it might be worthwhile testing more substances for this purpose. In addition, the increase of rMTT-DOI values from 10 min to 60 min exposure was most noticeable for the Cat 2B substances, indicating that the exposure time might be a crucial factor for separation of Cat. 2A and 2B.

Although damage to the cornea is the crucial driver of eye irritation for all GHS categories, conjunctiva damage gains more importance particularly as driver of irritation for GHS Cat. 2 classification [41]. Several chemicals are categorized as Cat. 2 mainly due to severity and/or persistence of the damage they produce to the conjunctiva in vivo. However, none of the already validated in vitro methods for eye irritation testing sufficiently addresses the conjunctival involvement. Therefore, it was our aim to develop a bioengineered conjunctiva model in order to explore whether it is possible to close the above-mentioned gap with an additional ocular tissue.

For this purpose the human hTERT-immortalized human conjunctiva epithelial cell line HCjE [49] was used to build up a full thickness and an epithelial conjunctiva equivalent, respectively. An immunohistochemical analysis of both models confirmed the expression of characteristic marker proteins. Cldn-1 staining was observed in all cell layers of the conjunctival epithelium which is in line with Yoshida [71], who found overall epithelial Cldn-1 staining in tissue

preparations of human conjunctivas. Regarding ZO-1 and Ocln we found also the same localization at the apical superficial tight junctions described by Yoshida in the native conjunctiva. Also functionality of the tight junctions was confirmed by measurement of TER in the epithelial conjunctiva equivalent. Evaluation of TER in the full thickness conjunctiva equivalent is was not possible due to technical reasons. Furthermore, our immunohistochemical analysis reveal within the epithelium of both models a mostly apical expression of the conjunctiva-specific cytokeratin CK-13 which is in line with Ramirez-Miranda [72] and Paladino [73] who described a similar distribution pattern of CK-13 in the native human conjunctiva and in a bovine 3D conjunctiva model, respectively.

In order to compare the effects of chemicals with conjunctival damage as the main driver of irritation [41] in both the corneal and in the conjunctival model, isopropyl acetoacetate and iso-propanol were selected from ECETOC list among 10 other test chemicals. However, when comparing the effects of these substances on conjunctiva and corneal 3D models, no biologically relevant differences were found in sensitivities towards the chemicals. Unlike the in vivo Draize test, where separation of Cat. 2A and 2B mainly depends on the degree of conjunctiva damage, this was not found in vitro when using 3D conjunctiva models.

A few comparative studies have been published so far in terms of cytotoxicity testing in corneal and conjunctival cultures, dealing mainly with pharmacological relevant compounds like benzalkonium chloride or thiomersal [74], [75], [76]. Due to best availability, most of these studies were undertaken with the Chang's human conjunctiva cell line [77] and in particular with the Wong-Kilbourne-Derivat of conjunctiva, clone 1-5c-4. Unfortunately, this cell line is described to be HeLa contaminated [78] and therefore it is not recommended to use it any more. Still, in line with our findings, cytotoxicity data generated with these cells did not hint to any biologically relevant differences in susceptibility between corneal and conjunctival cells.

Nonetheless, the conjunctiva full thickness model might be used for other studies, e.g. for basic biological questions using knock-out strategies of specific proteins. In addition, the epithelial conjunctiva model, which was used here mainly as an intermediate step for the generation of full thickness conjunctiva models may be useful, e.g. for the investigation of the influence of substances on barrier function.

Conclusions

In order to present an adequate, stand-alone strategy for the assessment of all 3 GHS categories of eye irritation we developed a MTT-based method to determine the initial depth of injury in 3D tissue models of the human eye. The test was applied to the previously developed cornea equivalent system and 25 reference chemicals of different GHS categories were tested. Our results reveal that the MTT-DOI test allows us to distinguish between the cytotoxic effects of all GHS categories in one test system. The overall concordance rate of 83% implies a

substantial agreement between the in vitro and in vivo estimates. The system is slightly over-predictive with respect to the non-irritant chemicals. The method is currently being tested in a ring trial with a small set of carefully selected chemicals. In order to meet the requirements for additional test systems assessing more specifically the conjunctiva involvement within an eye irritating response, we established a human cell based in vitro full thickness conjunctiva equivalent. The conjunctiva model reveals quite similar to in vivo conjunctiva regarding the initial depth of injury. However, it could not provide additional information to the cornea-based test method even when testing those chemicals which display conjunctiva damage prior to corneal effects, and thus seems to be dispensable for in vitro safety assessment testing. However, it may be beneficial for barrier function analysis and further biological questions.

Acknowledgments

We thank I. Gipson from Harvard Medical School in Boston, Massachusetts, USA, and S. Reichl from Technical University Braunschweig, Germany for placing the immortalized conjunctiva respectively cornea cells to our disposal.

Author Contributions

Conceived and designed the experiments: MZ-K JMB. Performed the experiments: MZ-K PH EW MB KM. Analyzed the data: MZ-K ME. Contributed reagents/materials/analysis tools: JMB IM. Contributed to the writing of the manuscript: MZ-K KM ME JMB IM.

References

1. **Draize J, Woodward G, Calvery H** (1944) Methods for the study of irritation and toxicity of substances applied topically to the skin and mucous membranes. J Pharmacol Exp Ther 82: 377–390.
2. **OECD** (2012) OECD Guidelines for the Testing of Chemicals No. 460: Fluorescein Leakage Test Method for Identifying Ocular Corrosives and Severe Irritants., Organisation for Economic Cooperation and Development, Paris, France. Available: http://www.oecd-ilibrary.org/docserver/download/9712241e.pdf?expires=1411129530&id=id&accname=guest&checksum=DE4660433959EEBF40750215101EDA48. Accessed 16 March 2014.
3. **Gautheron P, Dukic M, Alix D, Sina JF** (1992) Bovine corneal opacity and permeability test: an in vitro assay of ocular irritancy. Fundam Appl Toxicol 18: 442–449. DOI:10.1016/0272-0590(92)90142-5.
4. **Prinsen MK, Koeter HB** (1993) Justification of the enucleated eye test with eyes of slaughterhouse animals as an alternative to the Draize eye irritation test with rabbits. Food Chem Toxicol 31: 69–76.
5. **Barile FA** (2010) Validating and troubleshooting ocular in vitro toxicology tests. J Pharmacol Toxicol Methods 61: 136–145. DOI:10.1016/j.vascn.2010.01.001.
6. **Verstraelen S, Jacobs A, De Wever B, Vanparys P** (2013) Improvement of the Bovine Corneal Opacity and Permeability (BCOP) assay as an *in vitro* alternative to the Draize rabbit eye irritation test. Toxicol In Vitro 27: 1298–1311.
7. **Eskes C, Bessou S, Bruner L, Curren R, Harbell J, et al.** (2005) Eye irritation. Altern Lab Anim 33(1): 47–81.

8. **McNamee P, Hibatallah J, Costabel-Farkas M, Goebel C, Araki D, et al.** (2009) A tiered approach to the use of alternatives to animal testing for the safety assessment of cosmetics: eye irritation. Regul Toxicol Pharmacol 54: 197–209. DOI:10.1016/j.yrtph.2009.04.004.

9. **Hartung T, Bruner L, Curren R, Eskes C, Goldberg A, et al.** (2010) First alternative method validated by a retrospective weight-of-evidence approach to replace the Draize eye test for the identification of non-irritant substances for a defined applicability domain. ALTEX 27: 43–51.

10. **Takahashi Y, Hayashi T, Koike M, Sakaguchi H, Kuwahara H, et al.** (2010) An interlaboratory study of the short time exposure (STE) test using SIRC cells for predicting eye irritation potential. Cutan Ocul Toxicol 29: 77–90. DOI:10.3109/15569521003587327.

11. **Sakaguchi H, Ota N, Omori T, Kuwahara H, Sozu T, et al.** (2011) Validation study of the Short Time Exposure (STE) test to assess the eye irritation potential of chemicals. Toxicol In Vitro 25: 796–809. DOI:10.1016/j.tiv.2011.01.015.

12. **Takahashi Y, Hayashi K, Abo T, Koike M, Sakaguchi H, et al.** (2011) The Short Time Exposure (STE) test for predicting eye irritation potential: intra-laboratory reproducibility and correspondence to globally harmonized system (GHS) and EU eye irritation classification for 109 chemicals. Toxicol In Vitro 25: 1425–1434. DOI:10.1016/j.tiv.2011.04.012.

13. **Adriaens E, Dhondt MM, Remon JP** (2005) Refinement of the Slug Mucosal Irritation test as an alternative screening test for eye irritation. Toxicol In Vitro 19: 79–89. DOI:10.1016/j.tiv.2004.06.004.

14. **Adriaens E, Bytheway H, De Wever B, Eschrich D, Guest R, et al.** (2008) Successful prevalidation of the slug mucosal irritation test to assess the eye irritation potency of chemicals. Toxicol In Vitro 22: 1285–1296. DOI:10.1016/j.tiv.2008.02.018.

15. **Eskes C, Hoffmann S, Facchini D, Ulmer R, Wang A, et al.** (2014) Validation study on the Ocular Irritection(R) assay for eye irritation testing. Toxicol In Vitro 28(5): 1046–1065. DOI:10.1016/j.tiv.2014.02.009.

16. **Doucet O, Lanvin M, Thillou C, Linossier C, Pupat C, et al.** (2006) Reconstituted human corneal epithelium: a new alternative to the Draize eye test for the assessment of the eye irritation potential of chemicals and cosmetic products. Toxicol In Vitro 20: 499–512. DOI:10.1016/j.tiv.2005.09.005.

17. **Van Goethem F, Adriaens E, Alepee N, Straube F, De Wever B, et al.** (2006) Prevalidation of a new in vitro reconstituted human cornea model to assess the eye irritating potential of chemicals. Toxicol In Vitro 20: 1–17. DOI:10.1016/j.tiv.2005.05.002.

18. **Huhtala A, Salminen L, Tähti H, Uusitalo H** (2008) Corneal Models for the Toxicity Testing of Drugs and Drug Releasing Materials. In Ashammakhi N, editor. Topics in Multifunctional Biomaterials and Devices, 1(2): 1–23. Available: http://www.oulu.fi/spareparts/ebook_topics_multifunctional/abstracts/huhtala.pdf. Accessed 21 Mai 2009.

19. **Seaman CW, Whittingham A, Guest R, Warren N, Olson MJ, et al.** (2010) An evaluation of a cultured human corneal epithelial tissue model for the determination of the ocular irritation potential of pharmaceutical process materials. Toxicol In Vitro 24: 1862–1870. DOI:10.1016/j.tiv.2010.03.004.

20. **Kaluzhny Y, Kandarova H, Hayden P, Kubilus J, d'Argembeau-Thornton L, et al.** (2011) Development of the EpiOcular eye irritation test for hazard identification and labelling of eye irritating chemicals in response to the requirements of the EU cosmetics directive and REACH legislation. Altern Lab Anim 39: 339–364.

21. **Kolle SN, Kandarova H, Wareing B, van Ravenzwaay B, Landsiedel R** (2011) In-house validation of the EpiOcular eye irritation test and its combination with the bovine corneal opacity and permeability test for the assessment of ocular irritation. Altern Lab Anim 39: 365–387.

22. **Katoh M, Hamajima F, Ogasawara T, Hata K** (2013) Establishment of a new in vitro test method for evaluation of eye irritancy using a reconstructed human corneal epithelial model, LabCyte CORNEA-MODEL. Toxicol In Vitro 27: 2184–2192. DOI:10.1016/j.tiv.2013.08.008.

23. **OECD** (2013a). OECD Guidelines for the Testing of Chemicals No. 438: Isolated Chicken Eye Test method for identifying i) chemicals inducing serious eye damage and ii) chemicals not requiring classifications foreye irritation or serious eye damage. Organisation for Economic Cooperation and Development, Paris, France. Available: http://www.keepeek.com/Digital-Asset-Management/oecd/environment/test-no-438-isolated-chicken-eye-test-method-for-identifying-i-chemicals-inducing-serious-eye-damage-and-ii-chemicals-not-requiring-classification-for-eye-irritation-or-serious-eye-damage_9789264203860-en#page1. Accessed 21 March 2014.

24. **OECD** (2013b) OECD Guidelines for the Testing of Chemicals No. 437: Bovine Corneal Opacity and Permeability Test method for identifying i) chemicals inducing serious eye damage and ii) chemicals not requiring classification for eye irritation or serious eye damage. Organisation for Economic Cooperation and Development. Available: http://www.oecd-ilibrary.org/docserver/download/9713221e.pdf?expires=1411130561&id=id&accname=guest&checksum=5456793395AE41CA7938FF5D6D9C18DA. Accessed 25 April 2014.

25. **European Union** (2009) Guidance to Regulation (EC) No 1272/2008 on classification, labelling and packaging (CLP) of substances and mixtures. ECHA Reference: ECHA-09-G-02- EN. Available: http://www.iss.it/binary/cnsc/cont/Guida_CLP_II.pdf. Accessed 20 July 2014.

26. **OECD** (2012b) Draft OECD Guideline for testing of chemicals: The Cytosensor Microphysiometer Test Method: An in vitro Method for Identifying Ocular Corrosive and Severe Irritant Chemicals as well as Chemicals not classified as Ocular Irritants (21 December 2012). http://www.oecd.org/env/ehs/testing/DRAFT Cytosensor TG (V9)21 Dec 12_clean.pdf. Accessed 21 March 2014.

27. **Scott L, Eskes C, Hoffmann S, Adriaens E, Alepee N, et al.** (2010) A proposed eye irritation testing strategy to reduce and replace in vivo studies using Bottom-Up and Top-Down approaches. Toxicol In Vitro 24: 1–9. DOI:10.1016/j.tiv.2009.05.019.

28. **Hayashi K, Mori T, Abo T, Ooshima K, Hayashi T, et al.** (2012) Two-stage bottom-up tiered approach combining several alternatives for identification of eye irritation potential of chemicals including insoluble or volatile substances. Toxicol In Vitro 26: 1199–1208. DOI:10.1016/j.tiv.2012.06.008.

29. **Jester JV, Li HF, Petroll WM, Parker RD, Cavanagh HD, et al.** (1998a). Area and depth of surfactant-induced corneal injury correlates with cell death. Invest Ophthalmol Vis Sci 39: 922–936.

30. **Jester JV, Petroll WM, Bean J, Parker RD, Carr GJ, et al.** (1998b) Area and depth of surfactant-induced corneal injury predicts extent of subsequent ocular responses. Invest Ophthalmol Vis Sci 39: 2610–2625.

31. **Jester JV, Li L, Molai A, Maurer JK** (2001) Extent of initial corneal injury as a basis for alternative eye irritation tests. Toxicol In Vitro 15: 115–130.

32. **Jester JV** (2006) Extent of corneal injury as a biomarker for hazard assessment and the development of alternative models to the Draize rabbit eye test. Cutan Ocul Toxicol 25: 41–54. DOI:10.1080/15569520500536626.

33. **Jester JV, Ling J, Harbell J** (2010) Measuring depth of injury (DOI) in an isolated rabbit eye irritation test (IRE) using biomarkers of cell death and viability. Toxicol In Vitro 24: 597–604. DOI:10.1016/j.tiv.2009.10.010.

34. **Maurer JK, Parker RD, Jester JV** (2002) Extent of initial corneal injury as the mechanistic basis for ocular irritation: key findings and recommendations for the development of alternative assays. Regul Toxicol Pharmacol 36: 106–117.

35. **Zorn-Kruppa M, Tykhonova S, Belge G, Diehl HA, Engelke M** (2004) Comparison of human corneal cell cultures in cytotoxicity testing. ALTEX 21: 129–134.

36. **Zorn-Kruppa M, Tykhonova S, Belge G, Bednarz J, Diehl HA, et al.** (2005) A human corneal equivalent constructed from SV40-immortalised corneal cell lines. Altern Lab Anim 33: 37–45.

37. **Seeber JW, Zorn-Kruppa M, Lombardi-Borgia S, Scholz H, Manzer AK, et al.** (2008) Characterisation of human corneal epithelial cell cultures maintained under serum-free conditions. Altern Lab Anim 36: 569–583.

38. **Manzer AK, Lombardi-Borgia S, Schafer-Korting M, Seeber J, Zorn-Kruppa M, et al.** (2009) SV40-transformed human corneal keratocytes: optimisation of serum-free culture conditions. ALTEX 26: 33–39.

39. **Hahne M, Zorn-Kruppa M, Guzman G, Brandner JM, Haltner-Ukomado E, et al.** (2012) Prevalidation of a human cornea construct as an alternative to animal corneas for in vitro drug absorption studies. J Pharm Sci 101: 2976–2988. DOI:10.1002/jps.23190.

40. **Engelke M, Zorn-Kruppa M, Gabel D, Reisinger K, Rusche B, et al.** (2013) A human hemi-cornea model for eye irritation testing: quality control of production, reliability and predictive capacity. Toxicol In Vitro 27: 458–468. DOI:10.1016/j.tiv.2012.07.011.

41. **Barroso J, Alépée N, De Smedt A, De Wever B, Hibatallah J, et al.** (2013) The importance of understanding drivers of irritation in vivo for selection of chemicals used in the develop-ment and evaluation of in vitro eye irritation assays: Cosmetics Europe analysis. Poster presented at the In Vitro

Testing Indus-trial Platform (IVTIP) Spring 2013 Meeting, Southampton, UK, May 14–16, 2013. Available: https://www.cosmeticseurope.eu/downloads/6057.html. Accessed 15 May 2013.

42. **Adriaens E, Barroso J, Eskes C, Hoffmann S, McNamee P, et al.** (2014) Retrospective analysis of the Draize test for serious eye damage/eye irritation: importance of understanding the in vivo endpoints under UN GHS/EU CLP for the development and evaluation of in vitro test methods. Arch Toxicol 88(3): 701–723. DOI:10.1007/s00204-013-1156-8.

43. **ECETOC** (1998) Technical Report No. 48(2), Eye Irritation: Reference Chemicals Data Bank (Second Edition). European Centre for Ecotoxicology and Toxicology of chemicals, Brussels. Available: http://www.ecetoc.org/index.php?mact=MCSoap,cntnt01,details,0&cntnt01by_category=5&cntnt01template=display_list_v2&cntnt01order_by=ReferenceDesc&cntnt01display_template=display_details_v2&cntnt01document_id=226&cntnt01return. Accessed 15 August 2012.

44. **Barroso J, Alépée N, De Smedt A, De Wever B, Hibatallah J, et al.** (2014) The Importance of Understanding Drivers Of Irritation In Vivo for Selection of Chemicals Used in the Development and Evaluation of In Vitro Eye Irritation Assays: Cosmetics Europe Analysis; Poster auf SOT meeting, Phoenix, 23–27. March 2014. Available: http://www.congress.loreal.com/sot-2014/SOT-2014-Cosmetics-Europe-TFEI-DRoI.pdf. Accessed 15 August 2014.

45. **United Nations** (2011). Globally Harmonized System of Classification and Labelling of Chemicals (GHS), Fourth revised edition, UN New York and Geneva, 2011. Available http://www.unece.org/trans/danger/publi/ghs/ghs_rev04/04files_e.html. Accessed: 7 April 2013.

46. **Spielmann H, Liebsch M, Kalweit S, Moldenhauer F, Wirnsberger T, et al.** (1996) Results of a validation study in Germany on two in vitro alternatives to the Draize eye irritation test, HET-CAM test and the 3T3 NRU cytotoxicity test. Altern Lab Anim 24: 741–858.

47. **ICCVAM** (2006) Current Status of In Vitro Test Methods for Identifying Ocular Corrosive And Severe Irritants: Hen's Egg Test – Chorioallantoic Membrane Test Method Background Review Document. NIH Publication No: 06-4515. Appendix D. In Vivo and In Vitro Comparison of Ocular Irritancy Classification. Available: http://iccvam.niehs.nih.gov/docs/ocutox_docs/ocubrd/hetcam/hetcamappD.pdf. Accessed 18 April 2009.

48. **Araki-Sasaki K, Ohashi Y, Sasabe T, Hayashi K, Watanabe H, et al.** (1995) An SV40-immortalized human corneal epithelial cell line and its characterization. Invest Ophthalmol Vis Sci 36(3): 614–621.

49. **Gipson IK, Spurr-Michaud S, Argüeso P, Tisdale A, Ng TF, et al.** (2003) Mucin gene expression in immortalized human corneal-limbal and conjunctival epithelial cell lines. Invest Ophthalmol Vis Sci 44(6): 2496–2506.

50. **Kirschner N, Poetzl C, von den Driesch P, Wladykowski E, Moll I, et al.** (2009) Alteration of tight junction proteins is an early event in psoriasis: putative involvement of proinflammatory cytokines. Am J Pathol 175(3): 1095–1106.

51. **Schindelin J, Arganda-Carreras I, Frise E, Kaynig V, Longair M, et al.** (2012) Fiji: an open-source platform for biological-image analysis, Nature Methods 9(7): 676–682.

52. **Preibisch S, Saalfeld S, Tomancak P** (2009) Globally Optimal Stitching of Tiled 3D Microscopic Image Acquisitions. Bioinformatics 25(11): 1463–1465.

53. **Howell SL, Tyhurst M** (1974) Cryo-ultramicrotomy of islets of Langerhans. Some observations on the fine structure of mammalian islets in frozen sections. J Cell Sci 15(3): 591–603.

54. **Scheel J, Heppenheimer A, Lehringer E, Kreutz J, Poth A, et al.** (2011) Classification and labeling of industrial products with extreme pH by making use of in vitro methods for the assessment of skin and eye irritation and corrosion in a weight of evidence approach. Toxicol In Vitro 25(7): 1435–47. DOI:10.1016/j.tiv.2011.04.017.

55. **Wagoner MD** (1997) Chemical injuries of the eye: current concepts in pathophysiology and therapy. Surv Ophthalmol 41: 275–313.

56. **Dohlman CH, Cade F, Pfister R** (2011) Chemical burns to the eye: paradigm shifts in treatment. Cornea 30(6): 613–614. DOI:10.1097/ICO.0b013e3182012a4f.

57. **Jeon HS, Yi K, Chung TY, Hyon JY, Wee WR, et al.** (2012) Chemically injured keratocytes induce cytokine release by human peripheral mononuclear cells. Cytokine 59(2): 280–285. DOI:10.1016/j.cyto.2012.04.006.

58. **Eskes C, Bessou S, Bruner L, Curren R, Harbell J, et al.** (2004) Report for establishing the timetable for phasing out animal testing for the purpose of the Cosmetics Directive. Subgroup 3. Eye Irritation.

Available: http://ec.europa.eu/consumers/sectors/cosmetics/files/doc/antest/(5)_chapter_3/3_eye_irritation_en.pdf 2004. Accessed 20 August 2014.

59. **Raabe HA, Nash JR, Curren RD** (2008) The use of histopathology to improve the predictive capacity of the Bovine Corneal Opacity and Permeability (BCOP) assay. Poster at Linz Congress 2008. Suppl. Linz/2008 ALTEX 25, Supplement 1. Available: www.altex.ch/resources/Raabe.pdf. Accessed: 16 June 2014.

60. **European Union Risk Assessment Report.** CAS No: 108-88-3. EINECS. No: 203-625-9. Toluene. 2nd Priority List, Volume 30. (2003) EUR 20539 EN. European Union. Available http://echa.europa.eu/documents/10162/24a34bd6-55cd-4e28-ae24-5bae281bf3c2. Accessed 20 June 2014.

61. **Sugai S, Murata K, Kitagaki T, Tomita I** (1990) Studies on the eye irritation caused by chemicals in rabbits -1. A quantitative structure-activity relationships approach to primary eye irritation of chemicals in rabbits. J Tox Sci 15: 245–62.

62. **Guillot JP, Gonnet JF, Clement C, Caillard L, Truhaut R** (1982) Evaluation of the ocular-irritation potential of 56 compounds. Food Chem Toxicol 20: 573–82.

63. **Andersen I, Lundqvist GR, Mølhave L, Pedersen OF, Proctor DF, et al.** (1983) Human response to controlled levels of toluene in six-hour exposures. Scand J Work Environ Health 9: 405–418.

64. **Echeverria D, Fine L, Langolf G, Schork A, Sampaio C** (1989) Acute neurobehavioural effects of toluene. Br J Ind Med 46: 483–495. DOI:10.1136/oem.46.7.483.

65. **Von Burg R** (1993) Toluene. J Appl Toxicol 13, 441–446. DOI:10.1002/jat.2550130612.

66. **Van Goethem F, Hansen E, Sysmans m, De Smedt A, Vanparys P, et al.** (2010) Development of a new opacitometer for the bovine corneal opacity and permeability (BCOP) assay. Toxicol In Vitro 24: 1854–1861.

67. **Hayashi K, Mori T, Abo T, Ooshima K, Hayashi T, et al.** (2012) Two-stage bottom-up tiered approach combining several alternatives for identification of eye irritation potential of chemicals including insoluble or volatile substances. Toxicol In Vitro 26(7): 1199–208. DOI:10.1016/j.tiv.2012.06.008.

68. **Kojima H, Katoh M, Shinoda S, Hagiwara S, Suzuki T, et al.** (2014) A catch-up validation study of an in vitro skin irritation test method using reconstructed human epidermis, LabCyte EPI-MODEL24. J Appl Toxicol 34: 766–774.

69. **OECD** (2013) OECD Guidelines for the testing of chemicals No 439: In vitro skin irritation: Reconstructed human epidermis test method. National Institute of environmental health science. Available at htp.niehs.nih.gov/iccvam/suppdocs/feddocs/oecd/oecd-tg439-2013-508.pdf.

70. **ICCVAM** (2007) Test Method Evaluation Report - In Vitro Ocular Toxicity Test Methods for Identifying Ocular Severe Irritants and Corrosives. Interagency Coordinating Committee on the Validation of Alternative Methods (ICCVAM) and the National Toxicology Program (NTP) Interagency Center for the Evaluation of Alternative Toxicol ogical Methods (NICEATM). NIH Publication No.: 07-4517. Available: http://iccvam.niehs.nih.gov/methods/ocutox/ivocutox/ocu_tmer.htm. Accessed 18 April 2009.

71. **Yoshida Y, Ban Y, Kinoshita S** (2009) Tight junction transmembrane protein claudin subtype expression and distribution in human corneal and conjunctival epithelium. Invest Ophthalmol Vis Sci 50: 2103–2108.

72. **Ramirez-Miranda A, Nakatsu MN, Zarei-Ghanavati S, Nguyen CV, Deng SX** (2011) Keratin 13 is a more specific marker of conjunctival epithelium than keratin 19. Molecular Vision 17: 1652–1661.

73. **Paladino G, Marino C, La Terra Mulè S, Civiale C, Rusciano D** (2004) Cytokeratin expression in primary epithelial cell culture from bovine conjunctiva., Tissue and Cell 36: 323–332.

74. **Epstein SP, Chen D, Asbell PA** (2009a) Evaluation of biomarkers of inflammation in response to benzalkonium chloride on corneal and conjunctival epithelial cells. J Ocul Pharmacol Ther 25(5): 415–424. DOI:10.1089/jop.2008.0140.

75. **Epstein SP, Ahdoot M, Marcus E, Asbell PA** (2009b) Comparative toxicity of preservatives on immortalized corneal and conjunctival epithelial cells. J Ocul Pharmacol Ther 25(2): 113–119. DOI:10.1089/jop.2008.0098.

76. **Ayaki M, Yaguchi S, Iwasawa A, Koide R** (2008) Cytotoxicity of ophthalmic solutions with and without preservatives to human corneal endothelial cells, epithelial cells and conjunctival epithelial cells. Clin Experiment Ophthalmol 36(6): 553–559. DOI:10.1111/j.1442-9071.2008.01803.x.

77. **Chang R.S.** (1954) Continuous subcultivation of epithelial-like cells from normal human tissues. Proc Soc Exptl Biol Med 87: 440–443.

78. **Nelson-Rees WA, Daniels DW, Flandermeyer RR** (1981) Cross-contamination of cells in culture. Science 212(4493): 446–452.

Appendix III

Predicting the eye irritation potential of chemicals: A comparison study between two test systems based on human 3D hemi-cornea models

R. Tandon[1], **M. Bartok**[1*], M. Zorn-Kruppa[2], D. Gabel[1] and M. Engelke[1]

[1]Jacobs University Bremen, School of Engineering and Science, Campus Ring 1, 28759 Bremen, Germany

[2]University Medical Center Hamburg-Eppendorf, Department of Dermatology and Venerology, Martinistraße 52, 20246 Hamburg, Germany

*Corresponding author:

Abstract

In the present study we compared two different approaches recently introduced by us (Bartok et al. 2015; Zorn-Kruppa et al. 2014) which both aim for the correct prediction of chemicals according to the globally harmonized system of classification and labelling of chemicals (GHS) of potential eye irritatants. Both test systems are based on reconstructed human 3D hemi-cornea models which comprise a multilayered epithelium and a stroma with embedded keratocytes in a collagenous matrix. The effects of test chemicals after 10 and 60 minutes exposure were assessed from the quantification of cell viability using the MTT reduction assay. In the first approach the effects of test chemicals were evaluated by separately quantifying the damage inflicted to the epithelium and the stroma. In the second approach, depths of injuries (DOI) were quantified. Most of the test substances were chosen according to the study of Jester et al. (2010) with the intention to compare the predictivity of the two test systems based on reconstructed hemi-cornea models with the predictivity based on *ex vivo* rabbit corneas presented by Jester et al. (2010). Our results reveal that the extent of cell damage was dependent on the exposure time. A 60 minute exposure period is precondition for the clear differentiation of GHS 1 and GHS 2 and GHS nc materials for both types of models.

Introduction

The human eye is prone to irritation and damage by chemicals used in pharmaceuticals, cosmetics, household and agricultural products (Verstraelen et al. 2013). For safety reasons, such

chemicals need to undergo thorough toxicological assessment before they are incorporated in various consumer products (Cotovio et al. 2010). The Draize eye irritation test (OECD 2012a), is the only eye toxicity test officially accepted by the Organization of Economic Co-operation and Development (OECD) to predict the full range of irritation caused by different classes of eye irritants. However, the test has been criticized by many, questioning its test performance, reproducibility, use and interpretation of test scores, as well as its monetary and ethical aspects (Wilhelmus 2001). With the increasing concern over the scientific validity and ethical standards of such tests, the 7th amendment of the EU cosmetics directive has banned the use of animals for testing cosmetic ingredients for eye irritation since 2009 (Cotovio et al. 2010).

Efforts have been made to introduce alternative *in vitro* methods to assess the eye irritation potential of a substance. These *in vitro* methods range from simple assays using single cell lines to more complicated assays using isolated animal tissues or artificially reconstructed tissues. However, no method has gained acceptance as a complete regulatory replacement for the Draize eye irritation test (Scott et al. 2010).

Currently, only one cell-based test system and two ex vivo animal test systems have reached official regulatory acceptance (OECD 2012b; OECD 2013a; OECD 2013b). However, these test systems allow only the prediction of ocular corrosives and severe irritants (GHS 1). No single in vitro assay has been developed and validated as a full regulatory replacement for the Draize Eye Irritation test. Instead, the tests developed so far are intended to be used within the framework of an integrated testing strategy, either in a top-down or in a bottom-up approach (Hayashi et al. 2012; McNamee et al. 2009; Scott et al. 2010). These approaches, as in vitro alternatives to animal testing for the safety assessment, reveal their strengths preferably in the discrimination between severe and non-irritants. Test systems predicting GHS 2 substances directly are not yet available.

In an attempt to create a better *in vitro* eye irritation prediction system, different types of 3D corneal models have been proposed (Huhtala et al. 2008). Some models consist only of differentiated epithelium while other consists of epithelium with a stromal analogue in which corneal keratocytes are embedded in the collagen matrix. Previous studies have shown that the area and depth of initial injury can be used to determine the irritation potential of a chemical (Jester et al. 1998). Further studies have revealed that the extent of corneal injury can differentiate among categories of irritants. This was determined by evaluating the damages in

epithelium, stroma and the endothelium. The results were similar to those obtained from animal tests (Jester 2006; Jester et al. 2001). In the past, depth of injury in the cornea of *ex vivo* isolated rabbit eye (IRE-DOI) test was shown as a method that could differentiate among three categories of eye irritants of the globally harmonized system (GHS) of classification (Jester et al. 2010). In this method, the isolated rabbit eye is exposed to ocular irritants of different irritation potential. Then, the cornea is fixed and sectioned in order to study depth of injury in the epithelium and the stroma using biomarkers. The staining patterns of Tunel and Phalloidin stainings, which detect DNA fragmentation and intact actin filaments, respectively, were used to measure the DOI. The classification was based on the combined assessment of individual DOI caused to the stroma and the epithelium. The damage in each compartment showed proportionality to the severity of ocular irritant. Although IRE-DOI was able to classify most of the test substances into the 3 GHS categories, the irritation potential of some ocular irritants was underestimated by this method and needed several modifications for more accurate results (Jester et al. 2010). Furthermore, this method uses staining techniques which are quite expensive. In addition, the slaughtering of rabbits is required for isolation of rabbit eyes for the experiments, thus using about the same number of animals for classification.

In the present study, we used artificially reconstructed human 3D hemi-cornea models (Engelke et al., 2013). In one approach a collagen membrane was inserted between epithelium and stroma which allowed the separation and individual assessment of the damages after exposure to test chemicals in each of the compartments using MTT assay (Bartok et al. 2015). In this test system the prediction model was based on the cell viability and the combination of cut-off values in tissue viability from both epithelium and stroma. In the second approach, depth of injuries (DOI) in the hemi-cornea model was quantified based on the cell viability using the MTT assay (Zorn-Kruppa et al. 2014). Areas of metabolically active or inactive cells were quantitatively analyzed on cryosection images with ImageJ software analysis tools. By incorporating the total tissue thickness, the relative MTT-DOI (rMTT-DOI) was calculated. The prediction model of this test system is based on suitable viability cut-off values. We selected twelve test chemicals; most of them were chosen according to the study of Jester et al. (2010) in order to compare the predictivity of the test systems.

The aims of the study were to evaluate if these two different approaches allow the prediction of the test chemicals according to the GHS classification or if one approach is superior to the other;

and to identify the exposure time, which results in the best predictivity (10 or 60 minutes). In addition, the results obtained with the rMTT-DOI approach were compared to the results obtained from the IRE-DOI (Jester et al., 2010).

Materials and methods

Materials

Keratinocyte Growth Media (KGM®) with Bullet-kit and chemically defined Keratinocyte Growth Medium (KGM-CD®) were obtained from Lonza (Basel, Switzerland). Cell culture flasks, 6, 12, 24 and 96-well plates, penicillin/streptomycin (Pen/Strep) and phosphate buffered saline (PBS) with (++) and without (--) calcium and magnesium were from Biochrom (Berlin, Germany). 3-[4,5-Dimethylthiazol-2-yl]-2,5-diphenyl tetrazolium bromide (MTT) was from Sigma–Aldrich (Deisenhofer, Germany). TrypLE Express, 199 Media and Ham's F12 were from Invitrogen (Darmstadt, Germany). Tissue Tek Cryomold® biopsy vessels (10mm x10mm x 5mm), surgical disposable scalpels, Nunc cell culture inserts (0.5 cm^2, 3 µm pore size, polycarbonate), Menzel coverslips (24×50mm) and Superfrost® microscope slides, isopropanol, calcium chloride and PBS-- tenfold concentrated powder were from Omnilab (Bremen, Germany). The Cryomatrix was from Thermo Scientific (Limburg, Germany). Fluoromount-G was obtained from Southern Biotech (Birmingham, USA). Bola Teflon O-rings (1 cm outer and 0.7 cm inner diameter) were from Bohlinger GmbH (Grünsfeld, Germany). The Collagen Cell Carrier (CCC) was from Viscofan Bioengineering (Weinheim, Germany). The rat tail collagen solution was from CellSystems (Troisdorf, Germany).

Solutions

The 60% (w/v) sucrose solution was made in double distilled water. It was stored at room temperature (RT) and could be used for a maximum of 6 months. The instructions for MTT solution and F99 media preparation are described in the protocol published by Engelke et al. (2013). Reconstruction buffer was made as described by Bartok et al. (2015).

Cell culture and reconstruction of human 3D hemi-cornea models

Two types of cells, human corneal keratocytes (HCK) and human corneal epithelial (HCE) cells were used to construct the human 3D hemi-cornea models. HCK cells had been immortalized

with the SV-40 adenovirus and established by Zorn-Kruppa et al. (2005). The immortalized HCE cells (Araki-Sasaki et al. 1995) were received from the RIKEN cells bank (Tsukuba, Japan). Both types of cells were cultured following the procedure stated by Engelke et al. (2013). Two different types of hemi-cornea models were produced according to the protocol published by Bartok et al. (2015) and Zorn-Kruppa et al. (2014), respectively.

Chemical test protocol and data analysis

A set of 12 test chemicals, listed in Table 1, were applied on both hemi-cornea models with and without CCC membrane. The topical exposure of the models to the chemicals was for either 10 or 60 minutes. PBS ++ was used as negative control for both types of hemi-cornea models. Triton X-100 (0.3%) and isopropanol (ISP) were used as batch controls (BC) for hemi-cornea models with CCC membrane and the rMTT-DOI method, respectively. For models with CCC membrane, the optical density (OD) values corresponding to both the epithelial and stromal viability for each batch met the acceptance criterion as described by Bartok et al. (2015). In addition, the standard deviation calculated from tissue viabilities of 3 tissue replicates from one batch was less than 20%. Treatment with the test substances, washing steps, MTT application details (which were the same for both types of hemi-cornea models) were according to the protocol described by Bartok et al. (2015) and Zorn-Kruppa et al. (2014). Stroma and epithelium separation, optical density measurement and data analysis for hemi-cornea models with CCC membrane were done according to Bartok et al. (2015). For the hemi-cornea models prepared for cryosectioning, the paper published by Zorn-Kruppa et al. (2014) contains the protocol for the experimental procedure and the data interpretation on how to calculate the depth of injury (DOI).

Table 1. Test substances representing 3 different GHS categories of eye irritants

Test substances	Abbreviation	Chemical type	State	Supplier	CAS nr
Dodecane (neat)	DOD	organic	liquid	Sigma	112-40-3
Dimethyl sulfoxide (neat)	DMSO	surfactant	liquid	Grüssing	67-68-5
Potassium tetrafluoro borate	PTFB	Inorganic	liquid	Sigma	14075-53-7
Ethyl-2-methyl acetoacetate	EMAA	organic	liquid	Sigma	609-14-3
Acetone (neat)	ACT	aldehyde	liquid	Roth	67-64-1
Acetic acid (3% v/v in deionized water)	3% AA	non-surfactant acid	liquid	Sigma	64-19-7
Acetic acid (10% v/v in deionized water)	10% AA	non-surfactant acid	liquid	Sigma	64-19-7
Benzalkonium chloride (1% w/v in deionized water)	1% BAK	cationic surfactant	liquid	Sigma	63449-41-2
Benzalkonium chloride (10% w/v in deionized water)	10% BAK	cationic surfactant	liquid	Sigma	63449-41-2
Sodium hydroxide (8% w/v in deionized water)	8% NaOH	base	liquid	Sigma	1310-73-2
Sodium dodecyl sulfate (5% w/v in deionized water)	5% SDS	anionic surfactant	liquid	Roth	151-21-3
Sodium hypochloride (neat)	NaOCl	oxidizer	liquid	Sigma	7681-52-9
Cyclohexanol (neat, 99%)	CY	alcohol	liquid	Sigma	108-93-0
Parafluoroaniline (neat, 99%)	PF	organic	liquid	Sigma	371-40-4

Prediction models used for the classification of the test substances in GHS categories

The hemi-cornea models with a CCC-membrane between the stroma and the epithelium allowed the separation of these compartments after the chemical exposure. This made it possible to assess the cell viability in each of the compartments separately by using the MTT assay. The differentiation of all GHS categories of chemicals was based on an appropriate viability cut-off values set for both epithelium and stroma (Bartok et al. 2015). In the second test system, the hemi-cornea models, with no membrane between the stroma and the epithelium, were stained in MTT solution, frozen in liquid nitrogen and sectioned. The formazan crystals formed by the action of viable cells on MTT reagent were viewed under the microscope. The DOI was determined using ImageJ software, by calculating the ratio of thickness of the tissue without formazan crystals to the total thickness of the hemi-cornea tissue. The classification of the test

chemical into different GHS categories was done by using two DOI cut-off values described by Zorn-Kruppa et al. (2014).

Results

Assessment of stromal and epithelial viabilities of human 3D hemi-cornea models with CCC membrane

The stromal and epithelial viabilities were evaluated separately after 10 and 60 minutes exposure time, respectively. The stromal and epithelial viabilities of PBS++ (NC) treated models were set to 100%. For the models treated with other chemicals, the viability was calculated relative to that of the NC.

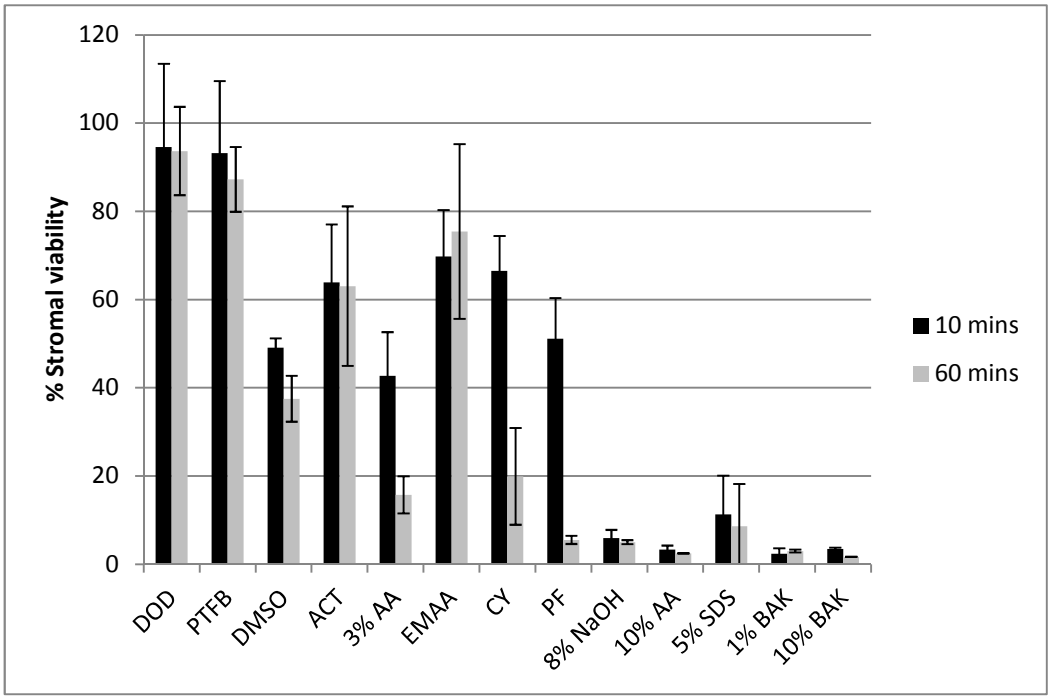

Figure 1. Stromal viability in human 3D hemi-cornea after 10 and 60 minutes exposure to chemicals.

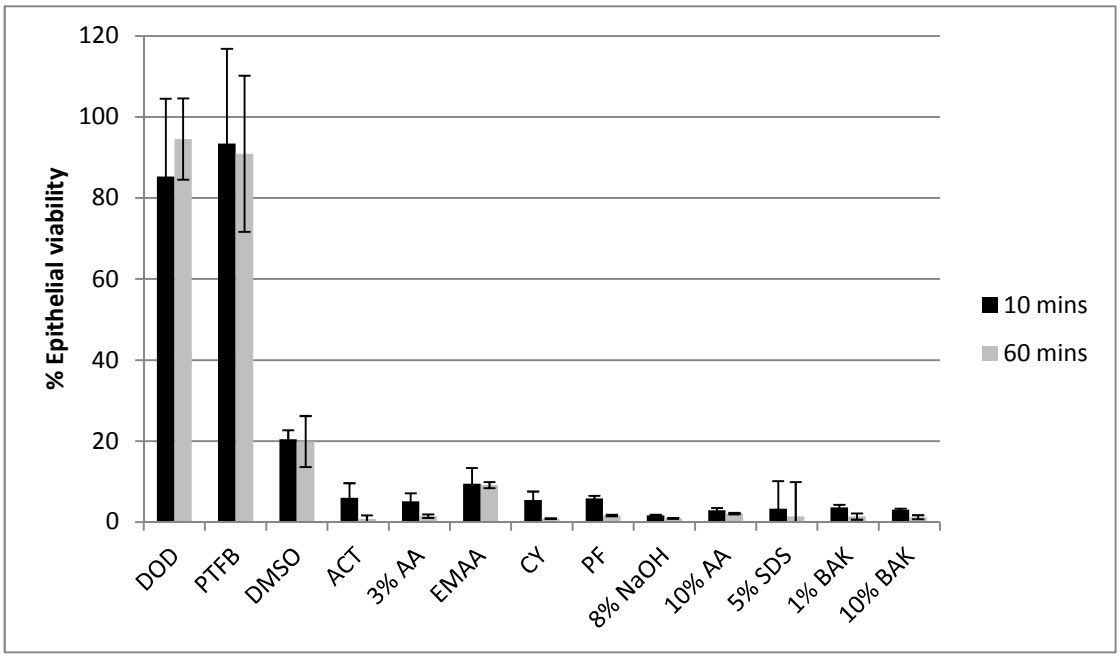

Figure 2. Epithelial viability in 3D hemi-cornea models after 10 and 60 minutes exposure to chemicals.

Figure 1 and 2 show the percentage (%) viability decrease for both the stroma and the epithelium after 60 or 10 minutes exposure time. Most of the chemicals that were tested in our study cause severe damage to epithelium for both 10 and 60 minutes exposure (Figure 1). While the epithelial viability for DMSO, PTFB and DOD is between 20- 95% compared to the NC, it was less than 10% for all other chemicals tested for both 10 and 60 minutes exposure.

In contrast, the stromal viability was dependent on the exposure time for some of the GHS 1 and GHS 2 chemicals. After 10 min exposure to PF and CY (GHS 1 category) stromal viabilities are about 51.1% and epithelial viabilities are about 66.5%, respectively. Indeed, the stromal viabilities after 10 minutes exposure to PF and CY are in the same range as ACT (63.9%), EMAA (69.8%) and 3% AA (42.7%), which are categorized as GHS 2 chemicals. Hence, the 10 minute exposure could not give clear differentiation between GHS 1 and GHS 2 chemicals. For NaOCl, no data for epithelial and stromal viability are available because the chemical completely dissolved the hemi-cornea models after the application.

After 60 minutes exposure, a better differentiation could be seen between GHS 2 and GHS 1 category chemicals. Figure 1 shows that the stromal viability of substances such as PF and CY decreased to 5.5% and 19.9%, respectively. For 3 % AA, an increased damage in the stroma was

observed after 60 minutes whereas the stromal viability was very similar for ACT and EMAA for both 10 and 60 minutes exposure.

Using the prediction models that were developed based on appropriate cut-off values for both the stromal and the epithelial viability after 60 min exposure of 60 min, we assigned the GHS category to the chemicals used in our study (Bartok et al. 2015). Analyzing the stromal and the epithelial viability, the substances such as PF, CY, 1% BAK, 8% NaOH, 10% AA, 5%SDS, 10% BAK, NaOCL and 3% AA were assigned as GHS 1 category; ACT and EMAA were categorized as GHS 2 category; DOD, DMSO and PTFB were assigned as GHS nc chemicals.

Evaluation of rMTT-DOI on human 3D hemi-cornea models

Figure 3a shows the cross section of a hemi-cornea model treated with PBS ++ (NC) for 60 minutes, in which formazan crystals are visible throughout the sectioned tissue. In Figure 3b, the long arrow indicates the total thickness of the model, and the shorter arrow represents the area where no formazan crystals can be seen. This in fact assigned to be the rMTT-DOI, where no viable cells are present.

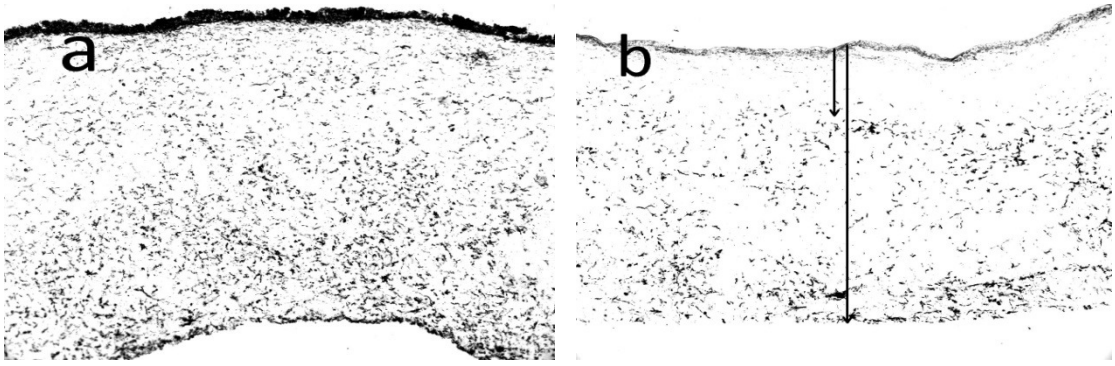

Figure 3. Cryosections of human 3D hemi-cornea models treated with PBS++ (a) and isopropanol (b) for 60 minutes. The short arrow shows the depth of injury, the long arrow shows the total tissue thickness (b).

Figures 4 and 5 show the cross sectioned hemi-corneas treated with different chemicals for 10 and 60 minutes, respectively. Figure 4a and 5a show the cross-sections of hemi-cornea models treated with DOD for 10 and 60 minutes, respectively. The distribution of formazan throughout the tissue cross-sections indicates that almost no damage has been caused to the hemi-cornea models by DOD. Looking at the distribution of formazan on hemi-cornea models treated with GHS 2 chemical ACT, it can be seen that it has penetrated the epithelial layer and caused partial

damage to the stroma for both 10 and 60 minutes exposure (Figure 4b and 5b). Despite being GHS 1 chemicals, PF (Figure 4c) and CY (Figure not shown) caused little damage to the stroma after 10 minutes exposure. However, the absence of formazan on tissue sections from Figure 5c indicates that PF damaged the stroma almost completely after 60 minutes.

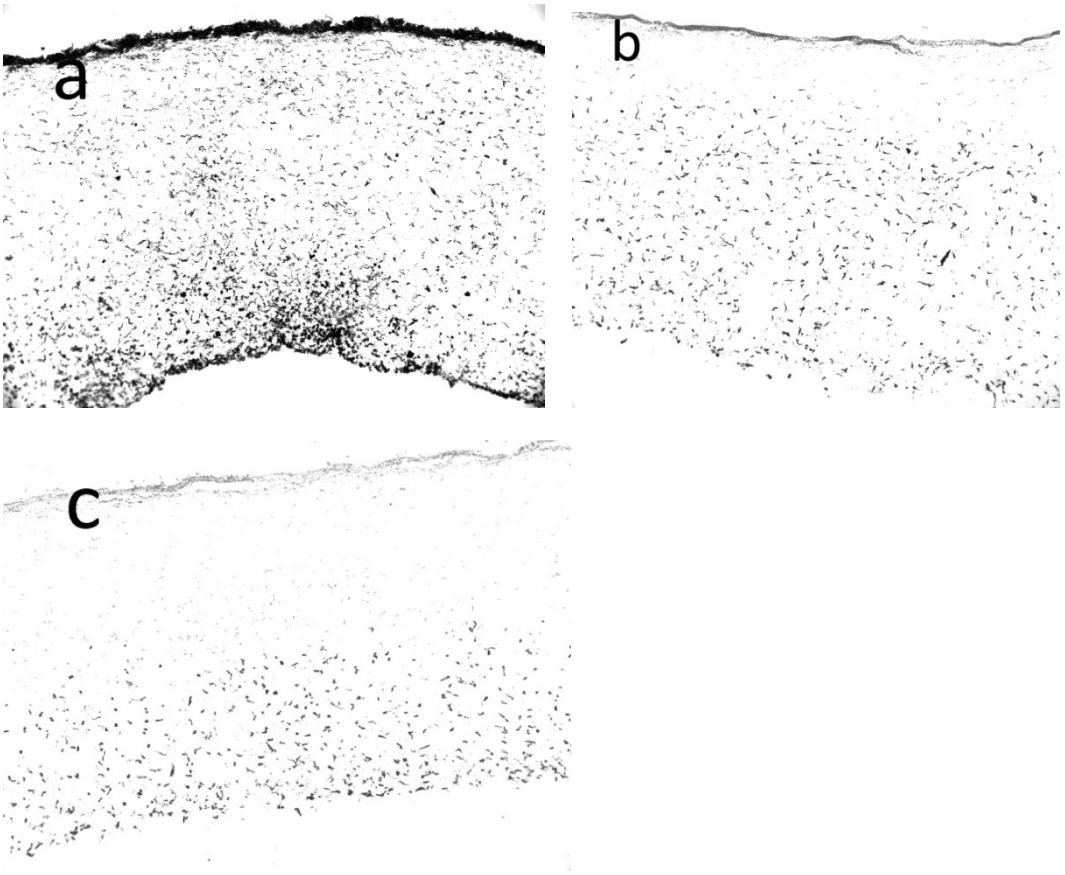

Figure 4. Cryosections on human 3D hemi-cornea models treated for 10 minutes with DOD (a), ACT (b), PF (c).

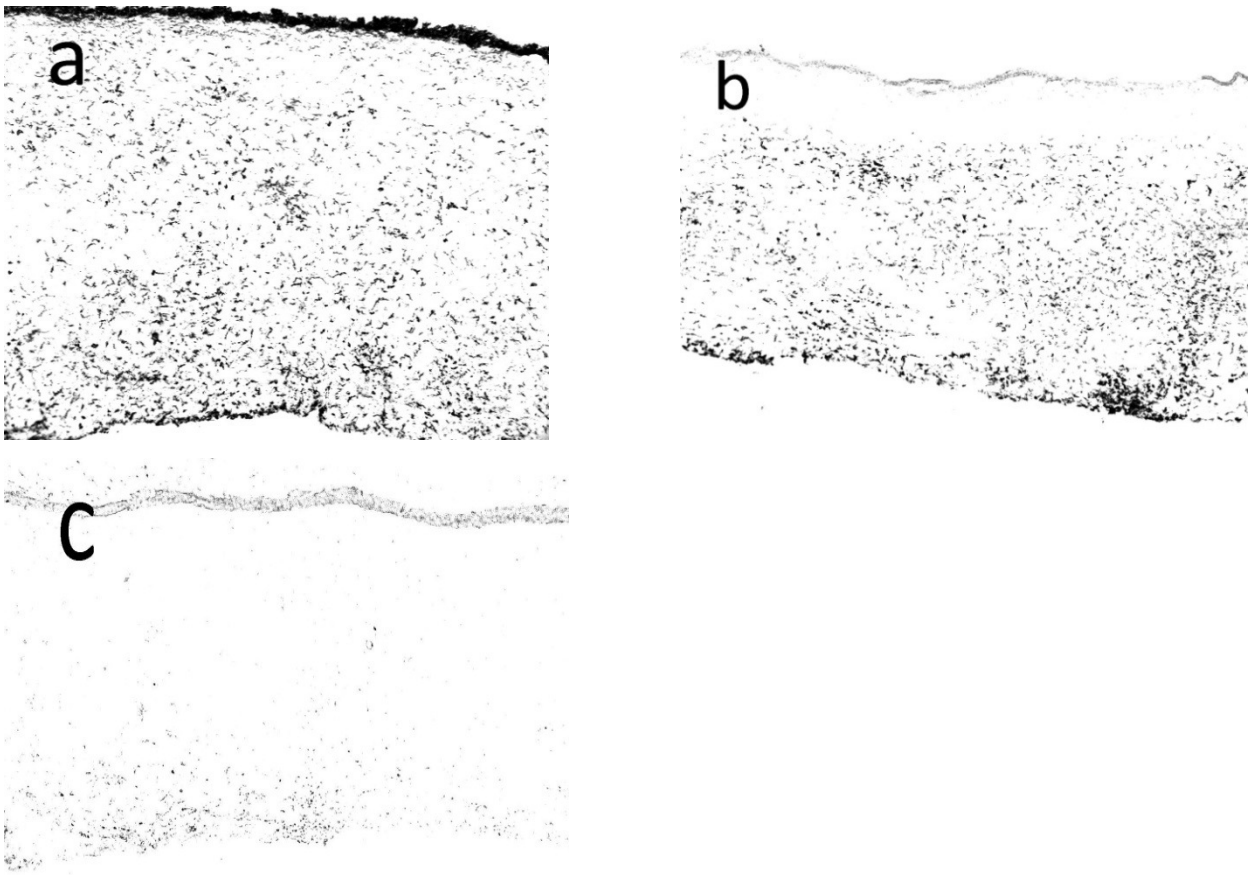

Figure 5. Cryosections on human 3D hemi-cornea models treated for 60 minutes with DOD (a), ACT (b), PF (c).

In Figure 6 the the rMTT-DOI for all test chemicals either after 10 or 60 minutes exposure are summarized in Figure 6. The rMTT-DOI was between 95-100 % on hemi-cornea treated with 1% or 10 % BAK, 10 % AA, 8% NaOH and 5% SDS both after 10 and 60 minutes exposure periods. The rMTT-DOI caused by GHS 2 chemicals, ACT, EMAA and 3% AA were in the range of 5% to 50%. No significant dependence on the exposure time was observed for theses GHS 2 test chemicals. The rMTT-DOI for DOD, DMSO and PTFB (GHS nc category) was very low and independent on the exposure period. In contrast, a strong dependence on the exposure time was measured for PF and CY (GHS 1 category): after 10 minutes exposure, CY and PF, induced only 30.5% and 42.6% rMTT-DOI, respectively, while a 60 minutes exposure led to almost 100% damage. From these results, it was clear that 10 minutes exposure was not enough for the clear discrimination between GHS 1 and GHS 2 category substances. No measurement of

rMTT-DOI could be done for NaOCl treated models as the models were completely dissolved after the application of the chemical.

Above results correspond to results from Zorn-Kruppa et al. (2014) who defined a preliminary prediction model based on the results of the 60 min exposures using two cut-off values for the in vitro classification of the test chemicals into the three GHS categories. According to this prediction model test chemicals of the study presented here with rMTT-DOIs of ≤ 5% are assigned to the non-irritant GHS nc and chemicals with rMTT-DOIs ≥ 90% are assigned to the severe irritant class (GHS 1). All other chemicals with intermediate rMTT-DOIs are predicted as Cat 2 chemicals. The predicted in vitro classifications for all the test chemicals are listed in Table 2.

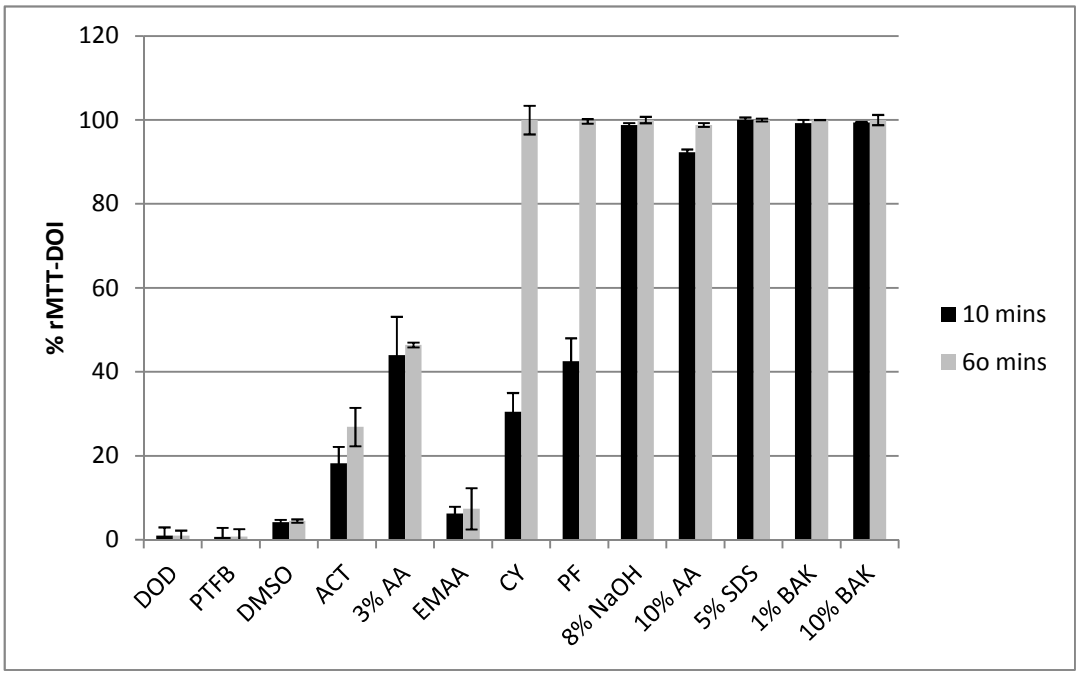

Figure 6. The comparison of rMTT-DOIs after 10 and 60 minutes exposure of chemicals to hemi-cornea models.

Table 2. Comparison of GHS category for test substances predicted by each *in vitro* prediction model with *in vivo* GHS classification

Test substances	*in vivo* GHS classification	*in vitro* GHS classification with CCC method	*in vitro* GHS classification with rMTT-DOI method
DOD	nc	nc	nc
DMSO	nc	nc	nc
PTFB	nc	nc	nc
EMAA	2	2	2
ACT	2	2	2
3% AA	2	1	2
10% AA	1	1	1
1% BAK	1	1	1
10% BAK	1	1	1
8% NaOH	1	1	1
5% SDS	1	1	1
NaOCl	1	1	1
CY	1	1	1
PF	1	1	1

Table 2 compares the predicted classes obtained from both test systems after 60 min exposure with in vivo Draize test categories. The prediction model developed by Zorn-Kruppa et al. (2014) and Bartok et al. (2015) was used for the assignment of the GHS class to the chemicals. The test system with CCC membrane correctly classified 13 out of 14 test substances. Only 3% AA was falsely classified as GHS 1 instead of GHS 2. The rMTT-DOI correctly classified all test substances used in this study.

Discussion

A set of test substances, previously used by Jester et al. (2010), and three additional test materials from the GHS nc category (DOD, DMSO and PTFB) and one from GHS 2 category (EMAA) were studied by using two different approaches based on artificially reconstructed hemi-cornea models. The GHS category of each substance was predicted by following the respective

classification methods described in papers published by Bartok et al. (2015) and Zorn-Kruppa et al. (2014). The aim was to first compare the agreement on the GHS categories of chemicals predicted by the two different test systems that were used in this study and later to compare the usefulness and prediction accuracy of these two methods with the IRE-DOI method presented by Jester et al. (2010).

In the beginning of our studies, an exposure time of 10 minutes was used for the two test systems introduced by Bartok et al. (2015) and Zorn-Kruppa et al. (2014). This exposure time was chosen as the lowest as we have concluded from former experiments (Engelke et al., 2013). Jester et al. (2010) used 10 seconds exposure time in his study. From our results, we deduced that in both test systems even 10 minutes exposure time was not enough to discriminate GHS 1 and GHS 2 category substances. Therefore, the chemical exposure time was increased to 60 minutes. Using the 60 min exposure period, all three GHS categories of eye irritants could be differentiated based on the extent of damage they caused to the models.

These results indicate that the decrease in tissue viability or depth of injury is a diffusion-controlled process which is basically dependent on the stromal part which constitutes at least 90% of the hemi-cornea. The diffusion of the tested chemicals is limited by their diffusion coefficient in the hydrous collagen and the cells serve as toxicity markers in this collagen matrix. From this point of view the hemi-cornea model displays a 3D-cell toxicity assay that, in contrast to standard cultured cell based assays, combines both the diffusion coefficient and inherent cell toxicity of the test chemicals.

Bartok et al. (2015) showed that the stromal and epithelial viabilities are inversely proportional to the severity of irritants. Our comparison study shows that this is true for both test systems. In line with the idea proposed by Engelke et al. (2013), that an irritant first damages the epithelium and later the stroma, our results show that non-irritants or slightly irritant substances (GHS nc), such as DOD, DMSO and PTFB, decrease only the epithelial viability while the stroma remains unaffected. For GHS 2 category irritants, such as 3% AA, EMAA and ACT, a decrease in stromal viability with the complete loss of epithelial viability was observed. Most of the test substances, used in this study, were classified in the GHS 1 category, leading to the complete loss of both stromal and epithelial viability. Sodium hypochlorite (NaOCl), completely dissolved the collagen stroma of the hemi-cornea models immediately after its application, probably because of its very low pH. Therefore, it was classified as GHS 1 category substance.

Conclusions

Our results for both test systems support the hypothesis made by Jester et al. (2006; 2010) and (Maurer et al. (2002)), who showed that the surface area and depth of initial corneal injury (DOI) in the epithelium and stroma, caused by chemicals of various classes in the rabbit eye, strongly correlate with the macroscopically observable severity and duration of ocular injury. The results from our study show that both of these methods can predict the GHS classification of an eye irritant substance. Despite the fact that these two models use the MTT reduction assay in two completely different ways to evaluate the effects of chemicals, there was a concordance in the GHS class predicted by these two methods for 13 out of 14 test substances used. Additionally, the MTT assay is a cheap, simple and widely accepted technique. Thus, one or the other method can be used as a good alternative to the controversial experiments like the Draize test and less accurate and more expensive test like the DOI-IRE.

References

Araki-Sasaki K, Ohashi Y, Sasabe T, et al. (1995) An SV40-immortalized human corneal epithelial cell line and its characterization. Invest Ophthalmol Vis Sci 36(3):614-21

Bartok M, Gabel D, Zorn-Kruppa M, Engelke M (2015) Development of an in vitro ocular test system for the prediction of all three GHS categories. Toxicol In Vitro 29(1):72-80 doi:10.1016/j.tiv.2014.09.005

Cotovio J, Grandidier MH, Lelievre D, et al. (2010) In vitro assessment of eye irritancy using the Reconstructed Human Corneal Epithelial SkinEthic HCE model: application to 435 substances from consumer products industry. Toxicol In Vitro 24(2):523-37 doi:10.1016/j.tiv.2009.11.010

Engelke M, Zorn-Kruppa M, Gabel D, Reisinger K, Rusche B, Mewes KR (2013) A human hemi-cornea model for eye irritation testing: quality control of production, reliability and predictive capacity. Toxicol In Vitro 27(1):458-68 doi:10.1016/j.tiv.2012.07.011

Hayashi K, Mori T, Abo T, et al. (2012) Two-stage bottom-up tiered approach combining several alternatives for identification of eye irritation potential of chemicals including insoluble or volatile substances. Toxicol In Vitro 26(7):1199-208 doi:10.1016/j.tiv.2012.06.008

Huhtala A, Salminen L, Tähti H, Uusitalo H (2008) Corneal Models for the Toxicity Testing of Drugs and Drug Releasing Materials Topics in multifunctional biomaterials and devices, Ed N Ashammakhi

Jester JV (2006) Extent of corneal injury as a biomarker for hazard assessment and the development of alternative models to the Draize rabbit eye test. Cutan Ocul Toxicol 25(1):41-54 doi:10.1080/15569520500536626

Jester JV, Li HF, Petroll WM, et al. (1998) Area and depth of surfactant-induced corneal injury correlates with cell death. Invest Ophthalmol Vis Sci 39(6):922-36

Jester JV, Li L, Molai A, Maurer JK (2001) Extent of initial corneal injury as a basis for alternative eye irritation tests. Toxicol In Vitro 15(2):115-30

Jester JV, Ling J, Harbell J (2010) Measuring depth of injury (DOI) in an isolated rabbit eye irritation test (IRE) using biomarkers of cell death and viability. Toxicol In Vitro 24(2):597-604 doi:10.1016/j.tiv.2009.10.010

Maurer JK, Parker RD, Jester JV (2002) Extent of initial corneal injury as the mechanistic basis for ocular irritation: key findings and recommendations for the development of alternative assays. Regul Toxicol Pharmacol 36(1):106-17

McNamee P, Hibatallah J, Costabel-Farkas M, et al. (2009) A tiered approach to the use of alternatives to animal testing for the safety assessment of cosmetics: eye irritation. Regul Toxicol Pharmacol 54(2):197-209 doi:10.1016/j.yrtph.2009.04.004

OECD (2012a) Acute Eye Irritation/Corrosion. OECD Guidline for Testing of Chemicals No. 405. In: chemicals OGftto (ed). Organisation for Economic Cooperation and Development, Paris, France

OECD (2012b) Fluorescein Leakage Test Method for Identifying Ocular Corrosives and Severe Irritants. OECD Guidline for the Testing of Chemicals No. 460. In: chemicals OGftto (ed). Organisation for Economic Cooperation and Development, Paris, France

OECD (2013a) Bovine Corneal Opacity and Permeability Test method for identifying i) chemicals inducing serious eye damage and ii) chemicals not requiring classification for eye irritation or serious eye damage. OECD Guidline for the Testing of Chemicals No. 437. In: chemicals OGfto (ed). Organisation for Economic Cooperation and Development

OECD (2013b) Test Guideline 438: Isolated Chicken Eye Test method for identifying i) chemicals inducing serious eye damage and ii) chemicals not requiring classifications for eye irritation or serious eye damage. OECD Guidline for the Testing of Chemicals No. 438. In: chemicals OGftto (ed). Organisation for Economic Cooperation and Development, Paris, France

Scott L, Eskes C, Hoffmann S, et al. (2010) A proposed eye irritation testing strategy to reduce and replace in vivo studies using Bottom-Up and Top-Down approaches. Toxicol In Vitro 24(1):1-9 doi:10.1016/j.tiv.2009.05.019

Verstraelen S, Jacobs A, De Wever B, Vanparys P (2013) Improvement of the Bovine Corneal Opacity and Permeability (BCOP) assay as an< i> in vitro</i> alternative to the Draize rabbit eye irritation test. Toxicology in Vitro 27(4):1298-1311

Wilhelmus KR (2001) The Draize eye test. Surv Ophthalmol 45(6):493-515 doi:10.1016/S0039-6257(01)00211-9

Zorn-Kruppa M, Houdek P, Wladykowski E, et al. (2014) Determining the Depth of Injury in Bioengineered Tissue Models of Cornea and Conjunctiva for the Prediction of All Three Ocular GHS Categories. PLoS One 9(12):e114181 doi:10.1371/journal.pone.0114181

Appendix IV

Graefes Arch Clin Exp Ophthalmol
DOI 10.1007/s00417-013-2342-3

BASIC SCIENCE

Brilliant Blue G as protective agent against trypan blue toxicity in human retinal pigment epithelial cells in vitro

Doaa Awad · Imke Schrader · Melinda Bartok · Neeti Sudumbrekar · Andreas Mohr · Detlef Gabel

Received: 12 November 2012 / Revised: 19 March 2013 / Accepted: 2 April 2013

Abstract
Background Combinations of trypan blue (TB), Brilliant Blue G (BBG) and polyethyleneglycol had been shown before to be less toxic to ARPE retinal pigment epithelial cells than TB alone. We studied systematically the influence of combinations of dyes on cell damage.
Methods ARPE cells were exposed to TB (concentration range 0.025 to 1 %), BBG (0.0025 to 0.5 %), and combinations of the two dyes, dissolved in phosphate buffered saline (PBS), for periods between 5 and 60 min. Cell damage was monitored with the WST-1 assay. The effect of different salt concentration was measured in the same way.
Results TB in concentrations of 0.075 % and higher was toxic to the cells already after 30 min incubation. BBG was toxic after 30 min in concentration of 0.1 % and higher, but had a protective effect on cells with incubation time of 5 min and concentrations up to 0.1 %. BBG at concentrations of 0.025 % protected against TB-induced damage at 5 min and 30 min incubation. Salt concentrations between 113 and 225 mM did not influence cell survival even after 30 min. In the presence of TB, propidium iodide bound strongly to the cells.
Conclusions BBG acts as a protecting agent against TB toxicity.

Keywords In vitro toxicity · Trypan blue · Brilliant Blue G · Combination toxicity · Osmolarity · Retinal pigment epithelial cells

D. Awad
Department of Biochemistry, Faculty of Science,
Alexandria University, Moharam Bek,
21511 Alexandria, Egypt

D. Awad · I. Schrader · M. Bartok · N. Sudumbrekar · D. Gabel
Department of Chemistry, University of Bremen,
PO Box 330440, 28334 Bremen, Germany

A. Mohr · D. Gabel
Cooperative Center Medicine, University of Bremen,
Bremen, Germany

A. Mohr
Opthalmological Clinic, Hospital St. Joseph Stift,
Bremen, Germany

M. Bartok · D. Gabel
School of Engineering and Science, Jacobs University Bremen,
Campus Ring 1,
28759 Bremen, Germany

D. Gabel (✉)
School of Engineering and Science, Jacobs University,
Campus Ring 1,
28791 Bremen, Germany
e-mail: d.gabel@jacobs-university.de

Introduction

An epiretinal membrane (ERM) is a pathological membrane formed over the macular area, which can greatly affect visual acuity. It is formed spontaneously in response to changes in the vitreous humor, or in patients with diseases triggering excessive collagen tissue response. Its removal can greatly improve vision [1]. Permanent restoration of vision is greatly aided by the concomitant removal of the internal limiting membrane (ILM) [2, 3]. Also for some stages of idiopathic macular hole surgery, removal of the ILM is assumed to be clinically beneficial [1]. Precise identification of ILM facilitates its complete removal. Since clear and complete identification of ILM is not easy, staining of ILM is recommended for that purpose. Numerous dyes are presently in clinical use for this purpose [4]. Among them are trypan blue (TB) and Brilliant Blue G (BBG). The clinically used concentration for TB is between 0.15 % and 0.25 %, that of BBG, 0.025 % (w/v) [3].

Recently, it has been suggested that combinations of dyes might be advantageous for staining of an epiretinal membrane as well as the internal limiting membrane in one step. The combination of TB and BBG was tested by us for toxicity [5]. Surprisingly, toxicity was not additive; rather, BBG appeared to have a protective effect against TB toxicity. As the combination of dyes was tested only in a limited concentration range (a range assumed to be optimal for the intended staining in preparation for surgery) and in the presence of polyethylene glycol (PEG), it was not possible to identify the cause of the apparent protective effect, and the dependence on the concentrations of the two dyes was not investigated.

We have therefore studied, in a systematic manner, the influence of combinations of BBG and TB on human retinal pigment epithelial cells (ARPE) and their time dependence. We have used the WST-1 assay for following cellular activity, an assay similar to the MTT assay, measuring the activity of intra- and extracellular dehydrogenases. In the literature, toxicity has also been assayed by measuring cell membrane permeability. We have therefore also tested the integrity of the cell membrane by running a propidium iodide (PI) assay, which stains cell nuclei of cells whose membrane is compromised.

As the literature [6–8] also has discussed the influence of changes in osmolarity on potential toxicity of dye preparations, we have varied the osmolarity of buffer solutions without dye and measured cell activity.

Materials and methods

Dye solutions

TB was a gift from Netherlands Institute for Innovative Ocular Surgery (NIIOS), Rotterdam, The Netherlands. Brilliant Blue G (BBG) was purchased from Sigma-Aldrich Co (Taufkirchen, Germany). TB and BBG dye powders were dissolved in phosphate buffered saline without Ca^{2+} or Mg^{2+} (PBS) to generate 1 % and 0.5 % (w/v) stock solutions, respectively. The dyes were diluted with PBS to the final concentrations used. PBS was chosen to allow comparison with the previous data [5]. All dye solutions were kept in the dark until use.

Solutions having different salt and buffer concentrations (NaCl concentrations between 75 and 300 mM) were prepared by diluting a 10 times concentrated PBS with distilled water. The tested solutions were incubated with ARPE cells for 30 min at 37 °C. PBS was used as negative control.

Cell culture and viability assay

ARPE cells (obtained from ATCC, LGC) were cultivated in a 1:1 mixture of Dulbecco's Modified Eagles Medium and Ham's F12 (DMEM-F12) supplemented with 10 % fetal bovine serum (FBS) and 1 % penicillin–streptomycin. Cells were cultured at 37° in an atmosphere of 5 % CO_2, and passaged by trypsinization with 0.25 %/0.02 % (w/v) trypsin/ethylenediaminetetraacetic acid (EDTA). ARPE cells were seeded at a density of 2×10^4 cells/well into 96-well flat bottomed plates and grown to confluence over 48 h.

Cell viability was examined using the cell proliferation reagent WST-1 (Roche Diagnostics GmbH, Mannheim, Germany). The tetrazolium salt WST-1 (4-[3-(4-iodophenyl)-2-(4-nitrophenyl)-2H-5-tetrazolio]-1,3-benzene disulfonate) is efficiently reduced by mitochondrial dehydrogenases in viable cells to a red soluble formazan. A decrease in the number of metabolically active cells (used here as a measure of cell viability) results in decrease in the overall activity of mitochondrial dehydrogenases, leading to a decrease in the amount of formazan dye formed. The produced formazan dye was quantified by a plate reader at 450 nm. The WST-1 reagent was diluted 10 times with DMEM-F12. After dilution, 100 µl WST-1 containing DMEM-F12 was added per well and incubated at 37 °C in a 5 % CO_2 for 90 min.

Experiments were performed to determine whether the presence of any residual dyes interferes with the WST-1 assay. Cells were incubated with TB, BBG or PBS, and then washed three times with PBS. DMEM-F12 was added instead of the WST-1 reagent. The optical densities at 450 nm were measured. No influence of the presence of residual dyes on the readings was found.

Experimental incubation

Time- and dose-dependent toxicities were examined. Once cells reached confluence, the growth medium was replaced with 50 µl of the experimental solution per well. After incubation, cells were washed three times with 100 µl of sterile phosphate buffer saline (PBS). Cell viability was then determined, with cells incubated with 50 µl PBS as control.

To determine the influence of the concentration of the dyes and different incubation times on viability, ARPE cells were exposed to 0.025, 0.075, 0.15, 0.25, 0.5, 0.75, 1 % TB for 5, 30 and 60 min, whereas BBG was used at concentrations of 0.0025, 0.0075, 0.025, 0.05, 0.1, 0.2, 0.3, 0.5 %.

In order to determine the influence of combining the clinically relevant concentration of TB (0.15 %) and BBG at different concentrations on the ARPE viability, combinations consisting of 0.025 % BBG and different concentrations of TB were also tested. The effect of varying osmolarity on cell viability was measured by incubating the cells with diluted solutions of a 10 fold concentrated PBS stock, with final concentrations of NaCl in PBS between 300 and 75 mM (corresponding to concentrations between twice and half of the normal concentration).

Uptake of propidium iodide

Uptake of propidium iodide (PI) was observed in a fluorescence microscope, as this had initially been described as an assay for cell membrane integrity [4] and cell viability [9]. The cells were seeded in flat bottomed 12 well plates at a density of 2×10^5 cells/well and incubated for 48 h at 37 °C. After the cells became confluent, they were incubated for 30 min with 500 µl of each test solution. Incubation with PBS was used as a negative control and with 70 % Ethanol as positive control. The cells were washed three times with PBS and incubated for 30 min at 37 °C with 10 µM PI and 20 µM H33342 solution prepared in cell culture media. After three washes with PBS, the cells were fixed with 8 % formaldehyde at 37 °C for 10 min, washed trice with PBS and analyzed under a Zeiss 100 microscope with 20× objective.

Statistical evaluation

The results are expressed as percentage of viable cells of controls (cells incubated with PBS). All experiments were carried out at least three times. Statistically significant differences between groups of data were calculated by GraphPad Instat; *P* values less than 0.05 were considered significant. All error bars pertain to this *P* level.

Results

The aim of our study was to examine the safety of different dyes and dye concentrations on ARPE cells in vitro. We therefore established that the dyes did not interfere with the WST-1 assay, where a red formazan is produced. Comparisons of the optical densities of cells which had been washed three times after incubation with TB or BBG with those incubated with PBS revealed that any of the two blue dyes possibly remaining in the well does not interfere with the WST assay (data not shown).

The time-dependent toxicity of 0.15 % and 0.25 % TB is shown in Fig. 1a. Cell survival is significantly reduced to 82 % and 62 %, respectively, with incubation times of 30 min, and to 59 % and 48 % following incubation for 1 h, but not for shorter times. In contrast, 0.025 % BBG is not significantly toxic even after 60 min incubation, and 0.05 % BBG only after 60 min (reduction to 81 % cell survival) (Fig. 1b). TB in concentrations of 0.15 % and 0.25 % is significantly toxic for ARPE cells after 30 min exposure. At a concentration of 0.25 % and 15 min incubation, TB was not significantly toxic.

Concentrations of TB up to 0.075 % were found to be nontoxic when ARPE cells were exposed for only 5 min (Fig. 1c). For incubation times of 30 and 60 min, already a 0.075 % dye solution reduced the viability significantly (to

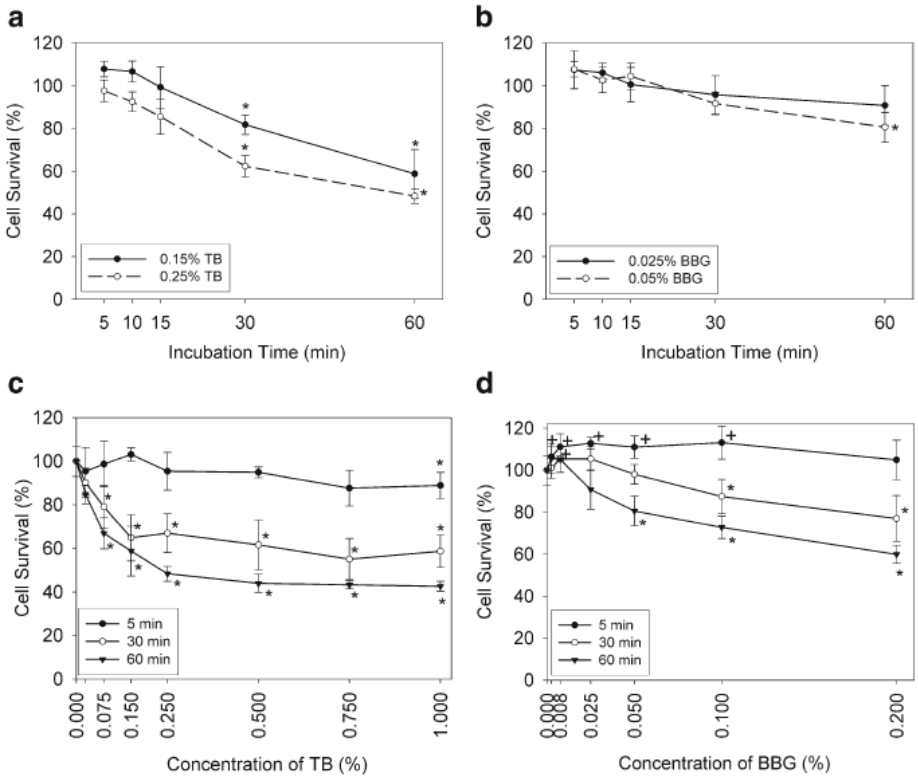

Fig. 1 Survival of ARPE cells after incubation with TB or BBG for different incubation periods. **a** Cells incubated with the clinically relevant concentrations of TB (0.15 % and 0.25 %). **b** BBG in clinically relevant concentrations (0.025 % and 0.05 %). **c** Viability of ARPE cells after 5 min, 30 min and 60 min exposure to TB at varying concentrations. **d** Viability of ARPE cells after 5 min, 30 min and 60 min exposure to BBG at varying concentrations. Data points with "*asterisk*": significantly lower survival than control ($p<0.05$); data points with "*plus sign*": significantly higher than control ($p<0.05$)

values of 79 % and 66 %, respectively). Concentrations higher than 0.25 %, while being toxic, did not lead to a further decrease in cell viability. There is a trend for TB to be more toxic following a 60-minute exposure, as compared to a 30-minute exposure, but this was significant ($p<0.05$) only at 0.25 % TB.

With BBG and exposure times for 30 min or 60 min, cell survival significantly decreased with high BBG concentrations (higher than 0.025 %) and with increasing incubation time. Exposure to BBG for 60 min was more toxic than exposure for 30 min with BBG concentrations of 0.05 % and higher. For concentrations of 0.2 %, cell survival was reduced to 75 % after 30 min and to 59 % after 60 min. In contrast, none of the concentrations tested led to reduced cellular activity when incubated for 5 min; on the contrary, the viabilities of cells incubated for 5 min with BBG concentrations lower than 0.2 % were all significantly higher than 100 % (Fig. 1d).

The dependence of BBG toxicity on time and concentration is thus different from that of TB.

Figure 2a shows cell survival as a function of varying TB concentrations with and without 0.025 % BBG at exposure time 5 min and 30 min. TB alone (0.075, 0.15, 0.25, 0.5 or 0.75 % TB) as well as its mixture with 0.025 % BBG was not significantly toxic when incubated with the cells for 5 min. Increasing the incubation time for TB to 30 min resulted in a significant decrease in cell viabilities (78 % at 0.075 % TB and 64 % at 0.15 % TB). The decrease was, however, significantly reduced by the addition of 0.025 % BBG. At 0.075 % TB, the addition of 0.025 % BBG resulted in complete restoration of cell viability (96 %), and at 0.15 % TB, BBG increased cell viability to 89 %.

When ARPE cells were exposed for 5 min to BBG alone in concentrations of 0.0075, 0.025, 0.05 or 0.1 %, the cell viability increased significantly to between 105 and 113 % (Fig. 2b). When 0.15 % TB was added, the increase in cell viability was still significant for concentrations of 0.025 % BBG and lower, and survival was 101 % even for the highest BBG concentration of 0.2 %. An exposure period of 30 min to BBG in concentrations lower than 0.1 % was found to have no effect on cell viability. For BBG concentrations of less than 0.1 % and an incubation time of 30 min, addition of 0.15 % TB significantly decreased the viability when compared to BBG alone.

As it has been discussed in the literature before that ARPE cells take up PI when damaged [9], cells exposed to different concentrations of TB, in the absence or presence of 0.025 % BBG, were incubated with PI after the exposure to the dyes and their removal through washing. Representative staining for PI are found in Fig. 3. When cells as positive controls had been damaged by exposure to ethanol, staining in the nuclei of the cells was evident. Following exposure to TB, intense staining of the whole cell body was found, and the staining did not co-localize with that of Hoechst 33342, which was used to detect the nuclei. We therefore conclude that PI staining is unsuitable for detecting the toxicity of TB.

The potential influence of changes in osmolarity on cell survival has been discussed in publications dealing with retinal pigment epithelial cells [6–8]. We have therefore tested the influence of salt concentration on the cell viability (Fig. 4). Following incubation for 30 min, only solutions with a total salt concentration of 75 and 300 mM induced a significant decrease in cell viability, whereas no significant decrease in viability was determined with any of the concentrations between these extremes (112.5, 135, 165, 225 mM). The control was cells incubated with PBS (150 mM).

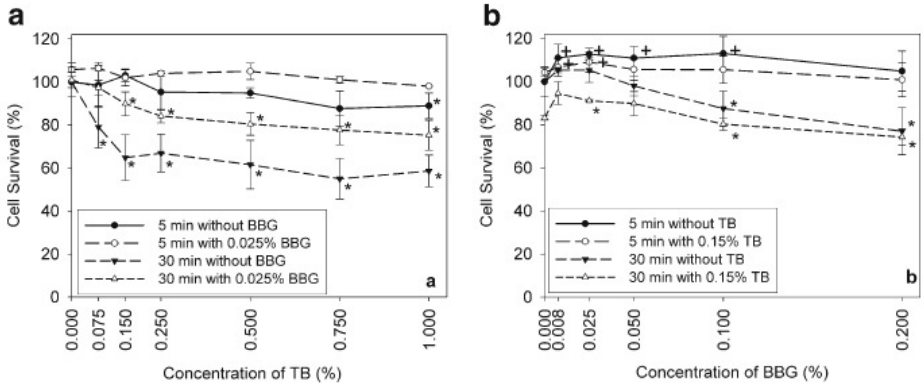

Fig. 2 **a** Survival of ARPE cells after incubation with varying concentrations of TB with and without 0.025 % BBG for 5 and 30 min. **b** Effect of different concentrations of BBG with and without 0.15 % TB incubated with the cells for 5 and 30 min on cell viability. Data points with "*asterisk*": significantly lower survival than control ($p<0.05$); data points with "*plus sign*": significantly higher than control ($p<0.05$). Values for incubation with the single dyes are identical to Fig. 1

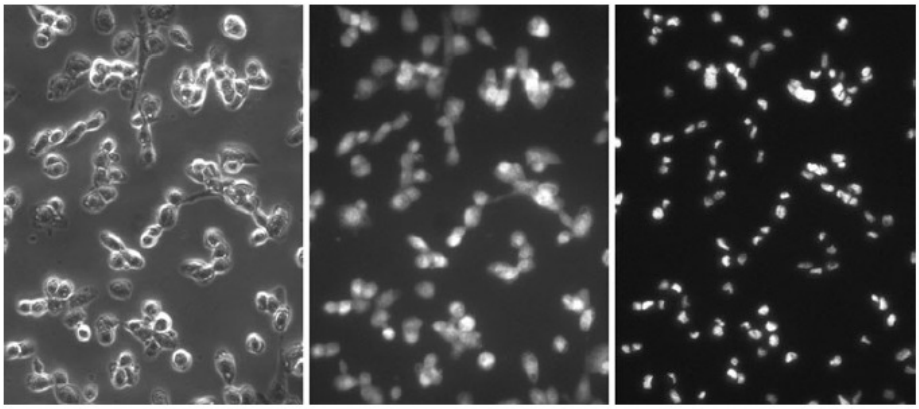

Fig. 3 Staining of cells with PI and Hoechst 33342 following exposure to TB 0.15 %. *Left*: phase contrast image. *Center*: PI staining. *Right*: staining with Hoechst 33342

Discussion

The combination of TB and BBG, in combination with polyethyleneglycol (PEG) to increase the density and viscosity of the solution (labeled as MembraneBlue-Dual™), has been found to enhance the staining effect of both ERM and ILM in one step. It facilitated removal of the membranes, as shown in a small retrospective comparative case study [10] and confirmed in a prospective multicenter study (Veckeneer, Mohr et al., submitted). The ease of removal was scored and found to be better for the combination that for BBG with PEG alone (labeled as ILM-Blue™).

The concentrations of TB and BBG used in the experiments were adopted from the concentrations in clinical use in vitreoretinal procedures or in eye banking (for a review see [11]). In the concentration range tested, TB had a much more pronounced toxic effect than BBG. On the basis of the results presented here, higher concentrations of the two dyes would only moderately increase the toxic effect on cells, and especially the toxic effect of TB is greatly reduced by BBG.

None of the toxic effects found can be caused by varying osmolarity of the different preparations; this cause has been implied by a number of authors [6–8]. We found that even drastic changes in osmolarity did not lead to relevant toxic effects within the first 30 min of exposure. This is in line with the results of Jackson et al. [8]. Previously, short-term exposure to hypoosmolar solutions containing indocyanine green solutions has been attributed to hypoosmolarity [7]. Recent work by Costa et al. investigated the effect of glucose and mannose in hypo- and hyperosmolar solutions on RPE cells [12]. The authors found that glucose exhibited a considerable toxic effect at all concentrations tested, whereas the same concentrations of mannitol did not affect cell viability. It is known from the literature that toxicity of benzalkonium chloride on conjunctival epithelial cells is potentiated by hyperosmolarity [13]. Such influences might be of importance also for the toxicity of dyes used in ocular surgery.

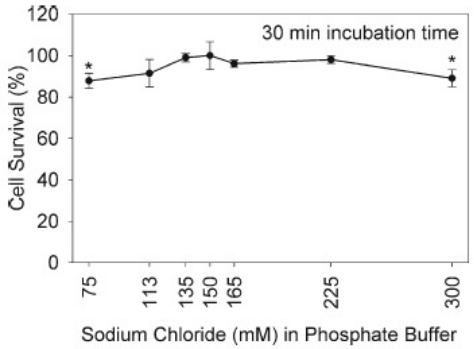

Fig. 4 Effect of concentration of PBS buffer on cell viability. Concentration is expressed for NaCl, with 150 mM corresponding to physiological conditions. Phosphate concentration at this NaCl concentration is 10 mM, and correspondingly lower or higher for lower or higher salt concentrations

Mannitol at physiological osmolarity increased cell survival to the same extent as seen here with BBG [12].

The toxicity of TB reaches a plateau of around 40 % cell survival at concentrations of 0.25 % and higher. Toxic effects not leading to complete reduction of cell function have been found by other authors [14]. They explained this by cells being in different stages of the cell cycle. We did not use synchronized cell cultures for our experiments, and thus we cannot exclude this as an explanation of the concentration dependence of the toxicity of TB.

BBG had a pronounced protective effect in our experiments, while at the same time being non-toxic in the concentration used. This was at first glance unexpected. It is, however, known from literature (e.g. [15]) that BBG acts as an antagonist on the P2X7 cell death purinergic receptor. The receptor is physiologically activated by extracellular ATP and leads to uptake of dyes and eventually apoptotic cell death [16].

The activation of the P2X7 receptor has been found to open channels large enough for fluorescent dyes such as PI to penetrate [16]. With TB, we did, however, find that the cell body, and not only the nucleus, is stained strongly. Therefore, we cannot conclude whether the protective effect of BBG is through its influence on the P2X7 receptor.

BBG has been found to have a protective effect not only in cell culture, but also in organs ex vivo and in vivo [17]. We therefore suggest that BBG might be used as an additive for other diagnostic and surgical short-term procedures whenever agents are limited in their dosage due to their inherent cellular toxicity.

Disclosures None

Funding/support This work has been supported by the Meyer-Schwarting Foundation Bremen

Financial disclosures None

Contributions of authors Design and conduct of the study (DA, DG, AM)

Collection, management, analysis, and interpretation of the data (DA, IS, MB, NS)

Preparation, review, or approval of the manuscript (DA, DG, AM).

Statement about Conformity with author information Not applicable

Other acknowledgments None

References

1. Christensen UC, Krøyer K, Sander B, Larsen M, Henning V, Villumsen J, la Cour M (2009) Value of internal limiting membrane peeling in surgery for idiopathic macular hole stage 2 and 3: a randomised clinical trial. Br J Ophthalmol 93:1005–1015
2. Kwok A, Lai TY, Yuen KS (2005) Epiretinal membrane surgery with or without internal limiting membrane peeling. Clin Exp Ophthalmol 33:379–385
3. Rodrigues EB, Maia M, Meyer CH, Penha FM, Dib E, Farah ME (2007) Vital dyes for chromovitrectomy. Curr Opin Ophthalmol 18:179–187
4. Morales MC, Freire V, Asumendi A, Araiz J, Herrera I, Castiella G, Corcostegui I, Corcostegui G (2010) Comparative effects of six intraocular vital dyes on retinal pigment epithelial cells. Investig Ophthalmol Vis Sci 51:6018–6029
5. Awad D, Schrader I, Bartok M, Mohr A, Gabel D (2011) Comparative toxicology of trypan blue, brilliant blue G, and their combination together with polyethylene glycol on human pigment epithelial cells. Investig Ophthalmol Vis Sci 52:4085–4090
6. Sippy BD, Engelbrecht NE, Hubbard GB, Moriarty SE, Jiang S, Aaberg TMJ, Aaberg TMS, Grossniklaus HE, Sternberg PJ (2001) Indocyanine green effect on cultured human retinal pigment epithelial cells: implication for macular hole surgery. Am J Ophthalmol 132:433–435
7. Stalmans P, Van Aken EH, Veckeneer M, Feron EJ, Stalmans I (2002) Toxic effect of indocyanine green on retinal pigment epithelium related to osmotic effects of the solvent. Am J Ophthalmol 134:282–285
8. Jackson TL, Hillenkamp J, Knight BC, Zhang JJ, Thomas D, Stanford MR, Marshall J (2004) Safety testing of indocyanine green and trypan blue using retinal pigment epithelium and glial cell cultures. Investig Ophthalmol Vis Sci 45:2778–2785
9. Kodjikian L, Richter T, Halberstadt M, Beby F, Flueckiger F, Boehnke M, Garweg JG (2005) Toxic effects of indocyanine green, infracyanine green, and trypan blue on the human retinal pigmented epithelium. Graefes Arch Clin Exp Ophthalmol 243:917–925
10. Kovacevic D, Mance TC, Markusic V (2011) "Brilliant Blue G" and "Membrane Blue Dual" assisted vitrectomy for macular hole. Coll Anthropol 35(Suppl 2):191–193
11. Rodrigues EB, Costa EF, Penha FM, Melo GB, Bottos J, Dib E, Furlani B, Lima VC, Maia M, Meyer CH, Hofling-Lima AL, Farah ME (2009) The use of vital dyes in ocular surgery. Surv Ophthalmol 54:576–617
12. Costa EF, Barros NMT, Coppini LP, Neves RL, Carmona AK, Penha FM, Rodrigues EB, Dib E, Magalhães O Jr, Moraes-Filho MN, Filho AASL, Maia M, Farah ME (2013) Effects of light exposure, pH, osmolarity, and solvent on the retinal pigment epithelial toxicity of vital dyes. Am J Ophthalmol 155:705–712
13. Clouzeau C, Godefroy D, Riancho L, Rostene W, Baudouin C, Brignole-Baudouin F (2012) Hyperosmolarity potentiates toxic effects of benzalkonium chloride on conjunctival epithelial cells in vitro. Mol Vis 18:851–863
14. Hollenbach PW, Nguyen AN, Brady H, Williams M, Ning Y, Richard N, Krushel L, Aukerman SL, Heise C, MacBeth KJ (2010) A comparison of azacitidine and decitabine activities in acute myeloid leukemia cell lines. PLoS One 5:e9001
15. Dutot M, Liang H, Pauloin T, Brignole-Baudouin F, Baudouin C, Warnet JM, Rat P (2008) Effects of toxic cellular stresses and divalent cations on the human P2X7 cell death receptor. Mol Vis 14:889–897
16. Virginio C, MacKenzie A, North RA, Surprenant A (1999) Kinetics of cell lysis, dye uptake and permeability changes in cells expressing the rat P2X7 receptor. J Physiol 519(Pt 2):335–346
17. Peng W, Cotrina ML, Han X, Yu H, Bekar L, Blum L, Takano T, Tian GF, Goldman SA, Nedergaard M (2009) Systemic administration of an antagonist of the ATP-sensitive receptor P2X7 improves recovery after spinal cord injury. Proc Natl Acad Sci U S A 106:12489–12493

Appendix V

Reduction of cytotoxicity of benzalkonium chloride and octenidine by Brilliant Blue G

M. Bartok*, R. Tandon, G. Alfaro-Espinoza, M. S. Ullrich and D. Gabel

School of Engineering and Science, Jacobs University Bremen, Campus Ring 1, 28759, Bremen, Germany

*Corresponding author

Abstract

The irritative effects of preservatives found in ophthalmic solutions, or of antiseptics used for skin disinfection is a consistent problem for the patients. The reduction of the toxic effects of these compounds is desired. Brilliant Blue G (BBG) has shown to meet the expected effect in presence of benzalkonium chloride (BAK), a well known preservative in ophthalmic solutions, and octenidine dihydrochloride (Oct), used as an antiseptic in skin and wound disinfection. BBG shows a significant protective effect on human corneal epithelial (HCE) cells against BAK and Oct toxicity, increasing the cell survival up to 51% at the highest BAK or Oct concentration tested, which is 0.01%, both at 30 min incubation. Although BBG is described as a P2x7 receptor antagonist, other selective P2x7 receptor antagonists, OxATP (adenosine 5'-triphosphate-2',3'-dialdehyde) and DPPH (N'-(3,5-dichloropyridin-4-yl)-3-phenylpropanehydrazide), did not reduce the cytotoxicity of neither BAK nor Oct. Therefore we assume that the protective effect of BBG is not due to its action on the P2x7 receptor. Brilliant Blue R (BBR), a dye similar to BBG, was also tested for its protective effect on BAK and Oct toxicity. In the presence of BAK no significant protective effect was observed. Instead, with Oct a comparable protective effect was seen with that of BBG. To ensure that the bacteriostatic effect was not affected by the combinations of BAK/BBG, Oct/BBG and Oct/BBR, bacterial growth inhibition was analyzed on different Gram-negative and Gram-positive bacteria. All combinations of BAK or Oct with BBG hinder growth of Gram-positive bacteria. The combinations of 0.001% Oct and BBR above 0.025% do not hinder the growth of *B. subtilis*. For Gram-negative bacteria, BBG and BBR reduce, but do not abolish, the antimicrobial effect of BAK nor of Oct. In conclusion, the addition of BBG at bacterial inhibitory concentrations is suggested in the ready-to-use ophthalmic preparations and antiseptic solutions.

Keywords

Brilliant Blue G; Brilliant Blue R; Benzalkonium chloride; Octenidine dihydrochloride; P2x7 receptor antagonist

Introduction

Brilliant Blue G (BBG) is widely used as a dye for proteins in gel electrophoresis. Its power to stain proteins has led to its application in vitreoretinal surgery for the staining of the internal limiting membrane (ILM), as it showed no toxic effects at the clinically suggested concentration, 0.025%, while showing good staining ability (Enaida et al. 2006). Later, BBG was found to be a great asset also in the treatment of the spinal cord injury, because it reduced the local inflammatory responses, showed protective effects towards the spinal cord neurons and improved the motor recovery (Marcillo et al. 2012; Peng et al. 2009). The authors paired the physiological function of BBG with its activity as a P2x7 receptor antagonist as the spinal cord neurons express this receptor abundantly at their surface. In previous studies, we showed that BBG protects ARPE retinal pigment epithelium cells against the toxicity of trypan blue (TB), which is another widely used dye for the staining of the ILM in eye surgery (Awad et al. 2013). This observation was unexpected, and no clear mechanism was proposed. Also, it was not known whether the protective effect of BBG was limited to TB, or whether it was more universal. Brilliant Blue R (BBR) is a dye very similar to BBG, which differs only by the absence of two methyl groups. BBR, in contrast to BBG, has never been used medically. In the literature, BBR is used only as a sensitive protein stain in polyacrylamide gel electrophoresis (Servaites et al. 2012). In this study we have tested the cytotoxicity of benzalkonium chloride (BAK) and octenidine (Oct) in combination with BBG or BBR in order to see whether there is any significant reduction in the toxicity of the compounds on human corneal epithelial cells (HCE). BAK is a widely used preservative in ophthalmic drops, even though it is known to have cytotoxic effects and easily causes inflammation on the eye surface (Ammar and Kahook 2011; Dutot et al. 2006; Liang et al. 2012; Paimela et al. 2012). Oct is an antiseptic agent for skin, mucous membranes and wounds, and is used in many preparations as a replacement for other antiseptics, because it shows a significantly higher efficiency already at very low concentrations (Hübner et al. 2010; Koburger et al. 2010). At the clinically and industrially used concentrations, both compounds show high cytotoxicity against mammalian cells. After only 5 minutes

incubation with HCE cells, less than 20% of the cells were found to be metabolically active. Interestingly, we found a high protective effect of BBG against the cytotoxic action of BAK and Oct, without an excessive reduction of the bacteriostatic effect.

Materials and Methods

Materials

Dulbecco's Modified Eagles Medium with Ham's F12 (DMEM + F12), BAK, BBG, BBR and OxATP (adenosine 5'-triphosphate-2',3'-dialdehyde) were purchased from Sigma-Aldrich (Schnelldorf, Germany). Oct was provided by Schülke & Mayr GmbH (Norderstedt, Germany). HCE cells were from Riken Bioresource Center (Tsukuba, Japan). WST-1 cell proliferation reagent was from Roche Diagnostics (Mannheim, Germany). Fetal bovine serum (FBS) and penicillin/streptomycin (Pen/Strep) were from Biochrom (Germany). Human epithelial growth factor (hEGF), insulin, amphotericin B, and L-glutamine were from Sigma-Aldrich (Steinheim, Germany), TrypLE Express was from Gibco (USA). DPPH (N'-(3,5-dichloropyridin-4-yl)-3-phenylpropanehydrazide) was synthesized as described by Lee et al. (Lee et al. 2012). The medium MHB (Mueller-Hinton Bouillon) was from Carl Roth (Germany).

Test solutions

BBG was used between 0.0025 and 0.075%, in combination with either BAK between 0.001 and 0.01%, or Oct between 0.002 and 0.01%. BBR was tested between 0.0025 and 0.05% in the presence of BAK at 0.004% and Oct at 0.003%. As negative control PBS was used. Each of these concentrations were also tested alone on HCE cells as well as on the below mentioned bacterial strains.

Cell culture and cell viability assay

HCE cells were cultivated in DMEM + F12 media, supplemented with 15% FBS, 1% Pen/Strep, 25 µg/ml amphotericin B, 5 µg/ml insulin, 10 ng/ml hEGF and 2 mM L-glutamine, at 37°C and 5% CO_2. The cells were passaged by trypsinization with TrypLE Express and seeded at a density of 20,000 cells/well in a 96-well, flat bottom plate and grown for 48 h prior to experiment. After the cells reached confluence, they were incubated with 50 µl/well of different test solutions for 5, 30 and 60 min at 37°C and then washed 3 times with PBS (w/o Ca^{2+} and Mg^{2+}). One hundred µl

of diluted WST-1 cell proliferation reagent (diluted 1:4 in PBS, then 1:10 in cell culture medium) was added to each well and incubated with the cells at 37°C for 4 h. The WST-1 reagent, which is a tetrazolium salt, is reduced to a red formazan dye by the mitochondrial dehydrogenases of metabolically active cells. We checked previously that the readings for this dye are not influenced by any remaining BBG (Awad et al. 2013). The amount of formazan dye formed was taken as a measure of cell survival. The absorbance of the plate was measured in an MR5000 plate reader (Dynatech) at 450 nm. All test solutions were tested in three independent experiments, with 6 to 12 measurements for each experiment.

Determination of inhibitory concentrations for bacterial cells

The Gram-positive bacteria *Bacillus subtilis, Clavibacter michiganensis* and *Paenibacillus sp.* as well as the Gram-negative bacteria *Escherichia coli* DH5α, *Pseudomonas putida* DSM 291 and *Vibrio sp.* Gal12 were used in the assay. The antimicrobial activities of the compound mixtures were assayed in micro-titer plates. For this, 100 µl of MHB were aliquoted into each well of the micro-titer plate, followed by 20 µl of a mixture of antimicrobial compounds and 100 µl of the bacterial suspension (approximately $2 \cdot 10^6$ cells/ml). Deionized water was used as negative control. All micro-titer plates were incubated overnight at 28 ºC, except for *E. coli* plates, which were incubated at 37 ºC. Following overnight incubation, the plates were examined for visible bacterial growth evidenced by the turbidity. Where no turbidity was seen, we assumed that there was no bacterial growth. For each compound, the assay was performed in triplicate in three independent experiments and in accordance with Jorgensen and Turnidge (2007).

Results

To investigate the influence of the time and the concentrations of BBG, BAK and Oct on the HCE cell viability, as well as their impact on the bacterial growth inhibition, the cells were exposed to different concentrations of these compounds. Our results showed that BAK was highly toxic for HCE cells. Already in concentrations of 0.001% and 5 min incubation, 30% cell loss was observed. For longer exposure, as would be used in wound treatment, concentrations of 0.002% reduced the cell survival to 20% or less. The inclusion of BBG, in the concentration of 0.025% used clinically for staining procedures, reduced the toxicity of BAK considerably (Fig. 1). This protective effect of BBG led to an increase of cell survival, with 50% at 5 min, 35% at

30 min and 27% at 60 min incubation at a concentration of BAK 0.01%, the highest concentration tested in this study.

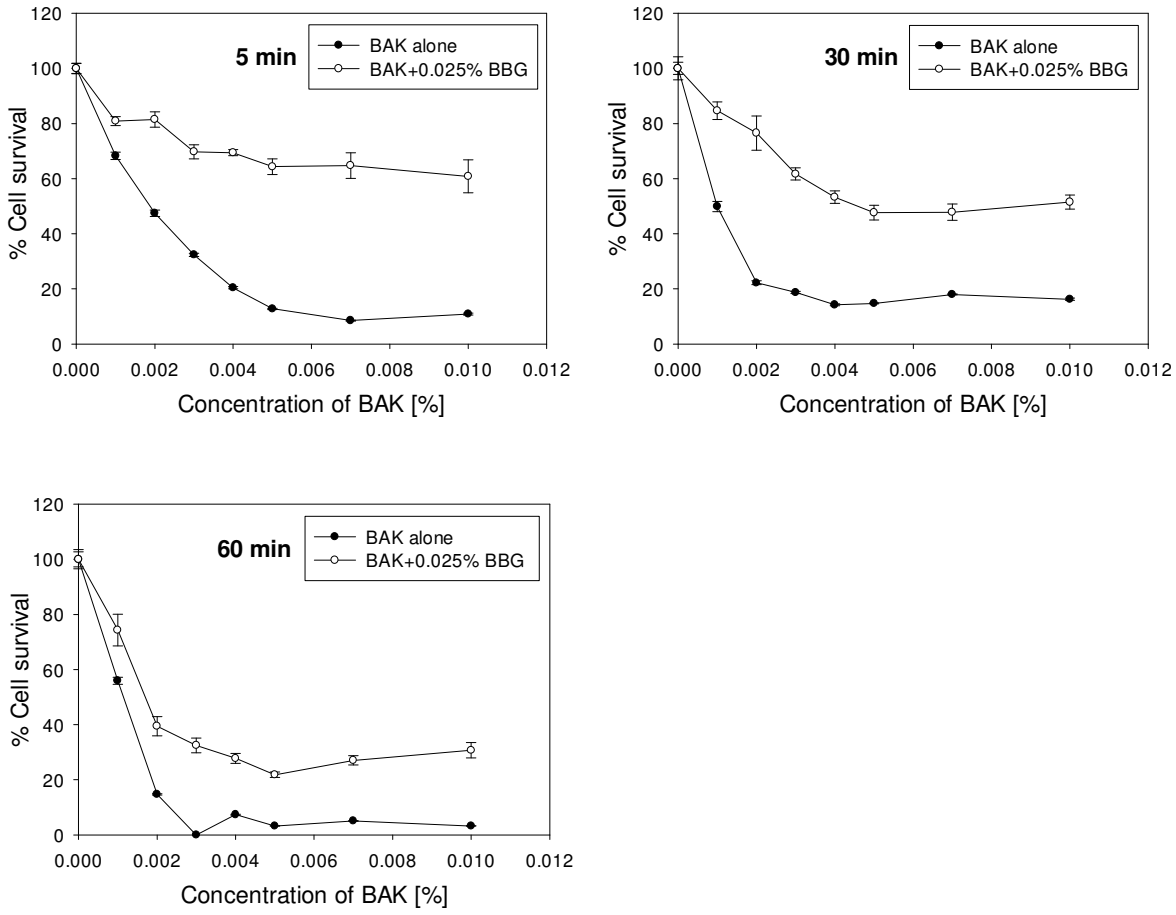

Fig. 1 Survival of HCE cells after exposure for 5, 30 and 60 minutes to different concentrations of BAK in PBS ("BAK alone") and in combination with 0.025% BBG. The error bars represent the standard deviations of 6 to 12 replicates performed within the same experiment.

The cell survival after exposure to BAK in the presence of different BBG concentrations is shown in Fig. 2. Even at low BBG concentrations, the compound showed significant increase of the cell survival: at 0.007% BBG, 67% of the cells survived exposure to 0.004% BAK, and 48% survived when exposed to 0.006% BAK. Without BBG, cell survival at these concentrations of BAK was around 15% (Fig. 1). At higher BAK concentrations, higher BBG concentrations have to be chosen; for example at 0.01% BAK with 0.015% BBG the cell survival increased to 37% and with 0.030% BBG to 46%, at 30 min incubation, whereas in the absence of BBG, cell survival of only a few percent was seen.

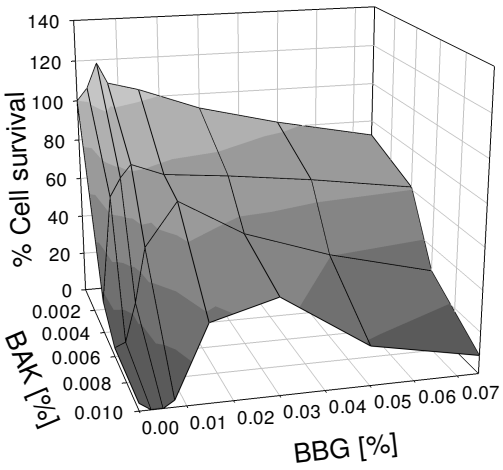

Fig. 2 Cell survival of HCE cells after exposure for 30 minutes to combinations of BAK and BBG in different concentrations.

Oct is an antiseptic agent which, in comparison with BAK, had a higher bacteriostatic effect, but at the same time was more toxic to the cells, as shown in Fig. 3a. BBG protected the cells against Oct toxicity even more than against BAK toxicity. After 5 min incubation with 0.009% Oct and 0.025% BBG, the cell survival increased to 95%, and after 30 min incubation, to 85%, while in the absence of BBG, Oct led to almost complete cell death. In order to find the most protective combination of Oct and BBG, different concentrations of BBG and Oct were tested in mixture for 30 min incubation (Fig. 3b). For 0.003% Oct, even 0.007% BBG abolished the toxicity of the antiseptic. For 0.007% Oct, a higher concentration of BBG, namely 0.025%, had to be applied, in order to achieve the same effect. At 0.01% Oct concentration, the minimal concentration of BBG needed was 0.025%, and the cell survival increased to 95%.

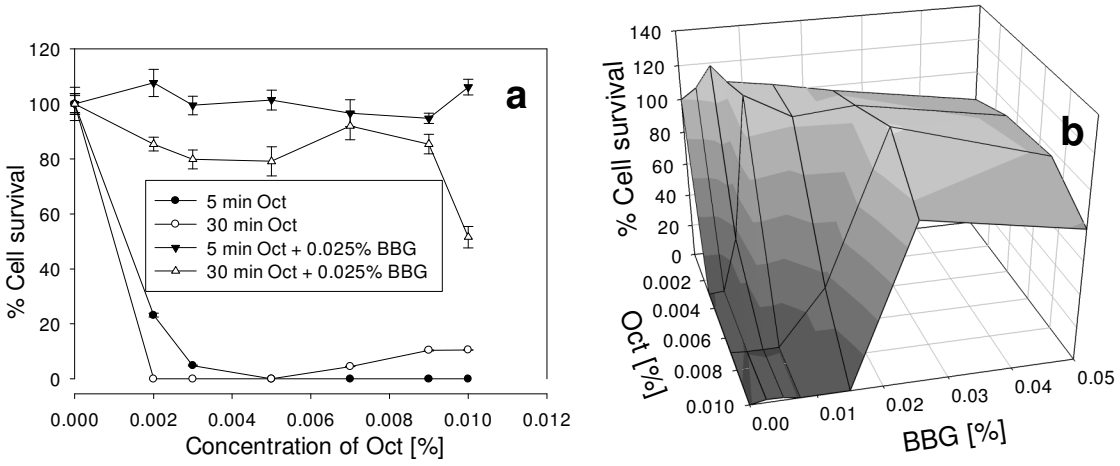

Fig. 3 Cell survival of HCE cells after exposure for 5 and 30 min to different concentrations of Oct with and without 0.025% BBG (**a**) and after exposure for 30 min to different combinations of BBG and Oct (**b**). The error bars represent the standard deviations of 6 to 12 replicates performed within the same experiment.

BBR is a dye which differs from BBG only by the absence of two methyl groups. This difference changed the protective activity of BBR against BAK significantly, but only slightly against Oct. At 0.004% of BAK there was no considerable cell survival in the presence of BBR at 0.025% or higher, while with BBG, the cell survival increased up to 74% (Fig. 4 a). The highest protective effect of BBR was obtained at 0.0075%, where the HCE cell survival increased to 52%. This was considerably less than the protective effect of BBG at the same concentration, which was 83%. At 0.003% of Oct BBR showed comparable protective effect with that of BBG (Fig. 4 b). The highest cell survivals at this Oct concentration was found at 0.015% and 0.025% BBR concentrations, which were 102% and 90%, respectively. In comparison, with BBG at the same concentrations the cell survival was 115% and 100%, respectively. Above 0.05% of BBR or BBG, in the presence of Oct, the HCE cells showed a considerable decrease in cell survival.

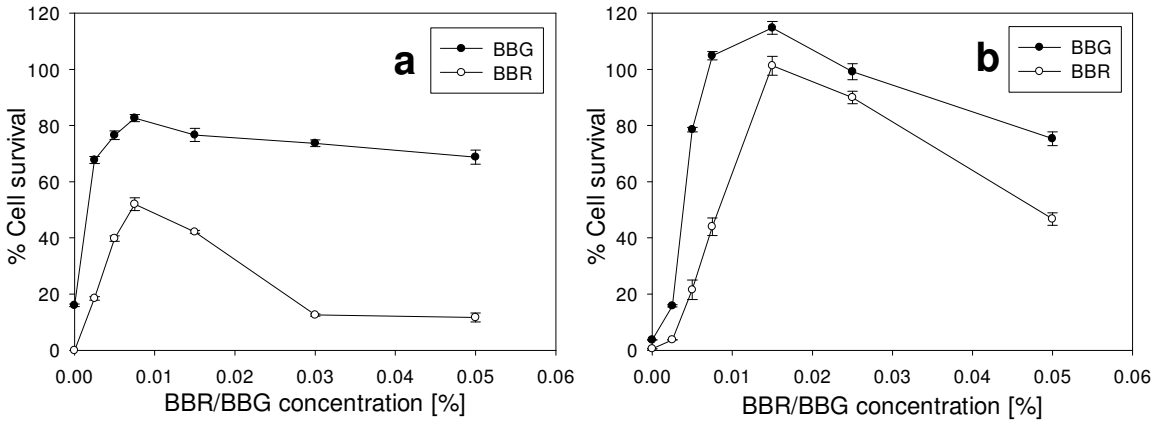

Fig. 4 Cell survival of HCE cells after exposure for 30 min to BBR or BBG, in the presence of 0.004% BAK (**a**) or 0.003% Oct (**b**). The error bars represent the standard deviations of 6 to 12 replicates performed within the same experiment.

To determine if the protective effect of BBG on antiseptics was due to its P2x7 receptor antagonist activity, other reported selective P2x7 receptor antagonists were tested in this study. One of them was OxATP. It is known as an irreversible P2x7 receptor antagonist, which blocks human P2x7 receptors at 10 μM concentration (Hibell et al. 2001; Wang et al. 2004). The other antagonist was DPPH, recently synthesized by Lee et al. (2012), which has an IC_{50} of 0.65 μM

with the ethidium bromide uptake assay. Neither OxATP, used between 2 µM and 2mM (preincubated for 30 min with HCE cells prior to exposure to BAK), nor DPPH, used between 0.1 µM and 10 µM, showed any protective effect against BAK toxicity, when BAK was present between 0.001 and 0.01%. Oct was tested between 0.003% and 0.01% only in the presence of DPPH and no protective effect of the P2x7 receptor antagonist was found (data not shown).

Bacteriostatic effect of Oct and BAK in the presence of BBG and BBR

Mixtures of BAK or Oct with BBG and BAK or Oct with BBR were used to determine the susceptibility of diverse bacterial strains towards the compound combinations. The BAK and Oct at concentrations between 0.002% and 0.01% inhibited the growth of all tested Gram-positive bacterial strains, even when mixed with the highest applied BBG concentration. In general, Gram-positive bacteria were more susceptible towards the compounds than Gram-negative bacteria. The inhibitory concentrations for Gram-negative bacterial growth were summarized in Fig. 5 and Fig. 6. All tested Gram-negative bacteria showed similar responses towards Oct and BAK when the same concentration of BBG was used. These results suggested that the growth of different bacterial organisms were efficiently inhibited by the use of 0.015 % BBG with 0.009 % BAK or 0.007 % Oct, as well as by the use of 0.007 % BBG with 0.005 % BAK or 0.003% Oct.

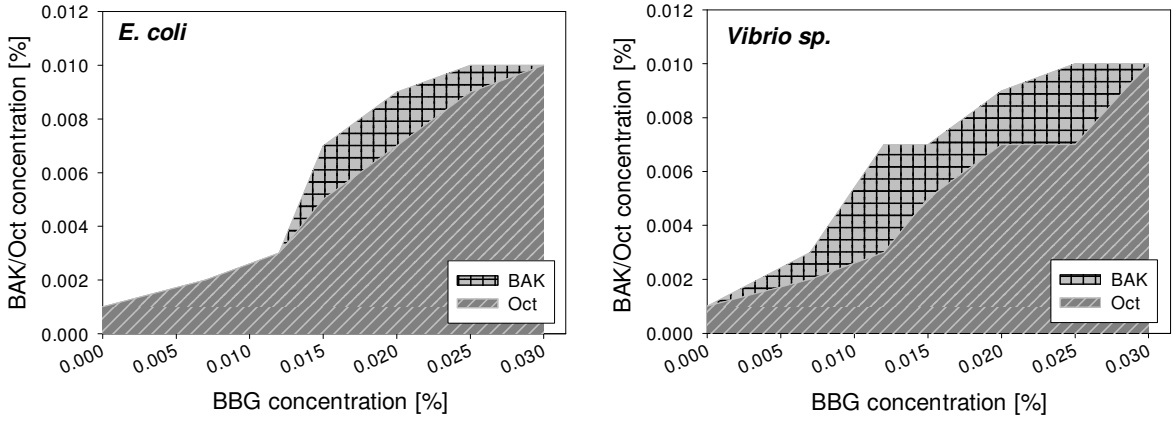

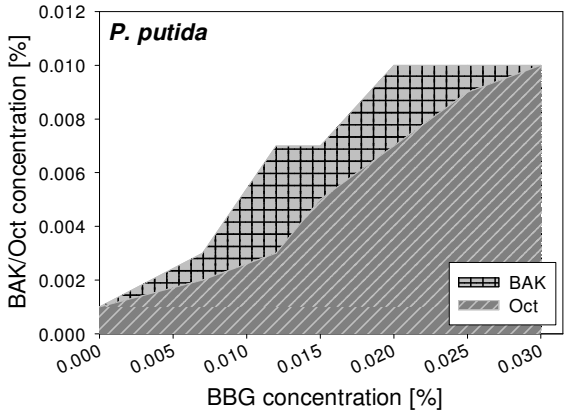

Fig. 5 Concentrations of BAK and Oct required to inhibit Gram-negative bacterial growth, when BBG is present. At combinations within the shaded area bacterial growth is observed; combinations above the shaded areas prevent bacterial growth.

BBR was assayed in combination with Oct on the Gram-negative and Gram-positive bacterial strains used before, to test whether BBR has the same bacterial inhibitory effect as BBG. The results showed that the bacterial growth of the Gram-positive bacterium, *B. subtilis* was not inhibited in presence of high BBR concentrations, i.e. 0.025% or 0.030% combined with 0.001% Oct. For the Gram-negative bacteria, increasing Oct concentrations were required with increasing BBR concentrations, similar to BBG (see Fig. 6). The results showed that the growth of all tested bacterial strains were inhibited by the use of 0.007% BBR with 0.005% of Oct, 0.012% BBR with 0.007% Oct and 0.020% BBR with 0.009% Oct. Combinations between BBR and BAK have not been investigated, because no significant protective activity of BBR on human cell lines was seen in presence of BAK.

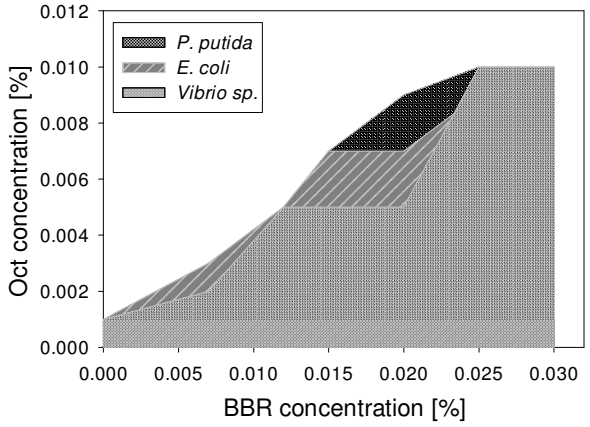

Fig. 6 Concentrations of BAK and Oct required to inhibit Gram-negative bacterial growth, when BBR is present. At combinations within the shaded area bacterial growth is observed; combinations above the shaded areas prevent bacterial growth.

The concentrations of BAK used in this study are in the range of concentrations used in commercially available eye drops, 0.004-0.02% (Liang et al. 2012), where 0.025% BBG exerted a significant cell viability increase on HCE cells. To achieve bacterial growth inhibition, as well as a significant increase of the cell viability, higher concentrations of BBG required higher BAK concentrations. The best combinations of these two compounds were 0.015% BBG for BAK between 0.008% and 0.01%, and 0.007% BBG for BAK between 0.004% and 0.006%. The HCE cell viability increased between 40-60% in the first set of combinations of BBG and BAK, and with 50-80% in the second set.

Oct was used in this study between 0.002% and 0.01%, because according to Hübner et al. (2010) 22.5 mg/l of OPE (Oct with phenoxyethanol) was sufficient to reduce with $3\log_{10}$ the bacterial growth after 30 min incubation. At these concentrations of Oct, 0.025% BBG increased the HCE cell survival by up to 100% at 30 min incubation. Also, BBR at the same concentration and incubation time increased the HCE cell survival up to 90%, when 0.003% Oct was present. To reduce the toxicity of the antiseptic agent, without affecting the bacterial inhibitory effect, we suggest the following combinations: 0.025% of BBG with 0.01% Oct; 0.015% BBG with 0.007% Oct; and 0.007% BBG with 0.003% Oct. With these combinations, the HCE cell survival increased by 35-115%.

Discussion

The inflammatory responses of the eyes or skin due to repeated contact with the preservatives and antiseptics used in different eye drops, wound disinfectants or cosmetical products, are unwanted side effects, which occur in many patients using these products on a daily basis. The reason for these inflammatory effects is the high toxicity of the compounds on the target cells. Therefore, reducing the toxicity of antiseptics and preservatives on human tissues, while maintaining their bacteriostatic effect, is desired. Ways to reduce these inflammatory effects, by combination of bacteriostatic agents with protective agents, were not yet investigated.

We found that the protective effect of BBG against BAK and Oct toxicity on human eye cells is remarkable. However, there are only limited numbers of possible combinations between different concentrations of BBG and BAK or Oct, at which the bacterial growth is inhibited. Very high

concentrations of BBG, 0.03% or higher, in the presence of either of the two antiseptics at the tested concentrations, no longer inhibits the bacterial growth of Gram-negative bacteria. BBR showed protective effects only against Oct toxicity, however this effect is slightly lower than that caused by BBG.

The microbiology experiments showed that the mixtures of BAK with BBG, Oct with BBG and Oct with BBR had stronger inhibitory effects on Gram-positive than on Gram-negative bacterial cells. Since the cell wall composition in both groups of bacteria differs remarkably (Silhavy et al. 2010), the hydrophobic outer membrane of Gram-negative bacteria might prevent the compounds from efficiently entering the cells. However, hydrophilic features of the compounds might aid the entrance of the antimicrobials into Gram-positive cells thus making them more susceptible. Previously McDonnell and Russell (1999) and Fazlara and Ekhtelat (2012) reported that BAK is more effective on Gram-positive bacterial organisms. They also mentioned that the mechanism of action of BAK, as a cationic quaternary ammonium compound, is based on the interaction of the negatively charged bacterial surface with the positively charged headgroup of BAK. After binding to the bacterial surface, BAK will enter the cell wall and cause its disruption and leakage of the cytoplasmic material to the outside. The mechanism of action of Oct has not been described yet, but we assume that it is similar to BAK, as both compounds have an amphiphilic structure, though Oct is a more complex molecule, with two cationic centers and long hydrophobic chains at both ends of the molecule. Oct and BAK have previously been successfully tested as antimicrobial compounds (Hübner et al. 2010; Sedlock and Bailey 1985). In comparison with BAK, Oct showed a higher efficiency against Gram-negative bacteria.

We have demonstrated here that BBG reduces the antibacterial effect of Oct and BAK for Gram-negative bacteria. Nevertheless, the use of certain concentration combinations of the compounds, presented in Fig. 5, will efficiently inhibit the growth of bacteria in eye drops, skin, mucous membranes and wound disinfectants, while protecting the epithelial cells against the cytotoxic action of the disinfectants. BBR reduces the growth of gram-negative bacteria less efficiently than BBG at any of the tested concentrations, when mixed with Oct.

Recently, Müller and Kramer (2008) defined the biocompatibility index (BI) of antiseptic compounds. They measured the IC_{50} value of the antiseptics on fibroblast cells and divided this value by the concentration at which 99.9% of the Gram-positive and Gram-negative bacteria are killed. A BI bigger than 1 means that an antiseptic compound is more toxic to bacterial

organisms in comparison to mammalian cells. In order to quantify, in our case, the effectiveness of the different concentration combinations of BBG and Oct or BAK in antiseptic treatments, a similar BI of the two antiseptic compounds in the presence of BBG will be defined as the next step of this study.

Previously Dutot et al. (2006) reported that BAK induces apoptosis in corneal and conjunctival cell lines through the activation of the P2x7 receptor. The activation of this receptor leads to pore formation and influx of Ca^{2+} and other extracellular molecules into the cell, but also to the escape of intracellular small metabolites (Chung et al. 2000; Dutot et al. 2006; Wang et al. 2004). The exact mechanism of the protective activity of BBG and BBR is not yet known. We assume, however, that it does not involve the P2x7 receptor, because other selective P2x7 receptor antagonists, OxATP and DPPH, did not show any protection against the cytotoxic effect of these antiseptics. Recently Jo and Bean (2011) showed that BBG at micromolar concentrations also causes inhibition of neuronal voltage gated sodium channels in neuroblastoma cells. The binding constants to these channels are far higher than those of the classic sodium channel blockers used in medical treatments of traumatic brain injury (Pitkanen et al. 2014). Further investigations are needed to elucidate on which target BBG and BBR acts when inhibiting the toxicity of BAK or Oct on HCE cells. To date, BBR has been less studied than BBG. This dye frequently occurs in the literature as a stain for the detection of proteins in polyacrylamide gel electrophoresis. No protective effect of the dye on human cells has been described yet, nor any activity on any cellular receptors.

The chemical interaction between negatively charged dye molecules and antiseptics, which have one (BAK) or two (Oct) positive charges, could be one reason, why BBG and BBR reduces the toxicity of Oct or BAK on HCE cells. This idea is supported also by our data, where certain mixtures between the dyes and the antiseptics reduce the bacteriostatic effect of the antiseptics on Gram-negative bacteria. This interaction could result in a compound that is no longer toxic to either the mammalian cells or to the Gram-negative bacteria. Interestingly, the bacteriostatic effect of the dye-preservative mixtures on Gram-positive bacteria is not affected by these interactions. In the literature it is mentioned that BBR, during the protein staining procedure, binds reversibly and particularly to positively charged parts of proteins (Tal et al. 1985), with a slightly different molecular mechanism than BBG (Lee et al. 2001). Casero et al. (1997) described studies of the interaction of the negatively charged BBG with several types of cationic

surfactants and the formation of dye-detergent premicellar aggregates at surfactant concentrations far below their critical micelle concentration. Ma et al. (2014) showed that BAK is able to interact with other negatively charged dye molecules, eosin Y and eosin B and form stable dye-surfactant aggregates. Additionally, Sütterlin et al. (2008) presented studies which showed that other negatively charged molecules, such as linear alkylbenzene sulfonate, naphthalene sulfonic acid, benzene sulfonic acid or SDS, can considerably modify the bacteriostatic effect of BAK on two Gram-negative bacterial strains, *P. putida* and *V. fischeri*.

Several preparations with BAK or Oct as an antiseptic are already commercially available. The combinations between Oct and BBG or BBR, or BAK and BBG, proposed by us in this study, will help in marking the disinfected area and in protecting the skin from possible irritations or inflammations caused by the antiseptics. The protective effect of BBG and BBR will also allow to use higher concentrations of the antiseptics in the ready-to-use preparations. The daily use of BBG-based solutions on the skin or in the eyes will have the side effect of staining the area of application surface blue. However, according to Peng et al. (2009) and our own experience, the staining disappears rapidly, and is gone about a week after the treatment. With BBR no such effect has been described yet in the literature, but we assume that it has a similar staining effect to BBG, because BBR is widely used as a high-sensitivity protein stain.

Acknowledgements

The research was partially funded by the Dr. Helmut und Margarete Meyer-Schwarting Stiftung. We are also grateful for the octenidine dihydrochloride gift from Schülke and Mayr GmbH.

Declarations

The authors declare that they have no conflict of interest.

References

Ammar DA, Kahook MY (2011) Effects of benzalkonium chloride- or polyquad-preserved fixed combination glaucoma medications on human trabecular meshwork cells. Mol Vis 17:1806-13

Awad D, Schrader I, Bartok M, Sudumbrekar N, Mohr A, Gabel D (2013) Brilliant Blue G as protective agent against trypan blue toxicity in human retinal pigment epithelial cells in vitro. Graefes Arch Clin Exp Ophthalmol 251(7):1735-40 doi:10.1007/s00417-013-2342-3

Casero I, Sicilia D, Rubio S, Perez-Bendito D (1997) Study of the formation of dye-induced premicellar aggregates and its application to the determination of quaternary ammonium surfactants. Talanta 45(1):167-80
Chung HS, Park KS, Cha SK, Kong ID, Lee JW (2000) ATP-induced [Ca(2+)](i) changes and depolarization in GH3 cells. Br J Pharmacol 130(8):1843-52 doi:10.1038/sj.bjp.0703253
Dutot M, Pouzaud F, Larosche I, Brignole-Baudouin F, Warnet JM, Rat P (2006) Fluoroquinolone eye drop-induced cytotoxicity: role of preservative in P2X7 cell death receptor activation and apoptosis. Invest Ophthalmol Vis Sci 47(7):2812-9 doi:10.1167/iovs.06-0224
Enaida H, Hisatomi T, Hata Y, et al. (2006) Brilliant blue G selectively stains the internal limiting membrane/brilliant blue G-assisted membrane peeling. Retina 26(6):631-6 doi:10.1097/01.iae.0000236469.71443.aa
Fazlara A, Ekhtelat M (2012) The disinfectant effects of benzalkonium chloride on some important foodborne pathogens. Am Eurasian J Agric Environ Sci 12(1):23-29
Hibell AD, Thompson KM, Xing M, Humphrey PP, Michel AD (2001) Complexities of measuring antagonist potency at P2X(7) receptor orthologs. J Pharmacol Exp Ther 296(3):947-57
Hübner N-O, Siebert J, Kramer A (2010) Octenidine dihydrochloride, a modern antiseptic for skin, mucous membranes and wounds. Skin Pharmacol Phys 23(5):244-258 doi:10.1159/000314699
Jo S, Bean BP (2011) Inhibition of neuronal voltage-gated sodium channels by brilliant blue G. Mol Pharmacol 80(2):247-57 doi:10.1124/mol.110.070276
Jorgensen J, Turnidge J (2007) Manual of Clinical Microbiology. In: Murray P, Baron E, Jorgensen J, Landry M, Pfaller M (eds) Antibacterial susceptibility tests: dilution and disc diffusion methods. 9th edn. ACM Press, Washington DC, p 1152-1172
Koburger T, Hübner N-O, Braun M, Siebert J, Kramer A (2010) Standardized comparison of antiseptic efficacy of triclosan, PVP–iodine, octenidine dihydrochloride, polyhexanide and chlorhexidine digluconate. J Antimicrob Chemother 65(8):1712-1719 doi:10.1093/jac/dkq212
Lee D, Lee EK, Lee JH, Chang CS, Paik SR (2001) Self-oligomerization and protein aggregation of alpha-synuclein in the presence of Coomassie Brilliant Blue. Eur J Biochem 268(2):295-301 doi:10.1046/j.1432-1033.2001.01877.x
Lee WG, Lee SD, Cho JH, et al. (2012) Structure-activity relationships and optimization of 3,5-dichloropyridine derivatives as novel P2X(7) receptor antagonists. J Med Chem 55(8):3687-98 doi:10.1021/jm2012326
Liang H, Brignole-Baudouin F, Riancho L, Baudouin C (2012) Reduced in vivo ocular surface toxicity with polyquad-preserved travoprost versus benzalkonium-preserved travoprost or latanoprost ophthalmic solutions. Ophthalmic Res 48(2):89-101 doi:10.1159/000335984
Ma W, Ma X, Sha O, Liu Y (2014) Two Spectrophotometric Methods for the Assay of Benzalkonium Chloride in Bandage Samples. J Surfactants Deterg 17(1):177-181 doi:10.1007/s11743-013-1446-4
Marcillo A, Frydel B, Bramlett HM, Dietrich WD (2012) A reassessment of P2X7 receptor inhibition as a neuroprotective strategy in rat models of contusion injury. Exp Neurol 233(2):687-92 doi:10.1016/j.expneurol.2011.06.008
McDonnell G, Russell AD (1999) Antiseptics and disinfectants: activity, action, and resistance. Clin Microbiol Rev 12(1):147-179

Müller G, Kramer A (2008) Biocompatibility index of antiseptic agents by parallel assessment of antimicrobial activity and cellular cytotoxicity. J Antimicrob Chemother 61(6):1281-7 doi:10.1093/jac/dkn125

Paimela T, Ryhanen T, Kauppinen A, Marttila L, Salminen A, Kaarniranta K (2012) The preservative polyquaternium-1 increases cytoxicity and NF-kappaB linked inflammation in human corneal epithelial cells. Mol Vis 18:1189-96

Peng W, Cotrina ML, Han X, et al. (2009) Systemic administration of an antagonist of the ATP-sensitive receptor P2X7 improves recovery after spinal cord injury. Proc Natl Acad Sci 106(30):12489-12493 doi:10.1073/pnas.0902531106

Pitkanen A, Immonen R, Ndode-Ekane X, Grohn O, Stohr T, Nissinen J (2014) Effect of lacosamide on structural damage and functional recovery after traumatic brain injury in rats. Epilepsy Res 108(4):653-65 doi:10.1016/j.eplepsyres.2014.02.001

Sedlock DM, Bailey DM (1985) Microbicidal activity of octenidine hydrochloride, a new alkanediylbis [pyridine] germicidal agent. Antimicrob Agents and Chemother 28(6):786-790 doi: 10.1128/AAC.28.6.786

Servaites JC, Faeth JL, Sidhu SS (2012) A dye binding method for measurement of total protein in microalgae. Anal Biochem 421(1):75-80 doi:10.1016/j.ab.2011.10.047

Silhavy TJ, Kahne D, Walker S (2010) The bacterial cell envelope. Cold Spring Harb Perspect Biol 2(5):a000414 doi:10.1101/cshperspect.a000414

Sütterlin H, Alexy R, Kümmerer K (2008) The toxicity of the quaternary ammonium compound benzalkonium chloride alone and in mixtures with other anionic compounds to bacteria in test systems with Vibrio fischeri and Pseudomonas putida. Ecotoxicol Environ Saf 71(2):498-505 doi:10.1016/j.ecoenv.2007.12.015

Tal M, Silberstein A, Nusser E (1985) Why does Coomassie Brilliant Blue R interact differently with different proteins? A partial answer. J Biol Chem 260(18):9976-80

Wang X, Arcuino G, Takano T, et al. (2004) P2X7 receptor inhibition improves recovery after spinal cord injury. Nat Med 10(8):821-7 doi:10.1038/nm1082

Appendix VI

Halogenated dodecaborate clusters as agents to trigger release of liposomal contents

Doaa Awad [a,b,c], Melinda Bartok [b,c], Farzin Mostaghimi [b], Imke Schrader [b], Neeti Sudumbrekar [b], Tanja Schaffran [b], Carsten Jenne [d], Jonny Eriksson [e], Mathias Winterhalter [c], Jürgen Fritz [c], Katarina Edwards [e], Detlef Gabel [b,c*]

Abstract: Halogenated dodecaborates, and especially dodecaiododododecaborate(2-), were found to trigger effectively the release of the contents of phospholipid liposomes, including liposomes containing distearoylphosphatidylcholine and cholesterol used clinically for cancer therapy. The basis of the release was studied with differential scanning calorimetry, cryo-transmission electron microscopy, and atomic force microscopy. When given at high concentration drastic morphological changes were induced by the dodecaborates. Use in triggered release is suggested.

Introduction

Liposomes are being used as carriers for a number of drugs, especially anti-cancer agents [1]. They accumulate in tumor tissue through the EPR effect (enhanced permeation and retention) through a leaky vasculature and the lack of lymphatic drainage in the tumor [2]. Encapsulation of drugs in liposomes leads to reduced toxicity and to longer circulation times. To be effective, the drugs need in most cases to be released from the liposomes. A variety of strategies for triggering the release of the liposomal contents has been tried. Such strategies would allow to wait for the optimal distribution of liposomes before their contents is released. With this, the therapeutic effect might be maximized and side effects due to uncontrolled release of the drug might be minimized. While some strategies rely on the specific environment of the tumor tissue, such as a lower pH value [3], others focus on the action of external agents such as ultrasound [4] or local hyperthermia [5]. For the latter modalities, the target site must be known in order to direct the external trigger for release. With the boron clusters presented here, the triggering agent can be administered systemically. The release of the drug is induced by the cluster compounds and will occur at the location where liposomes have accumulated.

Dodecaborate clusters are stable, ionic structures with dimensions similar to that of a phenyl ring. The parent cluster $B_{12}H_{12}^{2-}$ is of icosahedral shape and carries two negative charges. One or more of the hydrogen atoms can be replaced with functional groups, leading to the possibility for attaching them to organic structures [6]. When administered to patients for the intention of boron neutron capture therapy, the mono-sulfhydryl cluster mercaptoundecahydrododecaborate, $B_{12}H_{11}SH^{2-}$, (BSH) is found on the tumor cell membrane and moreover the compound is also capable of entering the cell nucleus [7].

We have previously investigated changes in liposome shape, permeability, and temperature-induced phase transition induced by substituted boron clusters, and found that, when given in sufficiently high concentrations, all boron clusters investigated so far changed the morphology of the liposomes. Leakage was not observed for all clusters, but phase transition temperatures were affected [8]. Binding was followed through measurement of zeta potential [8b, 8d], and, as expected, binding of the clusters leads to a negative potential, due to the negative charge of the clusters. On the basis of our previous results, it was suggested that the clusters capable of inducing liposome leakage could be used for triggered release of the contents of liposomes. In such an application, liposomes would first be allowed to distribute in the body, and accumulate, e.g., in tumor tissue. After the distribution phase, the injection of a suitable boron cluster compound could then trigger the release of liposomal content [8a]. Due to the small size and the good water solubility of the boron cluster compounds, they would distribute relatively freely in the body fluids and be able to reach liposomes in tumors.

BSH, which belongs to the compounds investigated previously, is capable of triggering release from dipalmitoylphosphatidylcholine (DPPC) liposomes, but not from liposomes consisting of distearoylphosphatidylcholine (DSPC) and cholesterol (Chol). Doxorubicin (Dox) encapsulated in the liposomes led to enhanced cell death [8a]. Dox is well soluble in water (around 10 mg/mL), but can be precipitated inside liposomes through active loading [9]. Since DSPC and

[a] Dr. Doaa Awad
Department of Biochemistry, Faculty of Science
Alexandria University
Moharam Bek, 21511 Alexandria, Egypt
[b] Dr. Doaa Awad, Melinda Bartok M.Sc., Farzin Mostaghimi B.Sc., Imke Schrader M.Sc., Neeti Sudumbrekar M.Sc., Dr, Tanja Schaffran, Prof. Dr. Detlef Gabel
Department of Chemistry
University of Bremen
PO Box 330440, D-28334 Bremen, Germany
[c] Prof. Dr. Detlef, Melinda Bartok, M.Sc., Prof. Dr. Mathias Winterhalter, Prof. Dr. Jürgen Fritz
Jacobs University Bremen
Campus Ring 1, D-28759 Bremen, Germany
D-28759 Bremen, Germany
e-mail d.gabel@jacobs-university.de
[d] Prof. Dr. Carsten Jenne
Fachbereich C – Anorganische Chemie
Bergische Universität Wuppertal
D-42119 Wuppertal, Germany
[e] Prof. Dr. Katarina Edwards, Jonny Eriksson
Department of Chemistry – BMC
Uppsala University
Box 579, S-75123 Uppsala

cholesterol are common constituents of liposomes loaded with, e.g., doxorubicin [10] we searched for boron cluster compounds with increased effect on liposomes, and therefore turned to perhalogenated clusters. Similar to BSH these clusters carry two negative charges, but due to the larger size of halogens in comparison with hydrogen, the perhalogenated clusters display a lower charge density. We expected them to interact more strongly with liposomes, due to reduced interaction with water [11] and the observed retention on chromatography matrices [12], and in analogy to the interaction of large and polarizable anions such as iodide with lipids [13].

Perhalogenation of dodecaborate can be readily achieved [14]. With increasing size of the halogen from F to I, the diameter of the cluster increases, and a systematic change of interaction potential can be anticipated. In the present we have studied and compared the interaction of $B_{12}H_{12}^{2-}$ (BH), $B_{12}F_{12}^{2-}$ (BF), $B_{12}Cl_{12}^{2-}$ (BCl), $B_{12}Br_{12}^{2-}$ (BBr), and $B_{12}I_{12}^{2-}$ (BI) with liposomes of varying composition. Our results show that the perhalogenated clusters interact increasingly strongly with increasing halogen size. Further, significant binding was observed already at concentrations where the clusters are non-toxic to mammalian cells in cell culture. Noteworthy, we found strong interaction and effective release of liposomal contents also from liposomes made from DSPC, Chol, and polyethyleneglycol distearoylphosphatidylethanolamine (DSPE-PEG).

Results and Discussion

Zeta potential

The binding curves pertinent to the association of the halogenated clusters to DSPC liposomes (Fig. 1 left) show the same sigmoidal pattern as those of other clusters to DMPC [8b] and DPPC [8d]. The apparent dissociation constants for DSPC (derived from the inflexion points of the curves) are 0.13 mM, 0.044 mM, and 0.017 mM for BCl, BBr, and BI, respectively, with limiting zeta potentials of around -60 mV for high concentrations of the clusters. For BSH on DMPC liposomes, we had previously determined a value of 0.23 mM [8b], and for $B_{12}H_{11}NR_3^{1-}$, between 28 mM for R = H and 0.018 mM for R = hexyl. The value for $B_{12}H_{11}SH$ on DPPC liposomes is 0.25 mM, and thus not very different from that for DMPC. The parent cluster BH has an apparent binding constant of 0.38 mM. For a detailed discussion about the association constants derived from zeta potential measurements, see [8d].

For DPPC liposomes (Fig. 1 right), the binding curves have a different appearance for BCl and BBr, and no limiting value for the zeta potential could be deduced. If one would assume similar limiting values of the zeta potential as for DSPC, BCl binds much less strongly than BBr, which in turn binds much less strongly than BI. For BI, an apparent dissociation constant of 8.7 µM is found, about half of the value observed for DSPC, while for DPhPC, the value was still lower (4.7 µM).

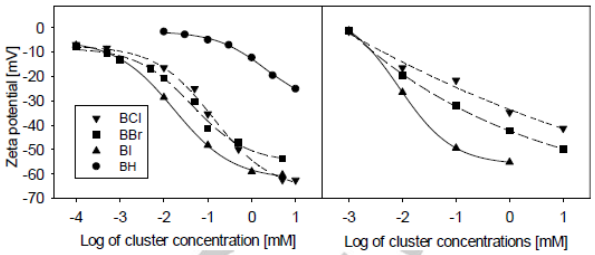

Figure 1. Zeta potential of DSPC liposomes (left) and DPPC liposomes (right), incubated with the clusters overnight in the indicated concentrations, and measured at 25°C in 10 mM Hepes pH 7.4.

The curves obtained for binding of BCl and BBr to DPPC are unusual in that they are not sigmoidal. This cannot be due to the morphological changes induced by the cluster, since, as reported in the next section, BCl and BBr caused structural changes of the liposomes that were qualitatively similar to those induced by BI.

Cryo-TEM and AFM

Halogenated clusters are capable of inducing drastic changes in the morphology of liposomes, and with BI, these changes are apparent already at lipid to cluster molar ratios as low as 10:1 (see Fig. 2 top right). It is evident that many of the liposomes have opened up and transformed into disk-like structures. Moreover, the remaining intact liposomes display a smooth surface (Fig 2 top right), in contrast to the angular appearance typically observed for phosphatidylcholine liposomes at temperatures below the main phase transition temperature (Fig. 2 top left).

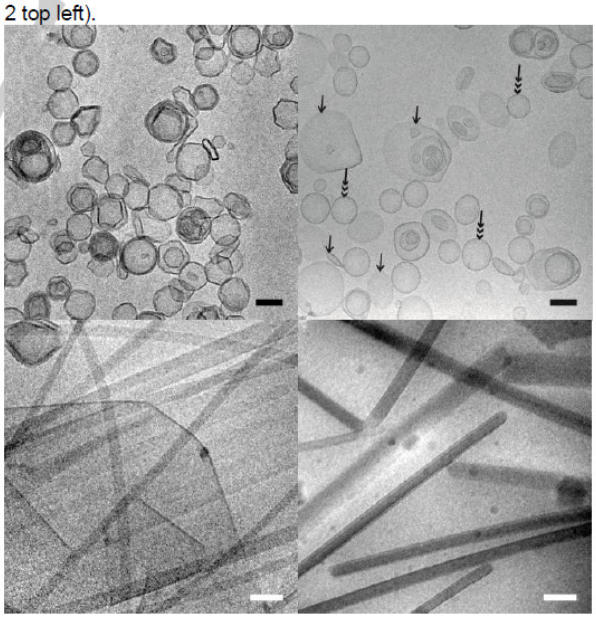

Figure 2. Cryo-TEM of DPPC liposomes. Top left. 5 mM DPPC. Top right: Incubation with 0.5 mM BI for 10 minutes at room temperature. Open structures and disks are pointed out by arrows with a single arrowhead, closed

liposomes with triple arrowheads Bottom left: Incubation with 16 mM BI for 10 minutes at room temperature. Bottom right: 50 mM BI after three cycles of DSC (maximum temperature 80°C). Scale bar in all pictures 100 nm.

At higher concentrations of BI, large sheets of lamellar material were frequently detected in the micrographs. In addition, long needle-shaped structures started to appear (Fig 2 bottom left). Following incubation with a large molar excess of BI over the lipid (10:1), liposomes and lamellar sheets disappeared and the samples were dominated by needles of different lengths, some as long as 10 µm, which could be followed across the electron microscopy grid at low magnification. Noteworthy, BI has a solubility well above 50 mM, and in cryoTEM no needle-like structures were found unless the lipid was present. At 50 mM BI, the needles formed in the presence of DPPC had a slightly irregular surface (data not shown). When the sample after DSC was investigated, smooth needles were found. As there is no contrast agent used in cryo-TEM, the electron dense appearance of the needles is most probably caused by iodine.

The limited thickness of the vitrified film formed during the cryo-TEM sample preparation excludes visualization of large (> 0.5 µm) structures potentially present in the original sample. In order to reveal any such structures, and to investigate the geometry of the needle-shaped crystals in more detail, selected samples were studied by AFM.

AFM images obtained from preparations of DPPC with BI at high concentrations show that the needle-like structures are not cylindrical in shape. Instead, the needles represent flat structures with heights of several tens of nm (Fig. 3). Defined islands of bigger height (rising by around 6 nm over the level of the structure on which they were found) can be discerned. It should be noted that the structures imaged by AFM are even more selected than those observed in cryo-TEM, since only structures adhering strongly to the mica can be analyzed.

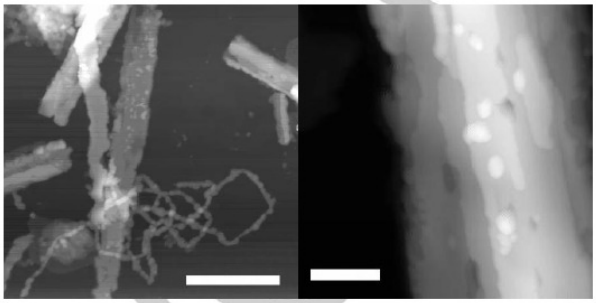

Figure 3. AFM image of a sample prepared from 5 mM DPPC and 50 mM BI adsorbed on a mica surface (left image: scale bar 1 µm, height range between black and white 150 nm; right image: scale bar 200 nm, height range 150 nm.

Significant changes in morphology were detected also upon incubation of the liposomes with the halogenated clusters BBr and BCl. In this case large lamellar sheets and open liposomes were detected by cryo-TEM at all concentrations investigated (between 0.05 and 50 mM, with 5 mM DPPC) (results not shown). Interestingly, in contrast to the case with BI, no needle-like structures were observed in any of the samples.

DSC

All clusters tested show a strong influence on thermally induced transitions in DSC.

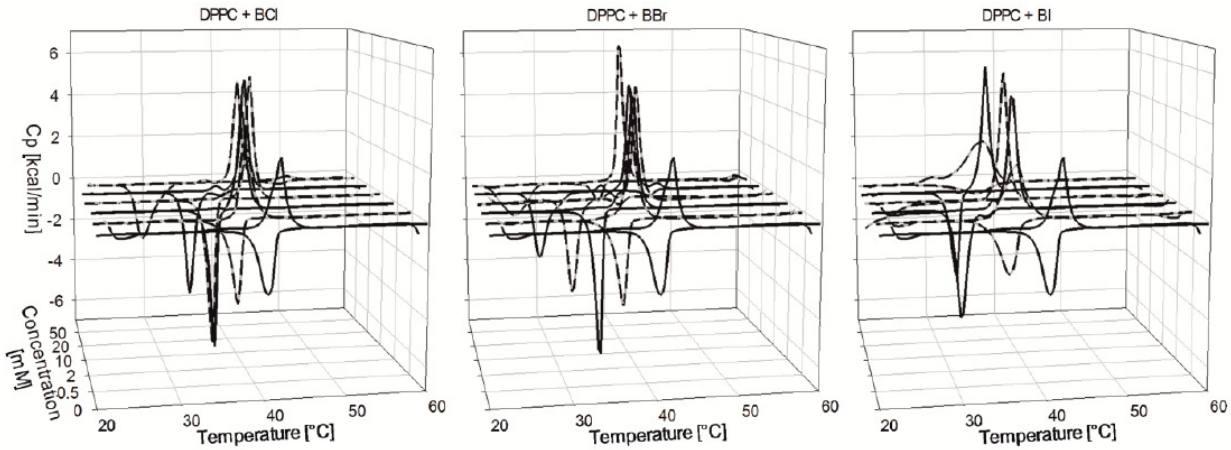

Figure 4. DSC scans of DPPC liposomes in the presence of the indicated concentrations of the clusters. Note that the scale of the concentration axis is not linear.

For DPPC (Fig. 4), the presence of the clusters leads to a slightly increased heat demand for the transition at intermediate and high concentrations. It also leads to increased separation of the transition temperatures (hysteresis) between the upscans and the downscans. This effect is especially pronounced for BBr, but present for all clusters at higher concentrations. For BI, a concentration of 50 mM leads to broadened transitions.

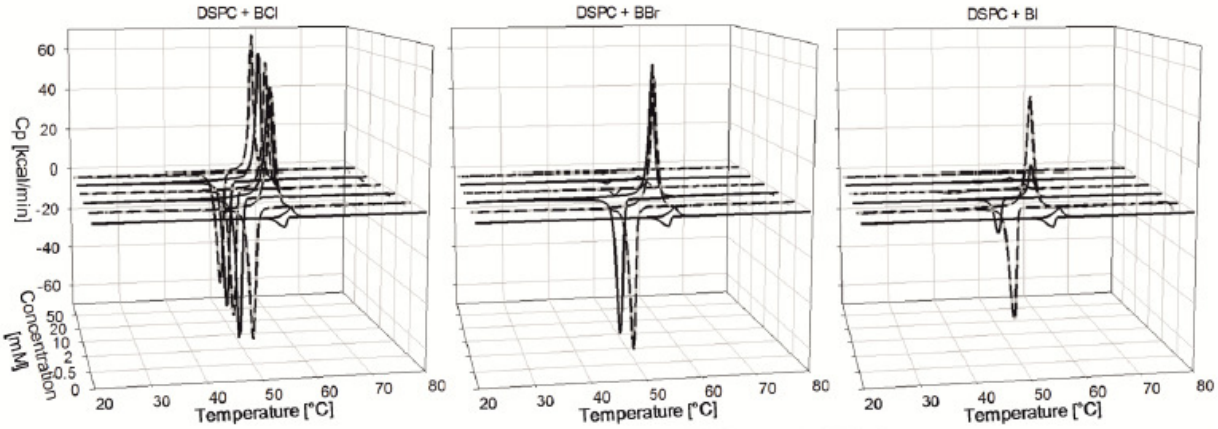

Figure 5. DSC scans of DSPC liposomes in the presence of the indicated concentrations of the clusters. Note that the scale of the concentration axis is not linear. The heat capacity scale of this Figure is different from that of Fig. 4.

When added to DSPC liposomes, all clusters have an effect different from that noted with DPPC liposomes (Fig. 5). At low concentrations (0.5 mM, with a lipid concentration of 5 mM), there is a drastic increase in the amount of heat required for the phase transition (553 kJ mol^{-1} for BCl at 0.5 mM as compared to 46 kJ mol^{-1} for the DSPC liposomes in the absence of clusters [15]). While this large heat demand is maintained for higher concentrations of BCl, it is reduced to very low values for BBr at concentrations above 2 mM, and at 50 mM BBr, no phase transition can be observed. For BI, the decrease of the heat demand sets in already beyond 0.5 mM, in contrast to DPPC.
For DSPC and BCl, the first upscans at 0.5 and 2 mM cluster concentration show a trace with two maxima, which disappear in the second and subsequent upscans. For BBr and BI, subsequent upscans were almost identical to the first one.

Leakage

Leakage is induced by halogenated clusters not only in DPPC liposomes, as observed before for non-halogenated clusters [8a], but also in DSPC liposomes (see Fig. 6). As expected, BI is most effective in inducing leakage but, surprisingly, BCl is more effective than BBr. Especially noteworthy is the effect which BI has on leakage. With this cluster, intermediate concentrations (around 0.1 mM) lead to a higher degree of leakage than with 0.5 mM. For all clusters, leakage comes to a halt after several minutes, but is not complete, at concentrations of 5 mM within the observation period of 10 min. This could be due to either incomplete leakage of all liposomes, or complete leakage of some liposomes, with others remaining intact.

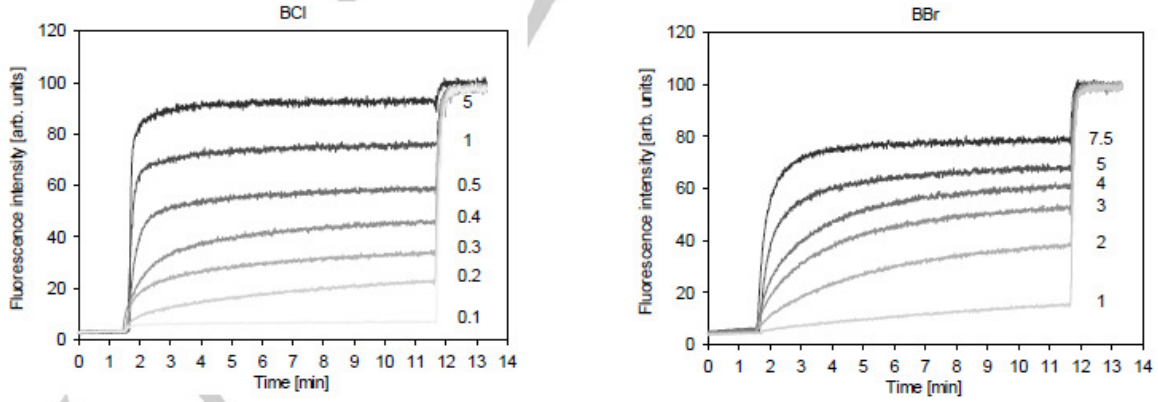

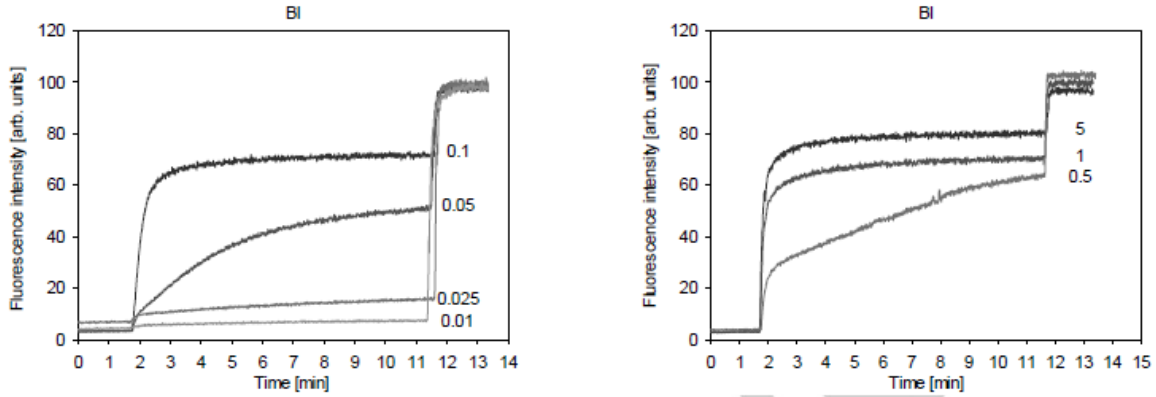

Figure 6. Leakage of CF induced by BCl (top), BBr (middle) and BI (bottom left for smaller concentrations, bottom right for higher concentrations) in DSPC liposomes at 37°C. Concentrations of clusters in mM are given next to the end of the curve before the addition of detergent.

When liposomes from DSPC and Chol (similar to those used in liposomal doxorubicin) are investigated, leakage cannot be induced by BCl at temperatures of 37°C, 45°C, and 53°C. These temperatures were chosen to be below the pretransition, at the beginning of the pretransition, and near to the main transition of the lipid melting (see Fig. 5). For these liposomes, BBr induces slow leakage at 1 mM concentration at 45°C, but not at 37°C nor at 53°C. In contrast, BI does induce leakage from these liposomes at all three temperatures (Fig. 7). In the presence of 5 mol% DSPE-PEG, leakage induced by BI at 37°C is initially rapid, but comes to a halt, whereas without PEG, leakage continues. Complete leakage from DSPC:Chol:DSPE-PEG liposomes at 37°C requires higher concentrations of BI, whereas an increase of BBr up to 5 mM does not result in complete release of CF from these liposomes.

With none of clusters did we observe a monotonous increase of the release of CF from the liposomes with increasing concentration of the clusters, neither with DSPC nor with DPPC. Of clinical relevance is the observation that not only liposomes prepared from pure phospholipids leak upon exposure to the halogenated clusters. Leakage can also be achieved from pegylated liposomes composed of DSPC and Chol in a 2:1 molar ratio (see Fig. 8). Also here, intermediate concentrations lead to a burst, followed by a longer lag period; at still higher concentrations, complete leakage is observed within the observation time period.

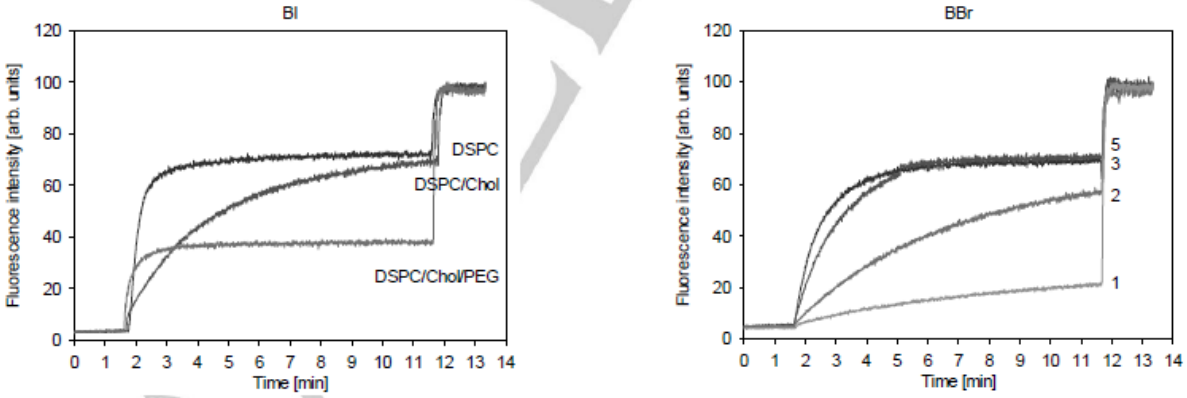

Figure 7. CF leakage from DSPC-containing liposomes induced by 1 mM BI at 37°C (left), and in DSPC:Chol:PEG liposomes by BBr (right). Concentrations of BBr in mM are given next to the end of the curve before the addition of detergent.

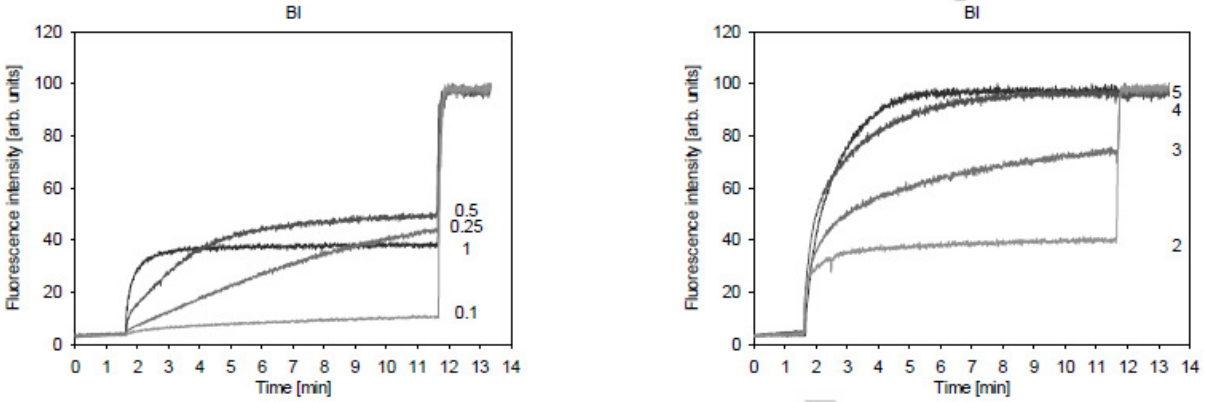

Figure 8. Leakage of CF induced by BI (left: small concentrations; right: high concentrations) from DSPC : Chol : DSPE-PEG2000 (61.66 : 33.33 : 5) liposomes at 37°C. Concentrations of BI in mM are given next to the end of the curve before the addition of detergent.

Toxicity of halogenated clusters

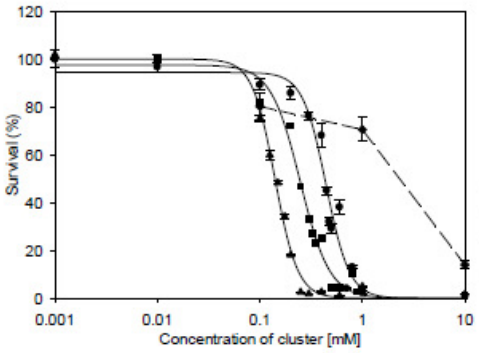

Figure 9. Survival of B79 cells incubated for 24 h with the halogenated clusters BF (diamonds), BCl (circles), BBr (squares), and BI (triangles). The solid lines are fits of a sigmoidal function to the data points, used to derive EC50 values. The line for BF is guidance to the eye.

BI was found to be the most toxic of the clusters investigated (Fig 9), with an EC50 value of 0.14 mM. The clusters BBr and BCl were found to be slightly less toxic than BI. Toxicity of BF is much lower than that of the other clusters, and it does not show the unusually steep dose response of the heavier halogens. The parent $B_{12}H_{12}^{2-}$ did not show cell toxicity in concentrations below 10 mM; at concentrations of 100 mM it damaged the cells because of osmotic effects similar to those of the equi-osmotic Na_2SO_4. Toxicity of the halogenated clusters is only around one order of magnitude higher than that of the clinically used BSH, while the disturbance of membrane integrity is much more pronounced for the halogenated clusters. With BSH, millimolar concentrations are needed to release CF from DPPC liposomes, and DSPC liposomes do not leak at all in the presence of BSH.

Table 1. EC50 values of boron clusters in V79 cells following a 24 h incubation

Compound	EC50 (mM)
BH	>10
BF	≈3
BCl	0.44
BBr	0.25
BI	0.14
BSH	2.8[a]

[a] Data from [8a].

In contrast, all halogenated clusters tested induce leakage in DPPC liposomes at 37°C when present in micromolar concentrations, and DSPC liposomes are unstable against the halogenated clusters at sub-millimolar concentrations (Fig. 6).

Discussion

The enthalpy of the phase transition of DSPC in the presence of all three clusters investigated (BCl, BBr, BI) is very much higher than that of pure DSPC, which is reported to be 11.5 kcal mol^{-1} [18]. Such high enthalpies are usually only found for inorganic oxides [19]. We have no explanation for these high values, nor for why these high values are observed only with DSPC. The melting points of the clusters are well above 100°C. Thus, even

if the lipid surface would serve as a nucleus for crystallization of the clusters, melting of these crystals would not be expected.

Previously, we had investigated the interaction of these and other boron clusters with immobilized egg phosphatidylcholine liposomes [20]. We found that especially BBr and BI interact so strongly with the liposomes that they could not be eluted, while BCl was not retained very strongly. The strong retention cannot be explained by a binding to the liposomal surface, as all three clusters have similar apparent association constants. An explanation for the strong retention of BI and BBr might therefore be interaction with the hydrophobic interior of the lipid bilayer. Interaction of iodide with the nonpolar part of the acyl chains of phosphatidylcholine has been found in molecular dynamics simulations [13, 21]. Experimentally, the binding of anions to phosphatidylcholine membranes appears to follow the Hofmeister series [22]

Release of the liposomal contents can occur through pores formed by the clusters, or through complete destruction of the liposomes. Partial release of the contents of all liposomes (as observed for the halogenated clusters) could be due to either a re-sealing of pores, or through complete destruction of only part of the liposomes. Cryo-TEM shows evidence for both possibilities, but cannot give information about pores in liposomes. For differentiation between the possibilities, fluorescence lifetime experiments have been used before [23]

Leakage is known to be influenced by the temperature-dependent state of the liposomes, with maximum permeability close to the temperature of the main phase transition [24]. For BI and DSPC we find rather uniform leakage with temperature, in contrast to BBr (leakage at 45°C, but not at 37°C and at 53°C). The BBr data are not consistent with the observations that leakage peaks around the temperature of the main transition.

Pores in lipid membranes can be characterized as being hydrophobic (i.e. their walls expose the hydrophobic tails of the lipids) or hydrophilic (the pore is at least partly covered by hydrophilic headgroups of the lipid) (see Fig. 10). These two possibilities of pore formation have been described as barrel-stave and toroidal pores [25]. In the case of hydrophobic pores, the clusters might coat the walls such that the hydrophobic lipid tails do not come in contact with water. For hydrophilic holes, the headgroups of the lipids can no longer be in close contact with each other. In this case, the clusters might fill the gaps between the headgroups.

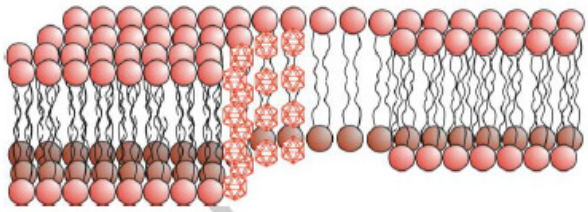

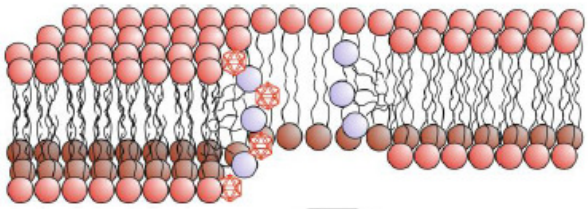

Figure 10. Models of pores with hydrophobic (top) and hydrophilic (bottom) walls, and the possible ways that the boron clusters can stabilize the holes. For the hydrophilic pore, the headgroups of lipids with exposure of hydrophobic chains to water are given in a different colour. Note that here and in the subsequent Figures, the relative size of the clusters to the lipid is only approximate.

Changes in liposomal structures by small ions have been observed in the past mostly for di- and trivalent cations [16]. Anions such as iodide have been shown to penetrate membranes without the induction of pores [17].

Support for the quasi-amphiphilic character of the clusters comes from recent molecular dynamics simulations. Hydrogen-substituted clusters have been investigated for their hydration shell [11]. The interaction with water was found to be weak, and a pronounced shell of hydration could not be detected. This might be due to the fact that the two negative charges of the cluster are not located at specific atoms, but are required to maintain the cluster framework and are thus very effectively delocalized. The halogenated clusters are still bigger in size, due to the increased van der Waals diameter (around 11 Å for BI as compared to 7 Å for BH) and the bigger volume in which the charges are distributed.

The barrel-stave pore might close through the formation of nanocrystalline arrays of the cluster such as shown in Fig. 11.

Figure 11. Possible explanation for closure of pores. Ordered arrays of the cluster are shown in the cross section of a hydrophobic pore. The cations required for electroneutrality are not shown.

The formation of long needles of crystal-like structure was unexpected. The electron dense structures seen in the cryo-TEM pictures of DPPC at high concentrations of BI (Fig. 2) are most probably very rich in iodine, this element being the most electron-dense in the mixture. AFM data indicates a flat rather than cylindrical geometry of the structures (Fig. 3). A possible interpretation of the needle-like structures is shown in Fig. 12. A core of lipids is surrounded by clusters in a crystalline arrangement. As BI does not form crystals on its own under these conditions, a core of lipid might serve as a nucleation site for crystal formation and growth. For the open sheets observed

in cryo-TEM pictures, such arrangement could stabilize the large open sheets which are found.
Needles and fibers from lipids have been observed before (for a review, see [26]). As cryo-TEM pictures represent electron density and thus BI, rather than the lipid itself, molecular interpretations must be different from those reviewed in [26].

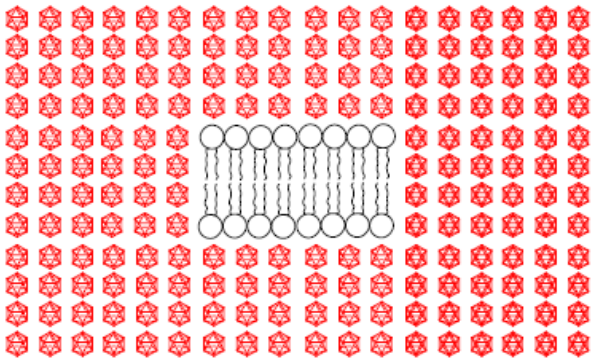

Figure 12. Interpretation of structures at high concentration. The cations required for electroneutrality are not shown.

Crystals of BCl have been described, in which the chlorine atoms of two clusters are in close contact to each other [27]. Thus, there are structural precedents to support the suggested formation of needles and other nanocrystalline arrangements.

Conclusions

The leakage induced by BI in sterically stabilized liposomes consisting of DSPC, Chol and DSPE-PEG, similar to those of Caelyx [28] and other liposomal preparations in clinical use for therapy in patients might make this cluster very suited for liposomal theapy with, e.g., liposomal doxorubicin. This would allow to trigger the release of liposomes after the distribution phase, and might therefore increase the therapeutic efficacy without increasing drug-related toxicity. Initial experiments show that BI does not lead to severely toxic events when administered intravenously to rats at 0.5 g/kg, translating into an estimated 4 mM concentration in blood based on published blood volumes [29] (Bassiouny, Awad, Gabel, in preparation).

Experimental Section

The halogenated clusters were synthesized according to published methods [14a, 14b]. They were used as sodium salts. DSPC, DPPC, and DSPE-PEG, with a PEG molecular weight of 2000, were from Lipoid (Ludwigshafen, Germany). Carboxyfluorescein (CF) was from Kodak/Aldrich (Deisenhofen, Germany). Ham F-10 Medium was supplied by Sigma Aldrich (Steinheim, Germany). WST-1 reagent was purchased from Roche Diagnostics (Mannheim, Germany).

Liposome preparation

Liposomes were prepared by thin film hydration in the buffers mentioned below, followed by five freeze-thaw cycles and 21 extrusions through a 100-nm polycarbonate membrane.

Zeta potential

For zeta potential measurements, liposomes (final concentration 0.5 mM) were incubated with different concentrations of the boron cluster anions overnight at room temperature. The buffer system was HEPES (1 mM, pH 7.4). Zeta potential measurements were performed with a Malvern Zetasizer Nano ZS (Malvern, England). For instrument control and data analysis, the software DTS (Nano) 5.0 was used.

Cryo-transmission electron microscopy (cryo-TEM)

A liposomal suspension containing 5 mM lipid, mixed with the appropriate boron cluster at the concentration specified, was placed on a copper grid coated with a perforated polymer film. Excess solution was removed in a custom-built environmental chamber under controlled humidity and temperature. Immediately after film preparation, the grid was plunged into liquid ethane held at a temperature just above its freezing point. The vitrified sample was mounted and examined in a Zeiss EM 902 A electron microscope, operating at an accelerating voltage of 80 keV in filtered bright field image mode at $\Delta E = 0$ eV. The temperature was kept below 108 K and images were recorded at defocus settings between 1 and 3 µm [30].

Differential scanning calorimetry (DSC)

The phase transitions of liposomes prepared from DPPC or DSPC in 10 mM Hepes buffer, 150 mM NaCl pH 7.4 were measured on a VP-DSC MicroCalorimeter (MicroCal, Northhampton, MA, USA) with MicroCal Origin 5.0 as the software for technical graphics and data analysis. Lipid at 5 mM concentration was used in the DSC measurements, and buffer was injected in the reference cell. Before injection, the liposomal suspension and buffer solution were degassed. Upscans and downscans were recorded in the temperature range between 20°C and 60°C for DPPC and between 20°C and 80°C for DSPC, with a scan rate of 90 °C/h and a filtering period of 2 s.

Leakage

The liposomes were prepared by hydration of a lipid film and subsequence polycarbonate membrane extrusion. A thin lipid film was prepared from DSPC or DPPC, Chol, and PEG-DSPE at molar ratios 61.66 : 33.33 : 5 mol%. The lipid film was hydrated with the appropriate volume of 100 mM carboxyfluorescein (CF) in 10 mM Hepes pH 7.4, adjusted to pH 7 with NaOH, and then vigorously agitated on a vortex mixer to obtain a suspension of multilamellar liposomes. The obtained suspension was then extruded through polycarbonate membrane with 100 nm pore size above the respective phase transition temperature to produce unilamellar liposomes. CF-containing vesicles were separated from the free CF by elution through a pre-packed column of Sephadex G-25 (GE Healthcare Bio-Sciences, Uppsala, Sweden. with 10 mM Hepes pH 7.4. The liposomal preparation was diluted to a final lipid concentration of 10 µM just before the measurements. The release of liposome content was followed by dequenching of CF. No quenching of CF by any of the boron clusters was observed; all data were normalized to 100% fluorescence after addition of Triton X-100 at 0.05% final concentration [8b].

Atomic force microscopy

For atomic force microscopy a Multimode AFM with a Nanoscope IIIa controller (Veeco, Germany) was used. Imaging was done with silicon cantilevers (RTESP, Veeco) in tapping mode in air. For sample preparation 5 mM DPPC solution was mixed with 50 mM BI in 10 mM HEPES. Ten µL of the sample solution was added to a freshly cleaved mica surface, incubated for 5 min, then shortly rinsed with nanopure water and dried under a nitrogen stream before imaging.

Toxicity

Chinese hamster lung fibroblasts (V79 cells) were used and cultivated with Ham's F10 medium and 10 % newborn calf serum at 37 °C and 5 % CO_2. Cells (10,000 per well) were seeded in 96-well plates and grown for 24 h. The cells were incubated with different concentrations of the halogenated derivatives for 24 h. Cell survival was determined using the WST-1 colour reagent, by incubating the cells for 4 h at 37°C with the reagent diluted 1:4 with phosphate-buffered saline (PBS) and then 1:10 with growth medium. Absorbance was measured at 450 nm.

Acknowledgements

We would like to acknowledge gift of DPPC, DSPC, and DSPE-PEG from Lipoid GmbH, Mannheim, Germany. For help with the synthesis of $K_2[B_{12}F_{12}]$ we are grateful to Janis Derendorf and Mathias Hill. KE gratefully acknowledges financial support from the Swedish Research Council and the Swedish Cancer Society.

Keywords: Triggered release • boron cluster • differential scanning calorimetry • cryo-transmission electron microscopy • distearoylphosphatidylcholine

[1] S. B. Lim, A. Banerjee, H. Önyüksel, *J Control Release* **2012**, *163*, 34-45.
[2] H. Maeda, H. Nakamura, J. Fang, *Adv. Drug Deliv. Rev.* **2013**, *65*, 71-79.
[3] X. Guo, J. A. MacKay, F. C. J. Szoka, *Biophys J* **2003**, *84*, 1784-1795.
[4] S. L. Huang, R. C. MacDonald, *Biochim Biophys Acta* **2004**, *1665*, 134-141.
[5] S. M. Park, M. S. Kim, S. J. Park, E. S. Park, K. S. Choi, Y. S. Kim, H. R. Kim, *J Control Release* **2013**, *170*, 373-379.
[6] aD. Gabel, D. Moller, S. Harfst, J. Rösler, H. Ketz, *Inorg Chem* **1993**, *32*, 2276-2278; bE. Justus, A. Vöge, D. Gabel, *Eur. J. Inorg. Chem.* **2008**, 5245-5250; cS. Hoffmann, E. Justus, M. Ratajski, E. Lork, D. Gabel, *J Organomet Chem* **2005**, *690*, 2757-2760.
[7] aB. Otersen, D. Haritz, F. Grochulla, M. Bergmann, W. Sierralta, D. Gabel, *J Neurooncol* **1997**, *33*, 131-139; bM. Neumann, U. Kunz, H. Lehmann, D. Gabel, *J Neurooncol* **2002**, *57*, 97-104; cM. Neumann, M. Bergmann, D. Gabel, *Acta Neurochirurgica (Wien)* **2003**, *145*, 971-975.
[8] aD. Gabel, D. Awad, T. Schaffran, D. Radovan, D. Daraban, L. Damian, M. Winterhalter, G. Karlsson, K. Edwards, *ChemMedChem* **2007**, *2*, 51-53; bD. Awad, L. Damian, M. Winterhalter, G. Karlsson, K. Edwards, D. Gabel, *Chem. Phys. Lipids* **2009**, *157*, 78-85; cT. Schaffran, E. Justus, M. Elfert, T. Chen, D. Gabel, *Green Chem.* **2009**, *11*, 1458-1464; dT. Schaffran, J. Li, G. Karlsson, K. Edwards, M. Winterhalter, D. Gabel, *Chem. Phys. Lipids* **2010**, *163*, 64-73.
[9] N. Dos Santos, K. A. Cox, C. A. McKenzie, F. van Baarda, R. C. Gallagher, G. Karlsson, K. Edwards, L. D. Mayer, C. Allen, M. B. Bally, *Biochim Biophys Acta* **2004**, *1661*, 47-60.
[10] N. J. Robert, C. L. Vogel, I. C. Henderson, J. A. Sparano, M. R. Moore, P. Silverman, B. A. Overmoyer, C. L. Shapiro, J. W. Park, G. T. Colbern, E. P. Winer, A. A. Gabizon, *Semin Oncol* **2004**, *31*, 106-146.
[11] K. Karki, D. Gabel, D. Roccatano, *Inorg Chem* **2012**, *51*, 4894-4896.
[12] P. Fan, J. Neumann, S. Stolte, J. Arning, D. Ferreira, K. Edwards, D. Gabel, *J. Chromatogr. A* **2012**, *1256*, 98-104.
[13] R. Vácha, P. Jurkiewicz, M. Petrov, M. L. Berkowitz, R. A. Böckmann, J. Barucha-Kraszewska, M. Hof, P. Jungwirth, *J. Phys. Chem. B* **2010**, *114*, 9504-9509.
[14] aD. V. Peryshkov, A. A. Popov, S. H. Strauss, *J Am Chem Soc* **2009**, *131*, 18393-18403; bW. H. Knoth, H. C. Miller, J. C. Sauer, J. H. Balthis, Y. T. Chia, E. L. Muetterties, *Inorg Chem* **1964**, *3*, 159-167; cV. Geis, K. Guttsche, C. Knapp, H. Scherer, R. Uzun, *Dalton Trans* **2009**, 2687-2694.
[15] K. P. Pauls, J. A. Chambers, E. B. Dumbroff, J. E. Thompson, *New Phytologist* **1982**, *91*, 1-17.
[16] aY. A. Ermakov, A. Z. Averbakh, A. I. Yusipovich, S. Sukharev, *Biophys J* **2001**, *80*, 1851-1862; bY. A. Ermakov, K. Kamaraju, K. Sengupta, S. Sukharev, *Biophys J* **2010**, *98*, 1018-1027.
[17] K. H. Klotz, R. Benz, *Biophys J* **1993**, *65*, 2661-2672.
[18] S. Ali, S. Minchey, A. Janoff, E. Mayhew, *Biophys J* **2000**, *78*, 246-256.
[19] *CRC Handbook of Chemistry and Physics*, 85th Edition ed., CRC Press, **2004**.
[20] P. Fan, S. Stolte, D. Gabel, *Anal Methods* **2014**, *6*, 3045-3055.
[21] J. N. Sachs, T. B. Woolf, *J Am Chem Soc* **2003**, *125*, 8742-8743.
[22] J. R. Rydall, P. M. Macdonald, *Biochemistry* **1992**, *31*, 1092-1099.
[23] H. Patel, C. Tscheka, K. Edwards, G. Karlsson, H. Heerklotz, *Biochim. Biophys. Acta* **2011**, *1808*, 2000-2008.
[24] aD. Papahadjopoulos, K. Jacobson, S. Nir, I. Isac, *Biochim. Biophys. Acta* **1973**, *311*, 330-348; bA. Blicher, K. Wodzinska, M. Fidorra, M. Winterhalter, T. Heimburg, *Biophys. J.* **2009**, *96*, 4581-4591.
[25] L. Yang, T. A. Harroun, T. M. Weiss, L. Ding, H. W. Huang, *Biophys J* **2001**, *81*, 1475-1485.
[26] J. H. Fuhrhop, W. Helfrich, *Chem. Rev.* **1993**, *93*, 1565-1582.
[27] aM. Nieuwenhuyzen, K. R. Seddon, F. Teixidor, A. V. Puga, C. Vinas, *Inorg Chem* **2009**, *48*, 889-901; bC. Knapp, in *Comprehensive Inorganic Chemistry 2nd ed, Vol. 1* (Ed.: J. Reedijk, Poeppelmeier, K.), Elsevier, Amsterdam, **2013**, pp. 651-679.
[28] P. F. Escobar, M. Markman, K. Zanotti, K. Webster, J. Belinson, *J Cancer Res Clin Oncol* **2003**, *129*, 651-654.
[29] H. B. Lee, M. D. Blaufox, *Journal of Nuclear Medicine* **1985**, *26*, 72-76.
[30] M. Almgren, K. Edwards, G. Karlsson, *Colloids Surf. A* **2000**, *174*, 3-21.

Appendix VII

Cellular interaction and uptake of liposomes containing dodecaborate cluster lipids: Implications for boron neutron capture therapy

Melinda Bartok[¶]*, Doaa Awad[ǀ], Joanna Wilinska[¶], Mitsunori Kirihata[§], Regine Süss[‡], Rolf Schubert[‡] and Detlef Gabel[¶]

[¶]School of Engineering and Science, Jacobs University Bremen, Campus Ring 1, D-28759 Bremen, Germany

[ǀ]Department of Biochemistry, Faculty of Science, Alexandria University, Moharam Bek, 21511 Alexandria, Egypt

[‡]Department of Pharmaceutical Technology and Biopharmacy, University of Freiburg, Hermann-Herder-Str. 9, D-79104 Freiburg, Germany

[§]Department of Biochemistry, Osaka Prefectural University, Sakai, Osaka, Japan

*Corresponding author

Note: Melinda Bartok and Doaa Awad contributed equally to this work.

Abstract

Recently we found that liposomes containing dodecaborate lipids intended for boron neutron capture therapy lead to massive hemorrhage in two different mouse tumor models, while not affecting the healthy organs *(Schaffran, T., Jiang, N., Bergmann, M. et al. (2014) Hemorrhage in mouse tumors induced by dodecaborate cluster lipids intended for boron neutron capture therapy. Int J Nanomedicine 9, 3583-90).* As we suspected that the liposomes interact specifically with endothelial cells in the tumor, we investigated the association and uptake of these liposomes in endothelial cells and in two different permanent cell lines by flow cytometry and fluorescence microscopy. Strong association of the liposomes with the cells, and uptake of both the boron lipid and a fluorescent marker lipid, was found even when the liposomes were sterically stabilized with polyethyleneglycol. Association was cell-type dependent, and HUVEC cells showed a particularly strong uptake. The results indicate that these lipids might preferentially be taken up in the vasculature, and their use in boron neutron capture therapy might therefore be limited.

Introduction

Boron neutron capture therapy (BNCT) utilizes the neutron capture reaction of ^{10}B with thermal neutrons. It is presently used clinically for treatment of brain tumors (*2, 3*) and head-and-neck tumors (*4, 5*). The compounds used in this therapy are p-dihydroxyborylphenylalanine (BPA) and $Na_2B_{12}H_{11}SH$ (BSH). For effective BNCT about 10-30 µg of ^{10}B per gram of tumor or 10^9 ^{10}B atoms per cell have to reach the affected tissue (*6*). For further enhancement of cell specificity and for increased uptake, targeting devices may be applied, which in BNCT are called "third generation" boron compounds (*7*). These delivery systems are designed for specific or overexpressed cell surface structures.

Our approach was to evaluate the suitability of liposomes as boron delivery devices. Liposomes are well-known systems used in cancer therapy for transporting chemotherapeutically active agents to tumors, and they have also been applied in experimental BNCT (*8*). Liposomes are able to transport large amounts of boron, either encapsulated in the interior of the liposome (*9*) or as lipid component with boron cluster compounds as headgroups (*8, 10*). While boron compounds encapsulated in liposomes might leak out, boron-containing lipids will allow to carry boron even when there is leakage of the liposomal content. Leakage of liposomes in the presence of boron clusters has been observed by us previously (*11*). The carrying capacity of liposomes prepared from boron lipids and helper lipids is at least equal to that of liposomes into which ionic boron cluster compounds have been encapsulated (*12*). The surface of the liposomes can be decorated with targeting agents (*13*).

We have recently prepared dodecaborate-containing lipids for BNCT (*12, 14-16*). The lipids form liposomes in the presence, and sometimes also in the absence, of helper lipids, and are of moderate to low toxicity. We tested these liposomes in mouse tumor models, and found that all lipid types led to hemorrhage in tumors, while the healthy tissues were seemingly unaffected (*1*). The onset of hemorrhage was rapid (within a few hours), and selective for tumor tissue in both of the tumor models tested (SCCVII squameous cell carcinoma in C3H mice and CT26/WT colon carcinoma in Balb/c mice). We hypothesized that the observed effect on the tumors was caused by the specific interaction of the liposomes with endothelial cells. In this work, we therefore compare the interaction and cellular uptake of boron-containing liposomes with HUVEC human umbilical vein endothelial cells as model for tumor endothelial cells, and human Kelly cells as a

cancer cell line. In addition, we used V79 Chinese hamster fibroblasts, as cell toxicity had been measured in these cells (*12, 14, 15*)

The tested lipids contain a pyridinium structure as manifold for two alkane chains, and dodecaborate as headgroup (*14*). Their structures are shown in Fig. **Error! Bookmark not defined.**. Interaction with cells was tested with fluorescence flow cytometry, and distribution in cells with fluorescence microscopy.

It had been shown before that liposomes interact with Kelly cells only when the liposomal surface is modified with an antibody recognizing the GD2-receptor that is overexpressed on Kelly cells, while non-targeted liposomes do not show cellular interaction (*17*).

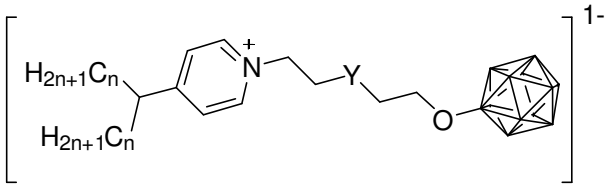

Y = no atom: **THF-S-n**
Y = O: **Dioxan-S-n**
Y = CH_2: **THP-S-n**
n = 12, 14, 16

Figure 1. Structure of the boron lipids used.

Materials and Methods

Materials

Phospholipids SPC, DSPC, DSPE-PEG_{2000} and EPG were gifts from Lipoid GmbH (Ludwigshafen, Germany). Cholesterol was obtained from Sigma-Aldrich (Steinheim, Germany), DPPE-NBD was from Avanti Polar Lipids (Alabama, Miss). The boron lipids (S-lipids) were synthesized as described by Schaffran et al. (*14*). Anti-BSH monoclonal antibody, clone A9H3, from purified IgG1 (affinity purified) was prepared at Osaka Prefectural University, Japan. Alexa Fluor 546 donkey anti-mouse IgG (H+L) was purchased from Invitrogen Molecular Probes (Göttingen, Germany). MobiGlow was obtained from MoBiTec (Göttingen, Germany). Kelly cells (human neuroblastoma cells) were purchased from DSMZ (Braunschweig, Germany) and V79 cells (Chinese hamster lung fibroblast cells) were from ATCC (Wesel, Germany). HUVEC cells (human umbilical vein endothelial cells), Medium 200 and LSGS Kit were

obtained from Life Technologies (Darmstadt, Germany). Trypsin 0.5% / EDTA 0.25%, RPMI 1640, Ham F-10, FCS, NCS and Penicillin/Streptomycin (Pen/Strep) were purchased from Biochrom (Berlin, Germany). Cold fish gelatin was from Sigma-Aldrich (Steinheim, Germany), Hepes and Triton X-100 from Acros Organics (Geel, Belgium), NaCl from Fluka (Buchs, Switzerland) and formaldehyde from Merck (Darmstadt, Germany).

Liposome preparation

Liposomes were prepared from DSPC:Chol:S-lipid (1:1:1 molar ratio) with 2 mol% DOPE-NBD, as a fluorescent marker. Control liposomes were made from SPC:Chol 2:1, DSPC:Chol 2:1 and SPC:Chol:EPG 1:1:1, respectively, with 2 mol% DOPE-NBD. DSPE-PEG_{2000} (2 mol%) was incorporated into the liposomes when indicated. The lipid mixture was dissolved in chloroform and dried under vacuum for 4 hours. The lipid film formed was hydrated with HBS (10 mM Hepes with 150 mM NaCl), subjected to 10 freeze-thaw cycles and extruded 21 times with a Liposofast hand extruder (Avestin, Mannheim, Germany), through a polycarbonate membrane with pore diameter of 100 nm (Avestin, Mannheim, Germany), by heating the lipid mixture above 60˚C, which is above the phase transition temperature of the DSPC lipid. The lipid concentrations were measured with the Stewart assay (*18*). The final concentrations were around 10 mM.

Liposome characterization (size and ζ potential)

A Zetasizer nano ZS device along with Zetasizer Software 6.01 and disposable Folded Capillary Cells or Zetamaster S with software PCS v1.41 (all Malvern Instruments, Malvern, U.K.) and semi-micro cuvettes Plastibrand (Carl Roth GmbH, Karlsruhe, GE) were used. Hydrodynamic particle diameter (Z-Ave) and ζ potential were determined. Samples were diluted with sterile filtrated (0.22 µm) HBS to a total lipid concentration of about 500 µM. Cuvette chamber temperature was 25 °C and sample equilibration time in the measurement cell was at least 2 min. All measurements were performed in triplicate with automatic selection of number of single runs per measurement (usually around 15 for Z-Average or 30 for ζ) as well as automatic attenuation selection. Smoluchowski approximation was used to calculate the ζ potential from the electrophoretic mobility. Voltage was set to device-bound minimum of 10 V, and thus only values for a monomodal distribution could be obtained.

Cell cultivation

Kelly cells were grown in RPMI 1640 medium supplemented with 10% FCS and 1% Pen/Strep and V79 cells were cultivated in Ham F-10 medium with 10% NCS and 1% Pen/Strep. For HUVEC cells, Medium 200 with an additional LSGS Kit was used. All cells were incubated at 37˚C with 5% humidified atmosphere.

Sample incubation for immunostaining

Cover slips (1.5 mm, Menzel, Germany) were cleaned with 10% HNO_3, sterilized in 70% ethanol, placed in 12-well plates and covered with 0.2% gelatin. Kelly, V79 and HUVEC cells were seeded at a density of 15 x 10^4, 10 x 10^4 and 20 x 10^4, respectively at 48 h prior to experiment. The incubation time was 2 h with various liposome concentrations (0.010, 0.075 and 2.5 mM), each at 37˚C. The THF-S-n and EPG containing lipids were also incubated at 4˚C with the cells, where mentioned. After incubation the cells were washed three times with PBS, fixed with 8% formaldehyde for 10 min at 37˚C, permeabilized with 0.2% Triton X-100, 5 min at room temperature (RT) and blocked with 10% FCS, 30 min at RT. The anti-BSH monoclonal antibody was diluted with the blocking solution to a concentration of 16 µg/ml and incubated with the cells 1 h at RT and then 24 h at 4˚C. The next day, the cells were washed three times with PBS and incubated with Alexa Fluor 546 labeled secondary antibody, 20 µg/ml prepared in blocking solution, for 1 h at RT. After three additional washing steps with PBS the cover slips were mounted on glass slides with 10 µl MobiGlow. Images were taken at 63x magnification with an AxioCam HRc camera on an LSM 510 Meta confocal laser scanning microscope equipped with argon/krypton gas and helium/neon lasers, controlled by a standard LSM 5 software (all Carl Zeiss, Germany). For all miscroscopic pictures, identical settings of gain etc. for each of the channels were used. For image analysis Zen Black 2012 software (Carl Zeiss, Germany) was used.

Flow cytometry measurements

The cells were seeded in 12-well plates (Kelly 2x10^5 cells/well, V79 1.5x10^5 cells/well and HUVEC 2.5x10^5 cells/well), 24 h prior to incubation. A medium change was performed 1 h prior to the experiment. The incubation with liposomes was for 2 h, at 37˚C and at 4˚C; the final lipid concentration given to the cells was either 0.075 mM or 0.010 mM. After incubation the cells were washed with PBS and harvested with trypsine/EDTA solution while shaking gently. The

cells were centrifuged and resuspended in 200 µl PBS. The samples were measured in a CyFlow Space apparatus with FlowMax software, version 2.82 (all Partec, Münster, Germany). For each sample, $3x10^4$ events were counted (excitation laser wavelength 488 nm, emission wavelength filter 516-556 nm). Fluorescence intensity of untreated control cells was used for gating. The fraction of treated cells showing higher fluorescence intensity than the gated cells was quantified.

Results

Liposome characterization

The different liposome preparations had diameters between 93 and 145 nm, with a polydispersity index of around 0.14. The ζ potential of the liposomes with boron lipids was around -45 mV, that of the EPG liposomes -36 mV. This charge was effectively shielded with the admixture of DSPE-PEG, and all of these liposomes had ζ potentials of around -5 mV.

Interaction of cells with liposomes

The association of liposomes containing either DSPC or SPC as helper lipid with V79 cells is shown in Figure **Error! Bookmark not defined.** (left). Generally, in all flow cytometry measurements we used as control SPC and DSPC liposomes, without the boron-lipid (B-lipid). Both of these controls showed little to no association with V79 cells. To mimic the influence of charge on cell uptake, we prepared liposomes containing EPG instead of the B-lipid and SPC as helper lipid. These liposomes showed lower cell association with V79 cells, in comparison with that in presence of B-lipids. An exception represented the THF-S-12 lipid liposomes, which had comparable uptake with that of the EPG containing liposomes. For all B-lipid liposomes, with or without PEG in their structure, the cell association was between 70% and 100%. The only exception from this trend was observed for THF-S-12, which had an association of about 32% for liposomes without the PEG lipid, and 53% for PEGylated liposomes. The highest cell association was obtained for THF-S-14, THF-S-16 and THP-S-16. Reduction of temperature to 4°C reduced the cell association to almost zero. The cell association of THF-S-14 with no PEG lipid is the only one noticeable at this incubation temperature.

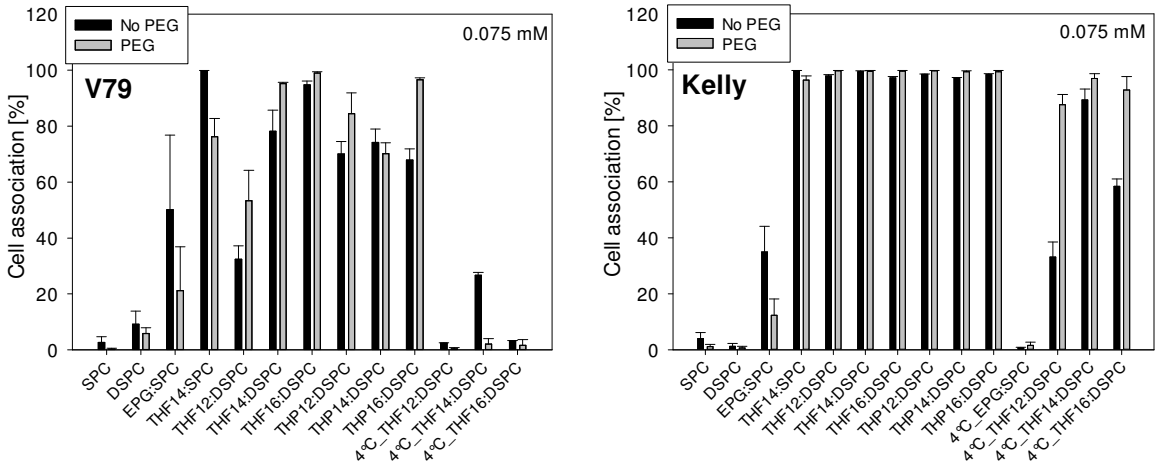

Figure 2. Cell association of 0.075 mM of liposomes, as measured by flow cytometry in V79 (left) and Kelly (right) cells. Where "4°C" is mentioned, the samples were incubated at 4°C with the liposomes, all other samples were incubated at 37°C.

The Kelly cells showed no association with the control liposomes at 37°C (Figure 2 (right)). The EPG containing lipid showed lower association with these cells than with V79 cells; cell associations were around 12% for PEGylated liposomes, and 35% for liposomes without the PEG lipid. For all B-lipid liposomes, the cell association with Kelly cells at 37°C was between 97% and 100%. We also observed that the PEGylation had only a minimal influence, with no significant differences between cells exposed to PEG liposomes or liposomes without the PEG lipid (see Figure 3). However, the reduction of the temperature to 4°C reduced the cell association of THF-S-12 and THF-S-16 containing liposomes, when no PEG lipid was present. All other samples presented an association of 87% to 97% with Kelly cells, which is comparable with that obtained at 37°C. The EPG containing lipid showed no cell association at 4°C. When using SPC instead of DSPC as helper lipid, similar values of cell association were obtained in V79 and Kelly cells.

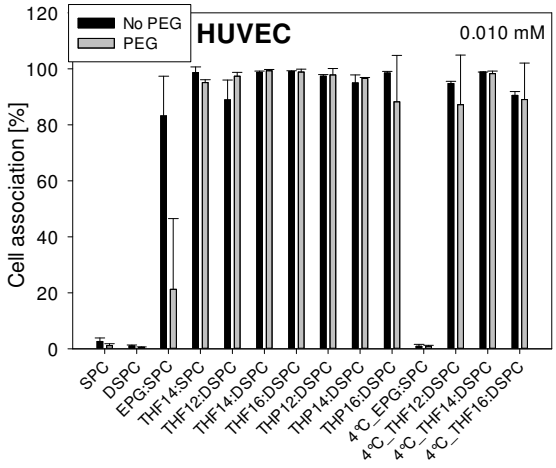

Figure 3. Cell association of liposomes at 0.010 mM concentration, as measured by flow cytometry in HUVEC cells. Where "4°C" is mentioned, the samples were incubated at 4°C with the liposomes, all other samples were incubated at 37°C.

At the liposome concentrations used for incubation with Kelly and V79 cells (0.075 mM total lipid), cell association of 100% was seen for both 37°C and 4°C in HUVEC cells, when they were exposed to B-lipid liposomes and EPG liposomes (data not shown). Therefore, we incubated the HUVEC cells with lower lipid concentration (0.010 mM). Even at this concentration the cell associations of the B-lipid liposomes were above 89%, when the incubation took place at 37°C, and above 87% at 4°C. The control liposomes, containing SPC or DSPC, showed no association with HUVEC cells. However, the EPG containing liposomes, at 10 μM lipid concentration and 37°C, were found in over 80% of the cells, when no PEG lipid was present, and only in 21% of the cells, when the liposomes were PEGylated. At 4°C the EPG liposomes showed no cell association. When the cells were incubated with the B-lipid liposomes at 4°C, a slight decrease in the cells association was observed, which was between 0-10%.

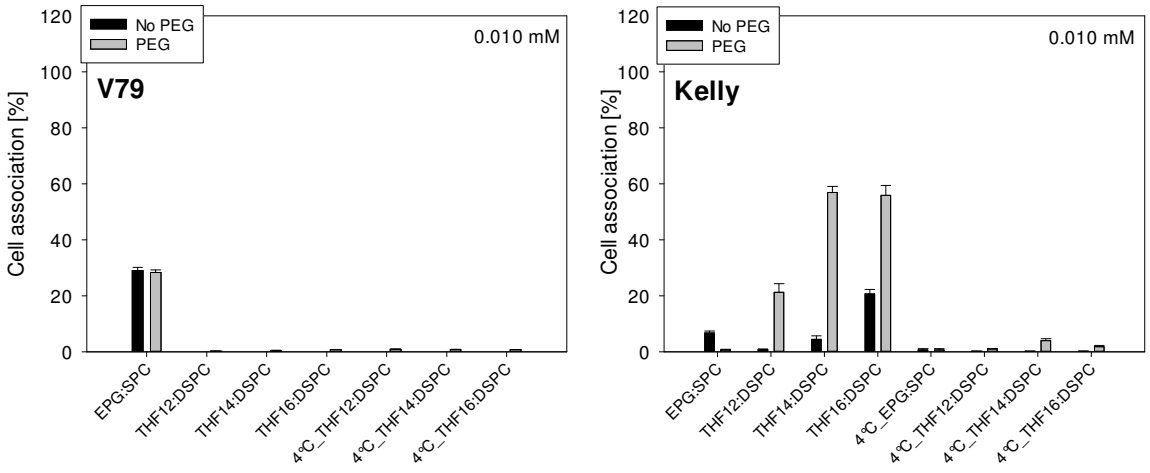

Figure 4. Cell association of liposomes at 0.010 mM, as measured by flow cytometry in V79 (left) and Kelly (right) cells. Where "4°C" is mentioned, the samples were incubated at 4°C with the liposomes, all other samples were incubated at 37°C.

In order to compare the cell association of the B-lipid liposomes between the three cell lines involved in this study, we incubated the V79 and Kelly cells with the liposomes also at 10 μM lipid concentration. The EPG lipid liposomes were used as control. In V79 cells there was no uptake of the liposomes at any B-lipid used, with or without the PEG lipid, neither at 37°C, nor at 4°C. However, the EPG lipid was found in about 29% of the cells. When Kelly cells were used, 56% of the cells have taken up the PEGylated B-lipid liposomes, in presence of THF-S-14 and THF-S-16 lipids, when the incubation temperature was 37°C. The THF-S-12 lipid caused a cell association in Kelly of only 21%. In the absence of PEG lipid, the B-lipids led to association of 1-20%. An incubation at 4°C led to no uptake in Kelly cells at 10 μM lipid concentration.

Microscopic localization of lipids in Kelly cells

The uptake of both the fluorescent lipid (NBD-lipid) and the boron lipid (B-lipid), as measured by antibody detection, was different for the different lipids, and was concentration dependent. As shown in Figure 5, for 0.075 mM of the liposomes the strongest uptake was found for THP-S-16, where the NBD-lipid and the B-lipid co-localized in the cytoplasma of the Kelly cells. In none of the staining images taken, when 0.075mM liposomes were used, was found any uptake in the cell nucleus. Also, the uptake of B-lipid at these concentrations was slightly lower than that of NBD-lipid.

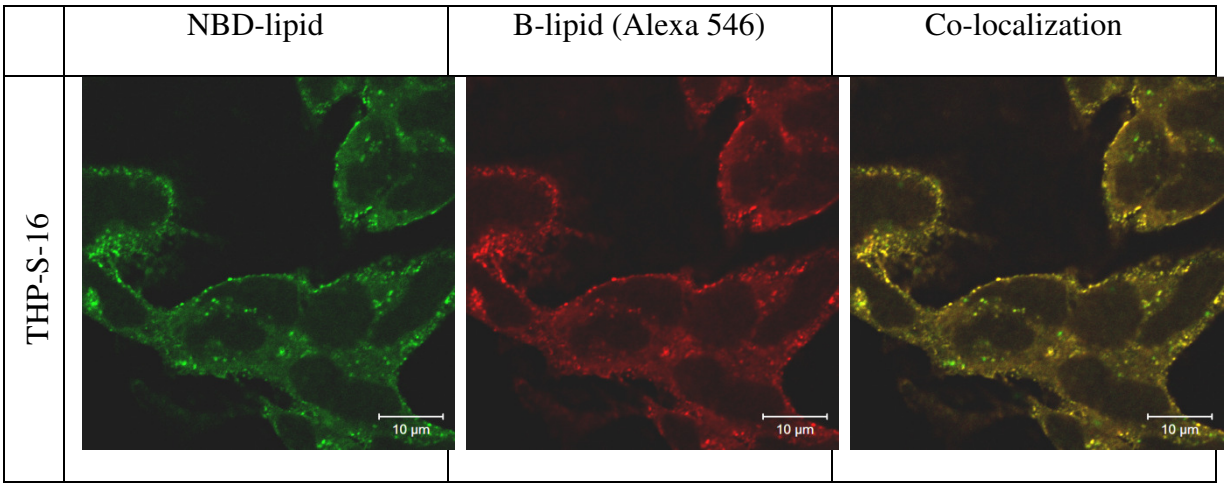

Figure 5. Localization of the THP-S-16 and the NBD-lipid in Kelly cells, when incubated at 37°C. The liposome concentration was 0.075 mM. The B-lipid is visualized by immuno-staining with the secondary antibody labeled with Alexa Fluor 546.

The liposome uptake experiments were performed also at 2.5 mM liposome concentration, because at this concentration a clear differentiation of the uptake of B-lipid and NBD-lipid, for different liposome preparations, was observed. In these conditions, the strongest uptake was found for THF-S-14 and THP-S-16 lipids, which were quite uniform throughout the cell body for the B-lipid, but the NBD-lipid had a lower accumulation in the cell nucleus in comparison to the cytoplasm (see Figure 6). In several preparations, cellular distribution of B-lipid and NBD-lipid did not coincide completely. Cell uptake of B-lipid was found to be low for THF-S-12, THF-S-16 and THP-S-12 lipids. In case of THF-S-12, also the NBD-lipid uptake was considerably lower than in case of other B-lipid liposomes. However, for THF-S-16 and THP-S-12 a strong NBD-lipid uptake was observed.

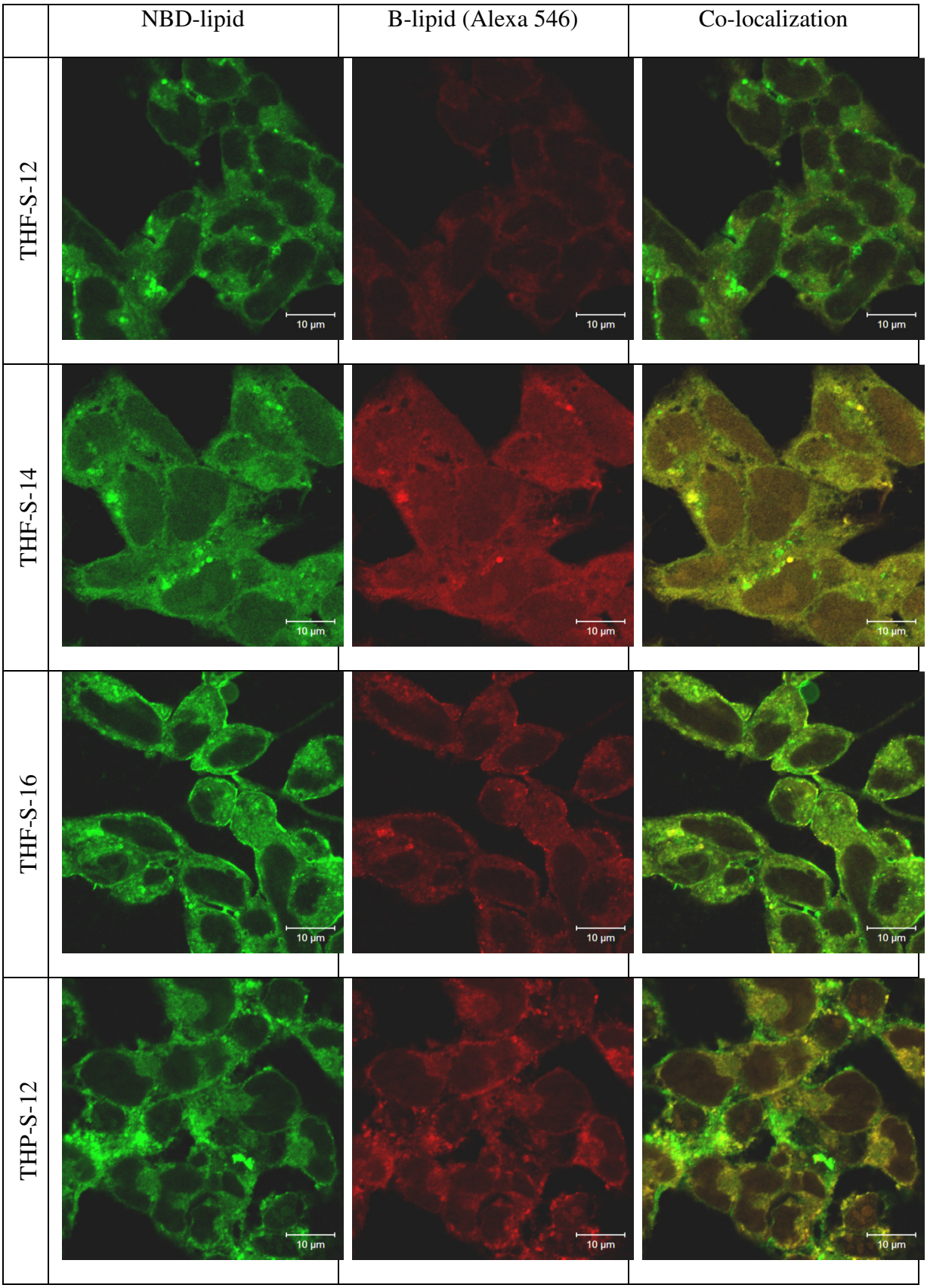
NBD-lipid
B-lipid (Alexa 546)
Co-localization
THF-S-12
THF-S-14
THF-S-16
THP-S-12
10 µm

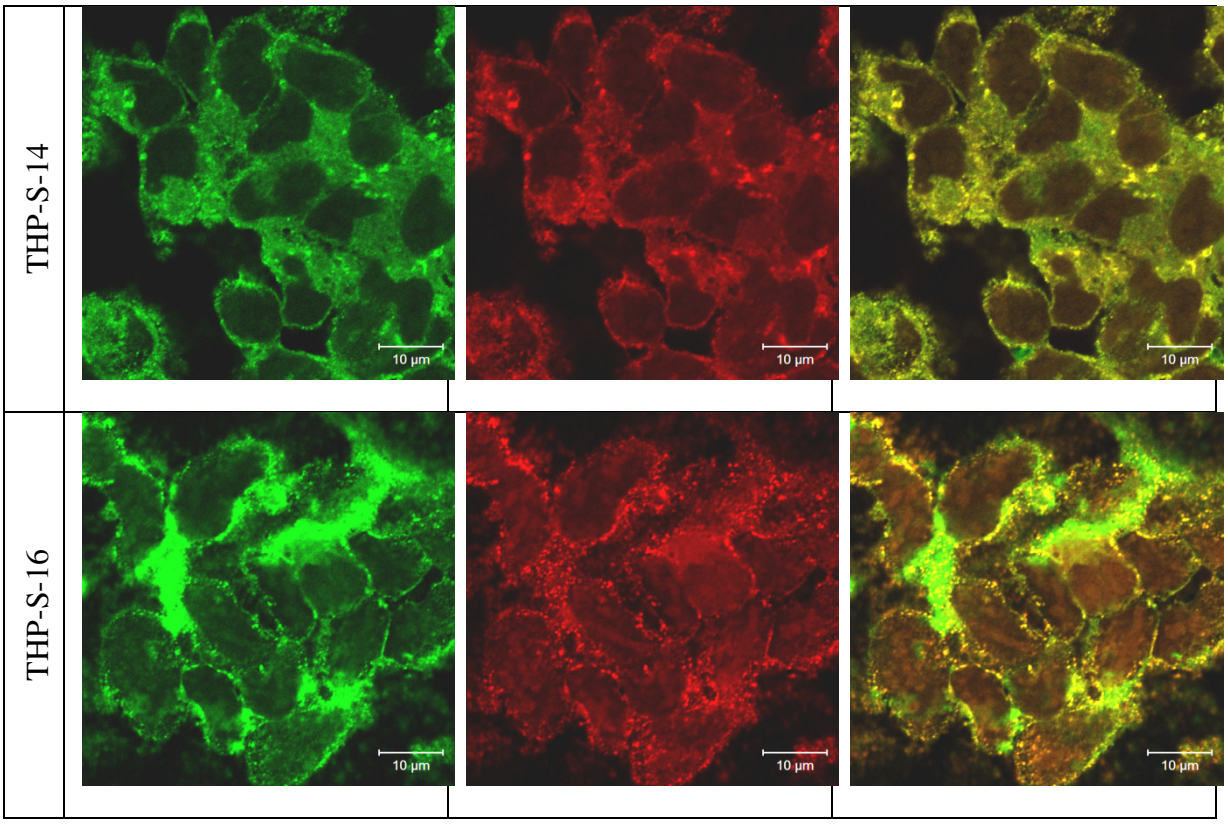

Figure 6. Localization of the B-lipids and the NBD-lipid in Kelly cells, when incubated at 37°C. The liposome concentration was 2.5 mM. The B-lipid is visualized by immuno-staining with the secondary antibody labeled with Alexa Fluor 546.

As the FACS measurements revealed a strong association of the B-lipid liposomes with Kelly cells also at 4°C, and the highest association of the PEGylated liposomes was obtained with THF-S-14 and THF-S-16 lipids, we stained the cells with two different concentrations of the THF-S-16 lipid liposomes (0.075 and 2.5 mM). The uptake at 0.075 mM, incubated at 4°C is comparable with the uptake at 37°C, when using the same concentration of the liposomes. However, the uptake of NBD-lipid, in case of 2.5 mM of liposomes, was significantly lower than the uptake at 37°C; instead, the B-lipid showed comparable uptake at both temperatures (data shown in the supplementary information).

Uptake of B-lipids in HUVEC cells

The HUVEC cells incubated with the B-lipid liposomes at 0.075 mM concentration showed similar uptake of the B-lipid and the NBD-lipid with that of Kelly cells at the same concentration. No significant uptake of the lipids was observed in these cells at 0.010 mM

concentration (data not shown). These results were in contrast with the results obtained in FACS measurements. We have no clear explanation for this. In the FACS measurements considerable cell association was seen also when EPG containing liposomes, without the PEG lipid, were incubated with HUVEC at 37°C. Therefore, we investigated the localization of these liposomes by fluorescence microscopy. The outcome was that the uptake of these lipids at 0.075 mM was similar to that of the B-lipids at the same concentration (data not shown).

Cellular uptake and localization in V79 cells

The uptake of the B-lipids and NBD-lipid was measured also in V79 cells, as the toxicity of the B-lipids was quantified previously in these cells (*13*). With V79 cells, the strongest association in FACS measurements was obtained for THF-S-16 and THP-S-16, when PEGylated liposomes were used. Therefore, we stained only these two B-lipid liposomes at 0.075 mM concentration with the cells. For both, the NBD-lipid showed a uniform uptake, all over the cell body. The uptake is comparable with that of Kelly at the same concentration. However, the B-lipid uptake was quite low in both cases (see in supplementary information).

The V79 cells incubated with the THF-S-n liposomes (n=12; 14; 16), at 2.5 mM, showed lower uptake for the NBD-lipid, but more intense uptake of the B-lipid, when compared to Kelly cells. For the THP-S-n lipids no considerable uptake of the NBD-lipid and B-lipid was observed (data not shown). However, when THP-S-12 was used a slight uptake of the B-lipid was noticed. This uptake was comparable with that of THF-S-16.

Discussion

The uptake of liposomes containing B-lipids in Kelly, V79, and HUVEC cells is quite unexpected. Previously, it has been reported that negatively charged liposomes with or without PEG layer do not associate much with HeLa cells (*19*). For positively charged liposomes, uptake is high in the absence of PEG, but almost completely inhibited by PEGylation (*20*).

Uptake between the three cell lines tested in this study is different. The reason cannot lie solely in different culture media or the serum content of the medium. Recently, HUVEC cells have been shown not to take up sterically stabilized liposomes more than what was found for other cell lines (*21*).

The reason for the uptake of B-lipid liposomes is unclear. Previously, the presence of negatively charged phospholipids and heparan sulfate glycoprotein has been made responsible for the

uptake of positively charged liposomes by endothelial cells (*22*). For the negatively charged boron lipids, such mechanism cannot be relevant. Uptake could be caused by strong interaction of boron clusters with membranes including the glycocalix. We have shown before that on carbohydrate chromatography matrices, boron cluster compounds are strongly retained (*23*). The interaction of clusters with water is unusual, and the energy required to remove water from the hydrate shell of the clusters is small (*24*). Thus, one might envisage that the cluster lipids might interact with the cell surface to a much higher degree than what is observed for other neutral or negatively charged lipids.

It is also unexpected that there was little difference between boron lipid liposomes containing PEG lipids and those lacking this steric stabilization. As boron lipids form stable structures even on their own (*12, 14, 15, 25*), we do not expect much exchange of boron lipids from the liposomes to smaller micelles, which would have to include also the fluorescent lipid (as this is monitored by flow cytometry, and is also found in microscopy). On the other hand, we cannot exclude such an explanation.

Recently, Nakamura et al. have described successful therapy of mouse tumors with dodecaborate-containing liposomes, encapsulating also $Na_2B_{12}H_{11}SH$ (*26*). In view of our results, the therapeutic efficacy could be caused by a selective destruction of the tumor vasculature, rather than a direct effect on the tumor stroma cells. Therefore, the uptake in HUVEC cells might be critical for use of these lipids in BNCT. If uptake of the liposomes in endothelial cells is predominant, it might be more effective for BNCT to enhance the targeting to these cells, rather than trying to target the liposomes to tumor stromal cells by one of the many mechanisms described for tumor targeting of neutral liposomes.

Krasnici et al. have found that the tumor vessels *in vivo* take up preferentially positively charged liposomes, in contrast to neutral and negatively charged liposomes, which extravasated unspecifically into the parenchyma (*27*). They explained this uptake with a charge related mechanism, where they assumed the presence of a negatively charged glycocalix on the endothelium of the microvessels, which could mediate the uptake. However, Lee at al. reported that the uptake of negatively charged liposomes containing PS (33 mol%) in J774 (murine macrophage cells) was 10-fold higher than the uptake of neutral liposomes with PC (*28*).

Previous *in vitro* experiments with rat liver endothelial cells showed that liposomes containing the negatively charged PS were taken up significantly in these cells, when the amount of PS lipid

was 30% of the total lipid concentration (*29*). The mechanism was assumed to be related to the broad ligand specificity of the scavenger receptors, present in these cells, which could mediate the binding and uptake of negatively charged liposomes. However, *in vivo* studies in rat liver showed only 25% uptake for the same liposomes.

In this study, we have not investigated the mechanism of uptake of the liposomes, nor to which compartments they distribute. Especially, we don't know whether the boron clusters are responsible for the uptake and whether neutral boron lipids with the same cluster as headgroup will also show uptake. Such studies are underway.

In conclusion, we have found that boron-containing liposomes associate strongest with HUVEC endothelial cells, more than with two other permanent cell lines. These observations might be relevant for the use of boron lipids in BNCT, and in other applications *in vivo*.

Acknowledgments

This work was financially supported by the Deutsche Forschungsgemeinschaft, DFG.

Abbreviations

BBE (bovine brain extract)

BNCT (boron neutron capture therapy)

BPA ((L)-4-dihydroxy-borylphenylalanine)

BSH ($Na_2B_{12}H_{11}SH$)

Chol (cholesterol)

DPPE-NBD (1,2-dipalmitoyl-sn-glycero-3-phosphoethanolamine-N-(7-nitro-2-1,3-benzoxadiazol-4-yl))

DSPC (1,2-distearoyl-sn-glycero-3-phosphocholine)

DSPE-PEG (1,2-distearoyl-sn-glycero-3-phosphoethanolamine polyethyleneglycol ($M_r \approx 2000$))

EPG (egg phosphatidylglycerol)

FCS (fetal calf serum)

GA-1000 (gentamicin sulfate and amphothericin-B additive)

HBS (hepes buffer saline, 10 mM Hepes with 150 mM NaCl, pH 7.4)

HUVEC (human umbilical vein endothelial cells)

NCS (newborn calf serum)

PBS (phosphate buffer saline, without $Ca^{2+}$and Mg^{2+}, pH 7.4)

PBS (phosphate buffered saline)

PC (phosphatidyl choline)

PEG (polyethyleneglycol)

Pen/Strep (Penicillin/Streptomycin).

PS (phosphatidylserine)

Rh-DPPE (Lissamine™ rhodamine B 1,2-dihexadecanoyl-sn-glycero-3-phosphoethanolamine

SPC (soy phosphatidyl choline)

References

(1) Schaffran, T., Jiang, N., Bergmann, M., Küstermann, E., Süss, R., Schubert, R., Wagner, F. M., Awad, D., and Gabel, D. (2014) Hemorrhage in mouse tumors induced by dodecaborate cluster lipids intended for boron neutron capture therapy. *Int J Nanomedicine 9*, 3583-90.

(2) Matsumura, A., Yamamoto, T., Tsurubuchi, T., Matsuda, M., Shirakawa, M., Nakai, K., Endo, K., Tokuue, K., and Tsuboi, K. (2009) Current practices and future directions of therapeutic strategy in glioblastoma: survival benefit and indication of BNCT. *Appl Radiat Isot 67*, S12-4.

(3) Sköld, K., Gorlia, T., Pellettieri, L., Giusti, V., H-Stenstam, B., and Hopewell, J. W. (2010) Boron neutron capture therapy for newly diagnosed glioblastoma multiforme: an assessment of clinical potential. *Br J Radiol 83*, 596-603.

(4) Kato, I., Fujita, Y., Maruhashi, A., Kumada, H., Ohmae, M., Kirihata, M., Imahori, Y., Suzuki, M., Sakrai, Y., Sumi, T., Iwai, S., Nakazawa, M., Murata, I., Miyamaru, H., and Ono, K. (2009) Effectiveness of boron neutron capture therapy for recurrent head and neck malignancies. *Appl Radiat Isot 67*, S37-42.

(5) Kankaanranta, L., Seppälä, T., Koivunoro, H., Saarilahti, K., Atula, T., Collan, J., Salli, E., Kortesniemi, M., Uusi-Simola, J., Valimaki, P., Makitie, A., Seppanen, M., Minn, H., Revitzer, H., Kouri, M., Kotiluoto, P., Seren, T., Auterinen, I., Savolainen, S., and Joensuu, H. (2012) Boron neutron capture therapy in the treatment of locally recurred head-and-neck cancer: final analysis of a phase I/II trial. *Int J Radiat Oncol Biol Phys 82*, e67-75.

(6) Fairchild, R. G., and Bond, V. P. (1985) Current status of 10B-neutron capture therapy: enhancement of tumor dose via beam filtration and dose rate, and the effects of these parameters on minimum boron content: a theoretical evaluation. *Int J Radiat Oncol Biol Phys 11*, 831-40.
(7) Soloway, A. H., Tjarks, W., Barnum, B. A., Rong, F.-G., Barth, R. F., Codogni, I. M., and Wilson, J. G. (1998) The chemistry of neutron capture therapy. *Chem. Rev. 98*, 1515-1562.
(8) Ueno, M., Ban, H. S., Nakai, K., Inomata, R., Kaneda, Y., Matsumura, A., and Nakamura, H. (2010) Dodecaborate lipid liposomes as new vehicles for boron delivery system of neutron capture therapy. *Bioorg. Med. Chem. 18*, 3059-65.
(9) Doi, A., Kawabata, S., Iida, K., Yokoyama, K., Kajimoto, Y., Kuroiwa, T., Shirakawa, T., Kirihata, M., Kasaoka, S., Maruyama, K., Kumada, H., Sakurai, Y., Masunaga, S., Ono, K., and Miyatake, S. (2008) Tumor-specific targeting of sodium borocaptate (BSH) to malignant glioma by transferrin-PEG liposomes: a modality for boron neutron capture therapy. *J Neurooncol 87*, 287-94.
(10) Li, T., Hamdi, J., and Hawthorne, M. F. (2006) Unilamellar liposomes with enhanced boron content. *Bioconjug Chem 17*, 15-20.
(11) Gabel, D., Awad, D., Schaffran, T., Radovan, D., Daraban, D., Damian, L., Winterhalter, M., Karlsson, G., and Edwards, K. (2007) The Anionic Boron Cluster (B(12)H(11)SH)(2-) as a Means To Trigger Release of Liposome Contents. *ChemMedChem 2*, 51-53.
(12) Justus, E., Awad, D., Hohnholt, M., Schaffran, T., Edwards, K., Karlsson, G., Damian, L., and Gabel, D. (2007) Synthesis, liposomal preparation, and in vitro toxicity of two novel dodecaborate cluster lipids for boron neutron capture therapy. *Bioconjug Chem 18*, 1287-93.
(13) Miyajima, Y., Nakamura, H., Kuwata, Y., Lee, J. D., Masunaga, S., Ono, K., and Maruyama, K. (2006) Transferrin-loaded nido-carborane liposomes: tumor-targeting boron delivery system for neutron capture therapy. *Bioconjug Chem 17*, 1314-20.
(14) Schaffran, T., Burghardt, A., Barnert, S., Peschka-Süss, R., Schubert, R., Winterhalter, M., and Gabel, D. (2009) Pyridinium lipids with the dodecaborate cluster as polar headgroup: synthesis, characterization of the physical-chemical behavior, and toxicity in cell culture. *Bioconjug Chem 20*, 2190-8.
(15) Schaffran, T., Lissel, F., Samatanga, B., Karlsson, G., Burghardt, A., Edwards, K., Winterhalter, M., Peschka-Süss, R., Schubert, R., and Gabel., D. (2009) Dodecaborate cluster lipids with variable headgroups for boron neutron capture therapy: synthesis, physical-chemical properties and toxicity. *J. Organomet. Chem. 694*, 1708-1712.
(16) Nakamura, H., Ueno, M., Lee, J.-D., Ban, S. H., Justus, E., Fan, P., and Gabel, D. (2007) Synthesis of dodecaborate-conjugated cholesterols for efficient boron delivery in neutron capture therapy. *Tetrahedron Lett 48*, 3153-3154.
(17) Lewrick, F. (2008), University of Freiburg.
(18) Stewart, J. C. (1980) Colorimetric determination of phospholipids with ammonium ferrothiocyanate. *Anal Biochem 104*, 10-4.
(19) Miller, C. R., Bondurant, B., McLean, S. D., McGovern, K. A., and O'Brien, D. F. (1998) Liposome-cell interactions in vitro: effect of liposome surface charge on the binding and endocytosis of conventional and sterically stabilized liposomes. *Biochemistry 37*, 12875-83.

(20) Pires, P., Simões, S., Nir, S., Gaspar, R., Düzgünes, N., and Pedroso de Lima, M. C. (1999) Interaction of cationic liposomes and their DNA complexes with monocytic leukemia cells. *Biochim Biophys Acta 1418*, 71-84.
(21) Luo, L.-M., Huang, Y., Zhao, B.-X., Zhao, X., Duan, Y., Du, R., Yu, K.-F., Song, P., Zhao, Y., Zhang, X., and Zhang, Q. (2013) Anti-tumor and anti-angiogenic effect of metronomic cyclic NGR-modified liposomes containing paclitaxel. *Biomaterials 34*, 1102-1114.
(22) Thurston, G., McLean, J. W., Rizen, M., Baluk, P., Haskell, A., Murphy, T. J., Hanahan, D., and McDonald, D. M. (1998) Cationic liposomes target angiogenic endothelial cells in tumors and chronic inflammation in mice. *The Journal of Clinical Investigation 101*, 1401-1413.
(23) Fan, P., Neumann, J., Stolte, S., Arning, J., Ferreira, D., Edwards, K., and Gabel, D. (2012) Interaction of dodecaborate cluster compounds on hydrophilic column materials in water. *J. Chromatogr. A 1256*, 98-104.
(24) Karki, K., Gabel, D., and Roccatano, D. (2012) Structure and dynamics of dodecaborate clusters in water. *Inorg. Chem. 51*, 4894-6.
(25) Justus, E., Awad, D., Hohnholt, M., Schaffran, T., Edwards, K., Karlsson, G., Damian, L., and Gabel, D. (2007) Synthesis, liposomal preparation, and in vitro toxicity of two novel dodecaborate cluster lipids for boron neutron capture therapy. *Bioconjug. Chem. 18*, 1287-1293.
(26) Koganei, H., Ueno, M., Tachikawa, S., Tasaki, L., Ban, H. S., Suzuki, M., Shiraishi, K., Kawano, K., Yokoyama, M., Maitani, Y., Ono, K., and Nakamura, H. (2013) Development of high boron content liposomes and their promising antitumor effect for neutron capture therapy of cancers. *Bioconjug Chem 24*, 124-32.
(27) Krasnici, S., Werner, A., Eichhorn, M. E., Schmitt-Sody, M., Pahernik, S. A., Sauer, B., Schulze, B., Teifel, M., Michaelis, U., Naujoks, K., and Dellian, M. (2003) Effect of the surface charge of liposomes on their uptake by angiogenic tumor vessels. *International Journal of Cancer 105*, 561-567.
(28) Lee, K. D., Nir, S., and Papahadjopoulos, D. (1993) Quantitative analysis of liposome-cell interactions in vitro: rate constants of binding and endocytosis with suspension and adherent J774 cells and human monocytes. *Biochemistry 32*, 889-99.
(29) Kamps, J. A. A. M., Morselt, H. W. M., and Scherphof, G. L. (1999) Uptake of Liposomes Containing Phosphatidylserine by Liver Cellsin Vivoand by Sinusoidal Liver Cells in Primary Culture:In Vivo–in VitroDifferences. *Biochem. Biophys. Res. Commun. 256*, 57-62.

Supplementary information for Appendix VII:

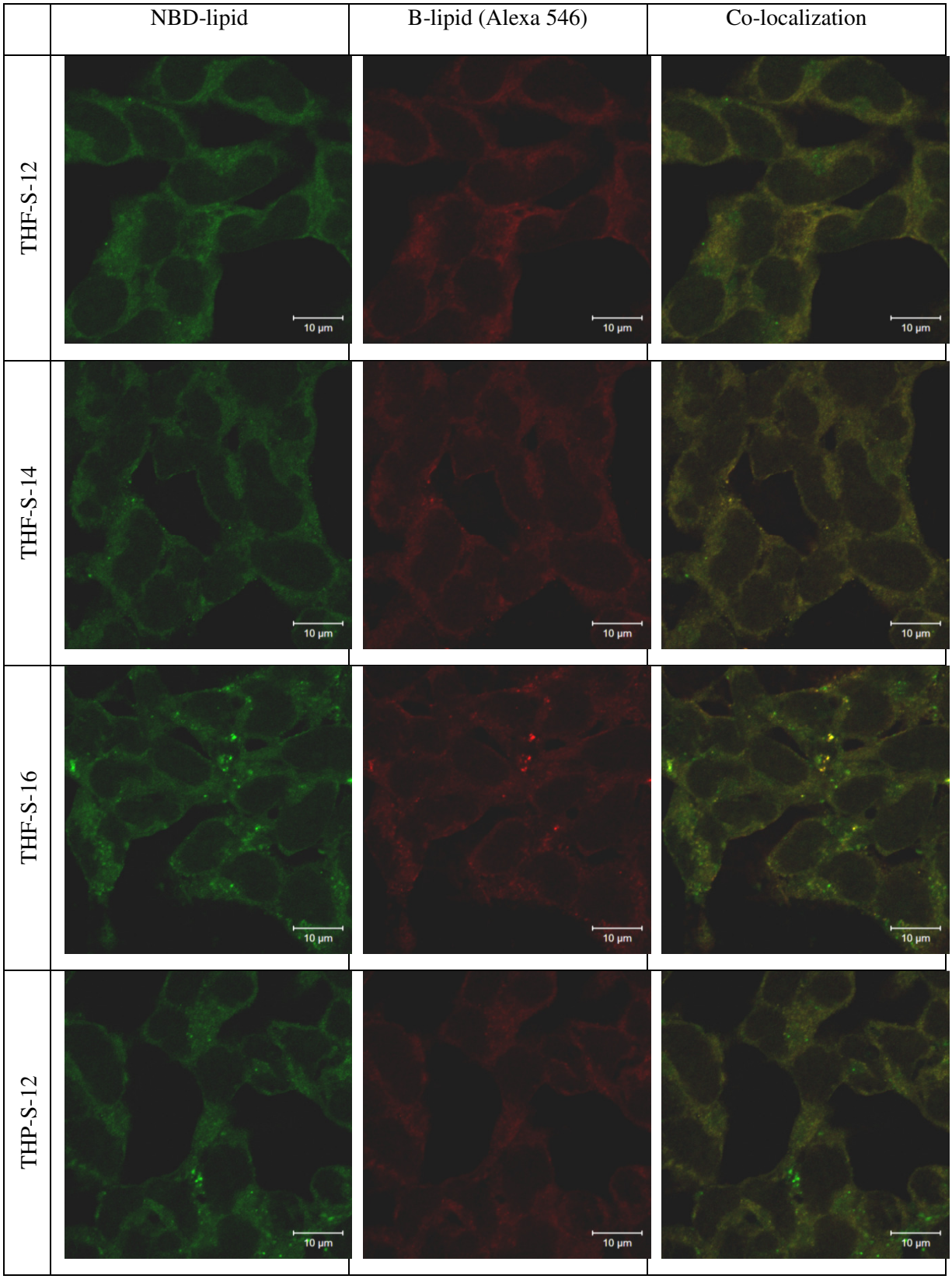

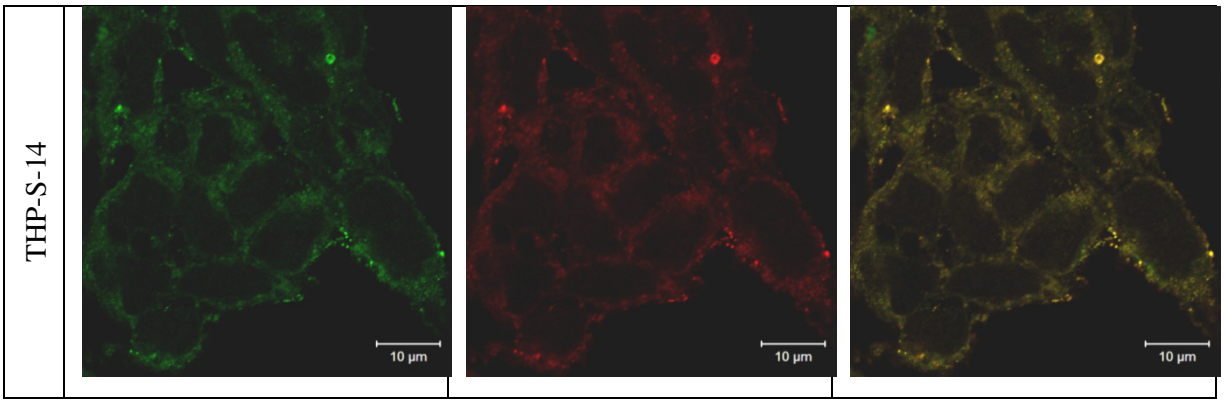

Figure 1S. Localization of the B-lipids and the NBD-lipid in Kelly cells, when incubated at 37°C. The liposome concentration was 0.075 mM. The B-lipid is visualized by immuno-staining with the secondary antibody labeled with Alexa Fluor 546.

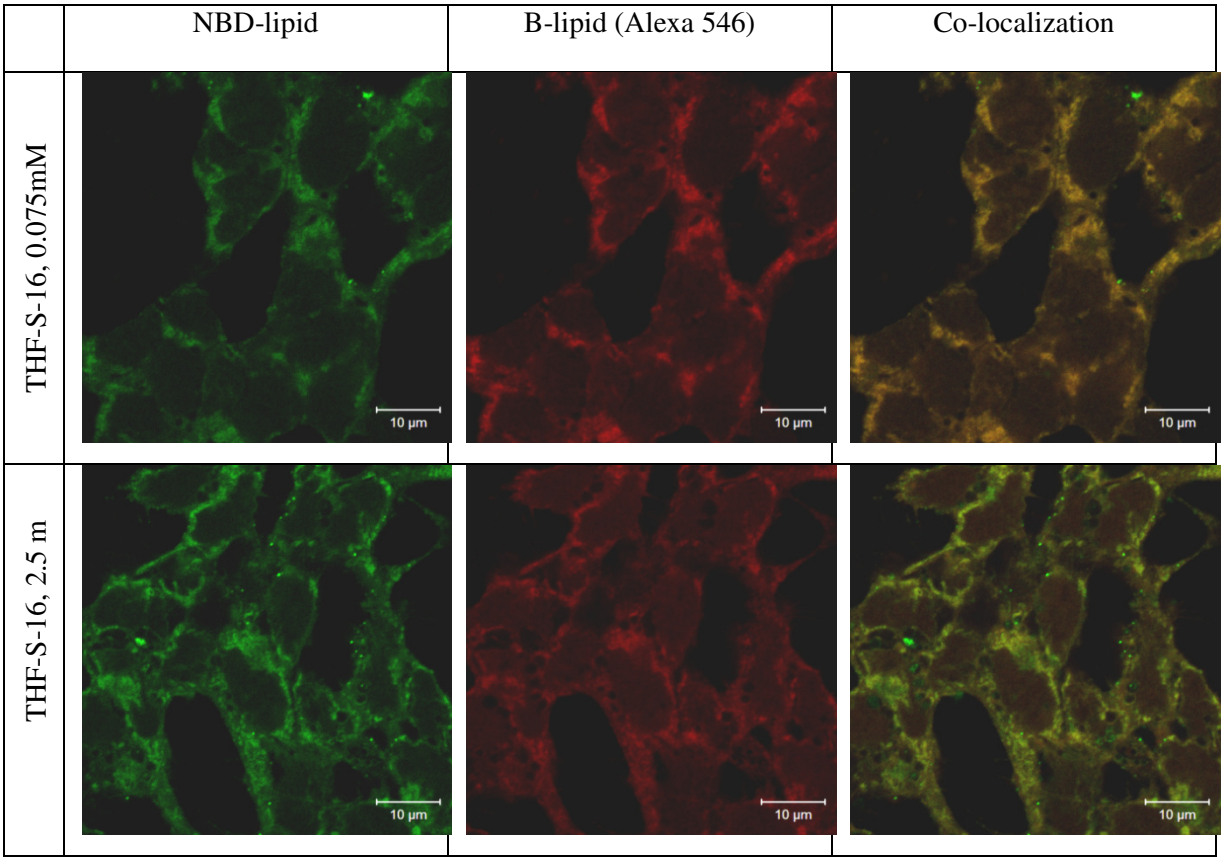

Figure 2S. Localization of the THF-S-16 lipid and the NBD-lipid in Kelly cells, when incubated at 4°C. The liposome concentrations were 0.075 and 2.5 mM. The B-lipid is visualized by immuno-staining with the secondary antibody labeled with Alexa Fluor 546.

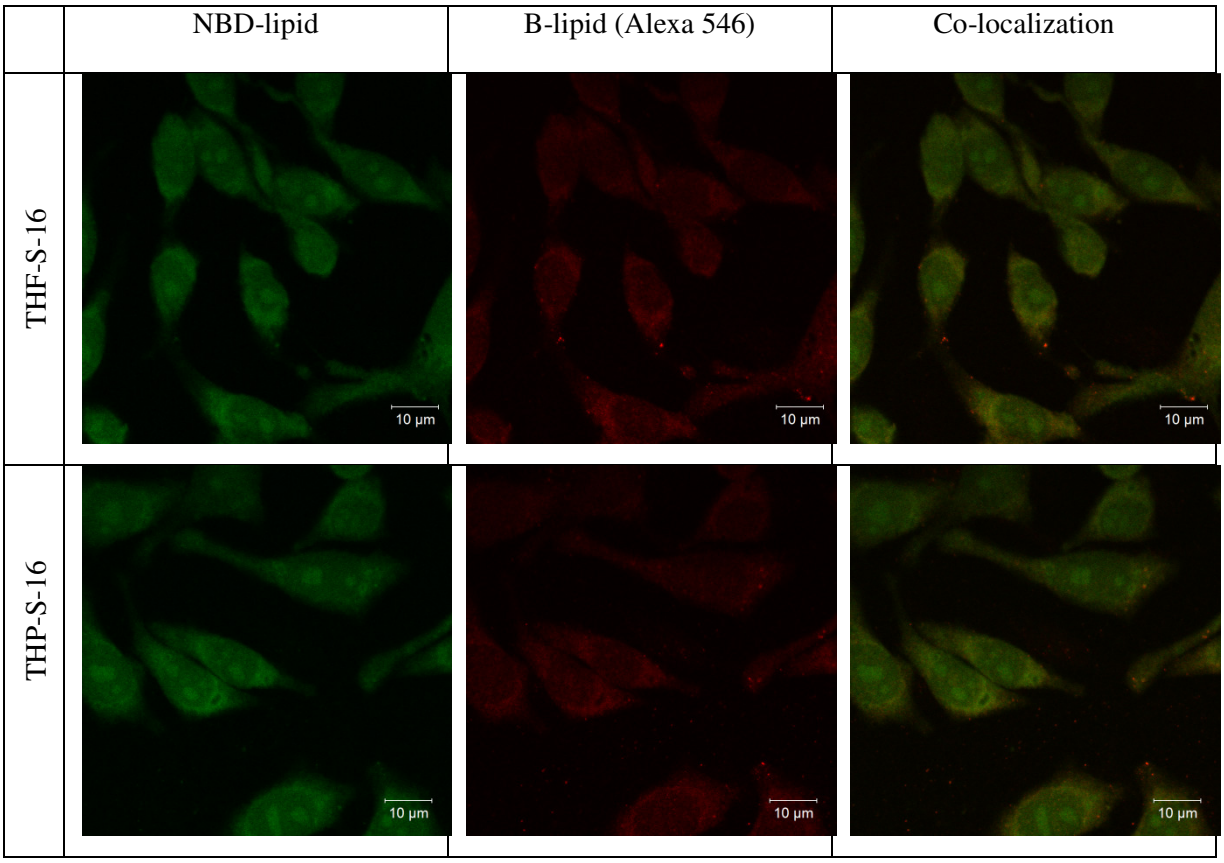

Figure 3S. Localization of THF-S-16, THP-S-16 and the NBD-lipid in V79 cells, when incubated at 37°C. The liposome concentration was 0.075 mM. The B-lipid is visualized by immuno-staining with the secondary antibody labeled with Alexa Fluor 546.

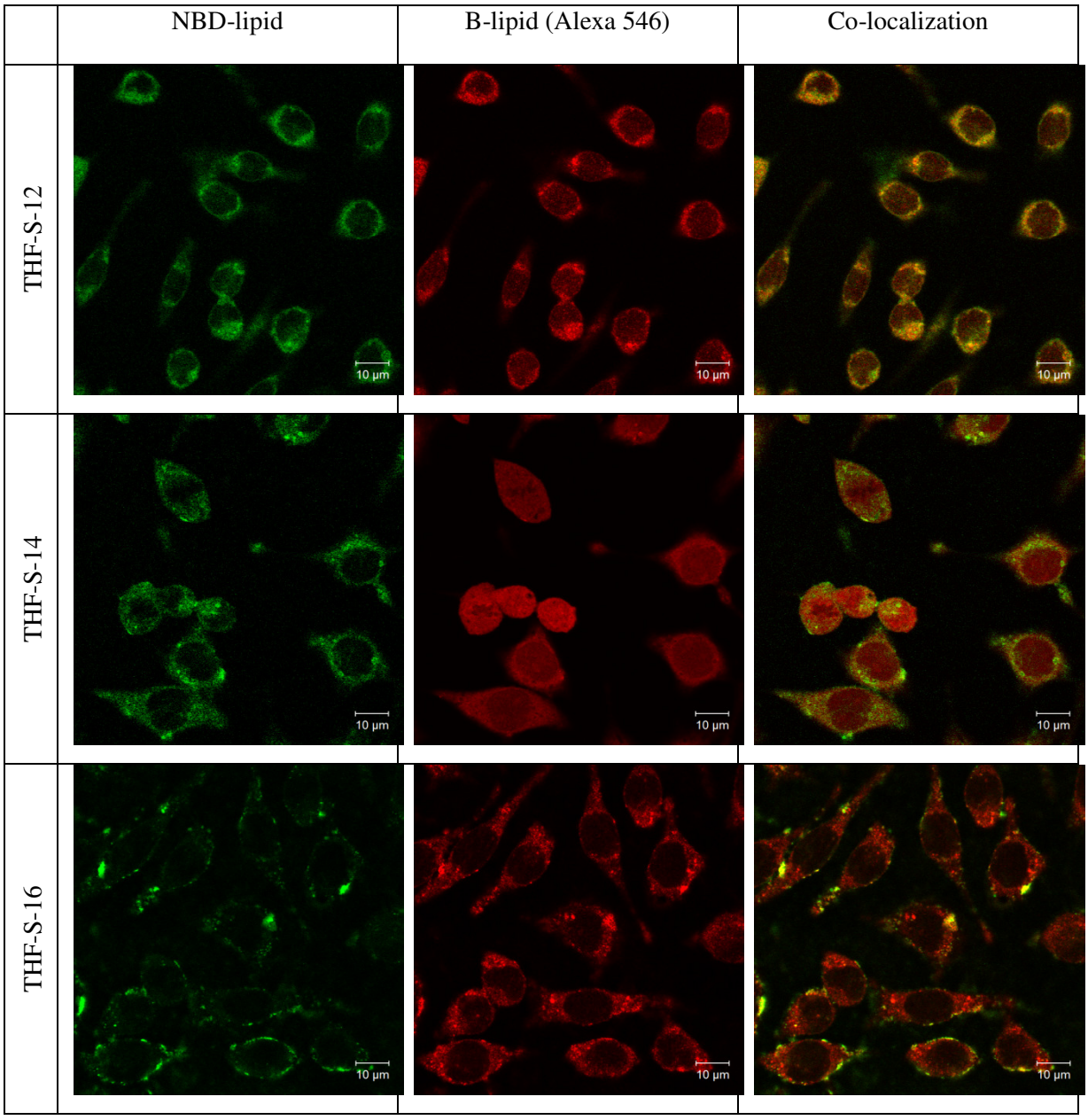

Figure 4S. Localization of B-lipids and the NBD-lipid in V79 cells, when incubated at 37°C. The liposome concentration was 2.5 mM. The B-lipid is visualized by immuno-staining with the secondary antibody labeled with Alexa Fluor 546.